論文 / 著書情報
Article / Book Information

題目(和文)	
Title(English)	Thermotropic Liquid Crystals in Rigid-rod Polyesters with Flexible Side Chains
著者(和文)	曽根正人
Author(English)	Masato Sone
出典(和文)	学位:工学博士, 学位授与機関:東京工業大学, 報告番号:甲第3157号, 授与年月日:1996年3月26日, 学位の種別:課程博士, 審査員:
Citation(English)	Degree:Doctor of Engineering, Conferring organization: Tokyo Institute of Technology, Report number:甲第3157号, Conferred date:1996/3/26, Degree Type:Course doctor, Examiner:
学位種別(和文)	博士論文
Type(English)	Doctoral Thesis

Thermotropic Liquid Crystals in Rigid-Rod Polyesters with Flexible Side Chains

A Dissertation

for the degree

DOCTOR OF ENGINEERING

by

Masato Sone

Department of Polymer Chemistry
Tokyo Institute of Technology
1996

Contents

Chapter 1

General Introduction

Liquid crystal is an intermediate state of aggregation between the crystalline solid and the amorphous liquid. Substance in this state is strongly anisotropic in some of the properties and exhibits a fluidity, which may be comparable to that of an ordinary liquid. The first observations of liquid crystalline behavior were made by Reinitzer[1] and Lehmann[2]. Several thousands of organic compounds are known to form liquid crystals[3]. A highly geometrical anisotropy in shape is essentially required for mesomorphism to occur. Anisotropic structural ordering in fluid phases has been of considerable interest to many scientists. Liquid crystalline polymers have a practical importance for their ability to orient while flowing and to maintain this orientation during the cooling process. Polymeric liquid crystalline materials have extremely long relaxation times but no elasticity. The properties enables good electro-optic performance over an extended range of temperature as well as good environmental stability.

In order to profitably discuss the structure and properties of polymeric liquid crystals it is necessary to describe and define several aspects of liquid crystallinity in small molecular compounds.

The majority of thermotropic liquid crystals are composed of rod-like molecules. They are classified broadly into three types: nematic, cholesteric and smectic which nomenclature was proposed by Friedel[4].

The nematic liquid crystal has some order in the direction of the molecules, but the centers of gravity of the molecules have no long range order. Thus the correlations in position between the centers of gravity of neighboring molecules are similar to those existing in a conventional liquid. The molecules are spontaneously oriented with their long axes approximately parallel. The preferred direction usually varies from point to point in the medium, but a uniformly aligned specimen is optically uniaxial, positive and strongly birefringent. The mesophase owes its fluidity to the ease

with which the molecules slide past one another while still retaining their parallelism. X-ray studies[5,6] indicate that some nematics possess a lamellar type of short-range order, i.e., they consist of clusters of molecules -called cybotactic groups[7]- the molecular centers in each cluster arranged in layers. In ordinary nematics the cybotactic groups, if they do exist, are smaller than can be detected by X-ray methods. A biaxial modification of the nematic has been discovered recently.

The cholesteric mesophase is also a nematic type of liquid crystal except that it is composed of optically active molecules. As a consequence the structure acquires a spontaneous twist about an axis normal to the preferred molecular direction. The twisted may be right-handed or left-handed depending on the molecular conformation. Optically inactive molecules or racemic mixtures result in a helix of infinite pitch which corresponds to the true nematic.

Smectic liquid crystals have stratified structures but a variety of molecular arrangements are possible within each stratification. Smectic phases are thus ordered higher than nematic phase. In smectic A the molecules are upright in each layer with their centers irregularly spaced in a liquid-like fashion. The interlayer attractions are weak as compared with the lateral forces between molecules and in consequence the layers are able to slide one another relatively easily. Hence this mesophase has fluid properties, though it is very much more viscous than the nematic. Smectic C is a tilted form of smectic A, i.e., the molecules are inclined with respect to the layer normal. Over a dozen other distinct smectic modifications have been identified. Some of them (S_B, S_E, S_G, S_H, S_J and S_K) have three-dimensional long-range positional order as in a crystal, though with weak interlayer forces (and hence energetically weak interlayer ordering), while some others, referred to as hexatic phases, have three dimensional long-range bond-orientational order, but without any long-range positional order[8,9]. The D phase has an overall cubic symmetry and thus is not smectics[10-12].

The first discotic liquid crystals of disc-shaped molecules were prepared and identified in 1977 by Chandrasekhar[13]. Since then a large number of

discotic compounds have been synthesized and a variety of mesophases discovered[14]. Structually, most of them fall into two distinct categories, the columnar and the nematic. Columnar phases exhibit genuine two dimensional long range order. The discotic columnar phases consists of discs stacked one on top of the other aperiodically to form liquid-like columns, the different columns constituting a two-dimensional lattice. The structure is somewhat similar to that of the hexagonal phase of soap-water and other lyotropic systems, but a number of variants of this structure have been identified: hexagonal, rectangular, tilted, oblique, etc. The nematic phase has an orientationally ordered arrangement of the discs without any long-range translational order. Unlike the classical nematic of rod-like molecules, this phase is optically negative. A cholesteric phase has also been identified. A smectic-like lamellar phase has been reported[15] but the disposition of the molecules in the layers has not yet been resolved.

Liquid crystalline polymers[16] are classified into three groups; main chain type, side chain type and rigid-rod type. The structures of polymers that form liquid crystals are illustrated schematically in Figure1-1. Mesogenic groups can be incorporated into polymer as side chains or as part of the main chain. The former case gives rise to the so-called side-chain liquid crystalline polymers, in which the chain conformation of the backbone is not significantly altered by the formation of mesophase[16]. Although the radius of gyration of the backbone appears to be different between the isotropic phase and mesophase or between the different mesophases according to the neutron scattering analysis, the polymeric and mesogenic effects are relatively uncoupled and the mesophase behavior is often predictable from the behavior of the low molecular weight mesogen.

On the other hand, if the mesogenic group forms part of the main chain as in main-chain liquid crystalline polymers[16,17], the polymer molecule must adopt a conformation and packing that is compatible with the structure of the mesophase. As a result, the polymeric and mesogenic properties are closely coupled. Alteration of the repeat unit may influence the molecular packing and result in the properties of the mesophase departing from those

of the low molecular weight mesogen. Conversely, the formation of a mesophase can affect the conformation of this type of polymer. Based on this concept of design of main chain liquid crystalline polymers, various new modifications of the liquid crystalline phases were observed recently. Watanabe et al.[16,17] report the thermotropic mesophase properties of main chain BB-n polyesters that can be constructed by an alternate arrangement of the mesogenic p,p'-bibenzoate unit and the flexible alkylene spacer with the carbon number of n. This homologous series of BB-n invariably form smectic mesophases; SA, SCA and SC, and cholesteric phases by the odd-even appearance of smectic structure resulting from a coupling of the polymeric and mesogenic effects, or the introduction of the chiral core in the intervening alkylene spacers. Moreover, Nakata et al.[17] report various characteristic smectic phases formed by the main chain type of polymers in which the mesogenic biphenyl moieties are linked by two different aliphatic spacers in a regularly alternate fashion.

Third type of the liquid crystalline polymers is named as "rigid-rod liquid crystalline polymers", which play the leading part in this thesis. Rigid rod polymers in solution were found to form liquid crystalline phases above a critical concentration depending on their axial ratio. Nematic or cholesteric liquid crystalline phases have been experimentally recognized and theoretically predicted by Onsager[18], Flory[19] and others[21,22]. Much less is known about other types of liquid crystals that may be formed by the rigid polymers, but recently experimental data indicate that rigid polymers may form liquid crystals that are neither nematic nor cholesteric. Livolant and Bouligand[23] and Lee and Meyer[24] have suggested from the analysis of microscopic textures that the synthetic polypeptide, poly(γ-benzyl glutamate), may form hexagonal columnar liquid crystals in its lyotropic solution. Watanabe et al.[25-29] also found the thermotropic hexagonal columnar phase in addition to the cholesteric phase in poly(γ-octadecyl L-glutamate). Strzelecka et al.[30] have reported that a smectic like phase in addition to a cholesteric phase can be seen in aqueous solutions of DNA, and subsequently, Livolant et al.[31] observed a columnar hexagonal phase in a similar DNA lyotropic system. The smectic A phase was also observed

in the lyotropic solution of tobacco mosaic virus by Meyer et al[32]. Smectic A and D phases were observed in the thermotropic mesophase of poly(γ-octadecyl L-glutamate) with a low degree of polymerization[27].

Kimura et al.[33] and Frenkel[34] have theoretically predicted that in hard-rod particles, smectic and columnar liquid crystals may appear as a result of an excluded-volume effect of the hard rods. A search for new liquid crystals of rigid polymers and their identification is continuing now in both the experimental and theoretical fields.

On the other hand, several interesting liquid crystalline phases with a characteristic layered structure have been found in the aromatic polyesters with long aliphatic side chains[35-63]. These liquid crystals can be easily distinguished from the nematic or cholesteric liquid crystals, but the structural details of these mesophases have not clearly been given.

OBJECTIVE of THIS THESIS

Over the past few years, there has been a considerable amount of effort directed towards the study of rigid-rod polyesters with long flexible side chains as a consequence of their ability to form thermotropic liquid crystalline phases[35-63]. The synthesized polymers reported in the literature[35-63] are listed in Figure 1-2. The most interesting result is that the rigid-rod polyesters with flexible side chains form a characteristic layered structure[37]. These layered structures are characterized by a lateral packing of the aromatic main chains into layers, with the fluid-like alkyl side chains occupying the space between the layers.

The object of this thesis is to systematically clarify the structural details of the layered segregated structure of rigid-rod polyesters with flexible side chains and to estimate the physical properties and phenomena, using different methods, where this structure plays a significant role.

In Chapter II, a series of rigid-rod polyesters with long alkyl side chains, denoted as B-Cn and H-Cn, have been prepared by condensing esters of pyromellitic acid with 4,4'-biphenol and hydroquinone, respectively. The alkyl side chain lengths were varied from hexyl (n=6) to octadecyl (n=18). These polyesters hvve been found to be easily soluble in common

solvents such as chloroform and tetrahydrofuran.

In Chapter III, we have analyzed in detail the thermotropic phase behavior and the mesophase structures of B-Cn polyesters. The results will be discussed as a function of side chain length. In this chapter, we would discuss the driving force for the formation of such a layered structure on the point of segregation between the aromatic main chains and aliphatic side chains. Moreover, the classification of layered mesophases is proposed on consideration of the positional order in the aromatic layers.

In Chapters IV, we have analyzed in detail the thermotropic phase behavior and the mesophase structures of H-Cn polyesters. The results will be discussed as a function of side chain length. In this chapter, we would discuss polymoph of H-Cn polyesters as a function of side chain length. The driving force for the formation of such a structure is thought of as the segregation between the aromatic main chains and aliphatic side chains.

In Chapter V, the main chain and side chain conformations in the layered crystals and mesophases of B-Cn polyesters are discussed based on the measurements from high resolution solid state ^{13}C NMR. Furthermore, an attempt has been made to interpret these spectra and estimate the polymer conformation by looking into the ^{13}C NMR shielding constants and performing total energy calculations using the FPT (finite perturbation theory) method within the INDO framework. This work makes it clear that the aromatic main chains take up anomal and confined conformations caused by the monolayer packing between layers of the aliphatic side chains.

In Chapter VI, the main chain and side chain conformations in the various segregated structures of H-Cn polyesters are discussed using high resolution solid-state ^{13}C NMR measurements. The behavior of the main chain conformation was elucidated from the observed ^{13}C NMR chemical shifts and calculations of the ^{13}C NMR shielding constant using the FPT method within INDO framework. In this study, a correlation between the chain conformation and the segregation of aromatic main chains and aliphatic side chains has been discussed.

In chapter VII, the state of interchain aggregation in the layered crystals

and mesophases of B-Cn polyesters is discussed from the fluorescence measurement as a function of temperature. In these layered crystalline and mesophases, charge transfer complexes between the adjacent main chains in the layers were found to be formed.

In chapter VIII, the state of interchain aggregation in the layered crystals and mesophases of H-Cn polyesters has again been discussed from the fluorescence measurement as a function of temperature. In these layered crystalline and mesophases, charge transfer complexes are also found to be formed between the adjacent main chains in the layers. Moreover a change in the charge transfer complexes was observed at the phase transition.

The concluding remarks of this dissertation will be summarized in the Chapter VIIII.

References and Notes

(1) Reinitzer,F. Monatscch Chem. 1888, **9**, 421.

(2) Lehmann,O. Z.Physikal. Chem. 1989, **4**, 462.

(3) Demus, D.; Demus,H.; Zaschko,H.(1974), Demus, D.; Zascheko,H.(1984) Flussige Kristalle in Tabellen, VEb. Deutscher Verlag fur Grundstoffindustrie, Leipzig.

(4) Friedel,G. Ann.Physique 1922, **18**, 273.

(5) Chistyakov,I.G.; Chaikovski, W.M. Mol.Cryst.Liq.Cryst. 1969, **7**, 269.

(6) de Vries,A. Mol.Cryst.Liq.Cryst. 1970, **10**, 219.

(7) Stewart,G.W. Discussions of Faraday Soc., 1933. p982.

(8) Birgeneau,R.J.; Litster,J.D. J.de Physs.Lett. 1969, **39**, 399.

(9) Pindak ,R.; Moncton ,D.E.; Davey ,S.C.; Goodby, J.W. Phys.Rev.Lett. 1981, **46**, 1135.

(10) Diele,S.; Brand,P.; Sackmann,H. Mol.Cryst.Liq.Cryst. 1972, **17**, 163.

(11) Tardieu,A.; Billard,J. J.Phys. (France) Colloq. 1976, **37**, C3-79.

(12) Etherington,G.; Leadbetter,A.J.: Wang,X.J.; Gray,G.W.; Tajbaksh,A. Liq.Cryst. 1986, **1**, 209.

(13) Chandrasekhar,S.; Sadashiva,B.K.; Suresh,K.A. Pramana 1977, **9**, 471.

(14) a)Levelut,A.M. J.Chem.Phys. 1983, **88**, 149. b) Destrade,C.; Fooucher,P.; Gasparoux,H.; Tinh,n.H.; Levelut,A.M.; Malthete,J. Mol.Cryst.Liq.Cryst. 1984, **106**,121. c) Chandrasekhar,S Adavances in Liquid Crystals, **Vol.5** (Ed. Brown,G.H.) p.47, Academic, New York (1982). d) Chandrasekhar,S. Phil. Trans. Roy.Soc. London 1983, **A309**, 93. e) Chandrasekhar,S.; Ranganath,G.S. Rep.Prog.Phys. 1990, **53**, 57.

(15) a) Giroud-Godquin,A.M.; Billard,J. Mol.Cryst.Liq.Cryst. 1981, **66**, 147.b)Ohta,K.;Muroki,H.;Takagi,A.;Hatada,K.;Ema,H.;Yamamoto,I.; Matsuzaki,K. Mol.Cryst.Liq.Cryst. 1986, **140**, 131. c) Ribeiro,A.C.; Martin,A.F.; Giroud-Godwin,A.M. Mol.Cryst.Liq.Cryst. Lett. 1988, **5**, 133.

(16) a)Blumstein,A. (ed) Liquid Crystalline Order in Polymers, Academic, New York (1978). b)Finkelmann,H.; Koldehoff,J.; Ringsdorf,H. Angew.Chem. Int.Ed.Engl. 1978, **17**, 935. c) Kostromin,S.G.;

Sinitzyn,V.V.;Talroze,R.V.;Shibaev,V.P.;Plate,N.A.Macromol.Chem. Rapid Commun. 1982, **3**, 809. d) Ringsdorf,H.; Schneller,A. Macromol.Chem.Rapid Comun. 1982, **3**, 557. e) Ciferri,A.; Krigbaum,W.R.; Meyer,R.B. (Eds.) Polymer Liquid Crystals, Academic, New York (1982). f) Samulski,E.T. Physics Today 1982, **35**, 40.

(17) a)Watanabe,J.; Hayashi,M. Macromolecules 1988, **21**, 278.;1989, **22**, 4083. b) Watanabe,J.; Hayashi,M.; Kinoshita,S.; Niori,T. Polym.J. 1992, **24**, 597. c)Watanabe,J.; Kinoshita,S.J.Phys.II France 1992, **2**, 1237. d)Watanabe,J.; Komura,H.;Niori,T. Liq.Cryst. 1993,**13**,455. e) Watanabe,J.; Hayashi,M.; Morita,A.; Niori,T. Mol.Cryst.Liq.Cryst. 1994, **254**, 221. f) Niori,T.; Adachi,S.; Watanabe,J. Liq.Cryst. 1995, **19**,139. g)Watanabe,J.; Hayyashi,M.; Morita,A.; Tokita,M. Macromolecules 1996 in press. h)Tokita,M.; Takahashi,T.; Hayashi,M.; Inomata,K.; Watanabe,J. Macromolecules 1996, in press.

(18) a)Watanabe,J.; Nakata,Y.; Shimizu,K. J.Phys.II Fance 1994, **4**, 581. b)Nakata,Y.; Watanabe,J. J.Mater.Chem. 1994, **4(11)**,1699.

(19) Onsager,L. Ann.M.Y.Acad.Sci., 1949, **51**, 627.

(20) Flory,P.J. Proc.R.Soc.London,Ser. 1956, **234**, 60.

(21) Grosberg,A.Y.; Khokhlov Adv.Polym.Sci. 1981, **41**, 53.

(22) Odijk,T. Macromolecules 1986, **19**, 2313.

(23) Livolant, F.; Bouligand, Y. J.Phys. 1986, **47**, 1813.

(24) Lee, S.; Meyer,R.B. Liq.Cryst. 1990, **7**, 451.

(25) Watanabe, J.; Ono, H.; Uematsu, I.; Abe, A. Macromolecules 1985, **18**, 2141.

(26) Watanabe, J.; Takashina, Y. Macromolecules 1991, **24**, 3423.

(27) Watanabe, J.; Takashina, Y. Polym. J. 1992, **24**, 709.

(28) Yamagishi, T.; Fukuda, T.; Miyamoto, T.; Yakoh, Y.; Watanabe, J. Mol. Cryst. Liq. Cryst. 1990, **7**, 155.

(29) Yamagishi, T.; Fukuda, T.; Miyamoto, T.; Yakoh, Y.; Takashina, Y.; Watanabe, J. Liq. Cryst. 1991, **10**, 467.

(30) Stzelecka, T.E.; Davidson, M.W.; Rill, R.L. Nature 1988, **331**, 457.

(31) Livolant, F.; Levelut, A.M.; Doucet, J.; Benoit, J.P. Nature 1989, **339**, 724.

(32) Wen, X.; Meyer, R.B.; Casper, D.L. D.Phys.Rev.Lett. 1989, **63**,2760.
(33) Kimura, H.; Tsuchiya, M.; J.Phys.Soc.Jpn., 1990, **59**, 3563.
(34) Frenkel, D. Liq.Cryst. 1989, **5**, 929.
(35) Ballauff, M. Macromol. Chem., Rapid Comun. 1986, **7**, 407.
(36) Ballauff, M. Angew. Chem., Int. Ed. Engl. 1987, **28**, 253.
(37) Ballauff, M.; Schmidt, G. F. Mol.Cryst.Liq.Cryst. 1987, **147**, 163.
(38) Stern, R.; Ballauff, M.; Wegner, G. Macromol. Chem., Macromol. Symp. 1989, **423**, 373.
(39) Rodrigues-Parada, J. M.; Duran, R.; Wegner, G. Macromolecules 1989, 22, 2507.
(40) Ebert, M.; Herrmann-Schenherr, O.; Wendorf, J.; Ringsdorf, H.; Tschirner, P. Liq. Cryst. 1990, **7**, 63.
(41) Adam, A.; Spiess, H. W. Macromol. Chem., Rapid Comun. 1990, **11**, 249.
(42) Frech, C. H.; Adam, A.; Falk, U.; Boeffel, C.; Spiess, H. W. New Polym. Mater. 1990, **2**, 267.
(43) Stern, R.; Ballauff, M.; Lieser, G.; Wegner, G. Polymer 1991, **32**, 2079.
(44) Harkmess, B. R.; Watanabe, J. Macromolecules 1991, **24**, 6759.
(45) Watanabe, J.; Harkness, B. R.; Sone, M. Polym. J. 1992, **24**, 1119.
(46) Cervinka, L.; Ballauff, M. Colloid Polym. Sci. 1992, **270**, 859.
(47) Sone, M.; Harkness, B. R.; Watanabe, J.; Torii, T.; Yamashita, T.; Horie, K. Polym. J. 1993, **25**, 997.
(48) Galda, P.; Kistner, D.; Martin, A.; Ballauff, M. Macromolecules 1993, **26**, 1595.
(49) Marz, K.; Lindner, P.; Urban, J.; Ballauff, M.; Fisher, E. W. Acta Polym. 1993, **44**, 139.
(50) Damman, S. B.; Mercx, F. R. P.; Kootwijk-Damman, C. M. Polymer 1993, **34**, 1891.
(51) Damman, S. B.; Mercx, F. P. M. J. Polym. Sci., Polym. Phys. 1993, **31**, 1759.
(52) Damman, S. B.; Mercx, F. P. M. J.; Lemstra, P. J. Polymer 1993, **34**, 2726.

(53) Damman, S. B.; Vroege, G. J. Polymer 1993, **34**, 2732.
(54) Kakimoto, M.; Orikabe, H.; Imai, Y. ACS Polym. Prep. 1993, **34**, 746.
(55) Steuner, M.; Hortz, M.; Ballauff, M. J. Polym. Sci., Polym. Chem. 1993, **31**, 1609.
(56) Watanabe, J.; Harkness, B. R.; Sone, M.; Ichimura, H. Macromolecules 1994, **27**, 507.
(57) Sone, M.; Harkness, B. R.; Kurosu, H.; Ando, I.; Watanabe, J. Macromolecules 1994, **27**, 2769.
(58) Damman, S. B.; Buijs, J. A. H. M. Polymer 1994, **35**, 2559.
(59) Damman, S. B.; Buijs, J. A. H. M.; van Turnhout, J. Polymer 1994, **35**, 2364.
(60) Buijs, J. A. H. M.; Damman, S..B. J. Polym. Sci.; Polym. Phys. 1994, **32**, 851.
(61) Tiesler,U.; Pulina,T.; Rehahn,M.; Ballauff,M.; Mol.Cryst.Liq.Cryst. 1994, **41**,525.
(62) Voigt-Martin, I. G.; Simon, P.; Bauer, S.; Ringsdorf, H. Macromolecules 1995, **28**, 236.
(63) Voigt-Martin, I. G.; Simon, P.; Yan, D.; Yakimansky, A.; Bauer, S.; Ringsdorf, H. Macromolecules 1995, **28**, 243.

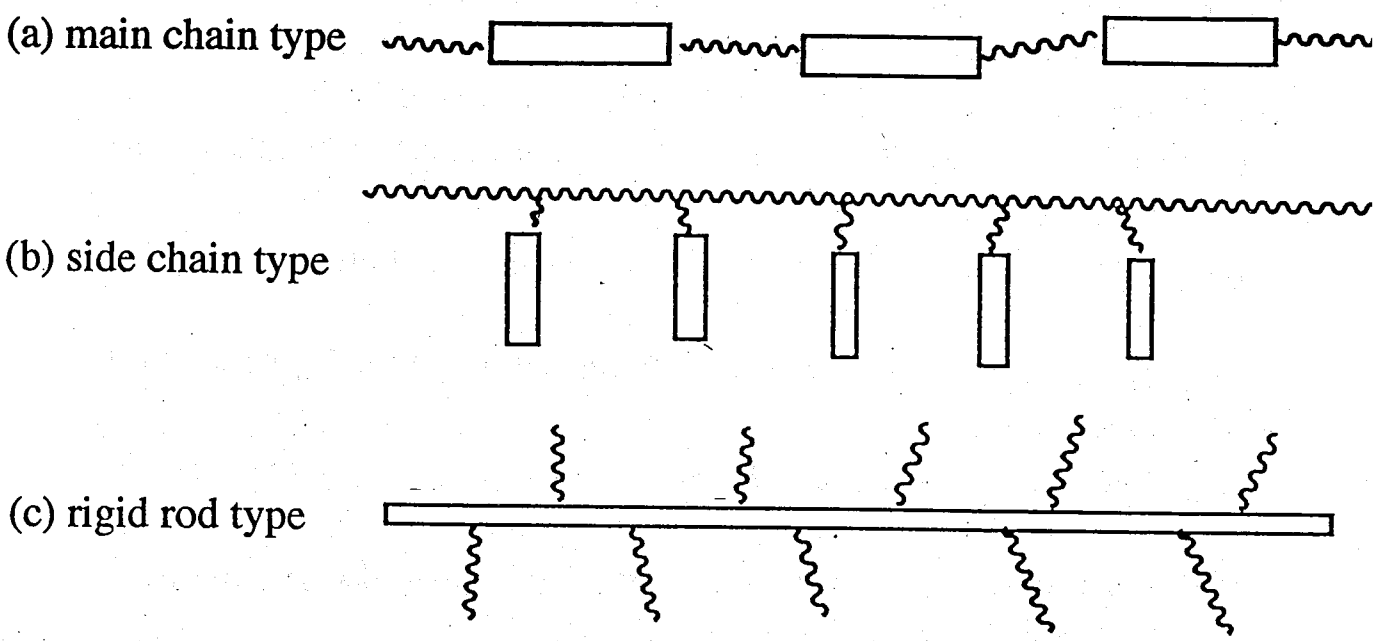

Figure 1-1. Schematic representations of three types of polymeric liquid crystals; (a) main chain type, (b) side chain type and (c) rigid rod type.

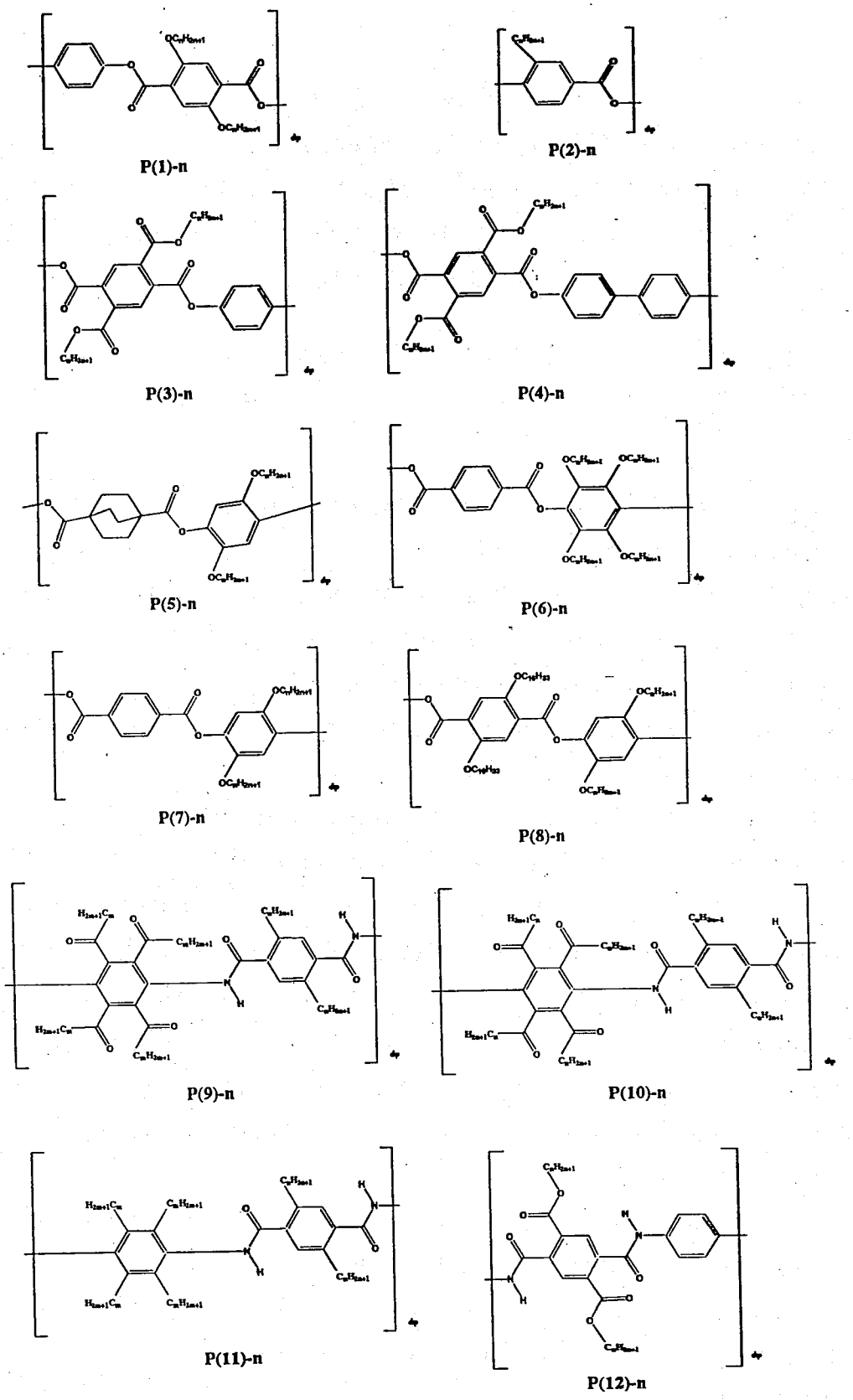

Figure 1-2. Rigid-rod aromatic polymer with flexible side chains as reported previously[35-63].

Chapter 2

Synthesis of Rigid-Rod Polyesters with Flexible Side Chains Based on Condencsation of 1,4-Dialkylesters of Pyromellitic Acid with 4,4'-Biphenol and Hyroquinone.

2-1. Introduction

There have been many reports in the literature concerning the preparation and liquid crystalline properties of rigid-rod polyesters with flexible side chians[1-29]. The objective of these studies has been to develop liquid crystalline materials with lower melting temperatures and greater solubilities than the simple rigid-rod polyesters with no side groups. As a result, not only have these goals been achieved but some very interesting liquid crystalline phases have also been observed.

There has recently been a report in the patent literature[40] concerning the preparation and purification of long-chain dialkyl esters of 1,2,4,5-benzenetetracarboxylic acid (pyromellitic acid). These materials can be prepared as a mixture by the reaction of pyromellitic dianhydride with a long-chain alcohol ($10 < n < 30$, where n denotes the number of carbon atoms in the chain) and then separated by their different solubilities in halogenated organic solvents. Isolation of the pure para isomer would yield a monomer from which several new rigid-rod polyesters with long n-alkyl side chains could be derived.

In this preliminary report we will discuss the liquid crystalline properties of two novel polyesters derived from the para isomer with n-tetradecyl side groups. These new polyesters were prepared as comonomers with hydroquinone and 4,4'-biphenol and are designated as H-Cn and B-Cn, respectively.

2-2 Synthesis

Materials and Methods

Tetrahydrofuran (THF) and toluene were distilled from $LiAlH_4$ prior to use. Triethylamine was distilled from NaH. Pyromellitic dianhydride (1,2,4,5-benzenetetracarboxylic dianhydride; Tokyo Chemical) and 1-hexanol, 1-octanol, 1-decanol, 1-dodecanol, 1-tetradecanol, 1-hexadecanol and 1-octadecanol (Tokyo Chemical) were used without further purification. Hydroquinone and 4,4'-biphenol (Mitsubishi Petrochemical) were obtained with a purity of 99.9 %.

^1H NMR spectra were obtained with a JEOL FX90Q spectrometer at frequency of 90 MHz. DSC measurements were performed on a Perkin-Elmer DSC-II calorimeter at a scanning rate of 10 °C/min. Wide-angle X-ray diffraction patterns of the polymers were recorded using a flat-plate camera mounted to a Rigaku-Denki X-ray generator emitting Ni-filtered Cu-Kα radiation. The temperature of the samples was controlled by placing the samples in a Mettler FP-80 hot stage mounted in the beam path. The film to specimen distance was determined by calibration with silicon powder. Optical microscopic observations of the liquid crystalline textures were made on Olympus BH-2 polarizing microscope equipped with a Mettler FP-80 hot stage.

1,4-Di-(1-tetradecylester) of 1,2,4,5,-Benzenetetracarboxylic Acid.

In a 500-mL round-bottomed flask, equipped with a magnetic stirbar, was placed 20 g (0.092 mol) of pyromellitic dianhydride and 39.3 g (2 mol equiv) of 1-tetradecanol. The flask was sealed with a drying tube, and the contents were slowly heated to 150 °C using an oil bath. After stirring for 45 min at 150 °C, the molten product was cooled, resulting in crystallization of the meta and para dialkyl esters of pyromellitic acid. To the flask was then added 400 mL of acetone, and the mixture was slowly stirred for approximately 12 hours. Filtration of the remaining solid materials yielded the pure para dialkyl ester product. The meta dialkyl ester (which also contained a small amount of the para isomer) could be recovered by

evaporation of the acetone extract. In a second purification step, the para dialkyl ester was washed with 200 mL of methylene chloride for about 3 hours. Filtration and drying of the product gave 18.4 g (31 % yield) of the para dialkyl ester.

The m- and p-di-(1-tetradecyl esters) of 1,2,4,5-benzenetetracarboxylic acid could be prepared as a mixture by reacting pyromellitic dianhydride with 1-tetradecanol at 150 °C. The para isomer was easily isolated from this mixture by taking advantage of the relatively high solubility of the meta isomer in acetone and thus washing the meta isomer away from the sparingly soluble para isomer. In the case of the di-n-tetradecylester, simple washing of the mixture with acetone results in the dissolution of the meta-isomer leaving the insoluble para-isomer that can be isolated by filtration.

This general procedure has been used to generate a series of 1,4-di-n-alkylesters of pyromellitic acid in which the alkyl moiety ranges from hexyl (n = 6) to octadecyl (n = 18). Considering the difference in solubility of the meta-isomer with varying side-chain lengths, the washing solvent had varied somewhat in the series. The different types of washing solvents used, the monomer melting point and the yield is recorded in Table 2-1. For the hexylesters of pyromellitic acid the para-isomer was further purified by recrystallization from toluene.

The purity of the para isomer was determined by ^{1}H NMR spectroscopy. Figure 2-1 shows the 1H NMR spectrum for the p-di-(1-tetradecyl ester) in DMSO-d_6. The signals in the region 0.5-2.0 ppm and at 4.2 ppm can be assigned to the aliphatic protons of the alkyl chain. The signal peak in the aromatic region at 7.9 ppm can be assigned to the two equivalent aromatic protons of the para isomer. The meta isomer shows two peaks in the aromatic region at 8.0 and 8.4 ppm ($CDCl_3$ solvent) that can be attributed to the two nonequivalent aromatic protons.

Diacid Chloride of the 1,4-Di-(1-tetradecyl ester) of 1,2,4,5-Benzenetetracarboxylic Acid.

Into a 50-mL round-bottomed flask, equipped with a magnetic stirbar,

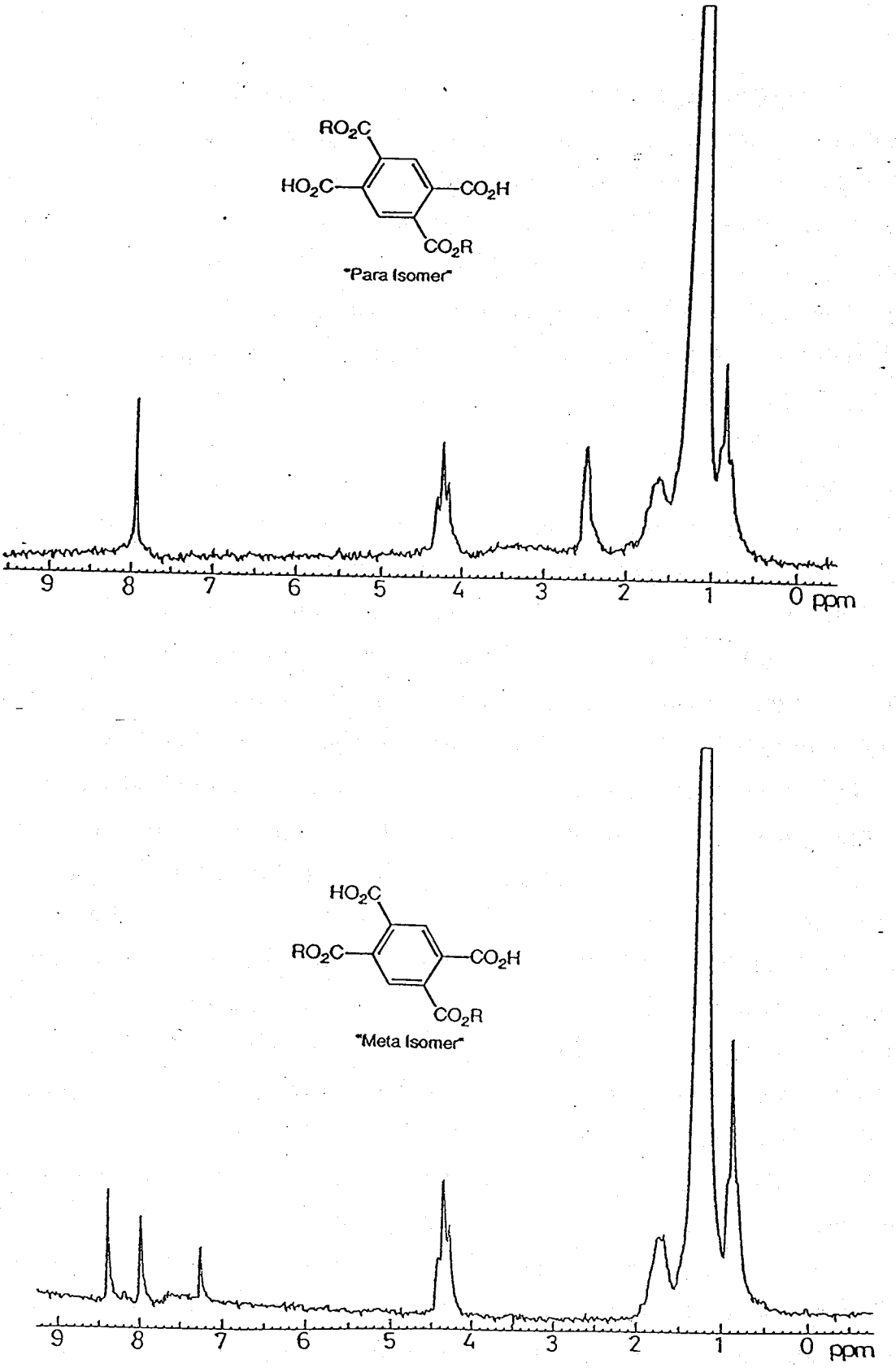

Figure 2-1. ^1H spectra of p-di-(1-tetradecyl esters) of 1,2,4,5-benzenetetracarboxylic acid in the DMSO-d_6 solution (upper) and that of m-isomer in the $CDCl_3$ solution (lower).

was placed 6.83 g (0.0106 mol) of the 1,4-di-(1-tetradecyl ester), 20 mL of THF, and approximately 4 mol equiv of thionyl chloride. The flask was equipped with a condenser and heated to reflux in an oil bath at 80-90 °C. After refluxing for 20 min, the THF and excess thionyl chloride were removed by distillation under reduced pressure. Residual thionyl chloride was removed by adding 10 mL of toluene to the solution and continuing the distillation under vacuum. The diacid chloride product was isolated as a light yellow solid.

Polyester.

In a 100-mL round-bottomed flask equipped with a magnetic stirbar, 1.165 g (0.0106 mol) of hydroquinone was dissolved in 30 mL of THF and slightly more than 2 equiv of triethylamine. In a separate 50-mL flask, exactly 1 mol equiv of the diacid chloride was dissolved in 10 mL of THF. This solution was then added over a period of 1 min to the rapidly stirred hydroquinone solution as it became cloudy due to the formation of triethylamine hydrochloride. In addition, there was a marked increase in solution viscosity as well as an increase in the temperature of the reaction vessel. To ensure complete transfer of the acid chloride, the 50-mL flask was rinsed with about 3 mL of THF and this was added to the reaction flask. The flask containing the polymer solution was then equipped with a condenser and drying tube and heated to reflux using an oil bath. After 30 min the polymer solution was cooled to room temperature and poured into 250 mL of methanol to yield a thin fibrous precipitate. The polymer was purified a second time by reprecipitating in THF solution with a 5-fold excess of methanol. The same procedure was used to prepare the biphenol polyester using biphenol instead of hydroquinone.

The polyesters H-Cn and B-Cn were found to be readily soluble in halogenated solvents such as chloroform and also soluble in THF. The ^{1}H NMR spectrum for the polymer B-C14 is shown in Figure 2-2. The broad signals located at 0.5-2.0 ppm and at 4.4 ppm can be assigned to the alkyl side chains. In the Aromatic region the broad signal located at 7.2-8.0 ppm can be assigned to the protons of the biphenyl moiety. The sharp

signal at 8.4 ppm can be assigned to the two equivalent aromatic protons of the p-alkyl ester component. Some negligible signals are also apparent in the aromatic region (8.1-8.3 ppm), and these may be attributable to end-group protons. The inherent viscosities of the H-C14 and B-C14 polyesters were 0.23 and 0.66 dL/g, respectively, as measured in THF at 25 °C.

The inherent viscosities of the H-Cn and B-Cn polyesters, ηinh, were measured in THF at 25 °C and are listed in the second column of Tables 2-2 and 2-3. All of the H-Cn and B-Cn polyesters prepared for this study were founded to form isotropic melts in the temperature region of 100 °C to 150 °C.

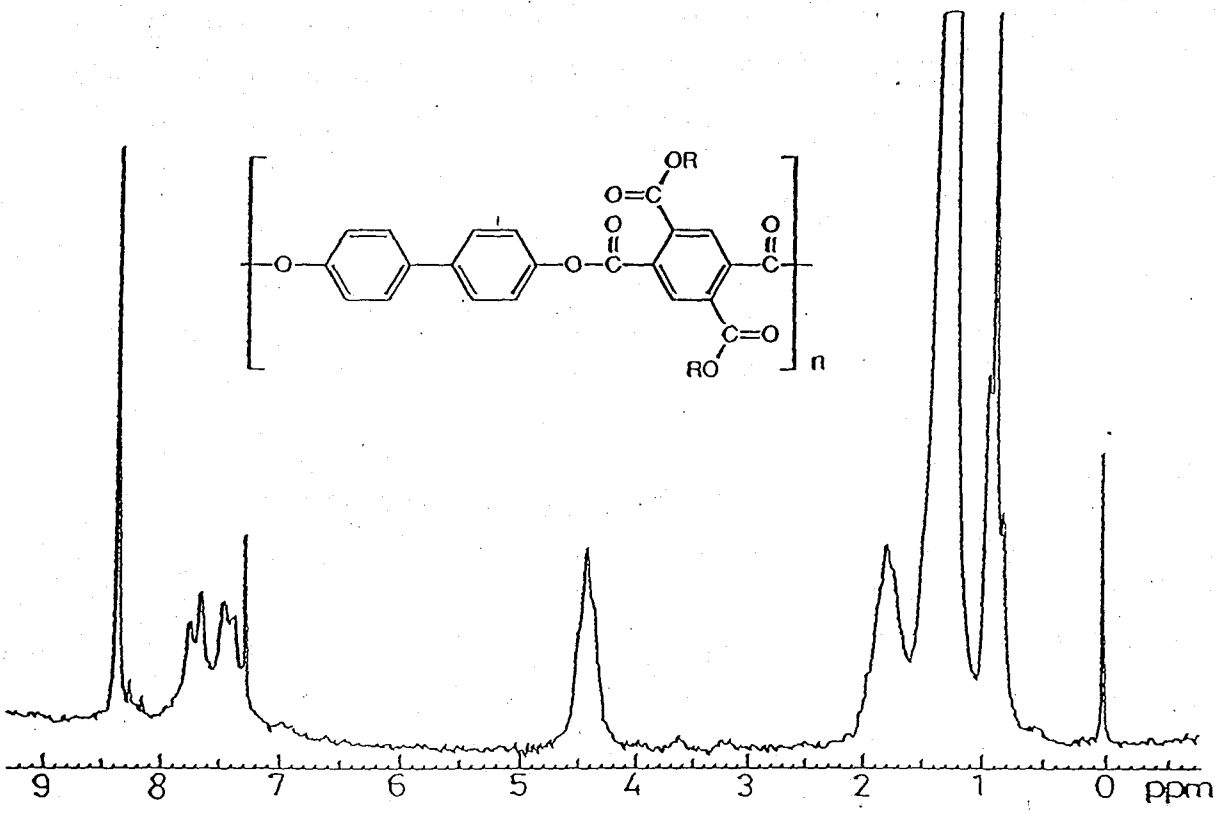

Figure 2-2. A ^{1}H spectrum for B-C14 polyesters in the $CDCl_3$ solution.

Table 2-1
Purification solvent, melting temperature and yields of 1,4-dialkylesters of pyromellitic acid.

1,4-dialkylesters of pyromellitic acid	melting point (°C)	washing solvent	yield (%)
C6	153--155	crystallized from toluene[a)]	34
C8	150--153	CH_2Cl_2	38
C10	150--154	CH_2Cl_2	37
C12	151--155	CH_2Cl_2	44
C14	151--155	Acetone/CH_2Cl_2[b)]	35
C16	153--154	Acetone/CH_2Cl_2[b)]	46
C18	151--153	Acetone/CH_2Cl_2[b)]	47

a) refer to the coment in text.
b) In these cases acetone was sufficient to purify the para isomer from the meta isomer however a second washing was performed to remove residual alcohol.

Table 2-2
Inherent viscosities and transition temperatures for H-Cn polyesters

Polymer	η_{inh}(dl/g)	T_1(°C)	T_2(°C)	T_i(°C)
H-C6	0.28	--	80	132
H-C8	0.38	--	82	124
H-C10	0.39	--	78	103
H-C12	0.57	--	99	128
H-C14	0.23	45	94	149
H-C16	0.31	43	101	146
H-C18	0.26	44	111	124

Transition temperature were recorded for the first heating DSC scans of the THF-cast films.

Table 2-3
Inherent viscosities and transition temperatures for B-Cn polyesters

Polymer	η_{inh}(dl/g)	T_1(°C)	T_2(°C)	T_i(°C)
B-C6	0.42	58	198	232
B-C8	0.59	--	61	190
B-C10	0.57	--	58	160
B-C12	0.71	--	79	164
B-C14	0.66	53	124	165
B-C16	0.49	50	--	126
B-C18	0.52	48	--	128

Transition temperature were recorded for the first heating DSC scans of the THF-cast films.

2-3 Reference and notes

(1) Ballauff, M. Macromol. Chem., Rapid Comun. 1986, **7**, 407.

(2) Ballauff, M. Angew. Chem., Int. Ed. Engl. 1987, **28**, 253.

(3) Ballauff, M.; Schmidt, G. F. Mol.Cryst.Liq.Cryst. 1987, **147**, 163.

(4) Stern, R.; Ballauff, M.; Wegner, G. Macromol. Chem., Macromol. Symp. 1989, **423**, 373.

(5) Rodrigues-Parada, J. M.; Duran, R.; Wegner, G. Macromolecules 1989, **22**, 2507.

(6) Ebert, M.; Herrmann-Schenherr, O.; Wendorf, J.; Ringsdorf, H.; Tschirner, P. Liq. Cryst. 1990, **7**, 63.

(7) Adam, A.; Spiess, H. W. Macromol. Chem., Rapid Comun. 1990, **11**, 249.

(8) Frech, C. H.; Adam, A.; Falk, U.; Boeffel, C.; Spiess, H. W. New Polym. Mater. 1990, **2**, 267.

(9) Stern, R.; Ballauff, M.; Lieser, G.; Wegner, G. Polymer 1991, **32**, 2079.

(10) Harkmess, B. R.; Watanabe, J. Macromolecules 1991, **24**, 6759.

(11) Watanabe, J.; Harkness, B. R.; Sone, M. Polym. J. 1992, **24**, 1119.

(12) Cervinka, L.; Ballauff, M. Colloid Polym. Sci. 1992, **270**, 859.

(13) Sone, M.; Harkness, B. R.; Watanabe, J.; Torii, T.; Yamashita, T.; Horie, K. Polym. J. 1993, **25**, 997.

(14) Galda, P.; Kistner, D.; Martin, A.; Ballauff, M. Macromolecules 1993, **26**, 1595.

(15) Marz, K.; Lindner, P.; Urban, J.; Ballauff, M.; Fisher, E. W. Acta Polym. 1993, **44**, 139.

(16) Damman, S. B.; Mercx, F. R. P.; Kootwijk-Damman, C. M. Polymer 1993, **34**, 1891.

(17) Damman, S. B.; Mercx, F. P. M. J. Polym. Sci., Polym. Phys. 1993, **31**, 1759.

(18) Damman, S. B.; Mercx, F. P. M. J.; Lemstra, P. J. Polymer 1993, **34**, 2726.

(19) Damman, S. B.; Vroege, G. J. Polymer 1993, **34**, 2732.

(20) Kakimoto, M.; Orikabe, H.; Imai, Y. ACS Polym. Prep. 1993, **34**, 746.

(21) Steuner, M.; Hortz, M.; Ballauff, M. J. Polym. Sci., Polym. Chem. 1993, **31**, 1609.
(22) Watanabe, J.; Harkness, B. R.; Sone, M.; Ichimura, H. Macromolecules 1994, **27**, 507.
(23) Sone, M.; Harkness, B. R.; Kurosu, H.; Ando, I.; Watanabe, J. Macromolecules 1994, **27**, 2769.
(24) Damman, S. B.; Buijs, J. A. H. M. Polymer 1994, **35**, 2559.
(25) Damman, S. B.; Buijs, J. A. H. M.; van Turnhout, J. Polymer 1994, **35**, 2364.
(26) Buijs, J. A. H. M.; Damman, S. B. J. Polym. Sci.; Polym. Phys. 1994, **32**, 851.
(27) Tiesler,U.; Pulina,T.; Rehahn,M.; Ballauff,M.; Mol.Cryst.Liq.Cryst. 1994, **41**,525.
(28) Voigt-Martin, I. G.; Simon, P.; Bauer, S.; Ringsdorf, H. Macromolecules 1995, **28**, 236.
(29) Voigt-Martin, I. G.; Simon, P.; Yan, D.; Yakimansky, A.; Bauer, S.; Ringsdorf, H. Macromolecules 1995, **28**, 243.
(30) Kamikita, M.; Awaji, H. Jpn. Kokai Tokkyo Koho JP 63,275-546 (88,275,546).

Chapter 3

Thermotropic Behavior and Phase Structure of Rigid-Rod Polyesters with Flexible Side Chains Based on 1,4-Dialkylesters of Pyromellitic Acid and 4,4'-Biphenol.

3-1 Introduction

There have been several recent reports in the literature on the preparation and the physical properties of rigid-rod polymers with long alkyl side chains[1-29]. The most interesting property of these materials is the ability to form layered structures in crystals and liquid crystals when the alkyl side chains reach a critical length. The α-helical poly(γ-alkyl L-glutamate)[30] were the first examples of this type of material, and more recently, aromatic polyesters and polyamids with long alkyl side chains have also been examined[1-29]. The layered phases are characterized by a segregated structure in which the rigid-rod main chains are packed into a layered structure, with the flexible side chains occupying the space between the layers. The formation of the layered structures is therefore not only due to main chain stiffness but also due to the binary molecular structure.

In this study, we have prepared a series of B-Cn polyesters in which the alkyl side chain length ranges from 6 to 18 carbon atoms and analyzed, in detail the thermotropic phase behavior and the mesophase structures. The results will be discussed as a function of side chain length.

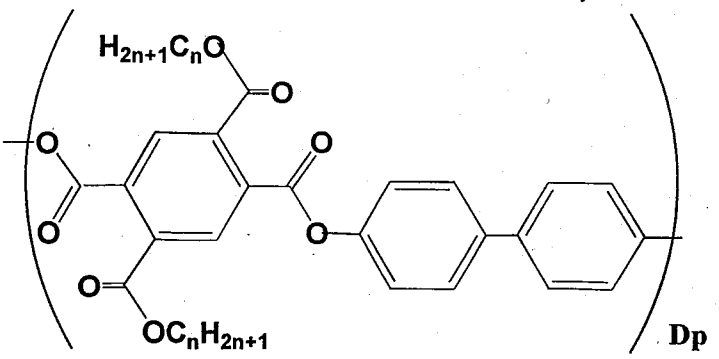

3-2 Experimental Section

Materials and Methods. The synthesis and characterization of the 1,4-dialkyl ester of pyromellitic acid has been described in Chapter II. The B-Cn polymers with n = 6-18 were prepared by converting the 1,4-dialkyl esters of pyromellitic acid to their respective diacid chlorides followed by condensation with 4,4'-biphenol. The inherent viscosities of these polymers are listed in the second column of Table 3-1.

DSC measurements were performed with Perkin-Elmer DSC II calorimeter at a scanning rate of 10 °C/min. Wide angle X-ray diffraction patterns of the polymers were recorded with a flat-plate camera mounted to a Rigaku-Denki X-ray generator emitting Ni-Filtered Cu Kα radiation. The temperature of the samples was controlled by placing them in a Mettler FP-80 hot stage mounted in the beam path. The film to specimen distance was determined by calibration with silicon powder. Optical microscopic observations of the liquid crystalline texture were made with an Olympus BH-3 polarizing microscope equipped with a Mettler FP-80 hot stage. ^{13}C CP/MAS NMR spectra were measured by means of a JNM-GX270 NMR (67.5 MHz) with a variable-temperature (VT) CP/MAS accessory. The sample (ca. 200 mg) was contained in a cylindrical rotor made of ceramic materials and spun at 4.0 kHz. The contact time was 2.0 ms with a repetition time of 5.0 s.

3-3 Results and discussion

Phase Behavior of B-Cn Polyesters The B-Cn polymers were all readily soluble in organic solvents such as THF and chloroform, and from these solutions fine thin films could be prepared by casting. Microscopic observation of these films on heating showed two transitions. At the first transition, T1, the solid crystalline phase changed to the fluid liquid crystalline phase, and at the transition, T1, the materials enter the isotropic phase. This transition behavior was also observed from the DSC transition temperatures on heating. They are listed in the third column of Table 3-1. The transition temperatures as determined by these two methods roughly correspond to each other although another DSC transition can be observed at around 50 °C for the B-C14, B-C16 and B-C18 polyesters (see curve a of Figure 3-1). This latter transition may not represent a thermodynamically stable state as it disappears on annealing at 80 °C. The transition temperatures recorded by both methods are plotted against n in Figure 3-2a, in which the open and closed circles are based on DSC and microscopic measurements, respectively. From this figure, one can observe that on heating the isotropization temperatures, Ti, decrease rapidly as n is increased from 6 to 10 but level off for the B-C10, B-C12 and B-C14 polyesters before falling somewhat again for the B-C16 and B-C18 polyesters. Similarly, the melting temperature of the crystal, T1, decreases but more substantially than Ti when n is increased from 6 to 10. With a further increase of n, Ti increases again and levels off for B-C14, B-C16 and B-C18. As a result, the liquid crystalline phase appears over a wide temperature range for the B-Cn polyesters that have side chains of an intermediate length.

The phase behavior observed on cooling is also shown in Figure 3-2b. The transition temperatures from the isotropic to liquid crystal phase are slightly lower than those observed on heating. An interesting point of this observation is that the B-C14, B-C16 and B-C18 polyesters show a new second transition (T2 transition) in the temperature region from 90 to 100 °C (refer to curve b in Figure 3-1). This can be interpreted as resulting

from a transition of one type of liquid crystal to another (i.e., a liquid crystal to liquid crystal transition) and will be described in greater detail later. The DSC cooling scans for the B-C8, B-C10 and B-C12 polyesters were relatively featureless, showing only a single phase transition from the isotropic to liquid crystal phase.

The liquid crystal to crystal transition has not been observed for the specimens with the exception of the B-C6 polyester when observed at a normal cooling rate of 10 °C/min. This can be thought of as to a greater degree of difficulty in forming crystallites from the longer side chain derivatives. Therefore, on cooling the B-C8, B-C10 and B-C12 polyesters to room temperature the liquid crystalline phase is retained and frozen. Also for the B-C14 and B-C16 and B-C18 polyesters, the liquid crystalline phase is frozen, but in these cases the side chains can crystallize at temperatures lower than 50 °C (see curves b and c in Figure 3-1). Reheating and recooling these materials gave phase transitions as shown in Figure 3-2b.

It should be noted here that these materials when cooled from the isotropic melt can be crystallized by annealing at around 80 °C for an extended period of time, although fairly prolonged annealing for 1 or 2 weeks is necessary for well developed crystallization to occur. The transition behavior of these annealed materials was found to be virtually identical to those observed for the cast films.

The phase behavior of the polyesters is, therefore, quite sensitive to their thermal history, which can be explained on the fact that kinetic factors lead to show crystal growth. We can also conclude that all specimens have the ability to form one type of liquid crystal (LC-1) whereas the B-C14, B-C16 and B-C18 polyesters can form an additional liquid crystal (LC-2) in the lower temperature region of LC-1. A comparison of parts a and b of Figure 3-2 reveals that the LC-1 is enantiotropic whereas the LC-2 is more like monotropic in nature. The isotropization enthalpy of LC-1 is about 0.15 kcal/(mol of repeat unit) and the enthalpy for the LC-1 to LC-2 transition is about 0.1 kcal/(mol of repeat unit).

Crystal Structure of B-Cn Polyesters At this point we will focus on the crystal structure of the B-Cn polyesters. Since the crystal structure obtained for both the as cast and annealed specimens is virtually identical, the X-ray diffraction pattern was examined for an oriented crystalline fiber which was spun from the isotropic melt and subsequently annealed at 80 °C for 2 weeks. Parts a and b of Figure 3-3 show the oriented crystalline patterns for the B-C6 and B-C18 polyesters, respectively. The diffraction pattern includes a number of layer line reflections as well as equatorial reflections, indicating that the crystal structure has three-dimensional order. The three-dimensional crystal lattice is obviously triclinic; however, a precise determination of the structure has so far not been performed successfully. Hence, we shall refer to the two-dimensional lattice projected along the polymer chain axis, which can be elucidated from the equatorial reflection profiles.

As listed in Table 3-2, the equatorial reflections include a series of h00 reflections. In addition, several other h10 reflections were observed. These reflections can result in a rough determination of the two-dimensional lattice structure (this is evident on comparing the observed and calculated values in parts a and b of Figure 3-4, with lattice constants of a = 10.0 Å, b = 4.55 Å and $\gamma = 103.1°$ for B-C6 and a = 23.1 Å, b = 3.46 Å and $\gamma = 94.0°$ for B-C18, respectively. Within these lattices, it is easy to show that the molecules adopt a layered structure in which the aromatic main chains are packed into a layer with a lateral spacing of b and the side chains occupy the space between layers separated by a sin γ. The main chains in the layer assume a fully extended conformation with a repeat length of 16.6 Å caluculated from the height (1/16.6 $Å^{-1}$) of the first layer line from the equatorial line.

The two-dimensional lattices were also determined for the other annealed fiber specimens. The layer spacing, a sin γ, and the molecular distance within a layer, b, is plotted against n in Figure 3-5. In this case data for the B-C10 polyesters is not included because of difficulty in obtaining a crystalline sample. The point to be noted here is that same value of around 4.6 Å is observed for the b axis in the shorter side chain B-Cn

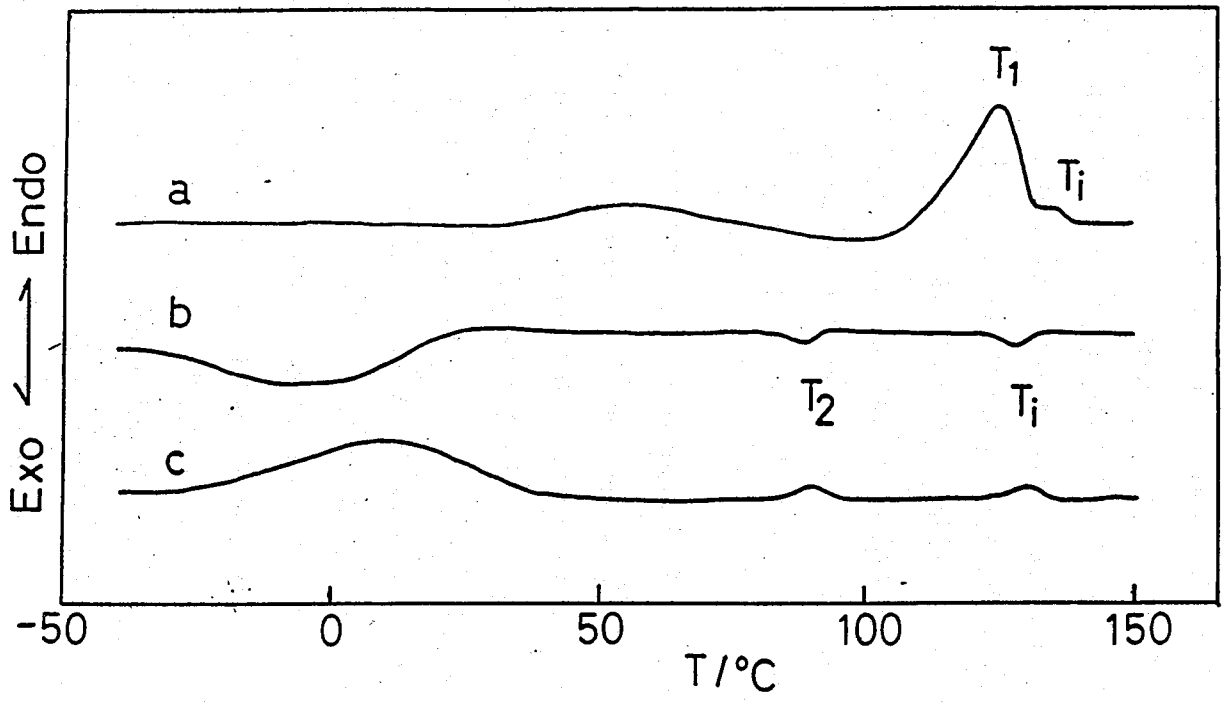

Figure 3-1. DSC thermograms of the B-C16 cast film observed on (a) first heating, (b) first cooling and second cooling.

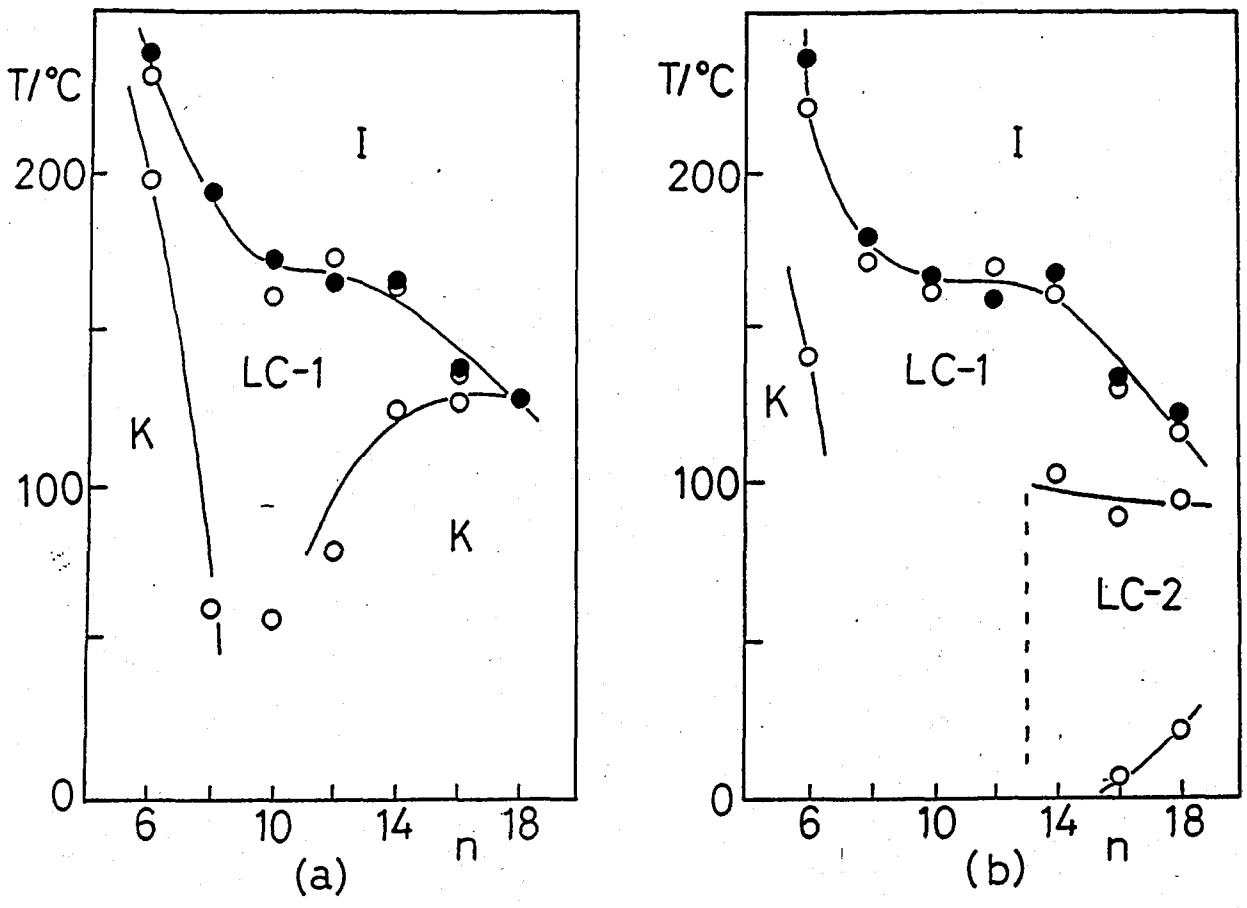

Figure 3-2. Variation of the transition temperatures with n (the number of carbon atoms in the alkyl side chain) as observed on (a) the first heating of as cast films and (b) cooling. The open circles are based on DSC thermograms and the closed circles are based on microscopic observations.

Table 3-1
Characteization for B-Cn polyesters

		heating			cooling		
Polymer	η_{inh}(dl/g)	T1(°C)	T2(°C)	Ti(°C)	Ti(°C)	T2(°C)	T1(°C)
B-C6	0.42	58	198	232	222	---	140
B-C8	0.59	--	61	190	172	---	30
B-C10	0.57	--	58	160	154	---	---
B-C12	0.71	--	79	164	168	---	---
B-C14	0.66	--	124	165	160	103	(-5)*
B-C16	0.49	50	--	126	160	89	(5)*
B-C18	0.52	48	--	128	129	94	(20)*

*These transition may be due to the crystalization of side chains (see the text).

Table 3-2
X-ray Data for the equatorial reflections observed
for B-C6 and B-C18 fibers

B-C6				B-C18			
dobsd(Å)		hk0	dcalcd*(Å)	dobsd(Å)		hk0	dcalcd*(Å)
9.73	vs	100	9.76	23.1	vs	100	23.0
4.88	s	200	4.88	11.5	s	200	11.5
4.48	s	110	4.43	7.68	m	300	7.68
3.73	vs	210	3.73	5.76	w	400	5.76
2.97	w	310	2.96	4.62	vw	500	4.61
2.36	vw	410	2.38	3.45	m	010	3.45
				3.40	m	110	3.38
				3.27	w	210	3.24
				3.06	vw	310	3.06
				2.87	vw	10	2.87

*Indeces and dcalcd are based on the unit cells cited in the text.

polyesters (B-C6, B-C8 and B-C12), whereas the longer side chain B-C14, B-C16 and B-C18 polyesters exhibit a fairly small value of 3.45 Å. This difference in the lateral packing distance is also reflected in the layer spacing. a sin γ, as it varies along the different lines with the side chain length, n, as found in Figure 3-5. Thus, the main chain packing within the layer appears in a different manner in the two series. This in turn indicates that the main chains must assume different conformations. The structure with the short spacing of 3.45 Å is particularly interesting since this distance corresponds to the van der Waals radius of the phenyl ring, and as a result this requires an unusual main chain conformation, with the aromatic rings forced to have a coplanar arrangement[31]. In fact, recent studies by solid-state ^{13}C NMR and Raman spectroscopies support such a peculiar conformation, the results of which will be reported in Chapter V.

The side chains located in the space between the main chain layers are also essentially in a crystalline form, and this could be studied by solid state ^{13}C NMR spectroscopy[32-35]. Figure 3-6 shows the spectra for the B-C18 crystal as observed in the range of 0-80 ppm, the signals of which can be assigned to the carbons of the alkyl side chain. The spectra of the LC-2 and isotropic phases are also shown in the same figure. The values of the chemical shifts for the peaks together with their assignment are listed in Table 3-3. The peaks in the vicinity of 30 ppm can be assigned to the interior CH_2 carbons and have been used to discuss the conformation and/or crystal structure of the alkyl chains. From reference data on n-alkanes and polyethylene, peak I at 34.2 ppm appears from the CH_2 carbons in an all-trans zigzag conformation in the crystalline phase and peak A at 30.1 ppm appears from the carbons in a noncrystalline state. The crystalline phase of B-C18, obviously, shows an intense peak I and a small peak A, indicating that some parts of the side chain are in a noncrystalline state. In contrast, the liquid crystalline and isotropic phases show only a peak A, indicating that they include just noncrystalline side chains.

Structure of Liquid Crystal-2 (LC-2) Phase LC-2 is a monotropic liquid crystal and appears on cooling the B-C14, B-C16 and B-C18 polyesters

(refer to Figure 3-2b). The viscosity of this phase is fairly high and so no characteristic optical texture could be detected. The X-ray diffraction pattern for the oriented LC-2 phase of B-C18 is shown in Figure 3-7a. The pattern includes several characteristic sharp reflections although the number of reflections have been reduced to a great extent as compared to the crystal diffraction pattern of Figure 3-3b. In the small angle region, two sharp equatorial reflections indexed by 100 and 200 were observed with spacings of 25.0 and 12.4 Å, respectively. In addition, two sharp meridional reflections with spacings of 16.6 (001) and 8.30 Å (002) were also observed. The weak 101 reflection also appears with a spacing of 13.9 Å. In the wide angle region, broad arcs with a spacing of 4.5 Å could be observed. This diffraction pattern is also typical of the LC-2 phase formed by B-C14 and B-C16. The X-ray data are listed in Table 3-4, and the spacings of the 100 reflections are plotted as closed circles against n in Figure 3-8.

It should be noticed that the spacing of the equatorial reflection approximates to that of the crystalline phase, indicating that the mesophase also assumes a layered structure. A 16.6 Å meridional reflection reveals that the main chains still assume a fully extended conformation as in the crystalline phase. The intensity of this reflection as well as the appearance of the second-order reflection indicates that there is a positional order along the chain axis in each layer. From the observation of the 101 reflection, the positional order may be more or less correlated between adjacent layers. The lack of a 010 reflection is characteristic of this mesophase and indicates that there is disorder in the lateral packing of the main chains. The ^{13}C NMR spectra, as mentioned above, demands that the side chains located between the layers must be disordered. These two latter facts as well as the fluidity of this phase undoubtedly differentiate this layered phase from the layered crystalline phase and give its liquid crystalline nature. An illustration of the layered structure in this mesophase is given in Figure 3-9.

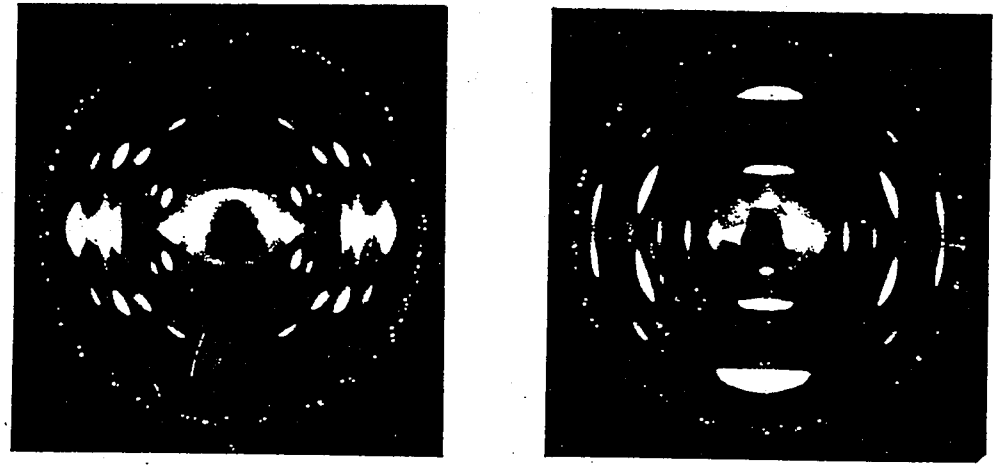

Figure 3-3. Oriented X-ray patterns of (a) B-C6 and (b) B-C18 crystalline fibers (see the text). Here, the fiber axis is oriented in the vertical direction.

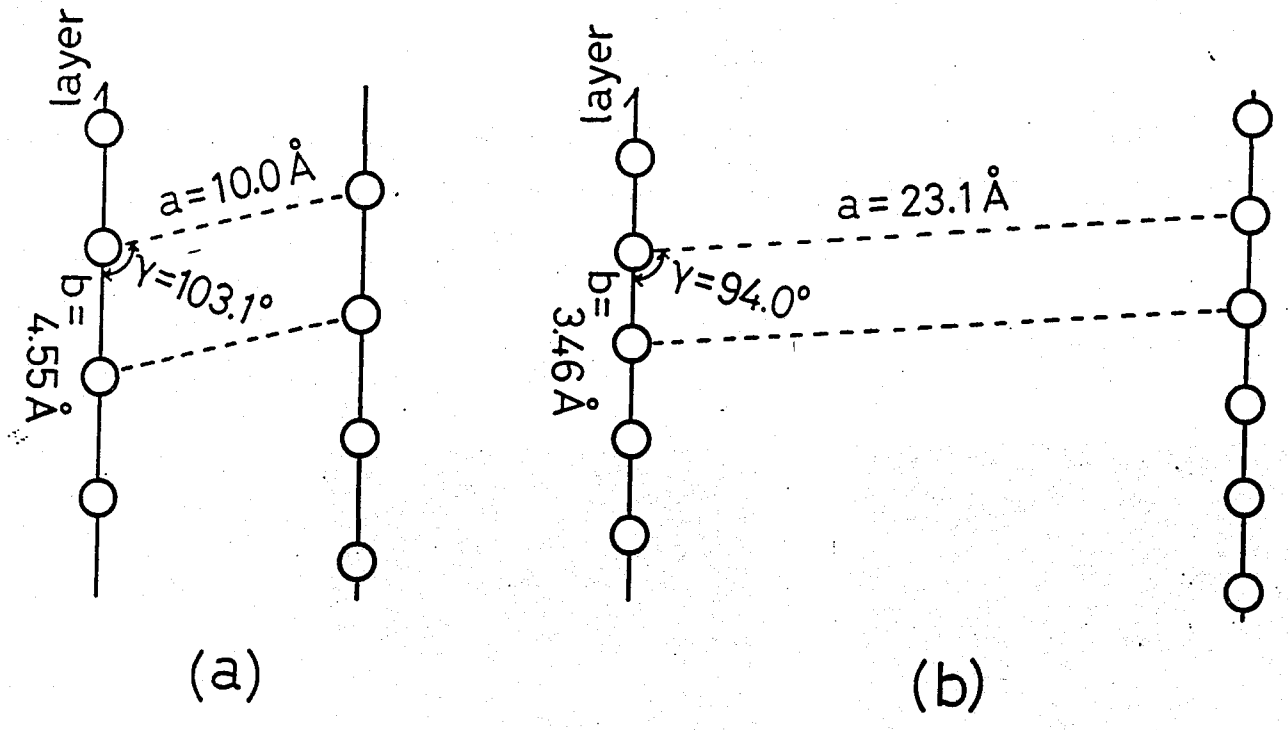

Figure 3-4. The two-dimensional lattices of (a) B-C6 and (b) B-C18 as elucidated from the equatorial reflections of the oriented X-ray pattern of Figure 3-3. The open circles in the layers indicate the position of the aromatic main chains.

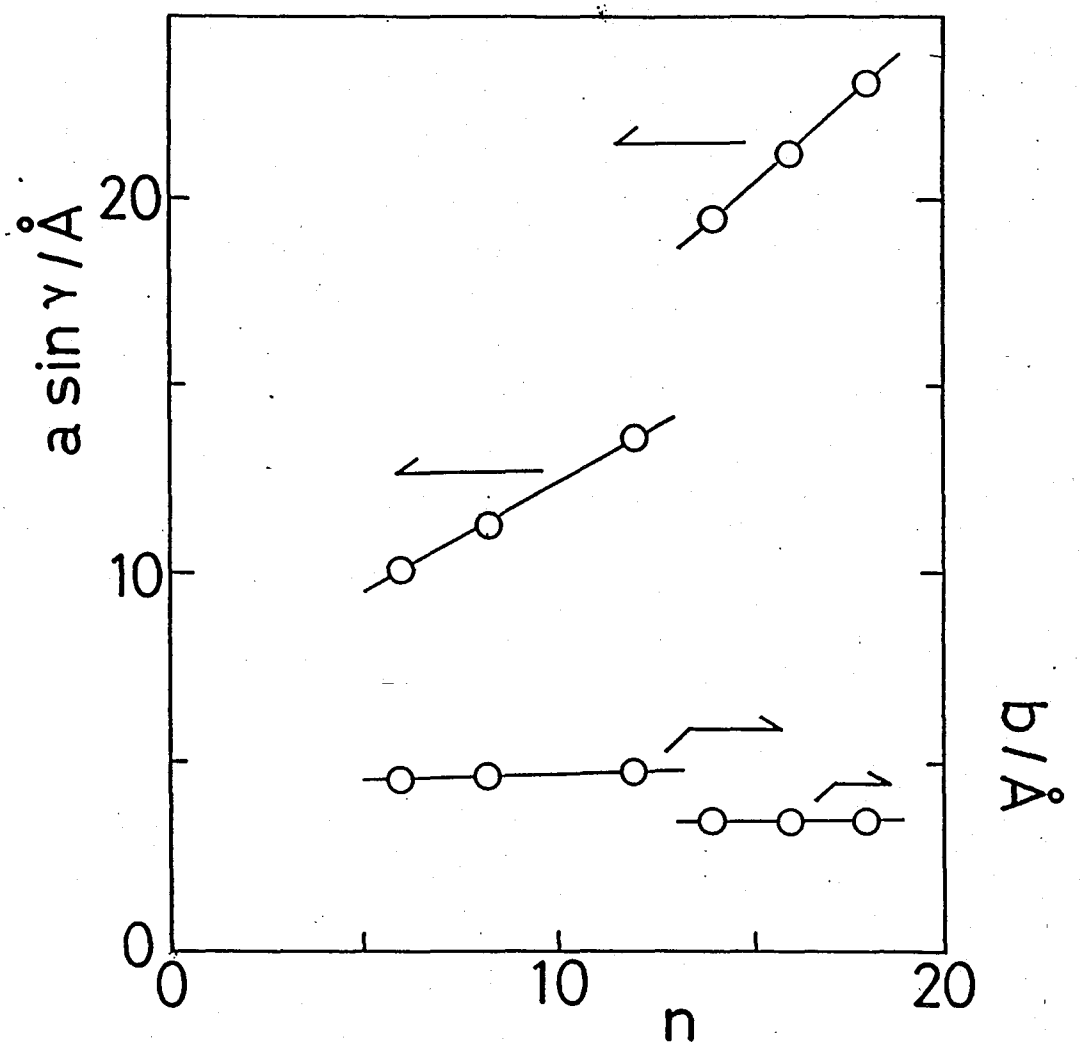

Figure 3-5. Variation of a sin γ and b (in the two-dimensional lattices) as a function of n (refer to Figure 3-4).

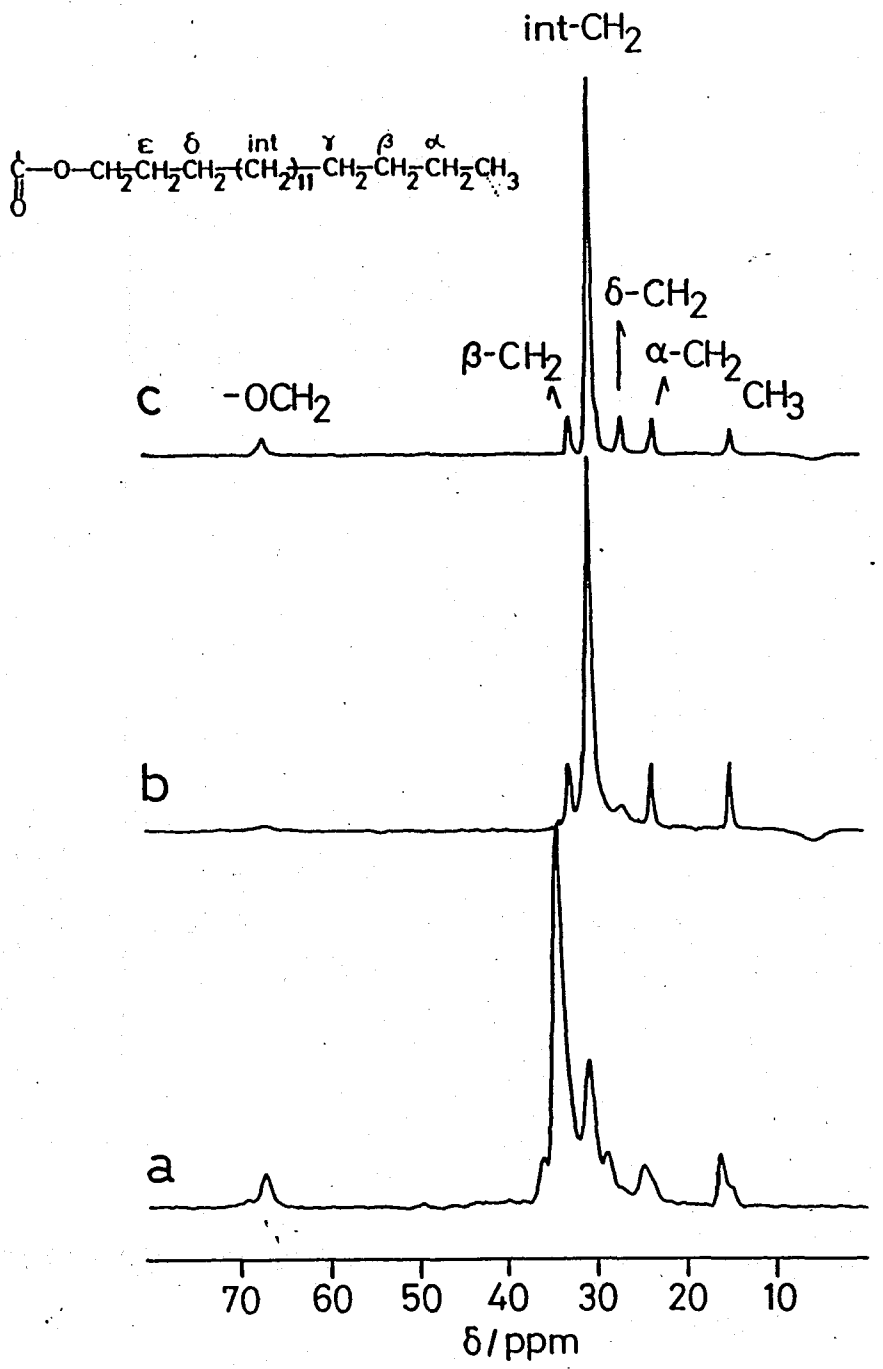

Figure 3-6. ^{13}C CP/MAS NMR spectra recorded for the aliphatic side chains of the B-C18 polyesters; (a) the crystalline phase at 20 °C, (b) LC-2 phase at 90 °C, and (c) the isotropic phase at 150 °C.

Structure of Liquid Crystal-1 (LC-1) Phase. LC-1 was found in all specimens. The X-ray pattern for the oriented LC-1 mesophase of B-C18 is shown in Figure 3-7b. Compared to the lower temperature LC-2 mesophase, the X-ray pattern for this mesophase is greatly simplified and exhibits only a few broad reflections. In the small angle region, one broad equatorial reflection with a spacing of 27 Å was observed. A very weak meridional arc with a spacing of 15.6 Å wass also observed. In the wide angle region, a broad arc with spacing of approximately 4.5 Å can be distinguished. This mesophase, thus, has no long range translational order, which is a characteristic feature of nematic mesophases. A similar pattern was observed for the LC-1 phases of the other B-Cn polyesters. In Figure 3-8, the spacings of the equatorial reflections are plotted as open circles against n, as measured for the mesophases at 100 °C. The spacing of the equatorial reflection increases monotonically from 15 to 27 Å when the value of n increases from 6 to 18, whereas the spacing of the meridional arc is almost constant at around 15.5 Å.

By optical microscopy, it was observed that this phase exhibits fluid behavior between glass slides and has an inversion wall texture like that of a nematic phase (see Figure 3-10). In areas where there is a free surface on one side, a Schlieren texture could also been observed. A similar texture has been observed for similar types of polyesters prepared by Ballauff at al[4]. The fluidity and microscopic Schlieren texture, thus, undoubtedly reflect the nematic like character of the mesophase.

In this case, however, the X-ray data do not support the conclusion that this is an ordinary nematic phase. The reason for this is that the spacing of the equatorial reflection is too large to accommodate the molecules in a nematic field. In an ordinary nematic phase, each molecule functions independently as a kinetic unit and therefore rotates freely around the long axis. If it was to apply to this system, spacings less than 10 Å are expected since the spacing should correspond to the average diameter of molecule. As found in Figure 3-8, however, the observed spacing of the equatorial reflection is as large as that observed for the LC-2 phase. A similar phenomenon has been observed for the nematic phases of polyamides

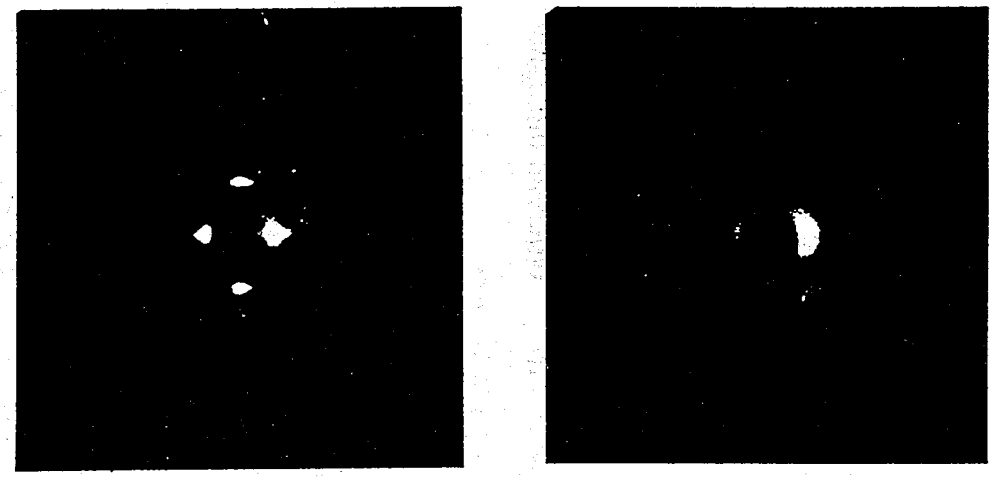

Figure 3-7. The oriented X-ray patterns of (a) the LC-5 phase and (b) the LC-1 phase of the B-C18 polyester.

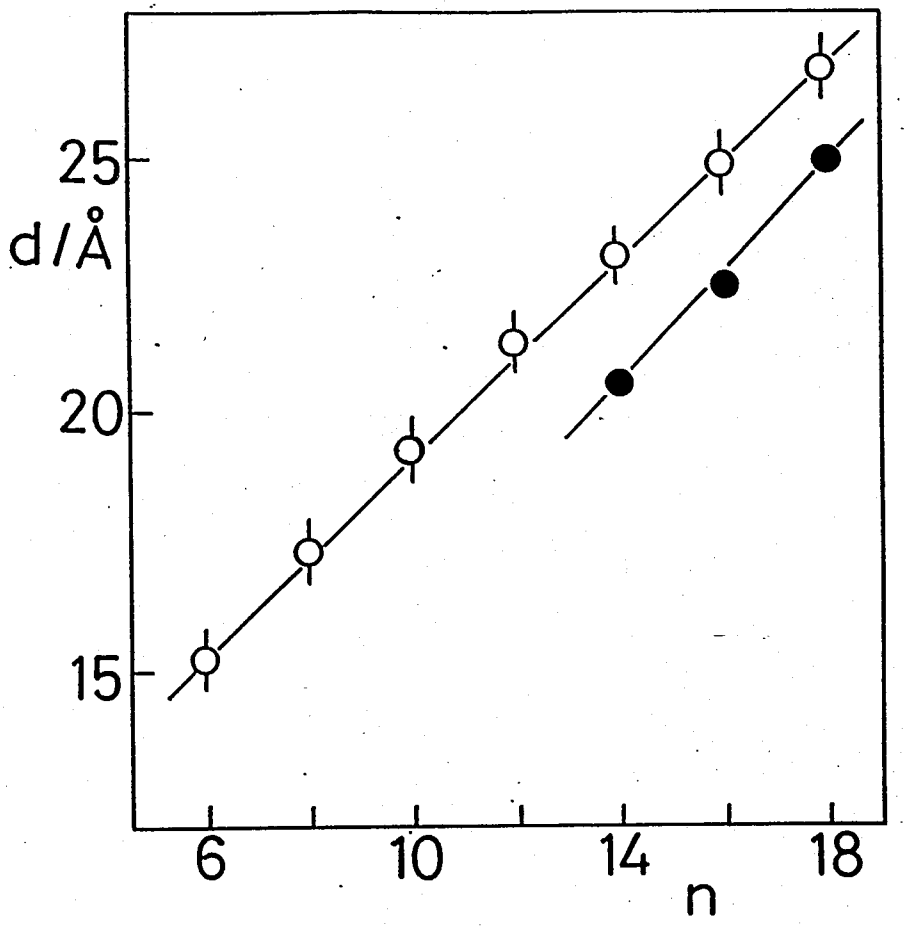

Figure 3-8. Plots of the spacings of the 100 reflections for the LC-2 and LC-1 against n. Here, the closed circles are observed for the LC-2 phases while the open circles are for the LC-1 phases.

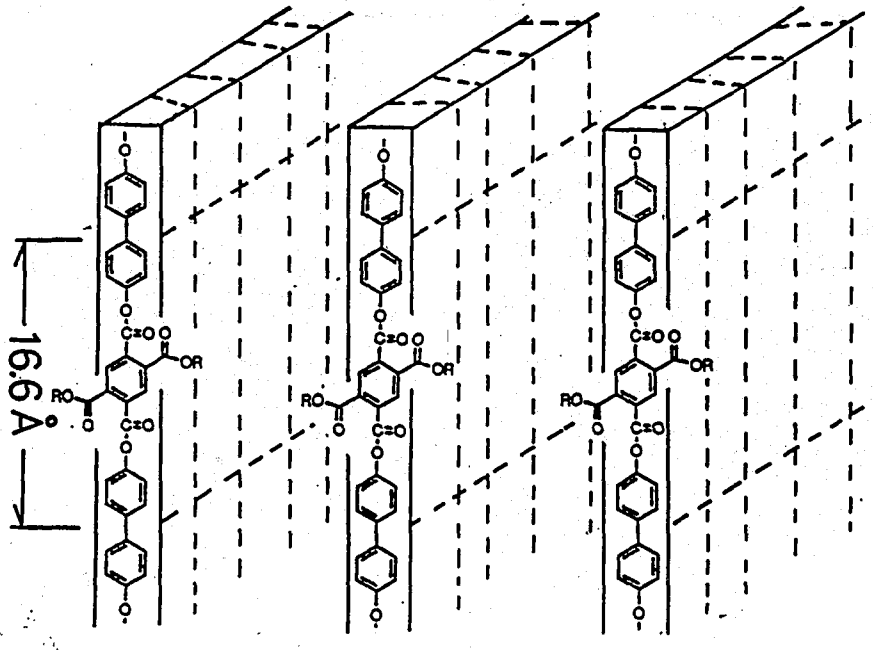

Figure 3-9. Schematic illustration of the layered structure for the LC-2 phase. Here, the fully extended main chains are packed into a layer with only a positional order along their main chain axes and the side chains in melt occupy the space between the layers.

with alkyl side chains as reported by Ebert et al[8,9].

To explain this pecularity, two possible nematic structures could be proposed as illustrated in parts a and b of Figure 3-11. One of these has been proposed for the polyamides, by Ebert et al.[6], in which each molecule functions as a kinetic unit but retains a boardlike shape as in the layered LC-2 (see Figure 3-11a). To retain such a broadlike shape, the polymer main chains should be coplanar and also the flexible side chains should have a strong tendency to remain within the planes defined by the backbone. For these polyesters, such a peculiar conformation appears unlikely in the nematic field since no specific intermolecular interactions can be expected[31]. As a more plausible model, it can be speculated that the main chains are still associated with each other to form a layer but the layers are piled up with greater degree of disorder (see Figure 3-11b). To produce such a disorder, the layer may be constructed with only short range order. We do not yet have decisive evidence as a basis for selecting one of the two possible structures.

Finally, it is noteworthy that both of the proposed nematic phases should be biaxial. In fact, the biaxiality has been observed in the above mentioned nematic phase of polyamides from the conoscopic method[9].

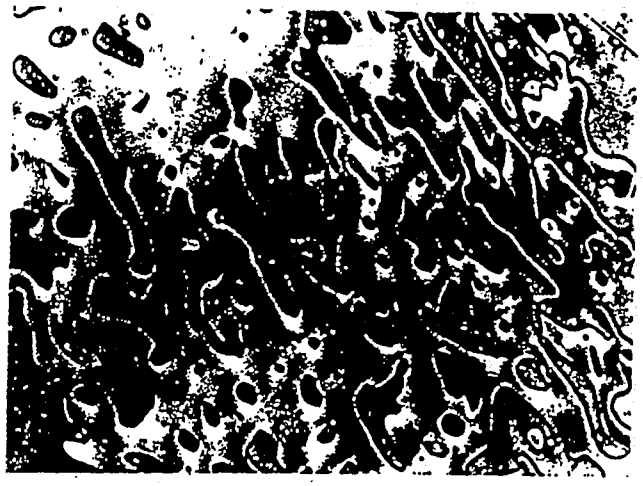

Figure 3-10. An optical microscopic photograph for the LC-1 phase of B-C10 exhibiting an inversion wall texture.

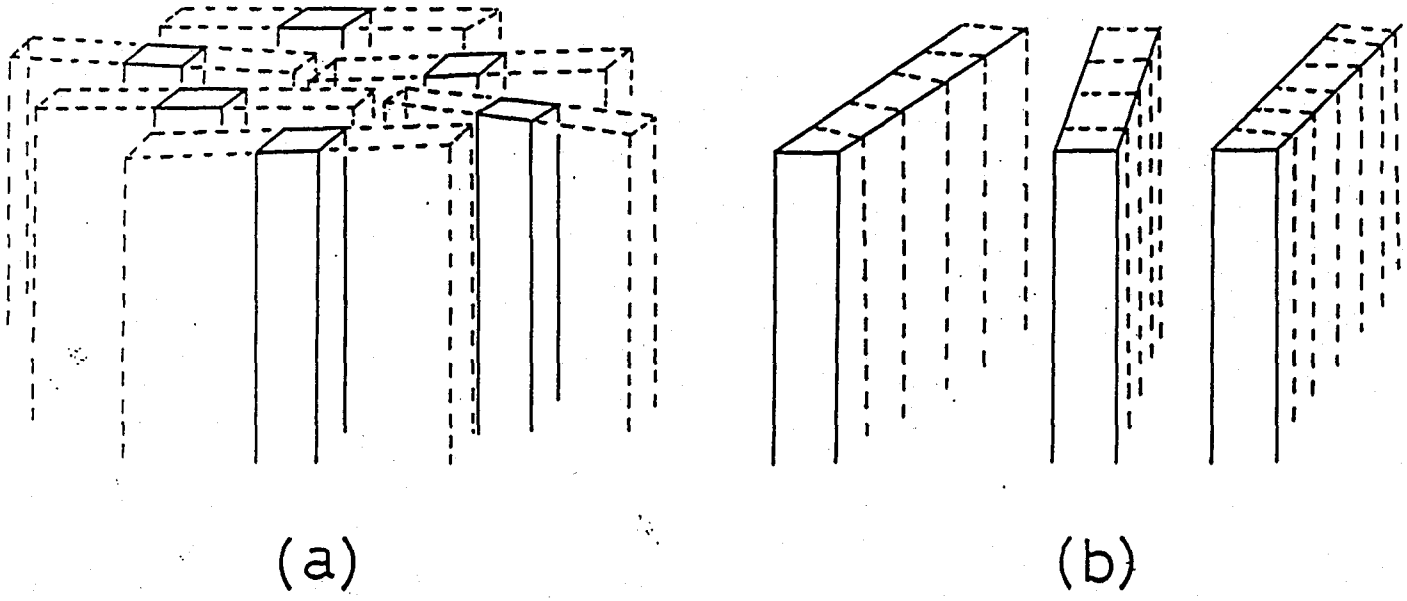

Figure 3-11. Two possible nematic structures for the LC-1 phase. In the nematic phase of (a), the molecules having a broad-like shape function as a kinetic unit. In contrast, in the nematic phase of (b), the main chains are associated with each other to form a layer, but the layers are piled up with a greater degree of disorder.

Table 3-3
^{13}C NMR chemical shifts for the aliphatic carbons of the B-C18 polyesters at various temperatures

	^{13}C NMR chemical shifts / ppm						
			Interior CH_2*				
Temp/°C	OCH_2	β	Cryst.	Amor.	δ	α	CH_3
25	67.1	35.9	34.2	30.8	28.7	24.5	16.1
90	67.0	32.7	--	30.5	26.7	23.4	14.6
148	67.0	32.3	--	30.1	25.5	23.0	14.3

*Cryst. and Amor. indicate the crystalline and noncrystalline state, respectively.

Table 3-4
X-ray data for the LC-2 phases

B-C14 dobsd(Å)	B-C16 dobsd(Å)	BC-18 dobsd(Å)
20.5 (100)	22.7 (100)	25.0 (100)
16.6 (001)	16.6 (001)	16.6 (001)
12.9 (101)	13.6 (101)	13.9 (13.9)
10.2 (200)	11.3 (200)	12.4 (200)
8.30 (002)	8.31 (002)	8.30 (002)

3-4 Concluding Remarks

To conclude, the B-Cn polyesters form layered crystalline and liquid crystalline phases in which the aromatic main chains are packed into a layer and the alkyl side chains are located in the space between the layers.

In the crystalline phase, the aromatic main chains are in a fully extended form with a repeating length of 16.6 Å and these are regularly packed within a layered structure. In addition, the side chains are also in a crystalline state between the layers. The X-ray pattern is indicative of a crystal structure with three-dimensional order, which demands that the positional correlation between adjacent layers is maintained through the side chain crystals. Thus, the crystal structure is likely built up by a close coupling of main chain crystals and side chain crystals. This coupling is also supported by the fact that both crystals melt at the same temperature. A study is now in progress to with greater accuracy determine the structure of the three-dimensional crystal lattice.

It is interesting to note that the main chains are packed into two different layered structures depending on the side chain length. For the B-Cn polyesters with side chains shorter than n = 12, the lateral packing distance of the main chains within a layer is 4.6 Å, but this reduces to 3.45 Å for the B-Cn polyesters with side chains longer than n = 14 (see Figure 3-4). The packing distance of 4.6 Å in the former group is reasonable for the main chains which have the twisted conformation in the most stable energy[7,39]. In contrast, the short spacing of 3.45 Å in the latter group indicates that the anomalously close packing of main chains requires a peculiar conformation in which the phenyl rings adopt a coplanar arrangement.

A difference in the packing structure between the two groups is also reflected in the melting temperature of the crystals. As shown in Figure 3-2a, the melting temperature drops significantly with an increase of n from 6 to 10 but then increases again with a further increase of n. The two distinct regions identified in the phase diagram are obviously related to the crystal structures. The decreasing region, observed for the short side chain B-Cn, corresponds to the lowering of the thermal stability of the

crystal structure, which is determined mainly by the polymer backbones with perhaps a slight perturbation by the shorter side chains. On the other hand, the regime of increasing thermal stability, observed with the longer alkyl side chain polyesters, corresponds to an enhancement of the thermal stability of the crystals. The structure in this case is strongly dominated by the crystallization of the long paraffin side chains, which also likely results in the anomalously dense packing of the backbones within a layer as described above.

LC-2, the lower temperature mesophase, also has a layered segregated structure similar to that of the crystalline phase although its fundamental structure is remarkably different in several aspects from the crystal structure. The main chains are still in an elongated conformation (a repeat length of 16.6 Å) as in the crystalline phase, but they are packed into a layer having positional order only along the chain axis but not in the lateral direction. The side chains are included between the layers in a noncrystalline form, which gives rise to the liquid crystalline fluidity of the phase. It is interesting to note that this type of liquid crystalline phase appears only for the B-Cn polyesters in which the alkyl side chains are longer than n = 14. The length of the side chains, hence, is a significant factor in determining the nature of the liquid crystalline phase.

This layered LC-2 has interesting features compared to the layered LC observed for the H-Cn polyesters. In the latter, the main chains are packed into a layer with positional order in the lateral direction but not along the chain axis. This is opposite to that in the LC-2 of B-Cn. Furthermore, Ballauff et al.[4] have reported in the layered mesophases formed by the polyesters that

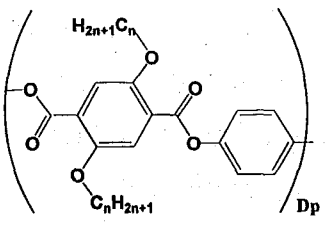

no positional order can be seen in any direction so far as the main chain packing within a layer is concerned. These observations suggest that

there are several types of layered mesophases which have different modes of packing the main chains into a layered structure as described below.

The LC-1 observed for all specimens displays a nematiclike optical texture, but a classical nematic phase cannot be postulated because of the large spacing of lateral packing between the molecules. At the present time, we can only propose a tentative model in which molecules retain a layerlike structure but there are frequent irregularities in the packing. A more detailed examination is needed for classification of the structure.

Finally, it is interesting to note that the basic features of the molecular packing into a layered mesophase are similar to those of discotic columnar phases[36,37]. In columnar phase, the column is formed by a stacking of the disklike molecules with the long alkyl side chains and core molecules arranged in space with a two dimensional lattice structure that may be hexagonal or rectangular. The different types of columnar phases have been classified on the basis of the packing array of the disklike molecules into column and the two dimensional packing array of columns[36]. In the present layered mesophase, the molecules have a broad-like shape and associate into a layered structure. In analogy to the discotic phases, the layered mesophases can be classified into several types on the basis of the packing arrangement of molecules into a layer[38]. This classification was initially proposed by Ebert et al.[9] who termed the layered mesophases "sanidic" and defined by Greek letter Σ. We are in agreement with this terminology, which can be extended to account for the four possible types of sanidic mesophases, ΣOb, ΣOu// , $\Sigma Ou_{\perp}$ and Σd. These have the following packing characteristics of the main chains within a layer:

1. ΣOb : having positional order in both directions parallel and perpendicular to the chain axis.

2. $\Sigma Ou_{\perp}$: having positional order only in a direction perpendicular to the chain axis.

3. ΣOu//: having positional order only in a direction parallel to the chain direction.

4. Σd ; having no positional order in any direction.

According to this classification scheme, the LC-2 in the present B-Cn

polyesters belongs to $\Sigma Ou\_$ while the layered mesophase of H-Cn belongs to $\Sigma Ou//$. Further, the layered mesophase reported by Ballauff et al.[4] can be classified into Σd. The validity of this classification scheme may be checked on a detailed structural examination of many types of layered mesophases.

3-5 Reference and notes

(1) Ballauff, M. Macromol. Chem., Rapid Comun. 1986, **7**, 407.

(2) Ballauff, M. Angew. Chem., Int. Ed. Engl. 1987, **28**, 253.

(3) Ballauff, M.; Schmidt, G. F. Mol.Cryst.Liq.Cryst. 1987, **147**, 163.

(4) Stern, R.; Ballauff, M.; Wegner, G. Macromol. Chem., Macromol. Symp. 1989, **423**, 373.

(5) Rodrigues-Parada, J. M.; Duran, R.; Wegner, G. Macromolecules 1989, **22**, 2507.

(6) Ebert, M.; Herrmann-Schenherr, O.; Wendorf, J.; Ringsdorf, H.; Tschirner, P. Liq. Cryst. 1990, **7**, 63.

(7) Adam, A.; Spiess, H. W. Macromol. Chem., Rapid Comun. 1990, **11**, 249.

(8) Frech, C. H.; Adam, A.; Falk, U.; Boeffel, C.; Spiess, H. W. New Polym. Mater. 1990, **2**, 267.

(9) Stern, R.; Ballauff, M.; Lieser, G.; Wegner, G. Polymer 1991, **32**, 2079.

(10) Harkmess, B. R.; Watanabe, J. Macromolecules 1991, **24**, 6759.

(11) Watanabe, J.; Harkness, B. R.; Sone, M. Polym. J. 1992, **24**, 1119.

(12) Cervinka, L.; Ballauff, M. Colloid Polym. Sci. 1992, **270**, 859.

(13) Sone, M.; Harkness, B. R.; Watanabe, J.; Torii, T.; Yamashita, T.; Horie, K. Polym. J. 1993, **25**, 997.

(14) Galda, P.; Kistner, D.; Martin, A.; Ballauff, M. Macromolecules 1993, **26**, 1595.

(15) Marz, K.; Lindner, P.; Urban, J.; Ballauff, M.; Fisher, E. W. Acta Polym. 1993, **44**, 139.

(16) Damman, S. B.; Mercx, F. R. P.; Kootwijk-Damman, C. M. Polymer 1993, **34**, 1891.

(17) Damman, S. B.; Mercx, F. P. M. J. Polym. Sci., Polym. Phys. 1993, **31**, 1759.

(18) Damman, S. B.; Mercx, F. P. M. J.; Lemstra, P. J. Polymer 1993, **34**, 2726.

(19) Damman, S. B.; Vroege, G. J. Polymer 1993, **34**, 2732.

(20) Kakimoto, M.; Orikabe, H.; Imai, Y. ACS Polym. Prep. 1993, **34**, 746.

(21) Steuner, M.; Hortz, M.; Ballauff, M. J. Polym. Sci., Polym. Chem.

1993, **31**, 1609.
(22) Watanabe, J.; Harkness, B. R.; Sone, M.; Ichimura, H. Macromolecules 1994, **27**, 507.
(23) Sone, M.; Harkness, B. R.; Kurosu, H.; Ando, I.; Watanabe, J. Macromolecules 1994, **27**, 2769.
(24) Damman, S. B.; Buijs, J. A. H. M. Polymer 1994, **35**, 2559.
(25) Damman, S. B.; Buijs, J. A. H. M.; van Turnhout, J. Polymer 1994, **35**, 2364.
(26) Buijs, J. A. H. M.; Damman, S. B. J. Polym. Sci.; Polym. Phys. 1994, **32**, 851.
(27) Tiesler,U.; Pulina,T.; Rehahn,M.; Ballauff,M.; Mol.Cryst.Liq.Cryst. 1994, **41**,525.
(28) Voigt-Martin, I. G.; Simon, P.; Bauer, S.; Ringsdorf, H. Macromolecules 1995, **28**, 236.
(29) Voigt-Martin, I. G.; Simon, P.; Yan, D.; Yakimansky, A.; Bauer, S.; Ringsdorf, H. Macromolecules 1995, **28**, 243.
(30) Watanabe,J.; Ono,H.; Uematsu,I.; Abe,A.; Macromolecules 1985, **18**, 2141.
(31) Coulter, P.; Windle, A.H. Macromolecules 1989, **22**, 1129.
(32) Yamanobe, T.; Tsukahara,M.; Komoto,T.; Watanabe,J.; Ando,I.; Uematsu,I.; Deguchi,K.; Fujito,T.; Imanari,M. Macromolecules 1988, **21**, 48.
(33) VanderHart,D.L.; J.Mag. Reson. 1981, **44**, 117.
(34) Earl, W.L.; VanderHalt, D.L. Macromolecules 1979, **12**, 762.
(35) Ishikawa, S.; Kurosu, H.; Ando,I.; J.Mol.Struct. 1990, **248**, 361.
(36) Destrade,C.; Foucher,P.; Gasparoux,H.; Tinh,N.H.;Levelut.A.M.; Malthete, J mol.Cryst.Liq.Cryst. 1981, **71**, 111.
(37) Chandrasekhar,S.; Ranganath,G.S. Prep.Prog.Phys. 1991, **53**, 57.
(38) In columnar phases, the columns associate with two-dimensional positional order, but in this case the layers are piled up with one-dimensional order. Hence, inour classification of the layered structures we do not consider the difference in the packing of layers but only the difference in the main chain packing into a layer.

Chapter 4

Thermotropic Behavior and Phase Structure in Rigid-Rod Polyesters with Flexible Side Chains Based on 1,4-Dialkylesters of Pyromellitic Acid and Hydroquinone.

4-1 Introduction

Rigid-rod polyesters with long flexible side chains have been investigated in a rapidly growing number of paper[1-29]. Most of these investigations were focusing either on the synthesis and the measurement of various physical static and dynamic properties in a layered liquid crystalline phases. An interesting property of these polyesters is to form liquid crystalline phase with layer modifications. It has been postulated that the driving force for the adoption of such a structure is a segregation of aliphatic and aromatic domains. In these layered structures, liquid crystallinity is the result of a partial or total lack of positional order within the layers with respect to the main chain packing and the fluid-like disordered alkyl side chains between the layers, The crystalline phase that developed from the layered mesophases also show that the main chains and side chains crystallize in a cooperative fashion.

In these layered structure, it is of considerable interest that an aromatic domains and an aliphatic domains are segregated[1-29]. Since the force of segregation plays an important role in determining the morphology, length of the side chain is presumed to influence the segregated structure. In fact, we previously reported that B-Cn forms two layered crystals and two mesophase depending on the length of alkyl side chains. This side chain length dependence of the morphology can possibly be compared with a fraction dependence of a A/B block copolymer.

An A/B block copolymer consists of two macromolecules bonded together. In the process of reaching equilibrium, such a material may

separate into distinct phases, creating domains of component A and B[30]. A dominant factor in the determination of the domain morphology is area-minimization of the intermaterial surface, subject to fixed volume fraction. It has been known that there exist three types of fundamental morphologies for the microdomain structure of block polymers, namely, spherical domain structure with cubic lattice, hexagonally packed cylindrical domain structure and alternating lamellar structure. The variation in morphology originates from the thermodynamical requirement associated with the incompressibility of polymeric liquids, i.e., the demand of uniform filling of the segments in domain space with the minimum free energy, while keeping the segmental density of each domain equal to the segmental density of the respective bulk polymers. If the component of the radius of gyration of the A-block chain parallel to the interface is similar to that of the B-block chain for A/B diblock polymers, interfaces of zero curvature (or infinite radius) are preferred in order to achieve uniform segmental distribution in domain space with the minimum free energy and the lamellar microdomain result. However, if the component of the radius of gyration parallel to the interface differs for the A-block and B-block chains, uniform packing of block chains in domains space with minimum free energy is possible only when the interface has a finite curvature resulting in the formation of cylindrical or spherical microdomains. Thus the morphology changes in the order of A spheres, A cylinders, A/B lamellae, B cylinders and B spheres as the fraction and hence the relative molecular volume of A component in A/B block polymer increases[29-33].

The rigid rod polyesters with flexible side chains have a binary molecular structure. Linear alkylene groups are bonded to rigid-rod aromatic polyesters. Although in this case length of the side chain is only variable parameter, various morphologies are expected as a function of side chain length. The objective of this work has been to examine the thermotropic behavior and the phase structure of H-Cn polyesters. Moreover, through discussion as a function of side chain length, we show how segregation influence the phase structure. A more detailed work on morphology of rigid-rod polyesters with flexible side chains is required. Thus, here we aim to

clarify the different morphologies caused by segregation of aliphatic side chains and aromatic main chains.

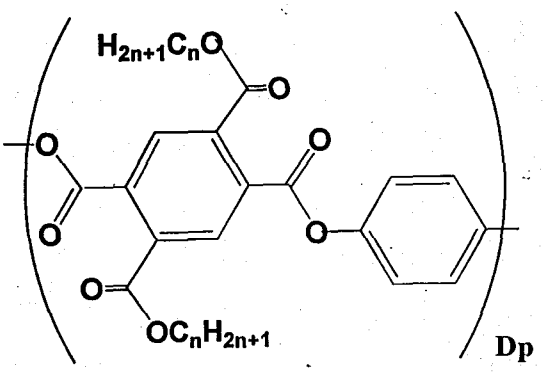

4-2 Experimental section

The synthesis and characterization of the H-Cn has been described in a previous report[10,11]. The H-Cn polymers with n = 6-18 were prepared by converting the 1,4-dialkylesters of pyromellitic acid to their respective diacid chloride followed by condensation with hydroquinone. The inherent viscosity of these polymers is reported previously[11].

DSC measurements were performed with a Perkin-Elmer DSC II calorimeter at a scanning rate of 10 °C/min. Wide angle X-ray diffraction patterns of the polymers were recorded with a flatplate camera mounted to a Rigaku-Denki X-ray generator emitting Ni-Filtered Cu Kα radiation. The temperature of the samples was controlled by placing them in a Mettler FP-80 hot stage mounted in the beam path. The film to specimen distance was determined by calibration with silicon powder. ^{13}C MAS NMR spectra were measured by means of a JNM-GX270 NMR (67.8 MHz) with a variable temperature (VT) CP/MAS accessory. The sample (ca. 200 mg) was contained in a cylindrical rotor made of ceramic materials and spun at 4.0 kHz. The contact time was 2.0 ms with a repetition time of 6.0 s.

4-3 Results and Discussion

[1] General phase behavior

The H-Cn polymers were all readily soluble in organic solvents such as THF and chloroform and from the solutions fine thin films could be prepared by casting[10]. Microscopic observation of the films of H-C12, 14, 16 and 18 on heating showed two transitions. On the first transition, T1, the solid crystalline phase changed to the fluid liquid crystalline phase and at the second transition, Ti, resulted in isotropic phase. H-C6, 8 and 10 show only crystal-isotropic transition.

From DSC thermograms of Figure 4-1, it is apparent that the H-C12 to 18 cast films exhibit similar transition behavior to that observed for the H-C16 film, with the exception that the degree of crystallinity of the crystalline phase decreases with a decrease in the length of alkyl side chains. This is evident from the calculated enthalpies for the T2 transition peaks as 12.7, 7.7, 5.0 and 1.0 kcal/mol for H-C18, 16, 14 and 12 respectively. The enthalpy of liquid crystal to isotropic phase transition is almost the same for all specimens, about 1 kcal/mol. A further reduction in the length of side chain results in DSC thermograms of the H-C10, 8 and 6 polyesters films exhibiting a direct transition from the crystal to isotropic phase and no liquid crystalline phase.

H-C10, 8 and 6 polyesters form high ordered crystals obtained on annealing the melt-quenched samples. H-C8 and 10 form only one type of crystal Km2 while H-C6 form another crystal at temperature lower than the Km2 crystal. The transition temperatures are summarized in Table 4-1.

The transition temperatures (open circles) based on the DSC data are plotted as a function of n in Figure 4-2. The Ti temperatures (closed circles) determined from the optical microscopy are also included in the same figure. From these results, it is obvious that the liquid crystalline phase appears for H-Cn polyesters where n is 12 or longer. An interesting aspect of this transition behavior is the trend where the isotropization

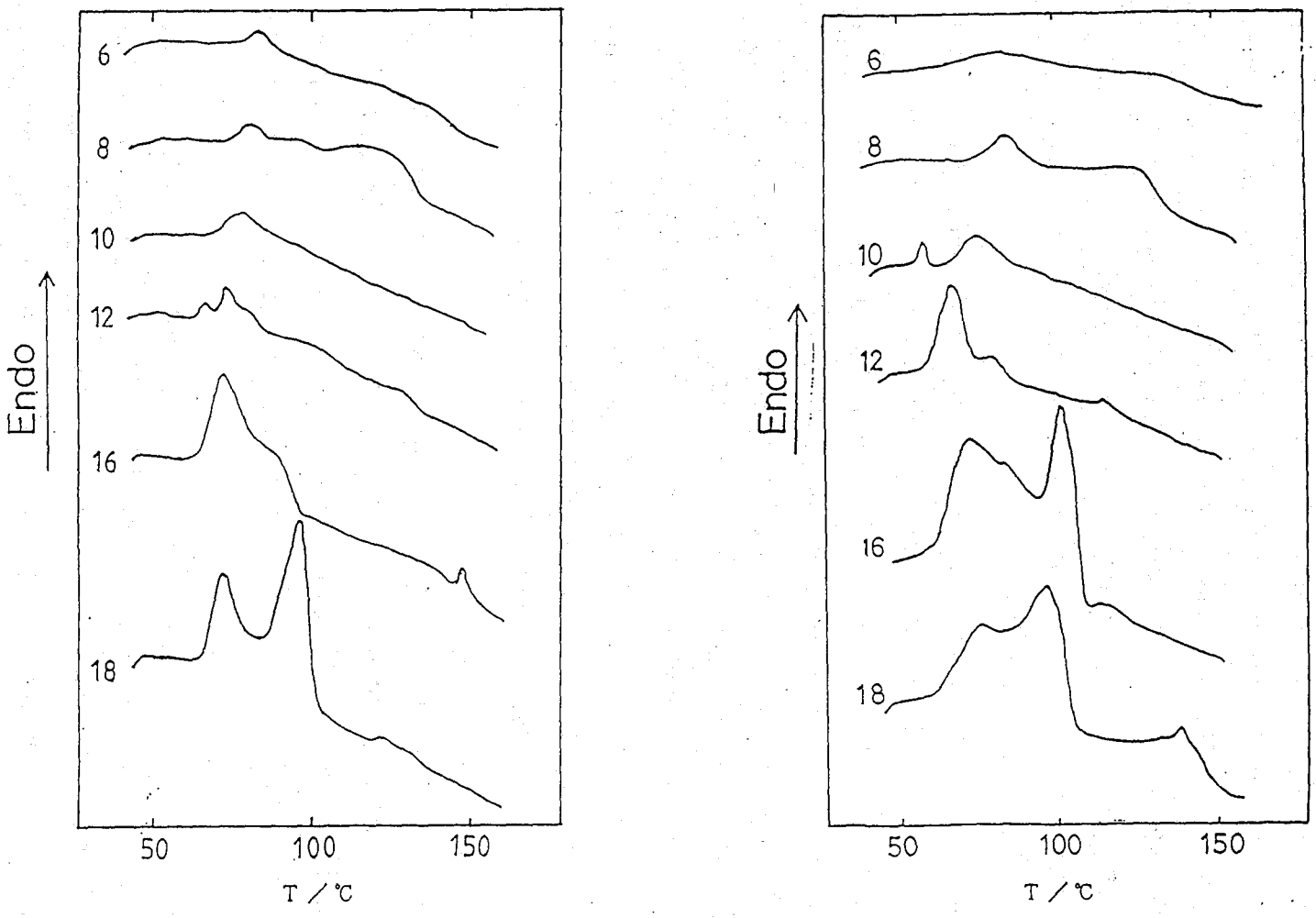

Figure 4-1. The DSC heating thermograms of the (a) THF cast films and (b) melt annealed sample of H-Cn.

Table 4-1
Inherent viscosities and transition temperatures for H-Cn polyesters

Polymer	η_{inh}(dl/g)	T_1(°C)	T_2(°C)	T_i(°C)
H-C6	0.28	--	80	132
H-C8	0.38	--	82	124
H-C10	0.39	--	78	103
H-C12	0.57	--	99	128
H-C14	0.23	45	94	149
H-C16	0.31	43	101	146
H-C18	0.26	44	111	124

Transition temperature were recorded for the first heating DSC scans of the THF-cast films.

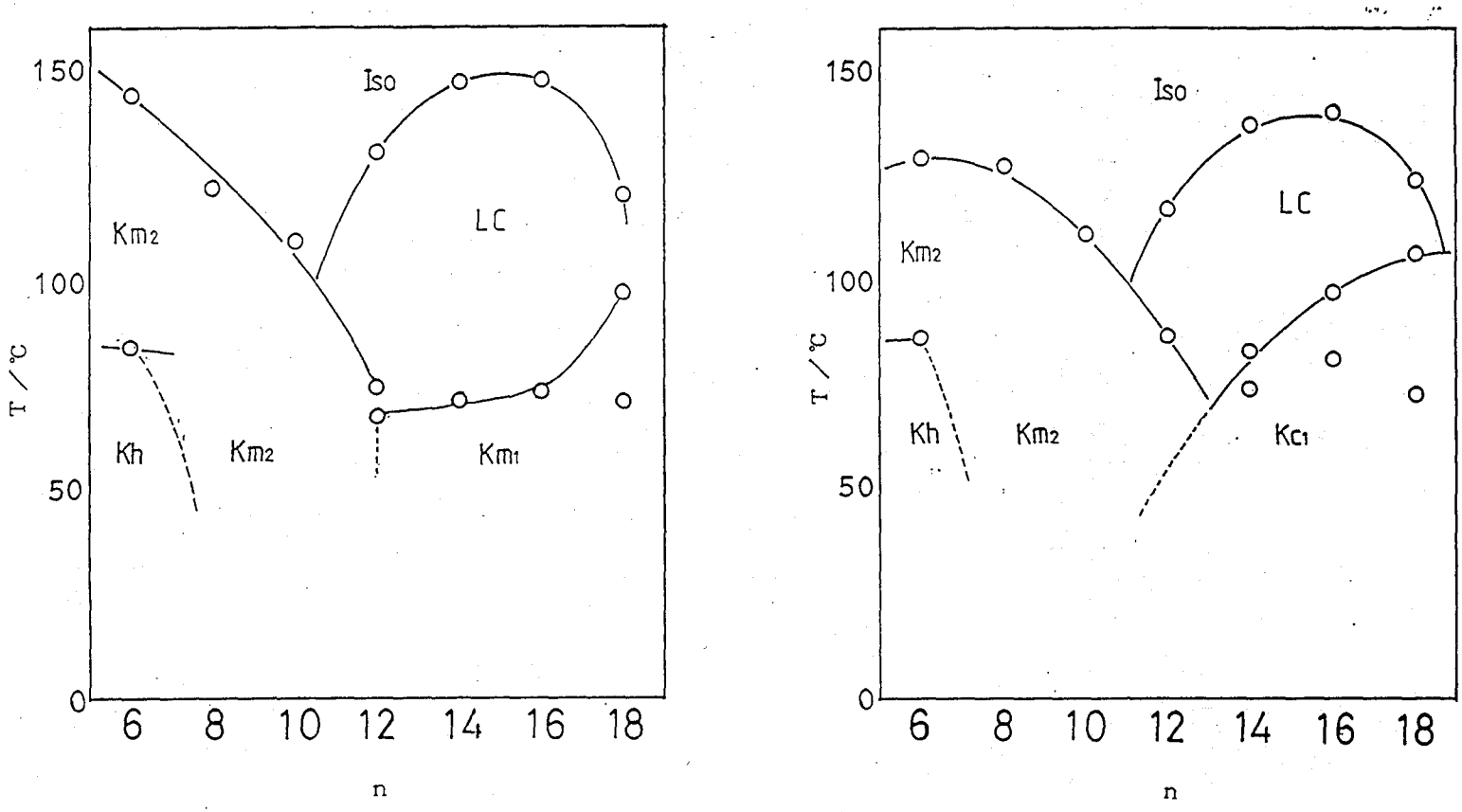

Figure 4-2. Variation of transition temperatures based on the heating DSC scan and optical microscopy with the number of carbon atoms in the alkyl side chain, n. (a) THF cast films and (b) melt annealed sample.

temperature of the crystalline phase, Ti, initially decreases as n increases from 6 to 10, but Ti for the liquid crystal increases with a further increase of n, exhibiting a maximum for H-C14. This indicates that the liquid crystalline phase arises not only as the result of a decrease in the crystal melting temperatures but also by an increase in the Ti temperatures for the liquid crystalline phases. A similar trend has also been observed for thermotropic alkyl ester derivatives of cellulose which exhibit a columnar hexagonal phase when the alkyl side chain is longer than an octyl group[39,40]. In the columnar phase, the individual column can be viewed as a type of micellar structure that results from differences in the polarity and/or geometric shape of the cellurose main chain and aliphatic side chain. Hence, for H-Cn polyesters we can conclude that the stability of the liquid crystalline phases may result from a segregation of the two components; the aromatic main chain and aliphatic side chain, which occurs most readily for long side chains[39,40]. An alternative explanation for the trend observed in Ti may be variations in the molecular weights of the polymers, but the viscosity data does not support this possibility.

The strong reflections at low angles together with their higher orders have seen at all temperatures revealed the presence of a layered structure, similar to the ones found in studies of related polyester systems. A linear relationship is found between the layer spacing d and the length of the side chains in terms of the number of C-atoms[2]. This experimental relationship is depicted in Figure 4-3. The open circles show the Bragg spacings found for the crystal (Kc) obtained by casting from THF solution and annealing for three weeks. H-C6 , 8 and 10 do not form a crystalline structure by casting from the solution. H-C12, 14, 16 and 18 form a layered liquid crystalline phase. The Bragg spacings found for this liquid crystal are shown as closed circles. And the open triangles are for the crystal (Km1) obtained on annealing the melt quenched sample. The H-C6, 8 and 10 do not form a liquid crystalline phase but the oriented fiber could easily be obtained by spinning in the isotropic state.

The closed triangles show Bragg spacings found in the crystal (Km2) obtained on annealing the melt spun fiber of H-C6, 8 and 10. Interestingly, H-C6

polyesters form the different crystalline modification (Kh) as obtained on annealing the melt spun fiber below 90°C. This long Bragg spacing is shown as a closed square. The linear relationship between the layer spacing and length of the side chains in Kc crystal is similar to that in "modification B" of the similar polyesters as reported by Ballauff et al[3]. Moreover, the relatioship in liquid crystalline phase is similar to that in "modification A".

Figure 4-4 shows the phase behavior of H-Cn polyesters as a function of side chain length.

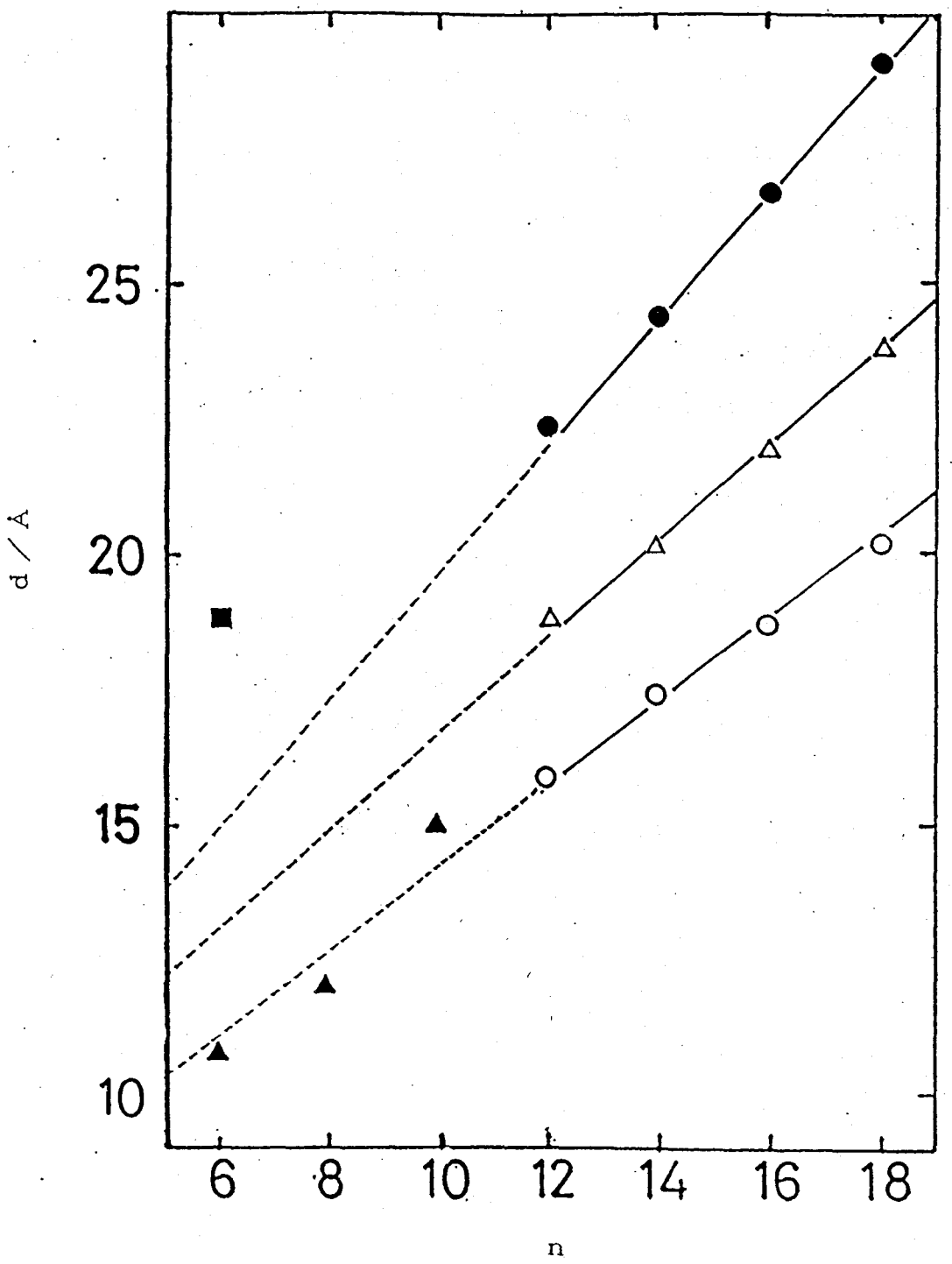

Figure 4-3. Plot of spacing of the Bragg spacing in the various phase vs. the carbon number of the alkyl side chain, n. The closed circles: liquid crystal. The open circles: Kc crystal as obtained by casting from THF solution. The open triangles: Km1 as obtained by annealing the melt-spun fibers. The closed triangles and the closed squares: Km2 and Kh, respectively, as obtained by annealing the melt-spun fibers.

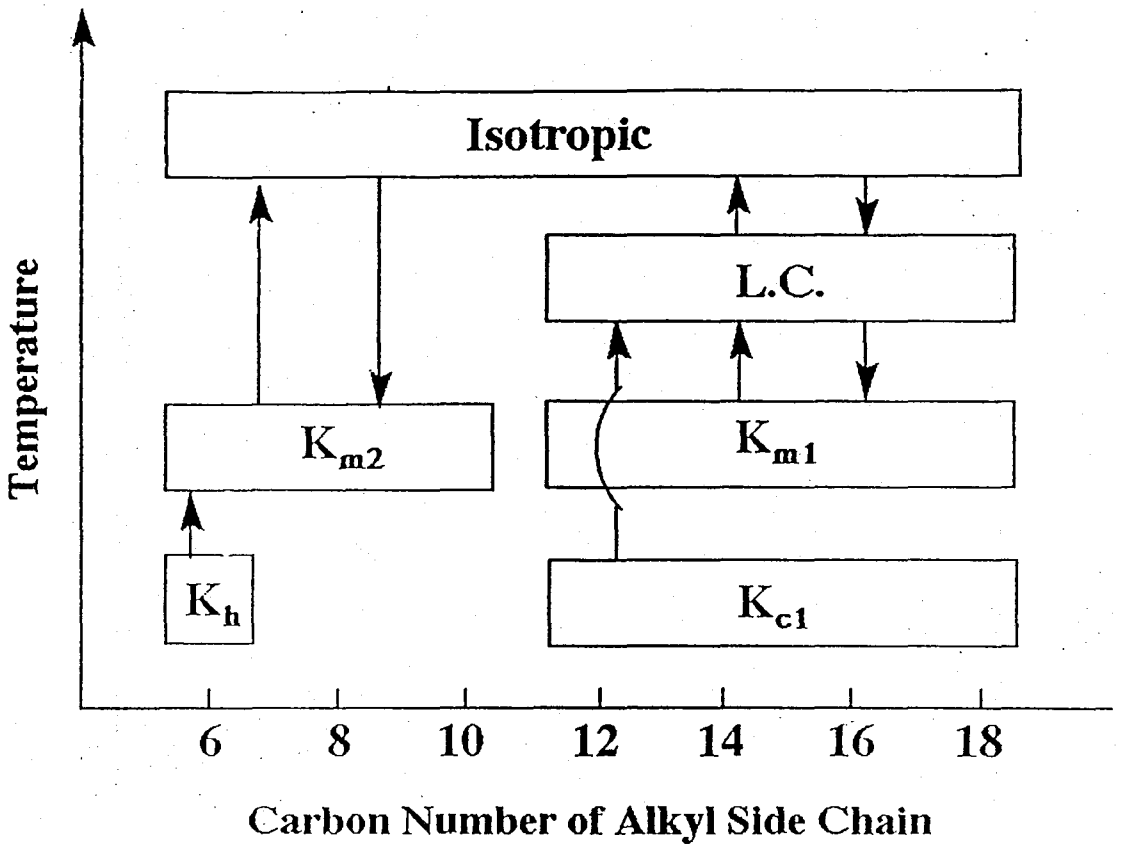

Figure 4-4. Schematic illustration of thermotropic phase behavior in H-Cn polyesters.

[2] Kc crystal

Figure 4-5(a) shows a typical example of X-ray diffraction pattern of Kc crystals of H-C16 polyester. The oriented specimen could not be obtained by casting from solution. Here, the observed reflections in the series h00 can be attributed to the layered structure that is formed with a layer plane parallel to film surface in the cast film. In the small angle region, many reflections were observed which reflect the formation of layered structure. Table 4-2 shows X-ray data for the equatorial reflections observed for Kc crystal of H-C16. Kc crystals were obtained by casting from THF or $CHCl_3$ solutions of H-C12 to 18. Characteristic h00 and 010 reflections were observed in the X-ray pattern of the Kc crystal of these series of polyesters. The layer spacing in this mesophase as revealed by X-ray analysis is shown to increase linearly with an increasing length of side chains. The observed increment of 0.82 Å per CH_2 unit suggests that the side chains are protruded normal to the main chain axis. The increment was also observed in rigid-rod polyesters with flexible side chains condensed by 2,5-dialkylterephtalic acid and hydroquinone. Ballauff classified this phase by modification B[2].

The characteristic point is that the distance of about 4.9 Å between the adjacent aromatic main chains, which is viewed in the crystals of the common aromatic polymers, independent of the side chain length. This interchain distance is observed in the crystal of ordinary aromatic polyesters. So, we can suggest that the aromatic main chains assume a twisted conformation. Figure 4-6 shows a TOSS ^{13}C CP/MAS NMR spectra for Kc of H-C16 polyesters. The chemical shift values of the aromatic main chains are completely same as those of diacetoxybiphenyl. Hence, the aromatic main chains take a stable and twisted conformation.

[3] Km1 crystal

Figure 4-5(b) shows a typical example of X-ray diffraction pattern of Km1 crystal of H-C16. This pattern shows 8 numbers of h00 reflections and 010 reflection, which suggests a highly ordered layered modification as shown in Table 4-2. Compared to the layered mesophase, the number

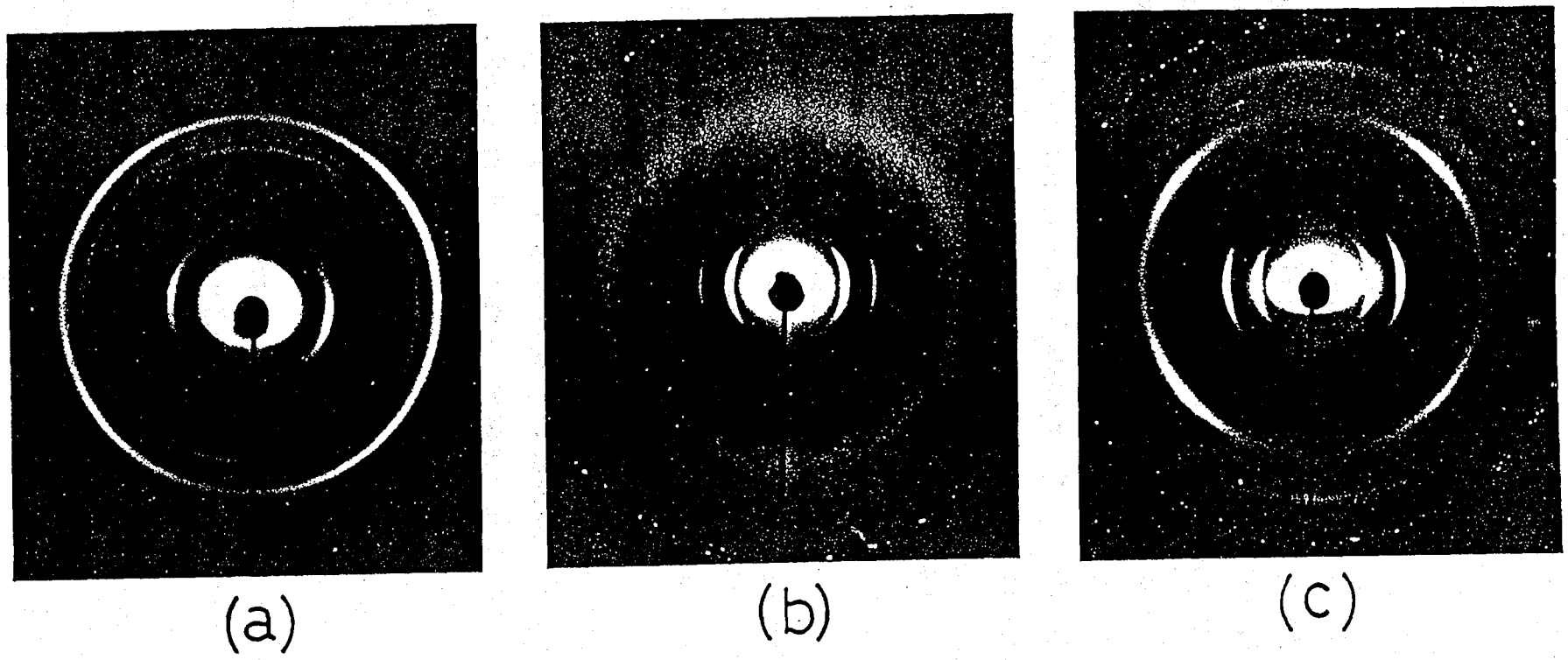

Figure 4-5. X-ray photographs of the as cast film of H-C16; (a) the crystalline phase (Kc) at 25°C; (b) liquid crystalline phase at 120°C; (c) melt-annealed sample (Km1) at 80°C. Here, the X-ray photographs were taken with the beam parallel to the film surface.

Table 4-2
X-ray data for the equatorial reflections observed for Kc and Km1 crystals of H-C16.

Kc				Km1			
dobsd Å	Int.	hk0	dcalcd Å	dobsd Å	Int.	hk0	dcalcd Å
18.8	vs	100		23.4	vs	100	22.2
9.29	s	200	9.29	11.1	s	200	11.1
7.87	vvw			7.25	s	300	7.40
6.75	w			5.45	m	400	5.55
6.10	vvw	300		4.39	s	500	4.44
5.35	vvw			3.90	m	010	010
4.89	m	010	4.89	3.65	w	600	3.70
4.58	w	400		3.21	vw	700	3.17
4.12	s			2.90	vvw	800	2.78
3.83	vw						
3.59	w	500					

Table 4-3
X-ray data for the liquid crystalline phase

	H-C12	H-C14	H-C16	H-C18
d_{100}(Å)	22.3	24.3	26.6	29.0
d_{200}(Å)	11.1	12.2	13.3	14.5
d_{300}(A)		8.13	8.87	9.72
d_{400}(Å)		6.07	6.65	7.28
d_{500}(Å)		4.89	5.32	
d_{010}(Å)	3.86	3.85	3.85	3.85

of h00 reflection and the off-meridional reflection increases. The characteristic value of this crystal is an interchain distance of about 3.92 Å observed as a 010 reflection. However, in this phase, hk0 reflections were not observed even though the alkyl side chains take an extended trans conformation concluded from solid state ^{13}C NMR. Thus, there are no interlayer correlation of the structural order in the aromatic main chain layers in this Km1 crystal. This result is different from that of crystals of B-Cn polyesters with layered modification.

The observed increment of 1.20 Å per CH_2 unit suggests that the side chains to protrude normal to the main chain axis. This increment is closed to the observed value in modification A as reported by Ballauff et al[3].

This interchain distance in aromatic layers is shorter than that in Kc crystal. In Kc crystal, the aromatic main chains are twisted. It can be assumed that the main chain takes an anomal conformation in Km2. Figure 4-6 shows solid state ^{13}C NMR spectrum of Km1 of H-C16 polyesters of Figure 5-7. Compared to Kc, the spectral shape of aromatic region is different in Kc. Thus, the aromatic main chains take an anomal conformation. The detailed analysis is reported in Chapter 5.

[4] Mesophase

The X-ray pattern of the liquid crystalline phase appear simple and an oriented pattern could be obtained for both as cast films and melt-spun fibers. The X-ray photograph of the liquid crystalline phase (Figure 4-5(c)), as observed for H-C16 film at 120 °C, includes a series of sharp equatorial h00 reflections with spacings of 26.6, 13.2, 8.73 and 6.59 Å. Two other wide angle reflections were observed. The first with a spacing of approximately 4.6 Å appears as a diffuse halo and the second appears as a sharp reflection with a spacing of 3.85 Å, showing stronger intensity on the meridional line. The X-ray study was also performed on oriented fibers spun from the isotropic melt. In this case, both, the h00 reflections and the 3.85 Å reflection appear on the equatorial line perpendicular to the fiber axis. A diffuse halo with a spacing of approximately 4.6 Å appears

with relatively stronger intensity on the equatorial line. Furthermore, weak meridional streaks with spacings of 12 Å and 6 Å also appear which are not familiar in the Kc crystal.

Similar X-ray patterns were observed for the liquid crystalline phases of H-C12, 14 and 18 as shown in Table 4-3. The only difference between them was the observed spacings for the h00 reflection, which increase linearly with an increase in n. All other reflections appear to have the same spacings and the same angular displacement in both film and fiber specimens. The X-ray data is listed in Table 4-3 and is presented in Figure 4-7.

The X-ray data is indicative of a layered structure for the liquid crystalline phase of the H-Cn polyesters, as illustrated in Figure 4-8. Here, the observed reflections in the series h00 can be attributed to a layered structure which contains a layer plane parallel to the film surface in the cast film or parallel to the fiber axis in the fiber specimen. Each layer is formed by a regular lateral packing of the aromatic main chains, as can be elucidated from the sharp reflection at 3.85 Å. A different angular displacement of this reflection relative to the h00 reflections has been observed between the film and fiber specimens. This could be explained by the different orientation of the layers in the film and the fiber specimens. The layers lie in a plane parallel to the film surface but with a random orientation of the layer axis (corresponding to the chain axis) while in the fiber specimen both the layer plane and layer axis lie parallel to the fiber axis. The main chain is in an extended conformation since the spacing of the meridional reflection, 12 Å, as observed in the fiber specimen, is in agreement with the value calculated by Erman et al., for a polyester with the same main chain repeat unit[41]. The appearance of this reflection as a weak streak indicates a random displacement of the main chain along the chain axis within a layer as in a nematic liquid crystal. The diffuse halo with a spacing of 4.6 Å can be attributed to the disordered alkyl side chains that occupy the space between the layers. Judging from the layer spacings, the side chains striking out of the neighboring layers interpenetrate into each other. The calculated densities based on this model are 1.08, 1.07, 1.05 and 1.05

g/ml for H-C12, H-C14, H-C16 and H-C18, respectively, which can be expected for these types of liquid crystals.

An examination of the sample density allows for further illustration of this layered structure. Returning to Figure 4-7, it is evident that there is a linear relationship between the layer spacing and the number of carbon atoms in the alkyl side chains. The slope gives an averaged increment of 1.12 Å per unit of n. The volume per two methylene (CH_2) units can therefore be given by 1.12 Å x 3.85 Å x 12.0 Å where the second and third factors are the distance between two main chains within a layer and the repeat length of the main chain, respectively. Thus, the density per CH_2 unit is calculated to be 0.90 g/ml which is somewhat larger than that (0.85 g/ml) of the amorphous phase of polyethylene.

[4] Km2 crystal

In this chapter, we will focus on the crystal structure for Km2 of the H-Cn polyesters with n = 6, 8 and 10. The X-ray diffraction pattern has been examined for an oriented crystalline fiber which was spun from the isotropic melt and subsequently annealed at 60 °C for H-C8 ,10 and 90 °C for H-C6 for 4 weeks. Figure 4-9 shows the oriented crystalline patters for the H-C6, 8 and 10. The diffraction pattern includes a number of layer line reflections as well as equatorial reflections, indicating that the crystal structure has three-dimensional positional order. The three dimensional crystalline lattice is obviously triclinic; however, precise determination of the structure has so far not been performed successfully. Hence, we shall refer to the two dimensional lattice projected along the polymer chain axis, which can be elucidated from the profile of equatorial reflections.

As listed in Table 4-4, the equatorial reflections include a series of hk0 reflections for Km2 crystals of B-C10, 8 and 6. These reflections could be allow a straightforward determination of the two dimensional lattice structure (which is evident on comparing the observed and calculated spacings in Table 4-4). The crystal lattices are illustrated in parts a, b and c of Figure 3-10, with lattice constants of a' = 12.15 Å, b' = 9.38 Å and γ' = 71.5° for H-C6 and a' = 12.6 Å, b' = 10.36 Å and γ' = 72.2° for H-C8 and a'

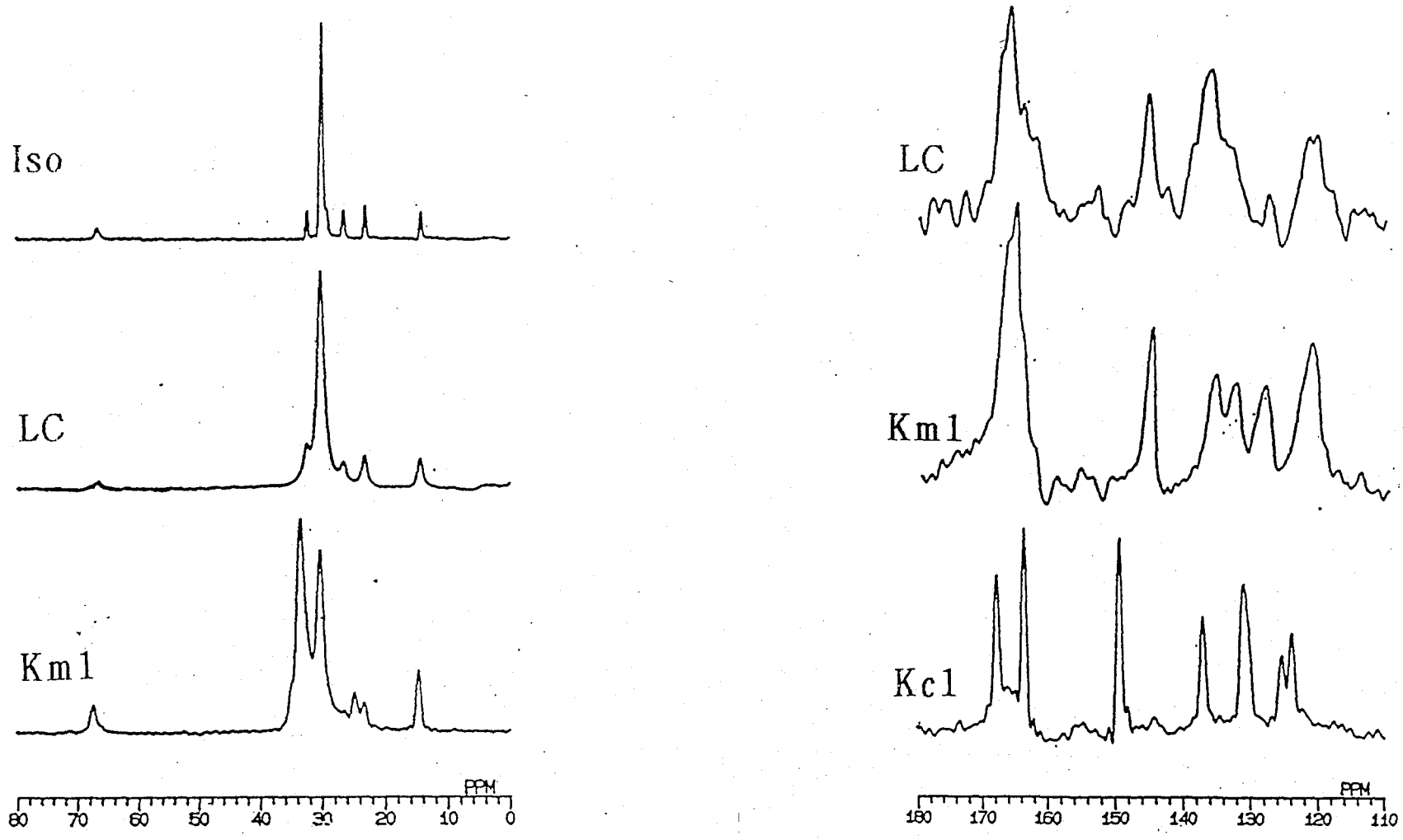

Figure 4-6. Solid state ^{13}C TOSS CP/MAS NMR Spectra of H-C16 polyesters in (a) Kc crystal, (b) liquid crystal and (c) Km1 crystal.

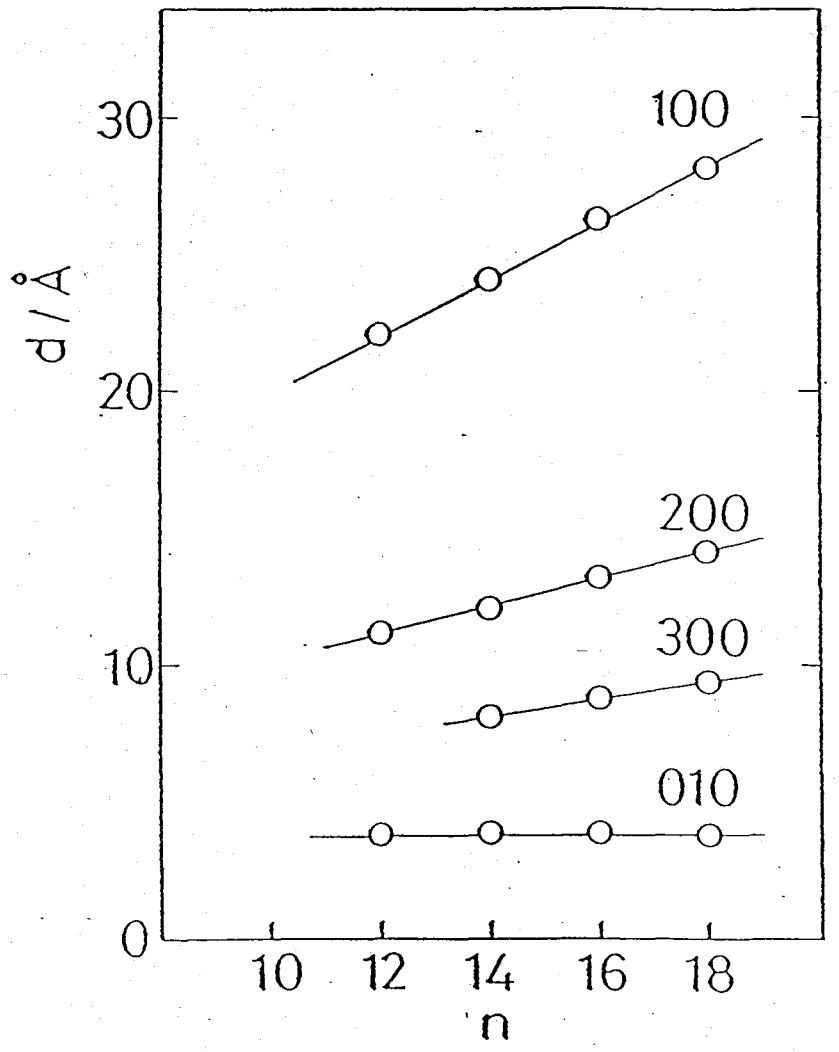

Figure 4-7. Plot of spacing the h00 and 010 reflections in the liquid crystalline phase vs. the carbon number of the alkyl side chain, n.

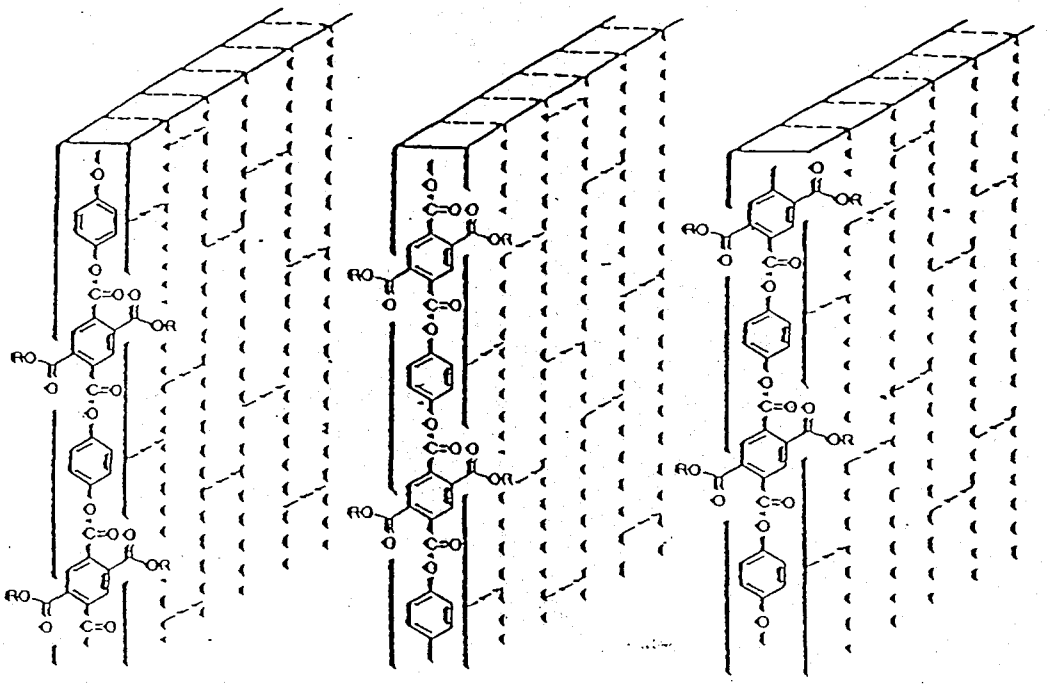

Figure 4-8. A proposed layered structure for the liquid crystalline phase. In this layered structure, the aromatic main chains in the extended form pack into layers with positional order only in the lateral direction, and the aliphatic side chains in the disordered form occupy the space between the layers.

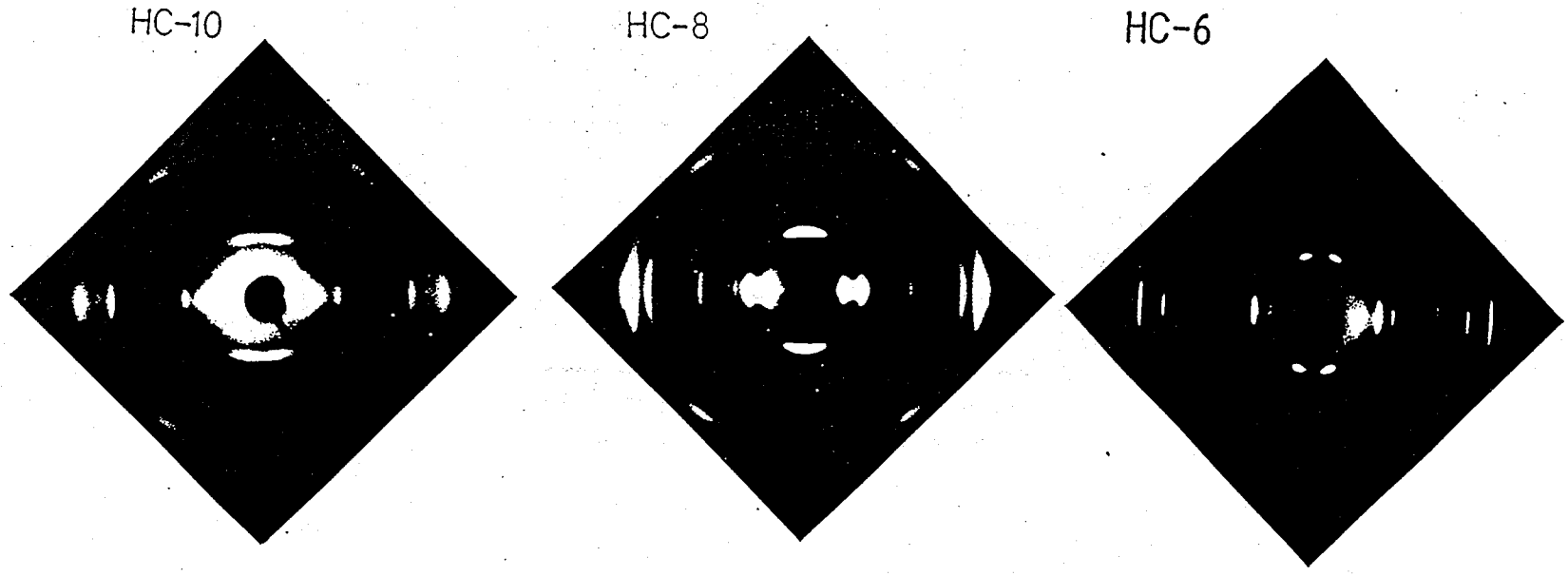

Figure 4-9. Oriented X-ray patterns of (a) H-C10, (b) H-C8 and (c) H-C6 crystalline fibers. Here, the fiber axis is oriented in tyhe vertical direction.

= 15.62 Å, b' = 9.44 Å and γ' = 78.0° for H-C10 respectively.

The number of polymers included in a two dimensional triclinic lattice can be deduced from density measurements. If this number is assumed to be true, the density, calculated from the known parameters of the hexagonal lattice and the molar mass, turns out to be about 0.62 gml^{-1} in all cases , which is actually half the true bulk density. It is obvious that a unit lattice includes two polymer chains. This strongly suggests that all the polymer molecule are crystallographically not equivalent.

Looking at the differences in polarity and/or geometric shape between the two groups in a molecule, it is easy to show that in Km2 the molecules adopt a layered structure in which the aromatic main chains are packed like zigzag sheet into a layer with a lateral spacing of half of b. The side chains occupy the space between the layers separated by a sinγ as shown in Figure 4-10. This phase resembles a model proposed by Adam and Spiess[7]. However, they proposed this phase as a real model of modification A as reported by Ballauff et al[2]. On the basis of former discussion, H-Cn polyesters with different side chain lengths form both phases; model A[7] (reported by Adam and Spiess) and Modification A[2] (reported by Ballauff). The main chains in the layer assume a fully extended conformation with a repeat length of 14 Å that can be elucidated from the height (1/16.6 $Å^{-1}$) of the first layer line from the equatorial line. From the value of b', interchain distance between the aromatic main chains is about 4.9 Å such that the main chain conformation is twisted. This structure is similar to the layered structure reported by Adam and Spiess[7].

The side chains located in the space between the main chain layers are completely in a amorphous state, which could be determined by solid-state ^{13}C NMR spectroscopy. Figure 4-11 shows the spectra for the H-C8 crystal as observed in the range of 0 - 180 ppm. The peaks in the vicinity of 30 ppm can be assigned to the interior CH_2 carbons and have been used to discuss the conformation and crystal structure of the alkyl chains. From reference data on n-alkanes and polyethylene, peak A at 30.1 ppm appears from the carbons in a noncrystalline state. It is interesting that although the side chain is amorphous, the main chains form three dimensional order.

Table 4-4

X-ray Data for the equatorial reflections observed for Km2 crystal of H-C6, H-C8 and H-C10

H-C6				H-C8				H-C10			
d_{obsd} Å	Int.	hk0	d_{calcd} Å	d_{obsd} Å	Int.	hk0	d_{calcd} Å	d_{obsd} Å	Int.	hk0	d_{calcd} Å
12.08	s	100	12.15	12.30	s	100	12.6	15.28	s	100	15.62
8.90	s	-110	8.46	9.87	w	-110	9.11	9.24	m	-110	8.74
6.22	w	200	6.07	6.61	m	200	6.30	7.55	w	200	7.81
5.76	w	-210	5.74	6.00	w	110	6.08			110	7.26
4.73	vvw	020	4.69	5.18	vvw	020	5.18	6.71	w	-210	6.60
4.45	m	210	4.26	4.97	w	-220	4.93	5.39	vvw	300	5.09
4.19	s	-310	4.02	4.58	m	210	4.55			210	5.36
3.70	vw	-320	3.51	4.15	s	300	4.20	4.89	s	-120	4.70
				3.97	w	-320	3.71	4.50	w	120	4.19
										-220	4.37
								4.06	m	-320	3.84
										120	4.19

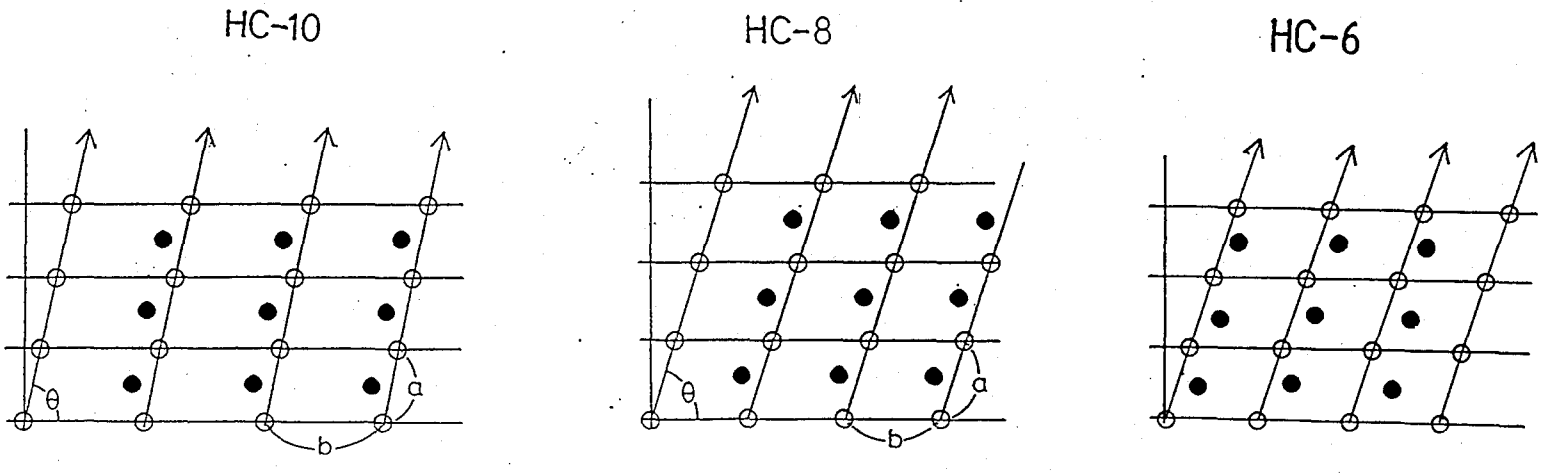

Figure 4-10 Two -dimensional lattices of (a) H-C10, (b) H-C8 and (c) H-C6 as elucidated from the equatorial reflections of the oriented X-ray patterns of Figure 3-8. The open and closed circles in the layers indicate the position of the aromatic main chains.

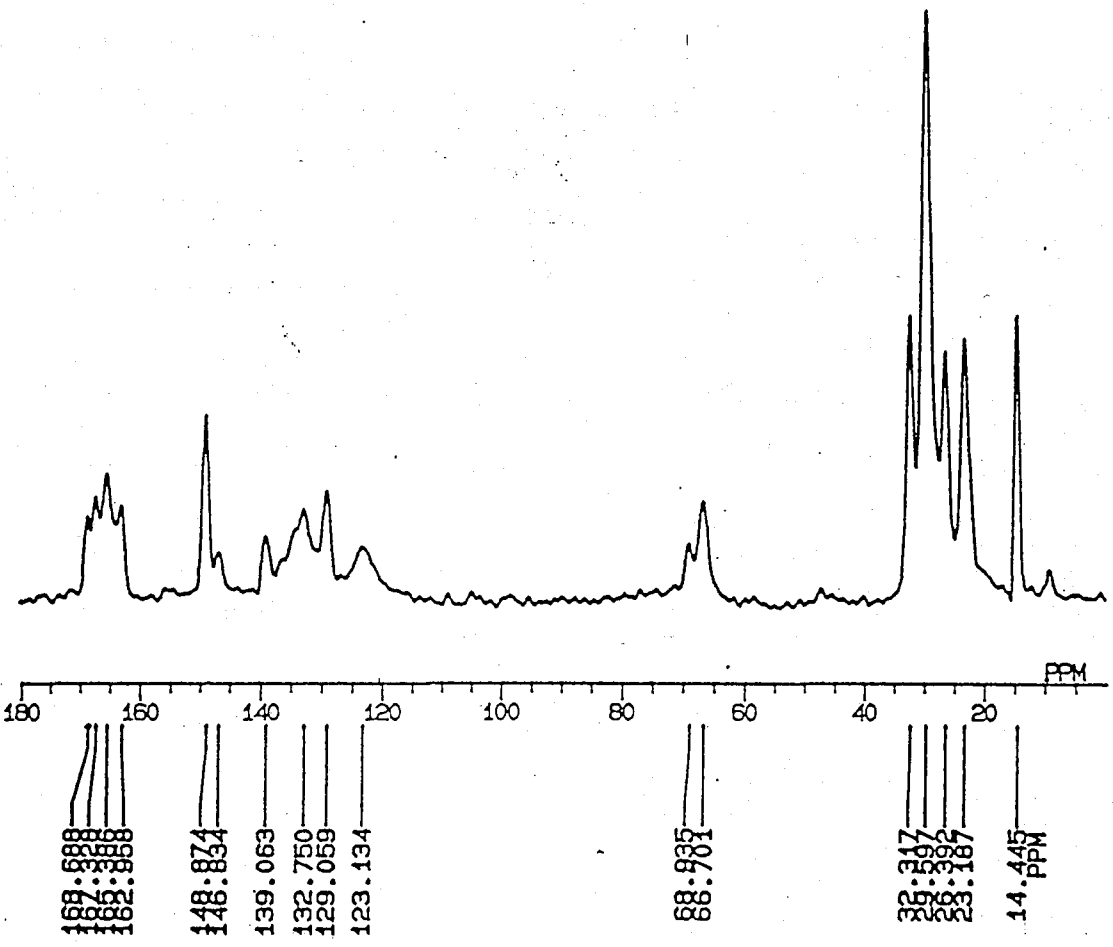

Figure 4-11. Solid state ^{13}C TOSS CP/MAS NMR Spectra of H-C8 polyesters in Km2 crystal.

However, there are a few reports on such a polymeric crystal. Next, the aromatic region show that the main chain conformation is same as Km1 is included in Km2. If the pair of the peaks of the Km1 is subtracted from the spectra of Km2, we can find the other pair. Since the spectrum shows the sharp peaks, in this crystal, the main chains take two confined conformations. Precise study of these conformations is reported in Chapter 5.

[5] Kh crystal

Kh crystal was obtained on annealing a melt-quenched sample at 50-90 °C for more than 1 week. Figure 4-12 shows an oriented crystalline pattern for Km2 and Kh of H-C6. The diffraction pattern includes a number of layer line reflections as well as equatorial reflections, indicating that the crystal structure has three dimensional order. The number of reflections are larger than that in Km2 crystal of the same polyesters. From the equatorial reflections, the crystal lattice is obviously hexagonal; however, a precise determination of the structure is still not complete. Hence, we shall refer to the two dimensional lattice projected along the equatorial reflection profiles.

As listed in Table 4-6, the equatorial reflections include a series of hk0 reflections. These reflections give easy determination of the two dimensional lattice structure. This crystal lattice has a hexagonal symmetry. The hexagonal lattice is illustrated in Figure 4-12, where the lattice constants are given by a = b = 31.7 Å. Considering the density, six numbers of the polyester have to be packed in a unit cell. Comparing the packing modification of Km2 crystal, the packing modification of Kh is proposed as shown in Figure 4-12. In this crystal, the aromatic main chains form a honeycomb-like network. Thus, the main chains are not packed into a layer so that we can suggest the main chain conformation is not confined, unlike in the layered structure. The ^{13}C solid state NMR spectrum of Kh crystal is shown in Figure 4-14. From this figure, it is clear that the main chain conformation is not confined. This result also supports the result that the conformation of all aromatic main chains is confined by monolayer packing.

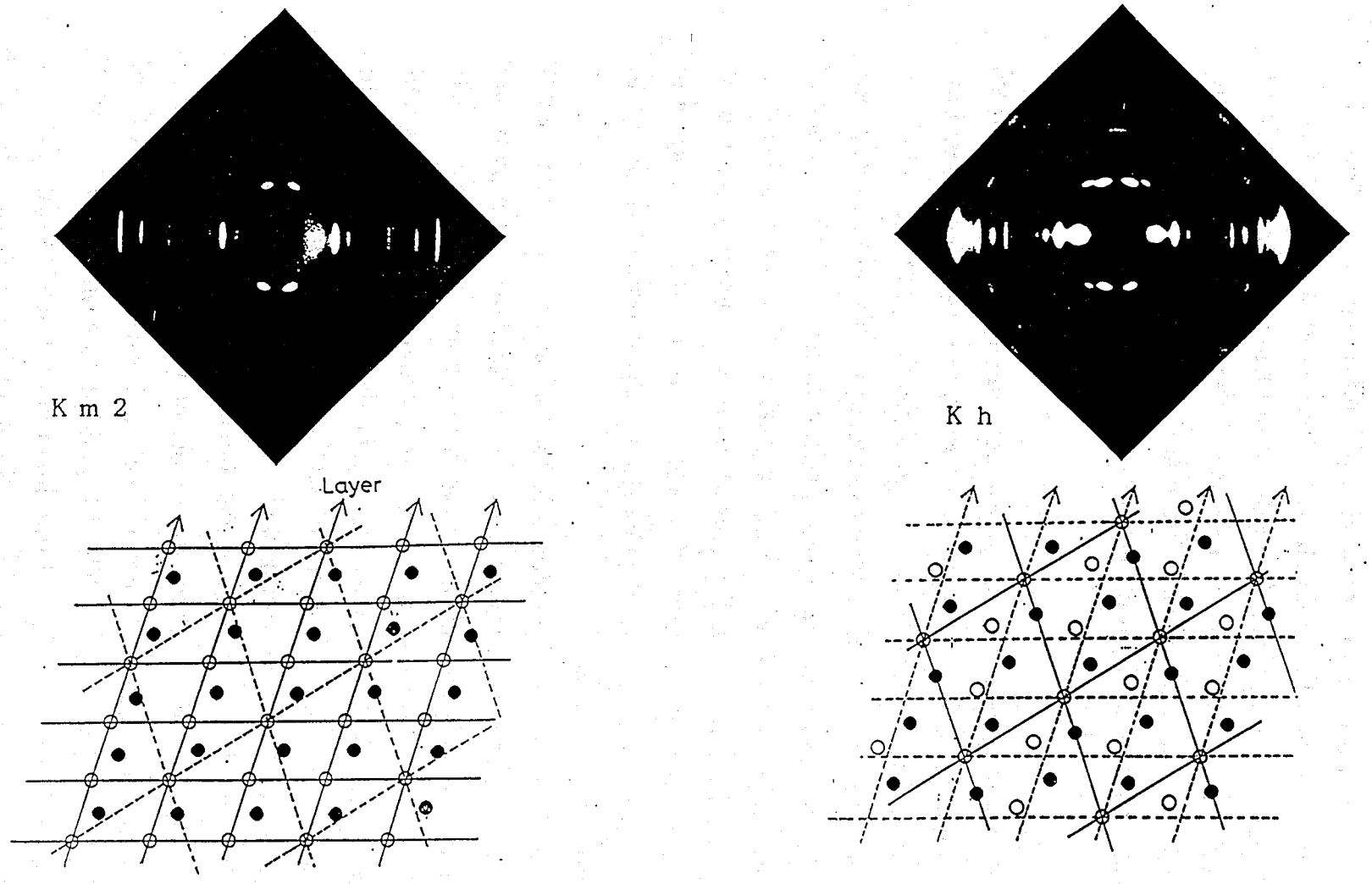

Figure 4-12. Upper: Oriented X-ray patterns of H-C6 crystalline fibers of Km2 and Kh. Here, the fiber axis is oriented in tyhe vertical direction. Lower: Two -dimensional lattices for Kc and Km2 of H-C6 as elucidated from the equatorial reflections of the oriented X-ray patterns. The open and closed circles in the layers indicate the position of the aromatic main chains. Unit cells are drown by rigid line.

Table 4-5
X-ray Data for the equatorial reflections observed for Kh crystal of H-C6

H-C6			
d_{obsd} Å	Int.	hk0	d_{calc} Å
18.82	s	110	18.3
15.75	s	200	15.9
10.88	s	300	10.6
8.86	w	310	8.80
7.93	w	400	7.93
6.29	vw	500	6.34
6.02	vw	420	5.99
5.72	w	510	5.70
5.19	w	430	5.21
4.63	w	440	4.58
4.44	vw	620	4.40
4.23	vw	710	4.20
4.06	vw	540	4.06

4-4 Concluding Remarks

To conclude, the H-Cn polyesters form three type of layered crystals, one layered mesophase and a hexagonal phase in which the aromatic main chains are aggregated like a layer and the alkyl side chains are surrounded by the aromatic layers.

H-Cn polyesters with n = 12 to 18 form two types of layered crystals and a layered mesophase in which the main chains are packed in a monolayer between aliphatic layers. In the two crystals Kc and Km1, the aromatic main chains are in a fully extended form with a repeating length of 14.0 Å and are regularly packed within a layered structure. In addition, the side chains are also in a crystalline state between the layers. The X-ray pattern is indicative of a crystal structure with three dimensional order, which demands that the positional correlation between adjacent layers is maintained with the help of side chain crystals. Thus, the crystalline structure is built up likely by a close coupling of main chain crystals and side chain crystals. The two crystals are different in the main chain packing. In Kc crystal, the interchain length between neighboring main chains is 4.89 Å, which is an ordinary value measured in crystals of an aromatic polyester without side chains. Km1 crystal, however, has an interchain length of about 3.85 Å in aromatic layers, which is unusual for ordinary aromatic polyesters.

Transition from Kc crystal to layered mesophase is irreversible. The layered mesophase changes to Km1 crystal. Sakurai et al. have reported reversible transitions between ordered morphologies for block copolymers in the presence of solvent[35]. It has long been recognized that the morphology observed in a bulk film may depend on the solvent from which the film is cast[36], selecting swelling of one block of the polymer by a preferential solvent may result in a different bulk morphology than that observed when a nonpreferential solvent is used. Such nonequilibrium morphologies are metastable below the glass transition temperatures of one or both blocks in the polymer; annealing the film at elevated temperatures hold in principle return the sample to the equilibrium morphology[31,37,38].

Liquid crystalline phase also has a layered segregated structure similar to

that of the crystalline phase although its fundamental structure is remarkably different in several ways from the crystal structure. The main chains are still in an elongated conformation (a repeat length of 14.0 Å) as in the crystalline phase, but they are packed into a layer having positional order only in the lateral direction and not along the main chain axis. The side chains are included between the layers in a noncrystalline form, which gives rise to the liquid crystalline fluidity of phase. It is interesting to note that the length between neighboring main chains in the mesophase is same as that in Km1 crystal. Hence, Kc crystal does not reverse back to liquid crystal and the packing modification in layered mesophase is stable. This type of liquid crystalline phase appears only for H-Cn with n = 12 to 18, which in turn implies that, the length of the side chains is a significant factor in determinating the nature of the liquid crystalline phase.

When n = 6, 8 and 10, H-Cn forms an individual layered crystal (Km2), with the main chains packed like a zigzag sheet as studied from the equatorial reflection profile of the oriented fiber. In the Km2 crystal, the aromatic main chains are in a fully extended form with a repeating length of 14.0 Å. In addition, the side chains are also in a molten state between the layers, while the X-ray pattern is indicative of a crystal structure with three dimensional order.

H-Cn also forms Kh at temperature lower than Km2. Kh is characterized as a high ordered crystal in which the aromatic layers are deformed to construct the hexagonal lattice with the side chains occupying the space. It might be confusing that the side chains are in an amorphous state when the X-ray diffraction pattern of the oriented sample shows highly ordered crystalline structure.

This dependence of morphology on side chain length is considered to be like a microphase separation of triblock polymers. In fact, Sekine et al report the mesomorphic properties and phase structure of B-n polyester[42].

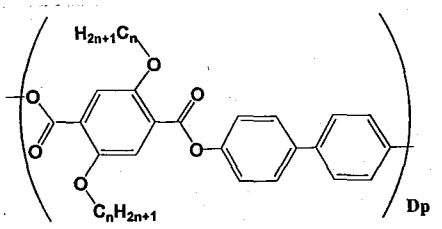

These polyesters form a nematic phase with the layered modification is left. Below the temperature range of nematic phase, B-n with n = 6 to 12 form columnar mesophase in which the aromatic layer is deformed to construct the honeycomb-like network with side chains surrounded by main chain layers. With longer side chains, these polyesters form the layered mesophase. This mesomorphic property may be considered to be a typical type of phase behavior of rigid-rod polyesters with flexible side chains. It is, moreover, a point to emphasize that a charge transfer interaction is less strong between the biphenyl and the 2,5-dialkoxyterephtalic acid moiety in the neighboring main chains. This study of the mesomorphic properties is now being done precisely. It will be reported in the future in more details[42].

In comparing to the phase behavior of B-Cn, H-Cn forms another new layered crystal Km2, in which the main chains are packed like a zigzag sheet. Km2 lies between the layered phase and a cylindrical phase. Hence, this phase can be considered like an intermediate phase similar to that observed in A-B block polymer. The intermediate phase, Km2, is a result of competition between the intermolecular interaction and segregation.

4-5 Reference and notes

(1) Ballauff, M. Macromol. Chem., Rapid Comun. 1986, **7**, 407.

(2) Ballauff, M. Angew. Chem., Int. Ed. Engl. 1987, **28**, 253.

(3) Ballauff, M.; Schmidt, G. F. Mol.Cryst.Liq.Cryst. 1987, **147**, 163.

(4) Stern, R.; Ballauff, M.; Wegner, G. Macromol. Chem., Macromol. Symp. 1989, **423**, 373.

(5) Rodrigues-Parada, J. M.; Duran, R.; Wegner, G. Macromolecules 1989, **22**, 2507.

(6) Ebert, M.; Herrmann-Schenherr, O.; Wendorf, J.; Ringsdorf, H.; Tschirner, P. Liq. Cryst. 1990, **7**, 63.

(7) Adam, A.; Spiess, H. W. Macromol. Chem., Rapid Comun. 1990, **11**, 249.

(8) Frech, C. H.; Adam, A.; Falk, U.; Boeffel, C.; Spiess, H. W. New Polym. Mater. 1990, **2**, 267.

(9) Stern, R.; Ballauff, M.; Lieser, G.; Wegner, G. Polymer 1991, **32**, 2079.

(10) Harkmess, B. R.; Watanabe, J. Macromolecules 1991, **24**, 6759.

(11) Watanabe, J.; Harkness, B. R.; Sone, M. Polym. J. 1992, **24**, 1119.

(12) Cervinka, L.; Ballauff, M. Colloid Polym. Sci. 1992, **270**, 859.

(13) Sone, M.; Harkness, B. R.; Watanabe, J.; Torii, T.; Yamashita, T.; Horie, K. Polym. J. 1993, **25**, 997.

(14) Galda, P.; Kistner, D.; Martin, A.; Ballauff, M. Macromolecules 1993, **26**, 1595.

(15) Marz, K.; Lindner, P.; Urban, J.; Ballauff, M.; Fisher, E. W. Acta Polym. 1993, **44**, 139.

(16) Damman, S. B.; Mercx, F. R. P.; Kootwijk-Damman, C. M. Polymer 1993, **34**, 1891.

(17) Damman, S. B.; Mercx, F. P. M. J. Polym. Sci., Polym. Phys. 1993, **31**, 1759.

(18) Damman, S. B.; Mercx, F. P. M. J.; Lemstra, P. J. Polymer 1993, **34**, 2726.

(19) Damman, S. B.; Vroege, G. J. Polymer 1993, **34**, 2732.

(20) Kakimoto, M.; Orikabe, H.; Imai, Y. ACS Polym. Prep. 1993, **34**, 746.

(21) Steuner, M.; Hortz, M.; Ballauff, M. J. Polym. Sci., Polym. Chem. 1993, **31**, 1609.
(22) Watanabe, J.; Harkness, B. R.; Sone, M.; Ichimura, H. Macromolecules 1994, **27**, 507.
(23) Sone, M.; Harkness, B. R.; Kurosu, H.; Ando, I.; Watanabe, J. Macromolecules 1994, **27**, 2769.
(24) Damman, S. B.; Buijs, J. A. H. M. Polymer 1994, **35**, 2559.
(25) Damman, S. B.; Buijs, J. A. H. M.; van Turnhout, J. Polymer 1994, **35**, 2364.
(26) Buijs, J. A. H. M.; Damman, S. B. J. Polym. Sci.; Polym. Phys. 1994, **32**, 851.
(27) Tiesler,U.; Pulina,T.; Rehahn,M.; Ballauff,M.; Mol.Cryst.Liq.Cryst. 1994, **41**,525.
(28) Voigt-Martin, I. G.; Simon, P.; Bauer, S.; Ringsdorf, H. Macromolecules 1995, **28**, 236.
(29) Voigt-Martin, I. G.; Simon, P.; Yan, D.; Yakimansky, A.; Bauer, S.; Ringsdorf, H. Macromolecules 1995, **28**, 243.
(30) Molau, G.E.; Block Polymers, Ed. by Aggarwal, S.L.; Plenum (1970).
(31) Thomas, E.L.; Alward, D.B.; Kinning, D.J.; Martin, D.C.; Handlin, D.L.Jr.; Fetter, L.J. Macromolecules, 1986, **19**, 2197.
(32) Herman, D.S.; Kinning, D.J.; Thomas, E.L.; Fetter, L.J. Macromolecules,1987, **20**, 2940.
(33) Hasegawa, H.; Tanaka,H.; Yamasaki, K.; Hashimoto, T. Macromolecules, 1987, **20**, 1651.
(34) Hajduk, D.A.; Gruner, S.M.; Rangarajan, P.; Register, R.A.; Fetter, L.J.; Honeker, C.; Albalok, R.J.; Thomas, E.L. Macromolecules, 1994, **27**, 490.
(35) Sakurai, S.; Hashimoto,T.; Fetters,L. J.Polym.Prep.Jpn. 1991,**40(3)**,770.
(36) Cohen,R.E.; Bates,F.S. J.Polym.Sci.Polym.Phys.Ed. 1980,**18**,2143.
(37) Sakurai,S.; Momii,T.; Taie,K.; Shibayama,M.; Nomura,S.; Hashimoto,T. Macromolecules 1986, **26**, 485.
(38) Sakurai,S.; Hasegawa, H.; Hashimoto, T.; Polym.Prep.Jpn. 1990, **39(3)**, 387.

(39) Yamagishi, T.; Fukuda, T.; Miyamoto, T.; Ichizuka, T.; Watanabe,J. Liq.Cryst. 1990, **7**,155.
(40) Yamagishi, T.; Fukuda, T.; Miyamoto, T.; Yakoh, Y.; Takashina, Y.; Watanabe, J. Liq. Cryst. 1991,**10**, 467.
(41) Erman, B.; Flory, J.J.; Hummel, J.P. Macromolecules 1980, **13**, 484.
(42) Sekine, N.; Sone, M.; Watanabe,J.; Kricheldorf, H.F. Macromolecules in press.

Chapter 5

Chain Conformation of B-Cn Polyesters in Layered Crystalline Phases and Mesophases Analyzed by High Resolution Solid-State ^{13}C NMR Spectroscopy.

5-1 Introduction

Over the past several years, there has been a considerable amount of effort directed towards the study of rigid-rod polyesters with long flexible side chains as a consequence of their ability to form thermotropic liquid crystalline phases. Rigid-rod aromatic polyesters with long flexible alkyl side chains form thermotropic phases but in this case they exhibit novel layered structures[1-29]. These layered structures are characterized by a lateral packing of the aromatic main chains into layers with the fluid-like alkyl side chains occupying the space between the layers. It has been postulated that the driving force for the adoption of such a structure is a segregation of the aliphatic and aromatic domains. In these layered structures, the liquid crystallinity is the results of a partial or total lack of positional order with respect to the main chain packing within the layers and also by the fluid-like disordered alkyl side chains between the layers[6,22]. The crystalline phases that develop from the layered mesophases also have a layered structure. In this case, X-ray studies have shown that the main chains and side chains crystallize in a cooperative fashion[12,22].

In these layered structures, it is of interest to determine how the aromatic main chains are packed into a monolayer, their conformation is presumed to be different from that observed in aromatic polymers without side chains. Furthermore, the main chain conformation may also be affected by how the surrounding alkyl side chains are accommodated into the space between the layers. In fact, several types of layered crystals and mesophases have been observed with different packing modifications[7-9,22], suggesting a plurality of aromatic main chain conformations.

The objective of this work has been to examine the main chain and side

chain conformations in the layered crystals and mesophases of the B-Cn polyesters, through the use of high resolution solid-state ^{13}C NMR. Furthermore, an attempt has been made to interpret these spectra and estimate the polymer conformation by considering the ^{13}C NMR shielding constants and performing total energy calculations using the FPT (finite perturbation theory) method within the INDO framework[30-34].

5-2 Experimental Section

The Synthesis of B-Cn polyesters (n; the carbon number of the alkyl side chain)

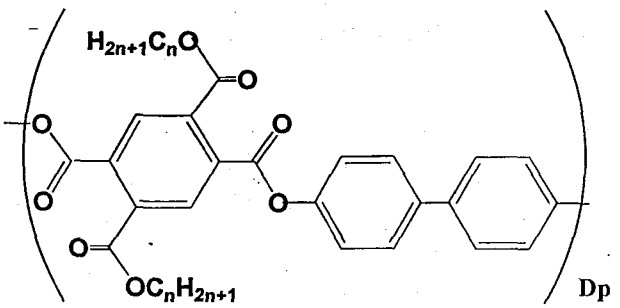

has been described in a Chapter 2. Here, the B-Cn polyesters with n = 6 to 18 were employed[10].

^{13}C MAS NMR spectra were recorded on a JNM GSX-270 NMR spectrometer operating at 67.8 MHz with cross polarization/magic angle spinning (CP/MAS) and variable temperature (VT) accessories. Samples were contained in a cylindrical rotor composed of zirconia with an O-ring and spun at speeds up to 4.0 kHz as controlled by a spinning controller. The contact time was 2.0 ms, and the repetition time was 3-6 s. The radio-frequency (rf) field strength was 60 kHz. Spectra were observed by the accumulation of 500-1000 scans so as to achieve a reasonable signal-to noise ratio. The ^{13}C chemical shifts were calibrated indirectly with adamantane as the external standard (29.5 ppm relative to tetramethylsilane). ^{13}C MAS NMR spectra for the crystalline phases were observed by the CP/MAS method, while those for the liquid crystalline and isotropic phases were observed by the gated decoupling/MAS method.

The ^{13}C NMR shielding constant and the total energy calculations for the model compounds were performed using the INDO method incorporated with the FPT method. The negative sign of the calculated ^{13}C NMR shielding means deshielding. The bond lengths and bond angles of a model compound as described by Coulter and Windle are shown later in Figure 5-8. The calculations were carried out as a function of the torsion angles by using a SUN SPARC station 2.

5-3 Results and Discussion

[1] Thermotropic Phase Behavior and Phase Structure of the B-Cn Polyesters

In our previous studies[10,13,22], we reported that the B-Cn polyesters form two layered crystals (K1 and K2) and two liquid crystalline phases (LC-1 and LC-2). The phase behavior depends on the side chain length as depicted in Figure 8-1.

In the layered K1 and K2 crystalline phases, the aromatic main chains are in a fully extended conformation with a repeat length of 16.6 Å and these are regularly packed within a layer. In addition, the side chains are also in a crystalline state between the layers. The X-ray pattern is indicative of a crystal structure with three-dimensional order, which demands that the positional correlation between adjacent layers is maintained through the side chains crystals. Thus, the crystal structure is likely built up by a close coupling of main chains crystals and side chain crystals. It is interesting to note that the main chains in the K1 and K2 crystals are packed in a different manner. For the K1 crystal, which is formed from the B-Cn polyesters with side chains shorter than n = 12, the lateral packing distance of the main chains within a layer is 4.6 Å, but this reduces to 3.45 Å for the K2 crystal in the B-Cn polyesters with side chains longer than n = 16. The polyester B-C14 has been found to have characteristics of both types of crystalline phases depending on the crystallization temperature. The packing distance of 4.6 Å in the K1 crystal is reasonable for the main chains in a stable twisted conformation. In contrast, the short spacing of 3.45 Å in the K2 crystal indicates an unusually dense packing of the main chains that requires a conformation in which all the phenyl rings adopt a coplanar arrangement.

The LC-2 phase, the lower temperature mesophase, also has a layered segregated structure similar to that of the crystalline phase although its fundamental structure is remarkably altered in several aspects from the crystal structure. The main chains are still in an elongated conformation (a repeat length of 16.6 Å) as in the crystalline phase, but they are packed

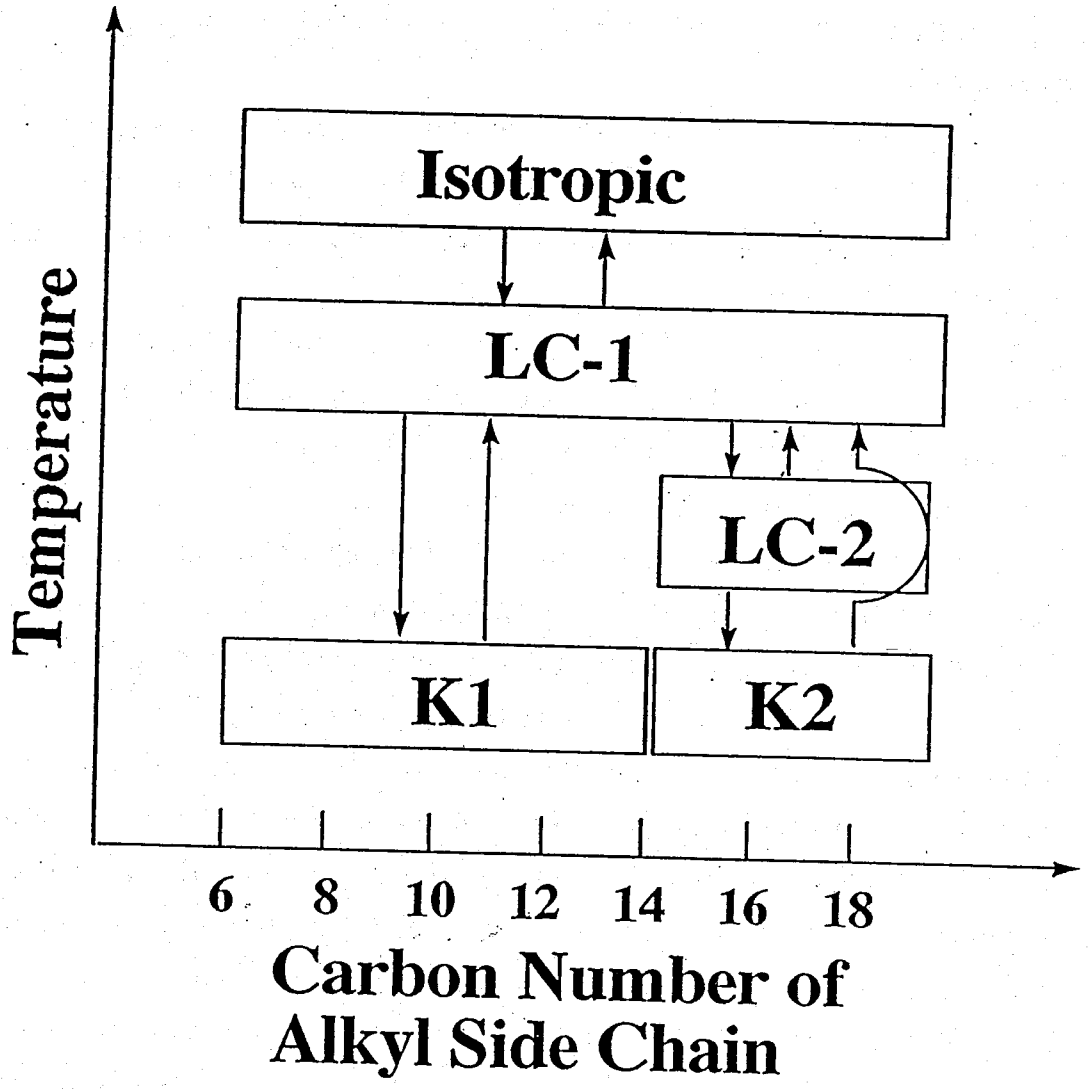

Figure 5-1. Schematic illustration of thermotropic phase behavior in B-Cn polyesters.

into a layer having positional order only along the chain axis but not in the lateral direction. The side chains placed between the layers are in a molten state, which gives rise to the liquid crystalline fluidity of the phase, This type of liquid crystalline phase appears only for the B-Cn polyesters in which the alkyl side chains are longer than n = 14 (see Figure 5-1).

The LC-1 phase, the higher temperature mesophase observed for all specimens, displays a nematiclike optical texture, but a classic nematic phase cannot be postulated because it still exhibits a lateral packing spacing as large as that in the LC-2 phase. A biaxial nematic phase has been tentatively proposed such that the layers are retained, but there are frequently irregularities in their packing.

This paper begins with an analysis of the main chain and side chain conformations in the layered K1 and K2 crystals, and in subsequent sections this is extended to measurements of the layered LC-1 and LC-2 mesophases.

[2] ^{13}C NMR Studies of the Layered K1 and K2 Crystals

The solid-state ^{13}C NMR spectra of these polymers in the aromatic and carbonyl regions were found to be rather complicated due to a large number of side bands resulting from the large anisotropy of the individual shielding tensors[30]. In order to eliminate the side bands, thus simplifying the spectra, total suppression of side band (TOSS) spectra was recorded. A typical example is shown in Figure 5-2 for B-C6 in the crystalline state. Here, the peaks in the region of 100-180 ppm can be assigned to the aromatic main chain carbons and the peaks in the region of 10-80 ppm to the aliphatic side chain carbons.

The clear resolution of the component carbon atom signals is extremely advantageous in attempting to elucidate the conformation of the polymer in the two different crystalline phases, K1 and K2 phases. Figure 5-3 shows ^{13}C TOSS CP/MAS spectra for B-Cn polyesters in the crystalline state as obtained by annealing for 1 week at 80 °C. According to these spectra, two types of crystalline modifications are different with respect to their main-chain conformations and intermolecular interactions. It is interesting to note here that the B-C14 polyester exhibits an NMR spectrum characteristic

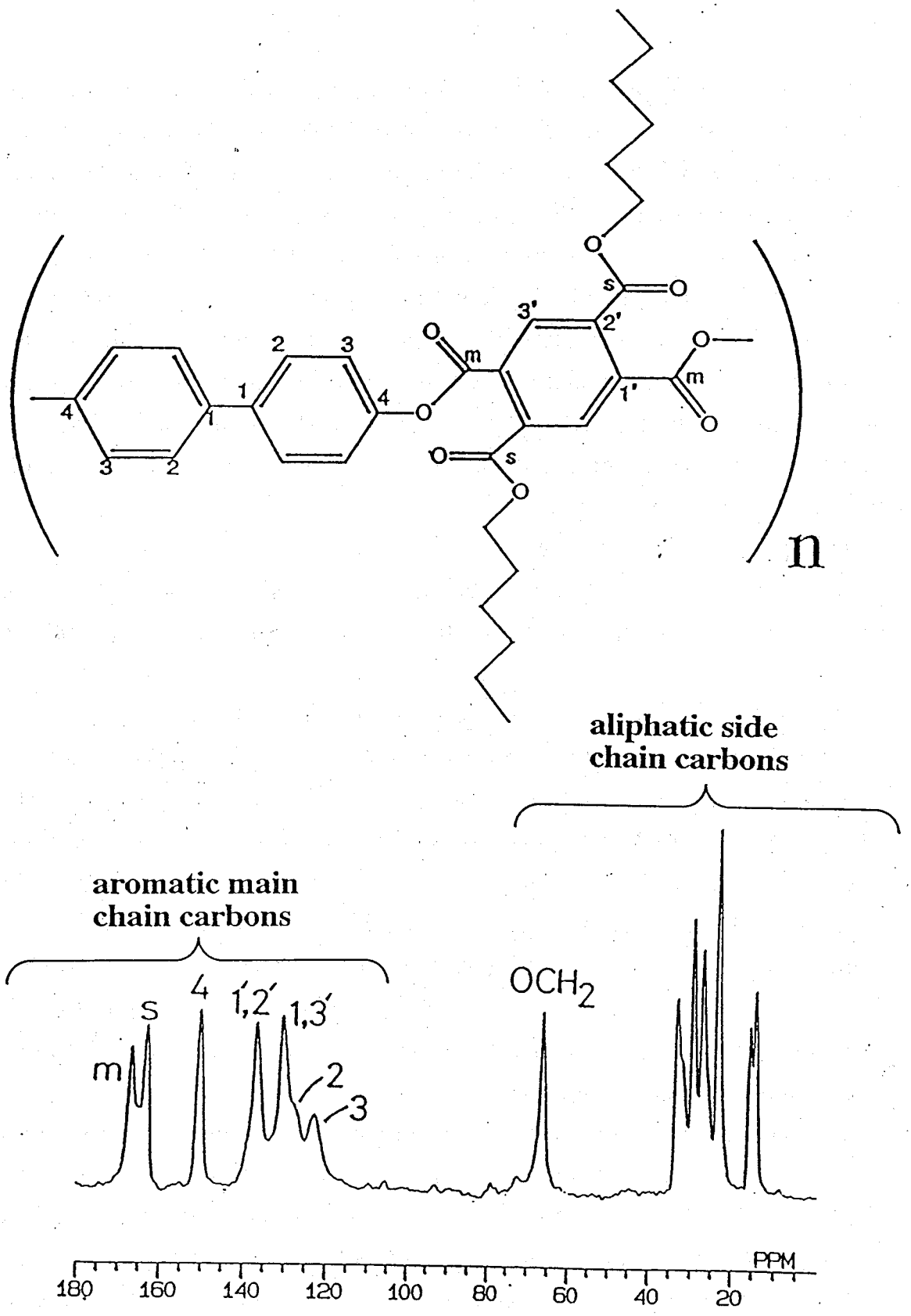

Figure 5-2. The ^{13}C TOSS CP/MAS spectrum as observed for the crystalline phase of B-Cn with peak assignments.

of both crystalline modifications are different with respect to their main chain conformations and intermolecular interactions. It is interesting to note here that the B-C14 polyester exhibits an NMR spectrum characteristic of both crystalline forms and thus its crystalline phase is bimorphic. These results agree with X-ray diffraction data[10,22].

In order to obtain information concerning the conformation of the polymer, it is first necessary to accurately assign the peaks in the ^{13}C NMR spectrum. To accomplish this, the NMR spectra of the crystalline polymers were measured using the dipolar dephasing method with a delay time of 60 μs, a typical example of which is shown in Figure 5-4 for the K1 crystal of B-C12 and the K2 crystal of B-C16. These data, together with the reference data, allow a well-defined assignment of the chemical shifts, which are given in Figure 5-2 and summarized in Table 5-1 and 5-2. According to these tables, there are three distinct differences between the chemical shifts for the K1 and K2 crystals. First, the chemical shifts for the higher field carbonyl carbon atoms of the pyromellitic ester moiety are different. Second, the number of aromatic carbon peaks are different. Third, the aliphatic signals indicate that there are differences in the state of the alkyl side chain crystals. Thus, we can come to a preliminary conclusion that two crystals are different in the conformation of the pyromellitic ester, biphenyl, and alkyl side chain moieties.

2-1 Main-Chain Conformation

At first, we shall focus on the main chain conformation. In order to discuss the relationship between the main chain conformation and chemical shifts, the possibility of intermolecular interactions between neighboring aromatic main chains that can contribute to the chemical shift values must be taken into consideration. In this aromatic polymeric system, electrostatic interactions may occur. In fact, it has been found that a charge transfer complex is formed between neighboring biphenyl and the pyromellitic ester moieties in both the layered crystals and mesophases[13]. Simons and Natansohn, however, have reported that even strong charge transfer complex formation without conformational change results in ^{13}C NMR chemical

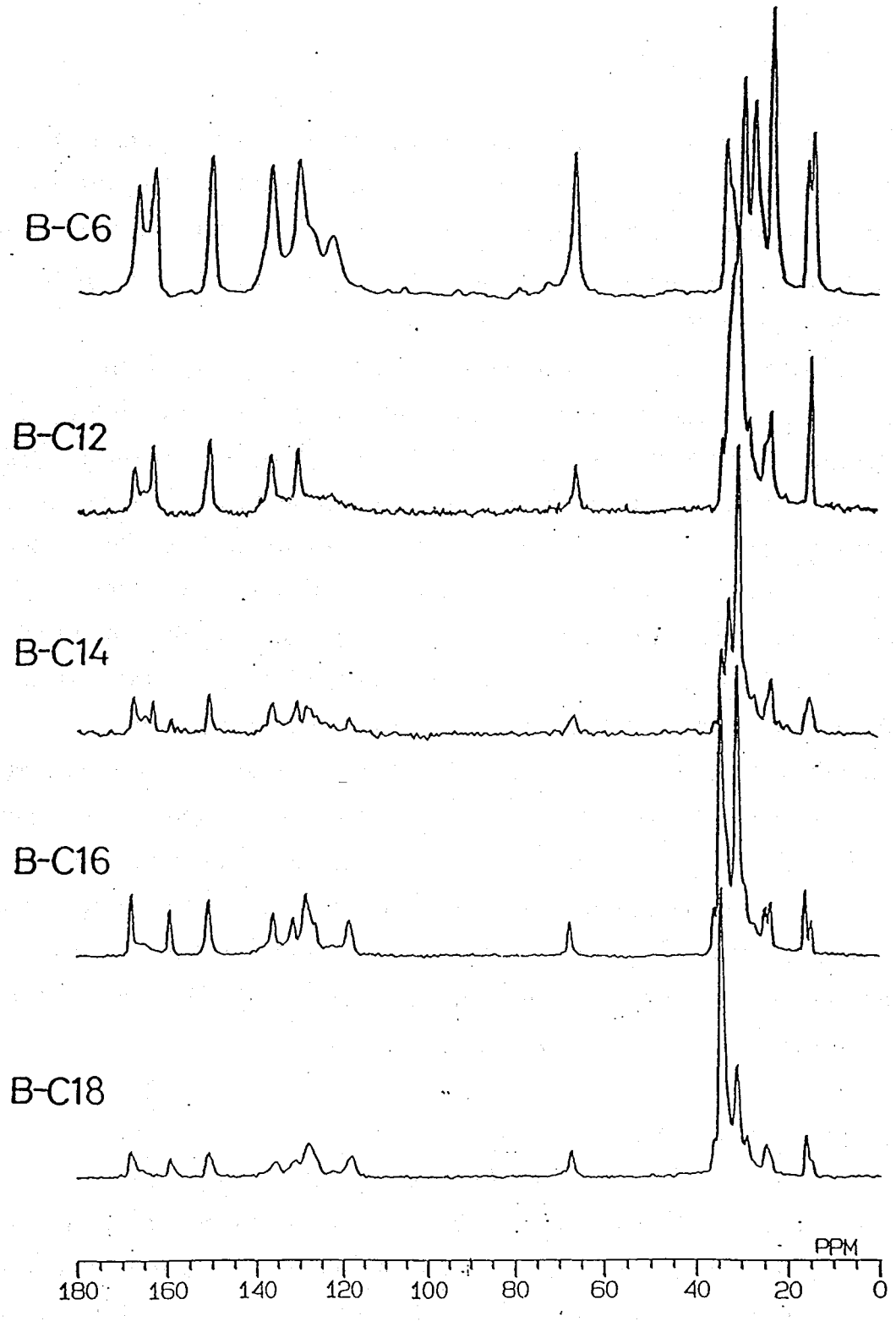

Figure 5-3. ^{13}C TOSS CP/MAS NMR spectra of the B-Cn polyesters in the crystalline state.

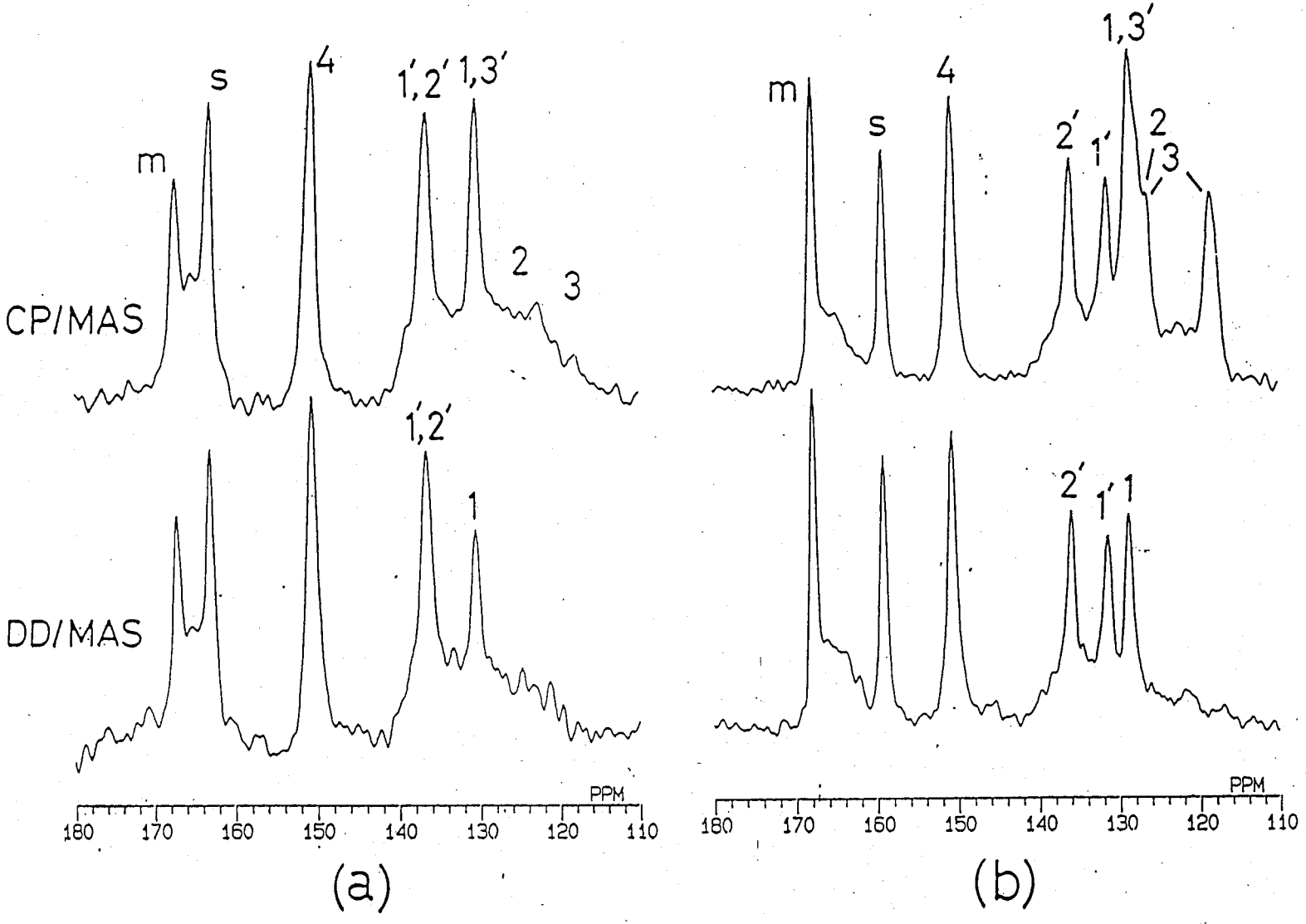

Figure 5-4. Expanded aromatic region of the ^{13}C MAS spectra for the two typical B-Cn crystals using CP and dipolar dephasing (DD) methods; a) the K1 crystal of the B-C12 polyester and b) the K2 vrystal of the B-C16 polyester.

Table 5-1
Observed ^{13}C NMR Chemical shifts for the aromatic carbons of the B-Cn polyesters in the crystalline state.

	Observed ^{13}C NMR Chemical shift (ppm)								
	C=O								
	m[a]	s[b]	C4	C1'	C2'	C3'	C1	C2	C3
B-C16soln[c].	165.5	164.7	150.2	134.6		130.0	130.0	128.3	121.5
K1 Crystal									
B-C6	167.5	163.5	150.7	136.1		130.0	130.0	128.0	122.8
B-C12	167.3	163.2	150.5	136.5		130.4	130.4	128.0	122.6
B-C14	167.3	163.2	150.5	136.5		130.4	130.4	128.0	122.6
K2 Crystal									
B-C14	167.6	158.8	150.6	136.0	131.5	130.0	128.0	128.0	126.2,117.8
B-C16	168.0	159.2	150.7	135.9	131.4	130.3	128.5	127.8	126.4,118.5
B-C18	168.1	158.2	150.9	135.6	131.0	130.1	128.1	128.1	126.2,118.4

m[a]; main chain s[b]; side chain c; $CDCL_3$ solution

Table 5-2
^{13}C NMR chemical shifts for the aliphatic carbons of the B-C18 polyesters at various temperatures

	^{13}C NMR chemical shifts / ppm						
		Interior CH_2*		α		CH_3	
Temp/°C	OCH_2	Cryst.	Amor.	Cryst.	Amor.	Cryst.	Amor.
B-C16 soln.[a]	66.8		29.7		22.7		14.1
K1 Crystal							
B-C6	66.3				23.4	15.7	14.4
B-C12	65.8	32.0	30.4		23.4		14.7
B-C14	66.3	32.3	30.4		23.2		15.0
K2 Crystal							
B-C14	67.3	33.9	30.3	24.6	23.2	16.1	14.8
B-C16	67.3	34.3	30.5	24.6	23.5	16.1	14.8
B-C18	67.1	34.2	30.7	24.6	23.5	16.1	14.9

*Cryst. and Amor. indicate the crystalline and noncrystalline state, respectively. a; $CDCl_3$ solution.

shift of about 1 ppm[39]. Thus, we have concluded that the chemical shift behavior is mainly influenced by the conformation of the aromatic main chains and the influence of intermolecular interactions on the ^{13}C NMR chemical shift values can be considered as being negligible.

Conformation of the Pyromellitic Ester Moiety Figure 5-5 shows schematically the ^{13}C NMR chemical shifts with their assignments for the carbon atoms of the pyromellitic ester moieties as measured for the K1 and K2 crystals. Two sharp peaks due to the main chain and side chain carbonyl carbons in the K1 crystals are observed at 167.5 and 163 ppm, respectively, whereas in the K2 crystal they appear at 167.5 and 159 ppm. The two aromatic carbons, C1' and C2', are observed as a single sharp peak at 136 ppm in the K1 crystal, but in the K2 crystal they are split into two sharp peaks at 131 and 136 ppm with equivalent intensities. The aromatic carbon C3' is observed at 130 ppm in both crystals. These results indicate that there is a remarkable difference in the conformation of the pyromellitic ester moieties between the K1 and K2 crystals.

As shown in Figure 5-6, four possible conformations can be considered for the pyromellitic ester moieties under the reasonable assumption that the ester groups are coplanar with the aromatic moiety. These conformations can be classified into two groups as follows. In models i and iii, a 180° rotation about an axis (a dashed line in Figure 5-6) drawn between the C1' and C2' atoms fails to superimpose the carbonyl functionalities, resulting in the C1' and C2' carbon atoms experiencing different electronic environments with different chemical shifts. In contrast, superpositioning is possible in models ii and iv. Hence, the electronic environment (or the chemical shift) for C1' and C2' should be the same. Of these two conformations ii and iv, conformation iv can be eliminated as a possibility because of the steric hindrance between the carbonyl oxygen atoms which would be forced to occupy positions in which the intermolecular distance is less than that required to accommodate the van der Waals radii.

As compared with the observed data, the pyromellitic ester moieties in the K1 crystal can be postulated to assume conformation ii. This conclusion

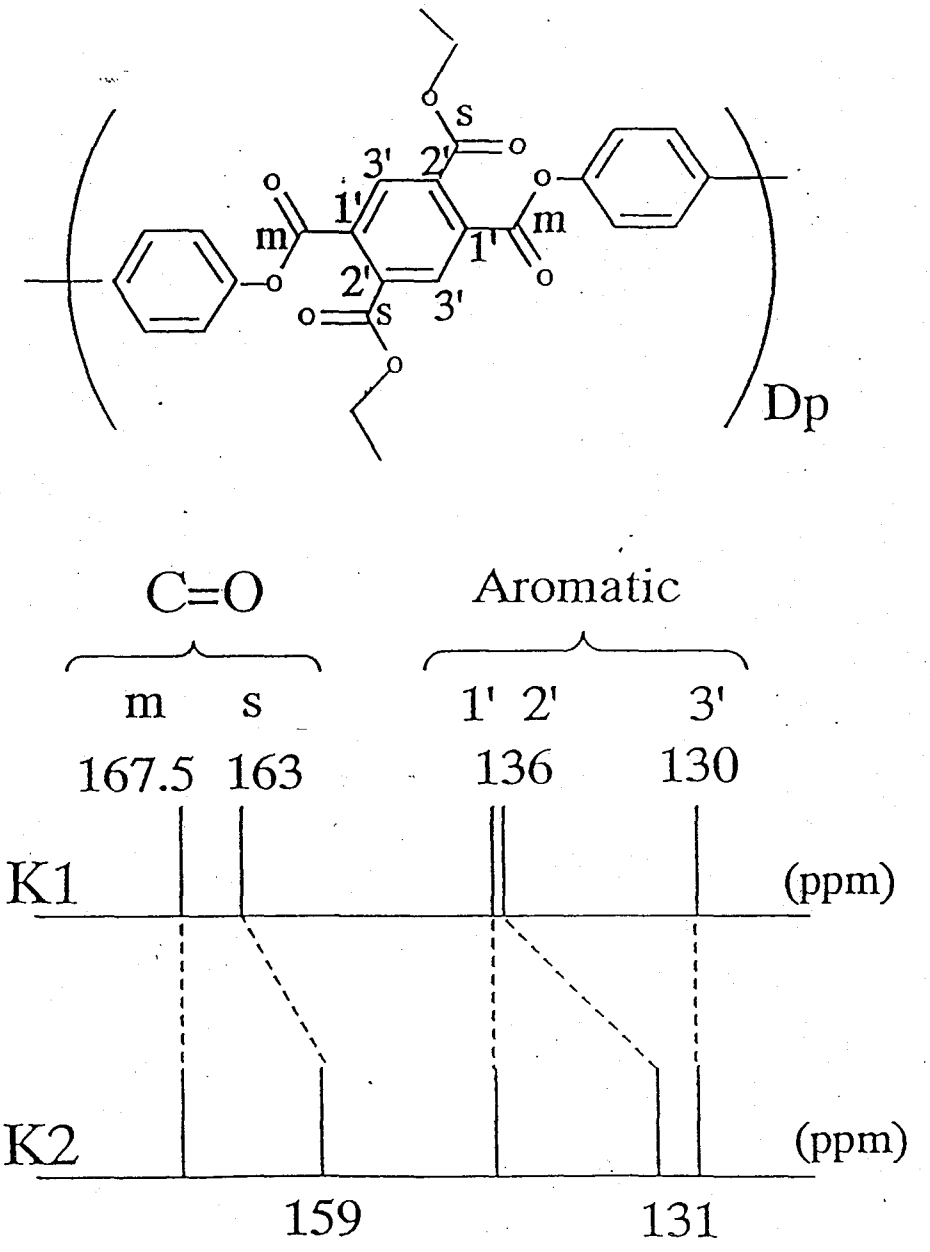

Figure 5-5. Diagram of the observed ^{13}C chemical shifts for the carbons of the pyromellitic ester moiety in the K1 and K2 crystals.

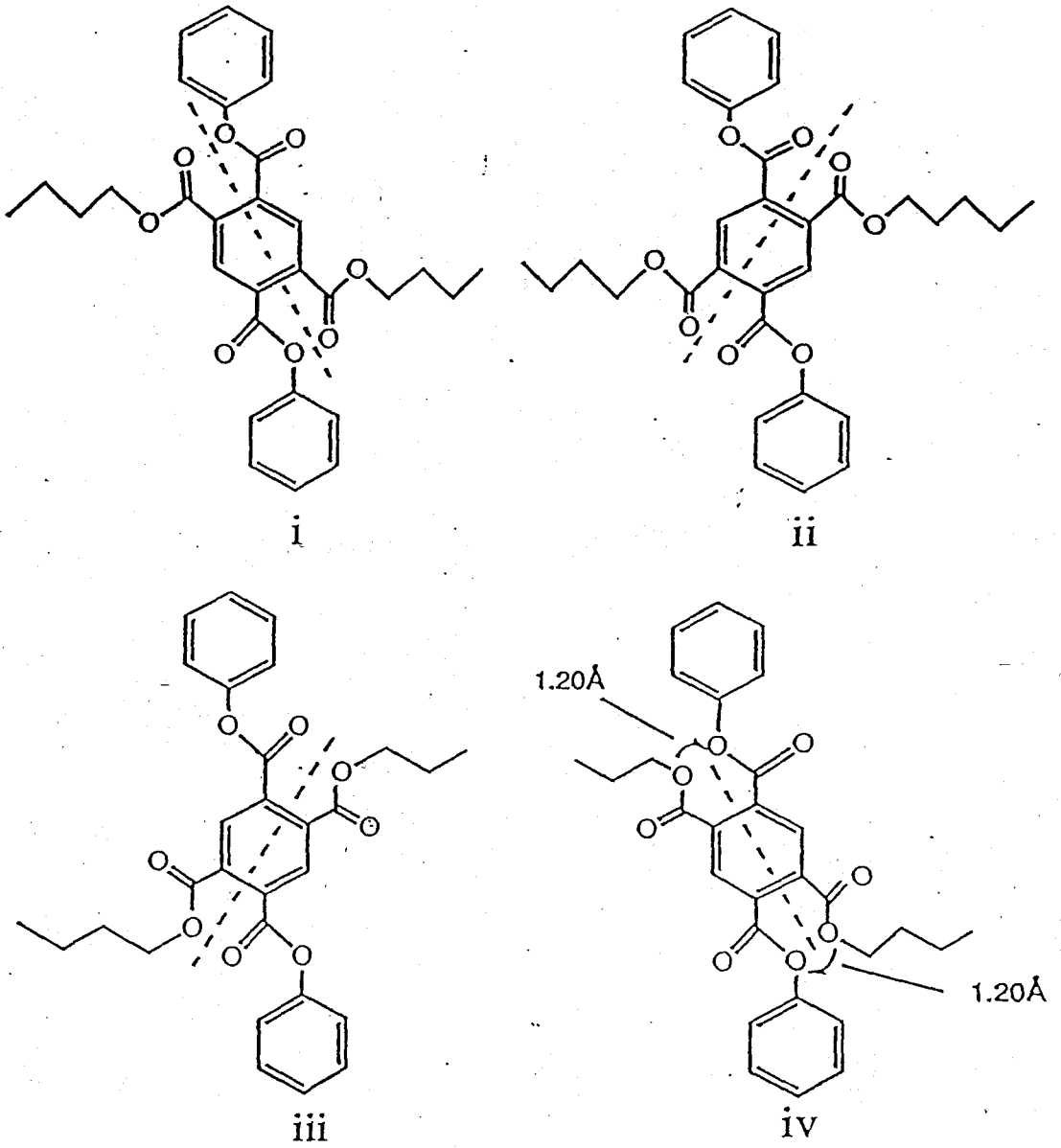

Figure 5-6. Four possible conformations for the pyromellitic ester moieties of B-Cn polyester.

is in agreement with the solution-state ^{13}C NMR study of benzenepolycarboxylic acids by Bruck and Rabinovits, in which the pyromellitic acid moieties in DMSO solution assume conformation ii, with the C1' and C2' carbons appearing as a single peak at 135.3 ppm[35]. The conformation of the pyromellitic ester moieties in the K2 crystal is believed to be either conformation i or iii. INDO calculations of a model compound indicate that conformation iii is more stable than conformation i and so may represent the conformation of the pyromellitic ester moiety in the K2 crystal.

Conformation of the Biphenyl Moiety Figure 5-7 illustrates the observed ^{13}C chemical shifts with their assignments for the carbons of the biphenyl moieties in the K1 and K2 crystals. A difference in the conformation of the biphenyl moieties in the two crystals is apparent. Both crystals show the same chemical shifts at 128 and 150 ppm for the C2 and C4 carbons, respectively, but the values for the C1 and C3 carbons are remarkably different (130 ppm for the C1 carbon and 123 ppm for the C3 carbon in the K1 crystal; 128 ppm for the C1 carbon and 126 and 118 ppm for the C3 carbon in the K2 crystal).

It is known that the two phenyl rings of the biphenyl moiety can rotate around the linking bond. It is also well-known that the most stable conformation for the biphenyl group is one in which the phenyl rings are twisted relative to each other. In addition, such a twisted conformation is preferred in solution and the isotropic melt. The chemical shifts determined for the isotropic solution and melt of B-C16 are listed in Table 5-4. It is interesting to note that these chemical shifts are quite similar to those in the K1 crystal. This leads to the simple conclusion that the biphenyl group in the Ka crystal assumes a twisted conformation as in solution and the isotropic melt and dictates that in the K2 crystal the biphenyl group assumes as anomalous conformation.

This conclusion is consistent with that deduced from the X-ray observation, according to which the molecular distance of 3.45 Å between neighboring main chains within a layer is unusually short in the K2 crystal relative to

the value (4.7 Å) in the K1 crystal[22]. The latter value can be expected for a twisted conformation, but the former value, corresponding to the van der Waals radius of the phenyl ring, can be accounted for only by a coplanar arrangement of the aromatic groups. It is therefore proposed that the difference in the chemical shift values, especially for the C1 and C3 carbons between K1 and K2, is due to this conformational difference.

To test this hypothesis, the INDO calculations of the total energy and ^{13}C NMR shieldings for the model compound of Figure 5-8 were performed as a function of the two torsion angles, ψ and ϕ, which correspond to the angles between the two phenyl rings in the biphenyl moiety and between the phenyl rings of the biphenyl and pyromellitic moieties, respectively (refer to Figure 5-9)., The geometric parameters given in Figure 5-8 are based upon X-ray diffraction data of aromatic ester compounds[40]. In performing the calculation, it was hypothesized that the carbonyl group and aromatic group of the pyromellitic ester moiety are coplanar[40]. Furthermore, it was presumed that the two pyromellitic ester moieties surrounding the biphenyl groups lie on the same plane, as shown in Figure 5-9. This is based upon X-ray data which indicates that the repeat distance along the chain axis corresponds to the length of the repeat unit in the polymer. Under these assumption, the calculations can be performed such that the torsion angles ψ and ϕ are varied under the condition of $\psi = 2\phi$ (refer to Figure 5-9).

Figure 5-10 and 5-11 show the variations of the total energy and the calculated ^{13}C NMR shieldings with the torsion angle ψ, respectively. It is apparent from Figure 5-10 that the twisted conformation with $\phi = 120°$ and $\psi = 60°$ is the most stable. It should be noted here that these values of ϕ and ψ are approximate to those which have been evaluated for the most stable conformations[40,42,43]. Furthermore, this figure also indicates that the coplanar conformation ($\phi = \psi = 0°$) is very stable, being approximately 20 kcal/mol less stable than the most stable twisted conformation. Thus, the coplanar conformation expected for K2 crystal is strongly disfavored.

From Figure 5-11, on the other hand, one can find that the chemical shifts strongly depend on the torsion angle ψ so as to allow the deduction

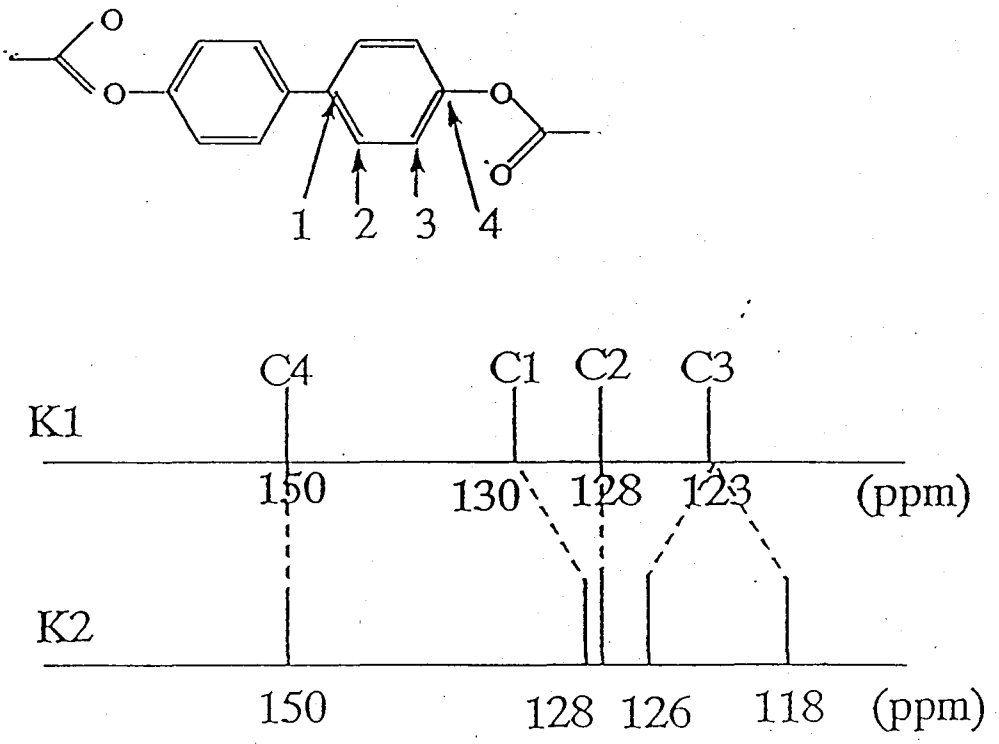

Figure 5-7. Diagram of the observed ^{13}C NMR chemical shifts of the carbons in the biphenyl moiety in the K1 and K2 crystals.

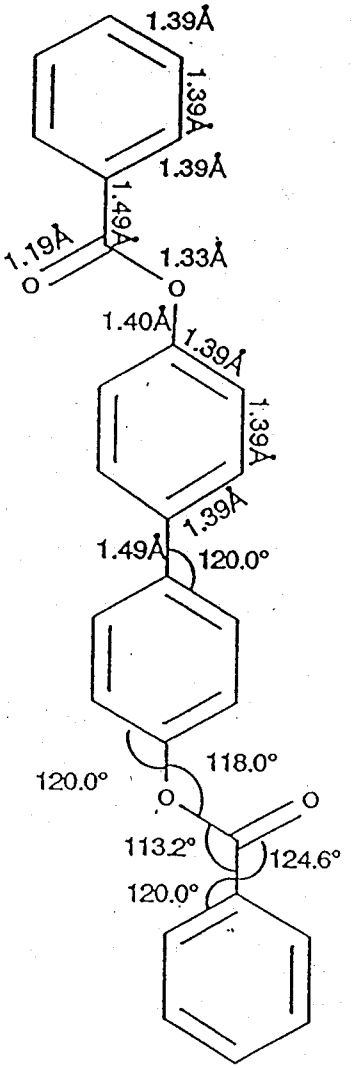

Figure 5-8. The model compound and the geometric parameters for the FPT-INDO calculation.

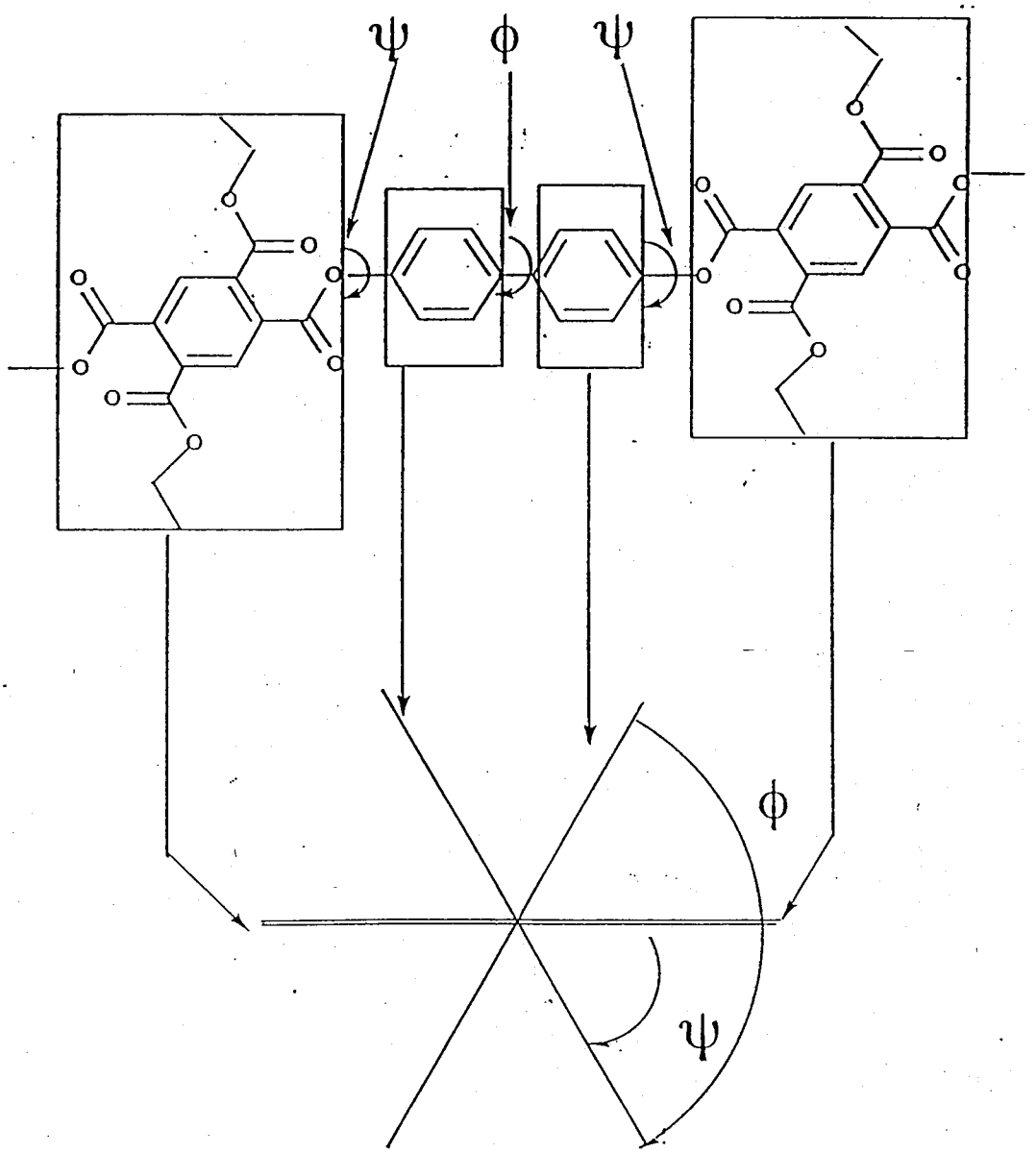

Figure 5-9. The torsion angles, ϕ and ψ, defining therelative twist between aromatic groups in the main chain.

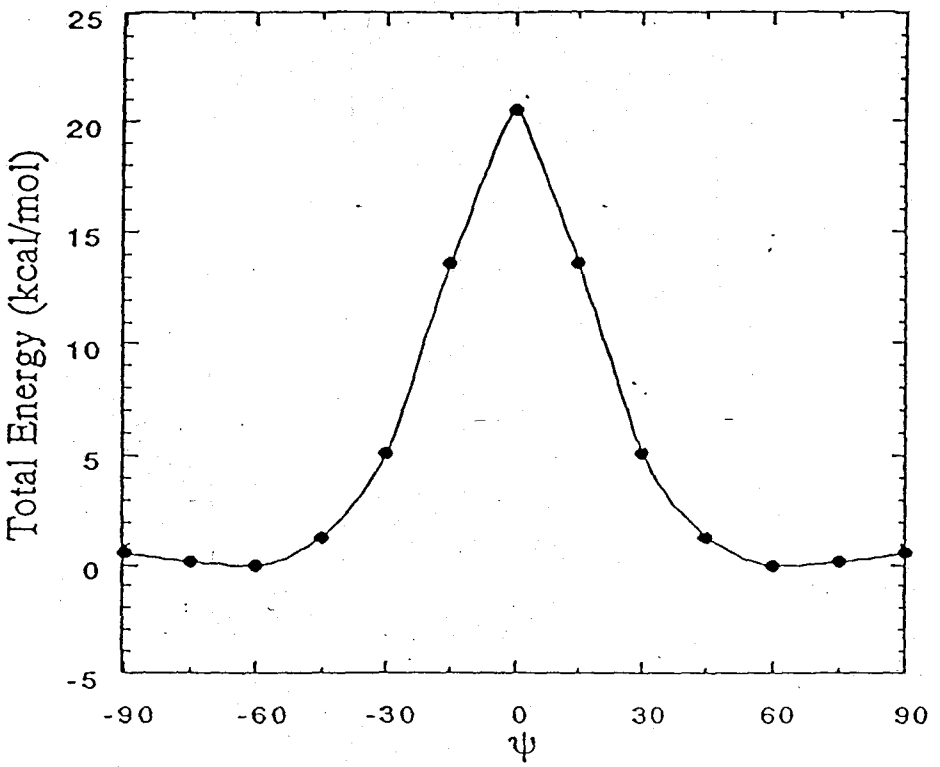

Figure 5-10. The calculated total energy as a function of the relative torsion angle, ψ, under the condition $\phi = 2 \times \psi$.

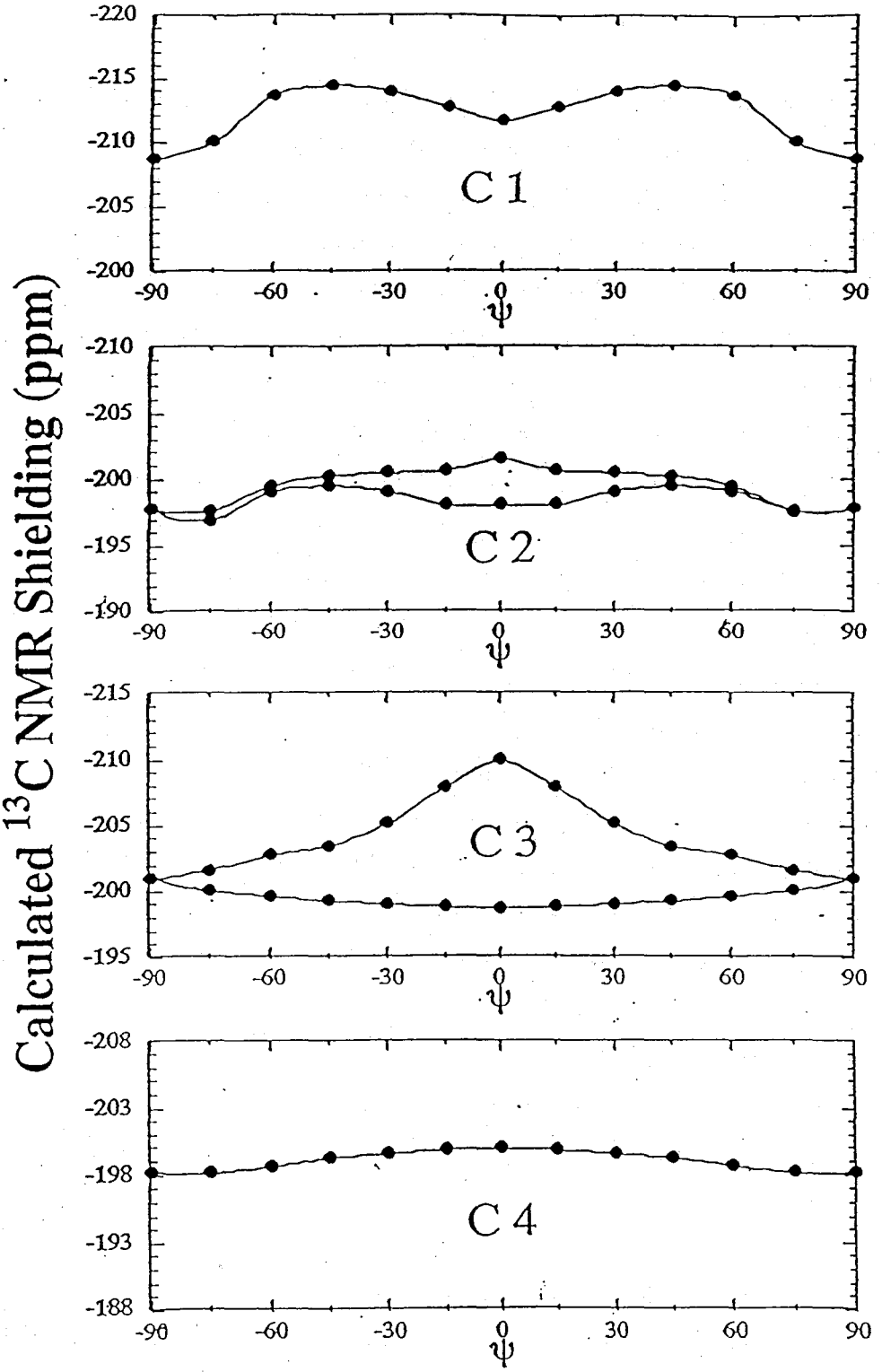

Figure 5-11. The calculated ^{13}C NMR shieldings of the carbons of the biphenyl moiety as a function of the relative torsion angle, ψ, under the condition $\phi = 2 \times \psi$. The negative sign indicates deshielding.

of the conformation based upon these values. The difference in the chemical shifts between the most stable twisted conformation and the anomalous coplanar conformation is striking. When ψ decreases from 60° to 0°, that is, when the conformation changes from the twisted from to the coplanar one, the C3 carbon signal undergoes a large splitting into two distinct components at higher and lower field and the C1 carbon peak shifts to a higher field. Moreover, with this conformational change, the C4 carbon peak does not change position and the C2 carbon peak undergoes only a slight splitting into two components. As compared with the observed data in Figure 5-7, this trend in the calculated ^{13}C NMR shieldings qualitatively corresponds to that observed experimentally. Thus, the FPT-INDO calculations support our suggestion that the main chain in the K1 crystal assumes a twisted conformation, while in the K2 crystal all of the aromatic rings of the main chain are in a nearly coplanar arrangement.

Recently, Tashiro et al. have reported that Raman spectroscopy is an effective method for examining the conformation of biphenyl groups based upon the detection of a Raman active band at about 420 cm^{-1} which appears for the twisted form of the biphenyl group but is absent in the coplanar form[44]. Our observations of the Raman spectra for the K1 and K2 crystals have supported the conclusion based upon the NMR studies. The results are shown in Figure 5-12.

In Figure 5-13 are illustrated the two distinct conformations of the aromatic main chains in the K1 and K2 crystals which are deduced from the overall data.

2-2 Conformation of the Alkyl Side Chain.

Figure 5-14 shows the expanded aliphatic region of the ^{13}C CP/MAS spectra for the K2 crystal of B-C16 and the K1 crystal of B-C12. The assignment of n-alkyl peaks is performed by reference data on n-alkanes as determined by VanderHart[36] and the observed chemical shifts are summarized in Table 5-2.

Ishikawa et al. have analyzed the crystalline phases of polymethylene by high resolution solid state ^{13}C NMR spectroscopy[37]. A similar analysis

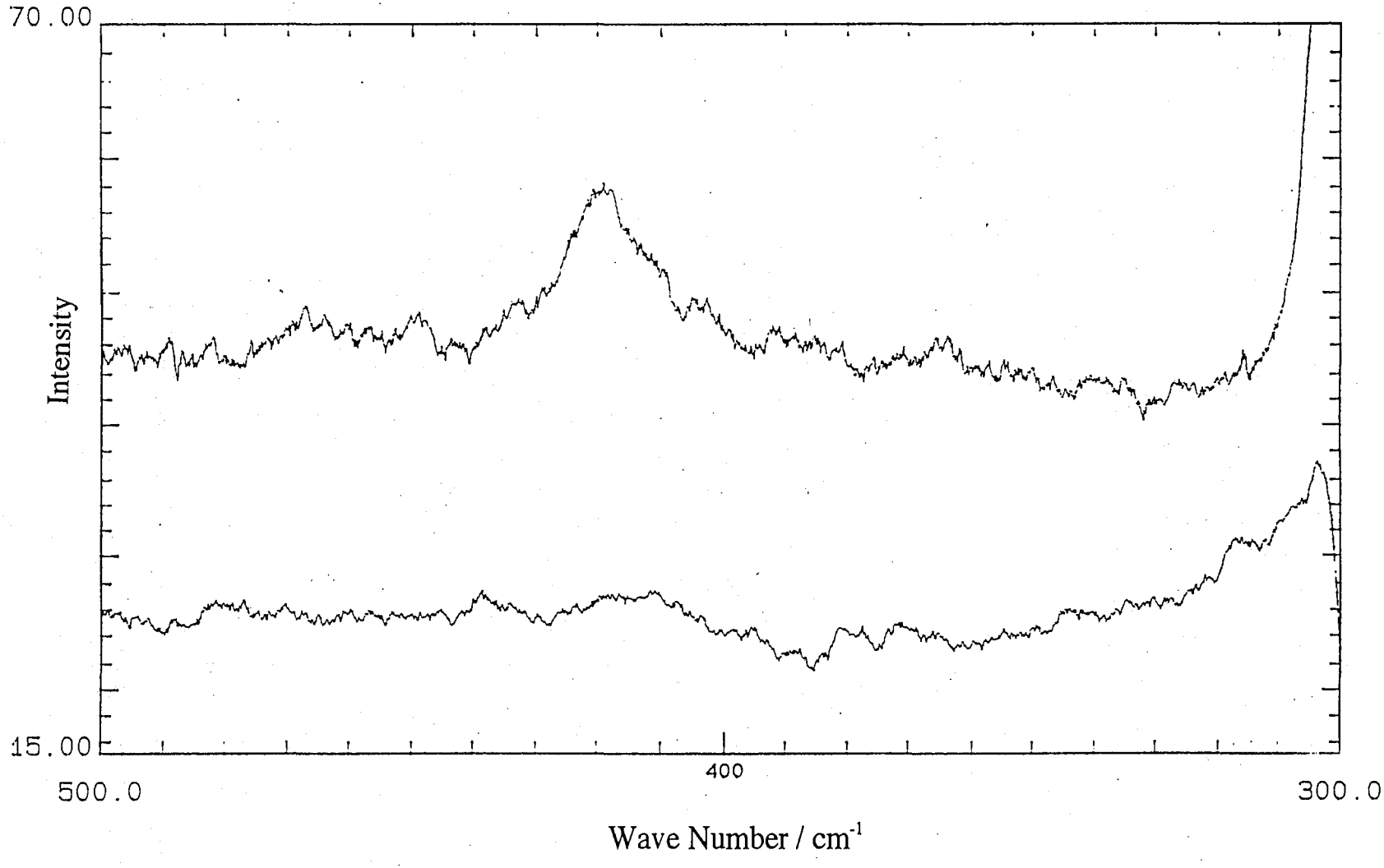

Figure 5-12. Raman spectra taken at room temperature for (a) K1 (BC-12) and (b) K2 (B-C16) crystals.

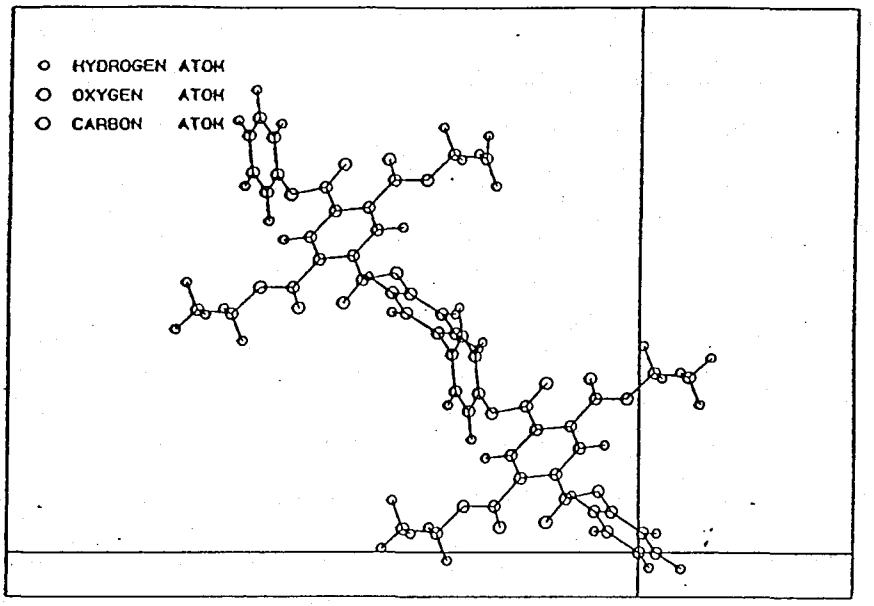

(a)

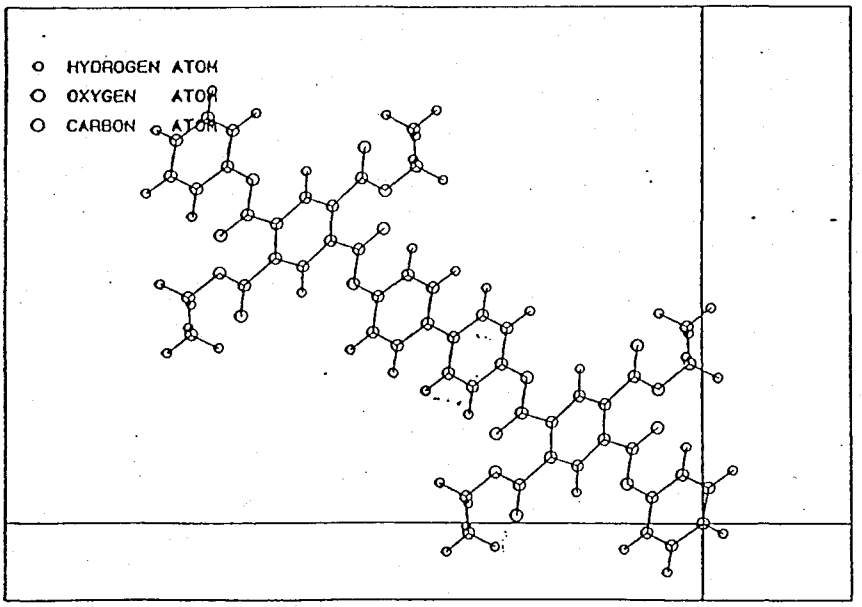

(b)

Figure 5-13. The chain conformations in (a) K1 and (b) K2 crystals according to the FPT-INDO calculation.

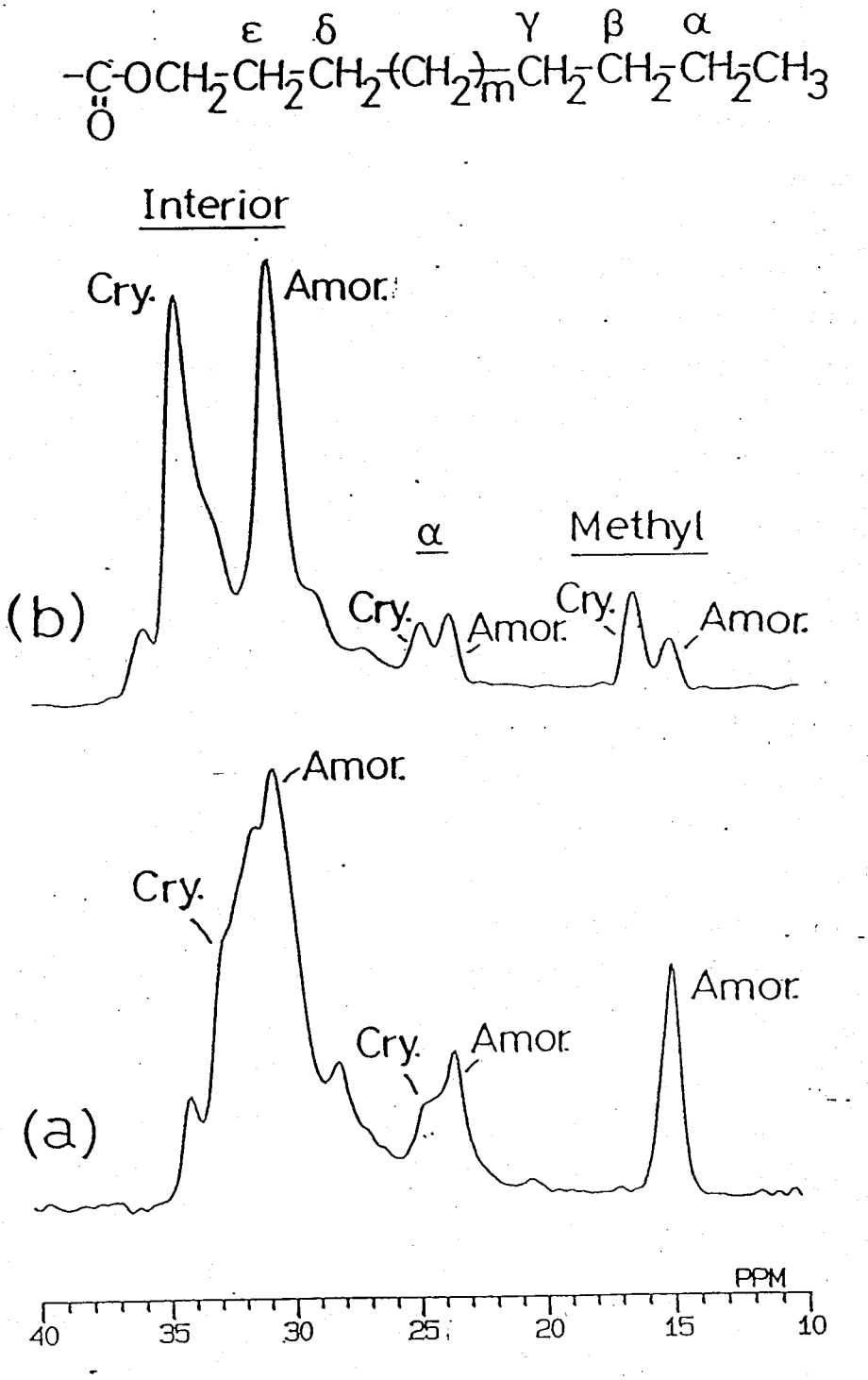

Figure 5-14. Expanded aliphatic region of the ^{13}C CP/MAS spectra for (a) the K1 crystal of BC-12 and (b) the K2 crystal of B-C16.

has been performed for the crystals of the alkyl side chains in poly(γ-octadecyl-L-glutamate)[38]. According to these studies, the signals for the methylene carbon atoms loaded in the interior of the chain appear at 32.8, 34.2, 33.2 and 30.5 ppm when these are in orthorhombic crystal, triclinic crystal, rotator and amorphous phases, respectively. The present results show that the methylene carbon atoms in the interior of the alkyl side chains in the K2 crystal of B-C16 appear at 30 and 34 ppm (see Table 5-2). In the K2 crystals, hence, the alkyl side chains crystallize into a triclinic form, although the amorphous part is also included to some extent. The triclinic crystalline form in the K2 crystal is supported by X-ray diffraction studies. On the other hand, the K1 crystal of B-C12 shows the main peak at 30 ppm, which is overlapped by a small peak at 32 ppm. The side-chain crystallization, thus, is not well progressing in this crystalline phase because of the short length of the side chain.

3. ^{13}C NMR Studies for LC-1 and LC-2 Mesophases

First, we shall focus on the side chain conformation in the mesophase. The expanded aliphatic region of the ^{13}C NMR spectra for the B-C16 polyester in the LC-2 phase together with the isotropic phase is shown in Figure 5-15. The ^{13}C chemical shifts are listed in Table 5-3. The chemical shift values clearly show that the aliphatic side chains are in a molten state and fluidlike in the LC-1 and LC-2 phases as well as in the isotropic phase. Furthermore, it is apparent from Figure 5-15 that in the liquid crystalline phases the half-widths of the O-CH_2 and δ-CH_2 carbon atoms, which are near the main chain, are larger than those of other carbons, although in the isotropic phase the widths of all the aliphatic carbons are almost the same. These differences are believed to originate from inhomogeneities in the molecular motion of the alkyl side chain. Therefore, in the layered liquid crystals, the aliphatic carbons near the main chain have less mobility than the other carbons. The formation of the layered structure is believed to restrict the molecular motion of the aliphatic carbon atoms near the main chains.

Figure 5-16 shows an expansion of the aromatic region of spectra for the

LC-1 (BC-12), LC-2 (BC-16) and isotropic phase (BC-16). The chemical shifts are listed in Table 5-4. Although the spectra are somewhat broad compared to those in the crystalline phases, we can reach the conclusion that the chemical shift values of LC-1 and LC-2 are similar to those of the K1 and K2 phases, respectively. This is especially evident in the spectra of the LC-2 and K2 phases which are identical, indicating that in this liquid crystalline phase all the aromatic groups are on a coplane, with the pyromellitic ester functionalities situated asymmetrically about an axis drawn between the C1' and C2' carbons. In the LC-1, the twisted conformation as in the K1 crystal can also be assumed according to the rough correspondence of the chemical shift values although a significant difference in the chemical shifts of the carbonyl carbons is observed (compare Table 5-1 and 5-4). This difference may result from a greater degree of molecular motion of the main chain and side chains in the mesophase.

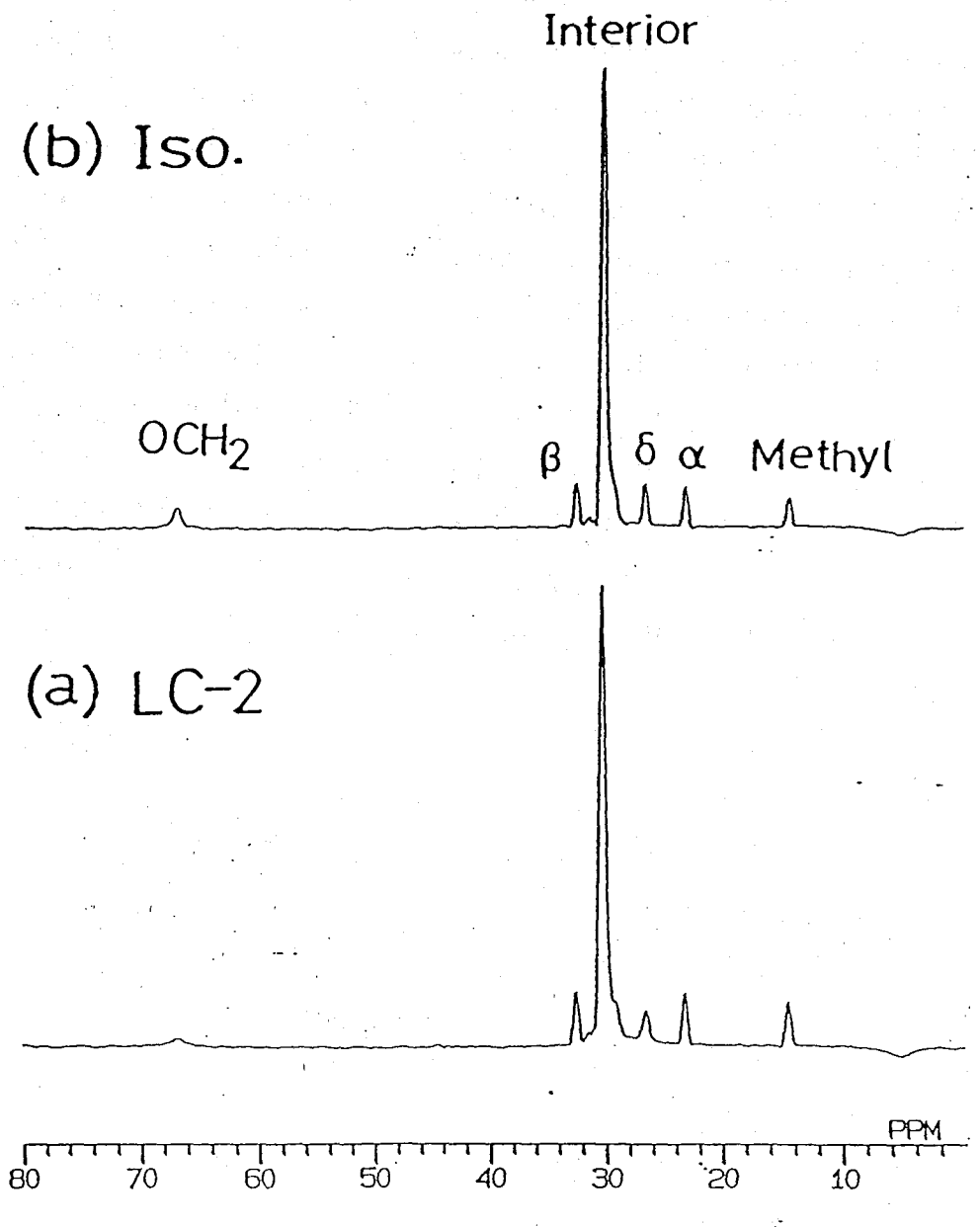

Figure 5-15. The expanded aliphatic region of the ^{13}C MAS spectra for (a) LC-2 and (b) isotropic phases of B-C16, as observed by the gated decoupling/MAS method.

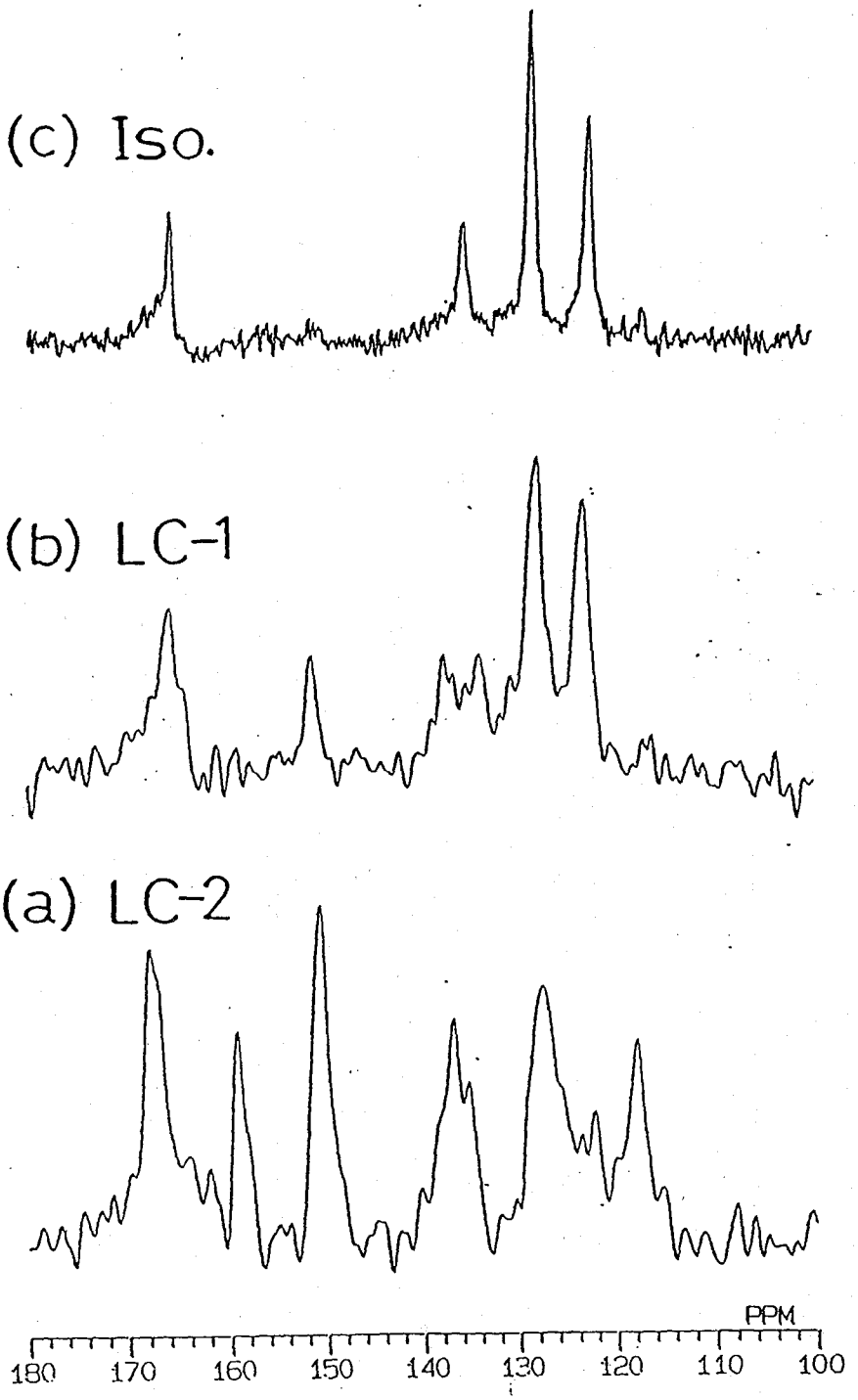

Figure 5-16. Expanded aromatic region of the ^{13}C CP/MAS spectra for (a) the LC-2 of B-C16 as observed by the Cp method, and (b) the LC-1 of B-C12 and (c) the isotropic phase of B-C16 as observed by the gated decoupling/MAS method.

Table 5-3

^{13}C NMR chemical shifts for the aliphatic carbons of the B-C18 polyesters at various temperatures

	^{13}C NMR chemical shifts / ppm								
			Interior CH_2*		δ	α		CH_3	
Temp/°C	OCH_2	β	Cryst.	Amor.	Cryst.		Amor.	Cryst.	Amor.
25(K2)	67.1	35.9	34.3	30.5	28.7	24.6	23.2	16.1	14.8
96(LC-2)	67.0	32.7		30.5	26.7		23.4		14.6
148(Iso.)	67.0	32.3	--	30.1	25.5		23.0		14.3

*Cryst. and Amor. indicate the crystalline and noncrystalline state, respectively.

Table 5-4

Observed ^{13}C NMR Chemical shifts for the aromatic carbons of the B-Cn polyesters in the crystalline state.

	Observed ^{13}C NMR Chemical shift (ppm)								
	C=O								
	m[a]	s[b]	C4	C1'	C2'	C3'	C1	C2	C3
Iso(B-C16)	165.7	164.2	150.8	134.8		130.3	130.3	128.2	121.9
LC-1(B-C12)	165.7	165.0	150.7	137.0	134.0	130.3	130.3	128.2	122.6
LC-2(B-C16)	168.1	158.2	150.7	136.6	131.0	130.0	128.6	128.6	126.0,118.0

m[a]; main chain s[b]; side chain c; $CDCL_3$ solution

5-4 Conclusion

High resolution solid state ^{13}C NMR spectra have provided detailed information about the main chain and side chain conformations in the crystalline and liquid crystalline phases of the B-Cn polyesters. In the K1 crystal, the biphenyl moieties assume a twisted conformation. In addition, the phenyl rings of the biphenyl and pyromellitic moieties are also twisted about the ester bond. In the K2 crystal, in contrast, all the aromatic rings in the main chain are on the same plane and side chains are packed into a triclinic lattice. In the LC-2 phase, the main chain conformation is the same as that in the K2 crystal although the side chains are in a molten state. In the LC-1 phase, on the other hand, the main chain conformation is similar to that observed in the K1 crystal.

FPT-INDO calculation as well as the reference data indicates that the twisted main chain conformation in the K1 and LC-1 phases is the most stable while the coplanar conformation in the K2 and LC-2 phases is to be strongly disfavored. When considering that the K2 and LC-2 phases arise from the B-Cn polyesters with side chains longer than n = 14, it is obvious that the anomalous coplanar conformation is the result of the long alkyl side chains segregating in the space between main chain layers. On this point, the results obtained in a previous study are interesting, in which the thermal stability of the K1 and K2 crystalline phases, i.e., the melting temperature, is remarkably altered by the side chain length. The melting temperature drops significantly with an increase of n from 6 to 10 but then increases again with further increase of n. The two distinct regions identified in the phase diagram are obviously related to the crystal structures or the polymer chain conformation. The decreasing region, observed for the shorter side chain B-Cn, corresponds to the lowering of the thermal stability of the K1 crystal, showing that its crystal structure is determined mainly by the polymer, backbone with a perturbation by the shorter side chains. On the other hand, the regime of increasing thermal stability, observed in the longer side chain polyesters, corresponds to an enhancement

of the thermal stability of the K2 crystal. The structure in the K2 crystal, hence, is strongly dominated by the crystallization of the long alkyl side chains. This may result in the anomalous coplanar conformation of the backbone and hence an anomalously dence packing of the backbones within a layer, although we cannot give answer as to why the coplanar conformation is still retained even in the LC-2 mesophase in which the side chains are in a molten state.

5-5 Reference and notes

(1) Ballauff, M. Macromol. Chem., Rapid Comun. 1986, **7**, 407.

(2) Ballauff, M. Angew. Chem., Int. Ed. Engl. 1987, **28**, 253.

(3) Ballauff, M.; Schmidt, G. F. Mol.Cryst.Liq.Cryst. 1987, **147**, 163.

(4) Stern, R.; Ballauff, M.; Wegner, G. Macromol. Chem., Macromol. Symp. 1989, **423**, 373.

(5) Rodrigues-Parada, J. M.; Duran, R.; Wegner, G. Macromolecules 1989, **22**, 2507.

(6) Ebert, M.; Herrmann-Schenherr, O.; Wendorf, J.; Ringsdorf, H.; Tschirner, P. Liq. Cryst. 1990, **7**, 63.

(7) Adam, A.; Spiess, H. W. Macromol. Chem., Rapid Comun. 1990, **11**, 249.

(8) Frech, C. H.; Adam, A.; Falk, U.; Boeffel, C.; Spiess, H. W. New Polym. Mater. 1990, **2**, 267.

(9) Stern, R.; Ballauff, M.; Lieser, G.; Wegner, G. Polymer 1991, **32**, 2079.

(10) Harkmess, B. R.; Watanabe, J. Macromolecules 1991, **24**, 6759.

(11) Watanabe, J.; Harkness, B. R.; Sone, M. Polym. J. 1992, **24**, 1119.

(12) Cervinka, L.; Ballauff, M. Colloid Polym. Sci. 1992, **270**, 859.

(13) Sone, M.; Harkness, B. R.; Watanabe, J.; Torii, T.; Yamashita, T.; Horie, K. Polym. J. 1993, **25**, 997.

(14) Galda, P.; Kistner, D.; Martin, A.; Ballauff, M. Macromolecules 1993, **26**, 1595.

(15) Marz, K.; Lindner, P.; Urban, J.; Ballauff, M.; Fisher, E. W. Acta Polym. 1993, **44**, 139.

(16) Damman, S. B.; Mercx, F. R. P.; Kootwijk-Damman, C. M. Polymer 1993, **34**, 1891.

(17) Damman, S. B.; Mercx, F. P. M. J. Polym. Sci., Polym. Phys. 1993, **31**, 1759.

(18) Damman, S. B.; Mercx, F. P. M. J.; Lemstra, P. J. Polymer 1993, **34**, 2726.

(19) Damman, S. B.; Vroege, G. J. Polymer 1993, **34**, 2732.

(20) Kakimoto, M.; Orikabe, H.; Imai, Y. ACS Polym. Prep. 1993, **34**, 746.

(21) Steuner, M.; Hortz, M.; Ballauff, M. J. Polym. Sci., Polym. Chem. 1993, **31**, 1609.
(22) Watanabe, J.; Harkness, B. R.; Sone, M.; Ichimura, H. Macromolecules 1994, **27**, 507.
(23) Sone, M.; Harkness, B. R.; Kurosu, H.; Ando, I.; Watanabe, J. Macromolecules 1994, **27**, 2769.
(24) Damman, S. B.; Buijs, J. A. H. M. Polymer 1994, **35**, 2559.
(25) Damman, S. B.; Buijs, J. A. H. M.; van Turnhout, J. Polymer 1994, **35**, 2364.
(26) Buijs, J. A. H. M.; Damman, S. B. J. Polym. Sci.; Polym. Phys. 1994, **32**, 851.
(27) Tiesler,U.; Pulina,T.; Rehahn,M.; Ballauff,M.; Mol.Cryst.Liq.Cryst. 1994, **41**,525.
(28) Voigt-Martin, I. G.; Simon, P.; Bauer, S.; Ringsdorf, H. Macromolecules 1995, **28**, 236.
(29) Voigt-Martin, I. G.; Simon, P.; Yan, D.; Yakimansky, A.; Bauer, S.; Ringsdorf, H. Macromolecules 1995, **28**, 243.
(30) Ando, I.; Yamanobe, T.; Kurosu, H.; Webb, G. A. Annu. Rep. NMR Spectrosc. 1990, **22**, 205.
(31) Ando, I.; Yamanobe, T.; Asakura, T. Prog. NMR Spectrosc. 1990, **7**, 839.
(32) Kurosu, H.; Yamanobe, T.; Ando, I. J. Chem. Phys. 1988, **89**, 5216.
(33) Sone, M.; Yoshimizu, H.; Kurosu, H.; Ando, I. J. Mol. Struct. 1993, **301**, 227.; 1994, **317**, 111.
(34) Asakawa, N.; Kurosu, H.; Ando, I.; Shoji, A.; Ozaki, T. J. Mol. Struct. 1994, **317**, 119.
(35) Bruck, D.; Rabinovits, M. Tetrahedron Lett. 1977, **47**, 4121.
(36) VanderHart, D. L.; J. Magn. Reson. 1981, **44**, 117.
(37) Ishikawa, S.; Kurosu, H.; Ando, I. J. Mol. Struct. 1990, **248**, 361.
(38) Yamanobe, T.; Tsukahara, M.; Komoto, T.; Watanabe, J.; Ando, I.; Uematsu, I.; Deguchi, K.; Fujito, T.; Imanari, M. Macromolecules 1988, **21**, 48.
(39) Simmons, A.; Natansohn, A. Macromolecules 1992, **25**, 3881.

(40) Coulter, P.; Windle, A.H. Macromolecules 1989, **22**, 1129.
(41) Uryu, T.; Kato, T. Macromolecules 1988, **21**, 378.
(42) Meurisse,P.; Lauprete,F.; Noel,C. Mol.Cryst.Liq.Cryst. 1984,**110**, 41.
(43) Akiyama,M.; Watanabe,T.; Kurihara,M. J.Phys.Chem. 1986, **90**, 1752.
(44) Tashiro,K.; Han,J.A.; Kobayashi,M.; Inoue,T. J.Am.Chem.Soc. 1990, **112**, 8273.

Chapter 6

Chain Conformation of H-Cn Polyesters in Layered Crystalline Phases and Mesophases Analyzed by High Resolution Solid-State ^{13}C NMR Spectroscopy.

6-1 Introduction

Several recent years, there has been a considerable amount of attention paid to the rigid-rod polyesters and polyamids with long alkyl side chains as a consequence of their ability to form thermotropic liquid crystalline phases[1-28]. Prior to and concurrent with these studies it was demonstrated that rigid-rod polymers with long flexible side chains such as poly(γ-octadecyl-L-glutamate) can form thermotropic cholesteric, smectic and columnar phases[29-33]. Rigid-rod aromatic polymers with long flexible side chains form thermotropic phases, but in this case they exhibit novel layered structures[1-28]. These layered structures are characterized by a lateral packing of the aromatic main-chains into layers, with the flexible alkyl side-chains occupying the space between the layers. It is interesting to focus that the basic features of the molecular packing into a layered mesophase are similar to those of discotic columnar phases. In columnar phases, the column is formed by a stacking of the disk-like molecules with the long alkyl side chains and core molecules arranged in space with a two dimensional lattice structure that may be hexagonal or rectangular. The different types of columnar phases have been classified on the basis of the packing array of the disklike molecules into columns. In the present layered mesophase, the molecules have a broad-like shape and associate into a layered structure. In analogy to the discotic phases, the layered mesophase can be classified into several types on the basis of the packing arrangement of molecules into a layer. This classification was initially proposed by Ebert et al., who termed the layered mesophase sanidic and defined by Greek letter Σ[9,22]. These have the following packing characteristics of the main chains within a layer; Σob, Σou// , Σou$_\perp$ and Σd[22].

In these layered structures, it is of interest to determine how the aromatic main chains are packed into a monolayer. Since the aromatic main chains are accommodated within the confined space of a monolayer, their conformation is presumed to be different from that observed in aromatic polymers without side-chains. In fact, several types of layered crystals and mesophases have been observed with different packing modifications, suggesting a plurality of aromatic main-chain conformations. In our previous study, we reported that the aromatic main-chain assumes a disfavored and confined coplanar conformation in the layered crystals formed by B-Cn polyesters[10,22,23].

H-Cn polyesters form three types of layered crystals and one type of cylindrical phase because of segregation between the aromatic main-chain and aliphatic side-chain domains. These polyesters are suitable for examining how the segregated structures are related to the main chain conformations.

The objective of this work has been to examine the main chain and side chain conformations in the different morphologies of H-Cn polyesters, by the use of high resolution solid-state ^{13}C NMR[23,34-38]. Furthermore, an attempt has been made to interpret these spectra and estimate the polymer conformation by considering the ^{13}C NMR shielding constant using the FPT (finite perturbation theory) method within the INDO framework[23,34-38].

6-2 Experimental

The synthesis of H-Cn polyesters (n, the carbon number of the alkyl side chain) has been described in Chapter 2. Here

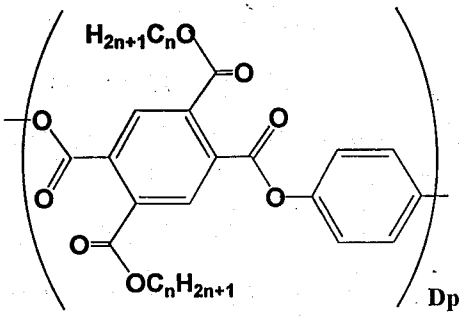

the H-Cn polyesters with n = 6-18 were employed.

^{13}C MAS spectra were recorded on a JNM GSX-270 NMR spectrometer operating at 67.8 MHz with cross polarization/ magic angle spinning (CP/MAS) and variable-temperature (VT) accessories. Samples were contained in a cylindrical rotor composed of zirconia with an O-ring and spun at a speed of upto 4.0 kHz monitored by a spinning controller. The contact time was 2.0 ms and the repetition time was 3-6 s. The 1H radio-frequency (rf) field strength was 60 kHz. Spectra were observed by the accumulation of 1000 to 3000 scans in order to achieve a reasonable signal-to-noise ratio. The ^{13}C chemical shifts were calibrated indirectly with adamantane as the external standard (29.5 ppm relative to tetramethylsilane)

The solid state ^{13}C NMR spectra of these polymers in the aromatic and carbonyl region were found to be rather complicated due to a large number of side bands resulting from the large anisotropy of the individual shielding tensors. In order to eliminate the spinning side bands, thus simplifying the spectra, the total suppression of spinning side band (TOSS) spectra were recorded. TOSS ^{13}C MAS spectra for the crystalline phases were observed by the CP method, while those for the liquid crystalline and isotropic phases were observed by the gated decoupling method.

In order to obtain information concerning the conformation of the

polymer, it was necessary to accurately assign the peaks in the ^{13}C NMR spectrum. The assignment of all the peaks wes based on reference data[39-42,45]. To accomplish this, the NMR spectra of the crystalline polymers were measured using the dipolar dephasing method within a delay time of 60 μs.

The ^{13}C NMR shielding constant and the total energy calculations for the model compounds were obtained using the INDO method incorporated with FPT method. The negative sign of the calculated ^{13}C shielding constant means deshielding. The bond lengths and bond angles of a model compound as described by Coulter and Windle[44] are shown later in Figures 6-4 and 6-6. The calculations were carried out as a function of the torsion angle by using a SUN SPARC station 2.

In this chapter, we shall focus mainly on the main-chain conformation. In order to discuss the relationship between the main-chain conformation and ^{13}C chemical shifts, the possibility of intermolecular interactions between neighboring aromatic main chains that can contribute to the chemical shift values must be taken into consideration. Kurosu et al. have clarified an effect of the intermolecular interaction on ^{13}C NMR chemical shifts of some kind of linear polymers in solid state through the ^{13}C NMR shielding calculation[36]. Actually, it has been found that a charge transfer complex is found between neighboring hydroquinone and pyromellitic ester moieties in the layered crystals and mesophases of H-Cn polyesters through the measurement of the CT fluorescence. Simons and Natansohn have reported that even strong charge transfer complex formation results in ^{13}C NMR chemical shifts of about 1 ppm without conformational change[43]. Otherwise, it is well known that effect of conformational change on ^{13}C chemical shifts is usually larger than 1 ppm[34,36]. Thus , we consider it reasonable that the chemical shift behavior is mainly influenced by the conformational change of the main- and side-chains and the influence of intermolecular interaction on the ^{13}C NMR chemical shift values can be considered as being negligible.

6-3 Results and Discussion

[1] Thermotropic Behavior of H-Cn Polyesters.

In Chapter 4[10,11], we reported that H-Cn polyesters form four types of crystals and a layered mesophase as a function of side chain length as shown in Figure 6-1.

With n = 12, 14, 16 and 18, H-Cn forms a highly ordered thermotropic mesophase (LC) and two crystalline phases (Kc and Km1) in layered structures. The Kc was obtained by casting from $CHCl_3$ and THF solution. The Km1 was obtained on annealing the quenched sample from liquid crystalline state at 60 °C for a month. In layered Kc and Km1 crystalline phases, the aromatic main chains are in a fully extended conformation with a repeat length of 12 Å and they are regularly packed within a monolayer. In addition, the side chains are also in a crystalline state between layers. It is of interest that the main chains in Kc and Km1 are packed in a different manner. For Kc, the lateral packing distance of the main chains within a layer is 4.9 Å, but this reduces to 3.85 Å for Km1. The packing distance of 4.9 Å in Kc is reasonable for the main chains in a stable twisted conformation. In contrast, the short spacing of 3.85 Å in Km1 indicates an unusual dense packing of the main chains that requires an anomal conformation.

With n = 6, 8 and 10, H-Cn forms a highly ordered crystal (Km2) having a layered structure, as obtained on annealing the quenched sample at 60°C from isotropic state. By casting the solution, we could not obtain crystal of H-Cn. In Km2, the aromatic main chains are in a fully extended conformation and are packed like a zigzag sheet in a layer.

H-C6 forms a cylindrical phase, denoted as Kh, in which the aromatic main chains are packed in a hexagonal lattice in the lower temperature region below Km2. The fact that Kh has three dimensional positional order was evident from the number of layer line reflections and equatorial reflection on the X-ray diffraction pattern of the as-spun fibers.

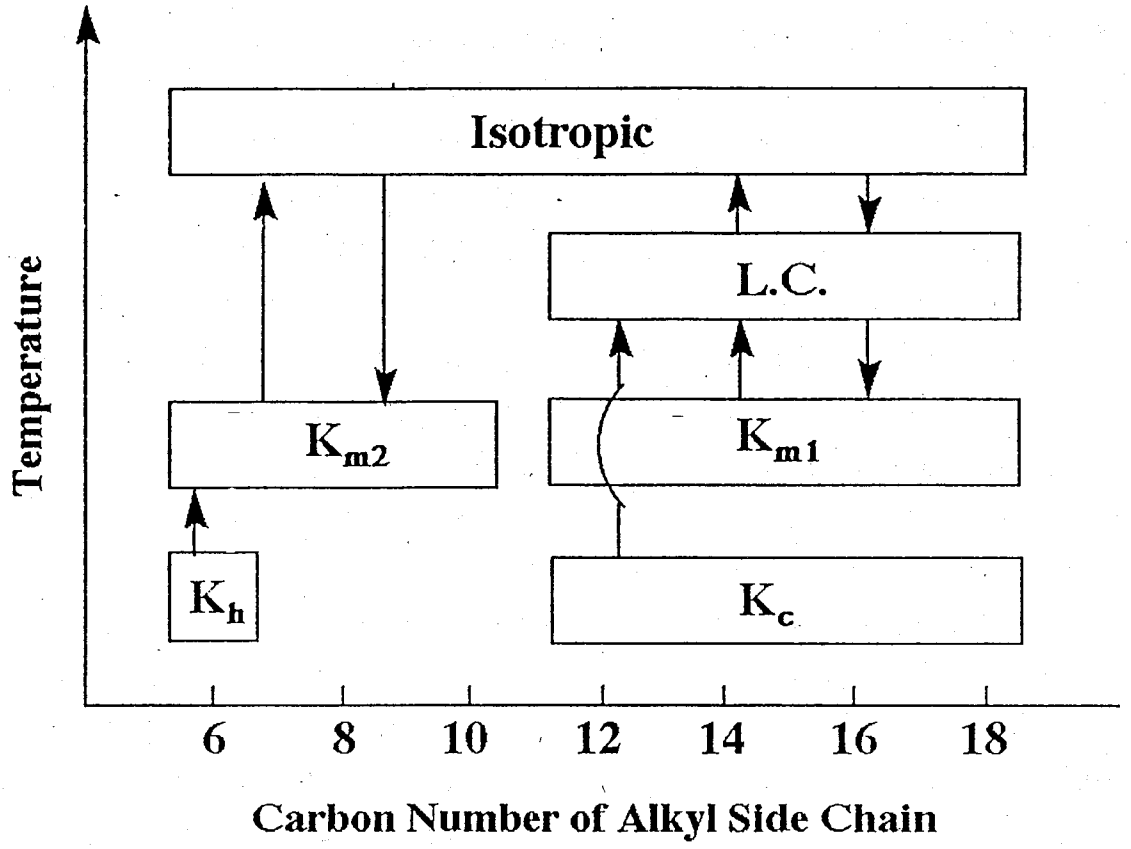

Figure 6-1. Schematic illustration of thermotropic phase behavior in H-Cn polyesters.

[2] Kc Crystal

H-Cn with n = 12 to 18 forms Kc crystal by casting from $CHCl_3$ or THF solution. In Kc crystals, the aromatic main chains are fully extended with repeat length of 12 Å and they are regularly packed within a monolayer. The lateral packing distance of the main chains within a layer is 4.9 Å, which is reasonable for the stable conformation of the aromatic polymers.

Figure 6-2 shows ^{13}C CP/MAS spectra for H-C16 in the Kc crystals. The observed ^{13}C chemical shift values are summarized in Table 6-1. At first, we will focus on the pyromellitic ester moiety. Two sharp peaks due to the main and side chain carbonyl carbons in Kc were observed at 167.9 and 163.6 ppm, respectively. The aromatic carbon peaks, C1', C2' and C3', were observed at 137.1, 131.0 and 130.0 ppm, respectively.

As discussed in previous studies about B-Cn, four plausible conformations can be considered for the pyromellitic ester moieties under the reasonable assumption that the ester groups are coplanar with the aromatic moiety. Comparison with the conformational analysis of B-Cn in the layered crystals shows that the conformation of the pyromellitic ester moieties in Kc is believed to be either conformation i or iii as shown in Figure 6-3.

To distinguish i and iii, the FPT-INDO calculations of the ^{13}C NMR shieldings for the model compound of Figure 6-4 were performed. The geometric parameters given in Figure 6-4 are based on X-ray diffraction data of aromatic ester compounds. Figure 6-5 shows a diagram of the calculated ^{13}C NMR chemical shifts of the carbons in the pyromellitic moiety. From this Figure, it is clear that there is little difference in the ^{13}C chemical shifts of all carbons between conformation i and iii, while the positions of the peaks in the pyromellitic moiety are exchanged with each other between two carbonyl carbons, m and s, and two aromatic carbons C1' and C2'. Conformation iii is 5 kcal/mol and more stable than conformation i. From the above results and calculation, we cannot determine the exact conformations for Kc, i or iii.

X-ray diffraction pattern of Kc crystal shows that the main chains are fully extended. To maintain linearity of the main chain backbone, it is clear that the main chain ester bonds assume an all-trans conformation. From

the chemical shift values of C1' and C2' carbons, the pyromellitic moieties takes the conformation i or iii. These two conformations must not be mixed in one unit of pyromellitic moieties because if these are mixed, the NMR signals of a conformation ii should be observed. From this point of view, the conformation of the pyromellitic moieties in Kc could be one of the two conformations i or iii. Next, when conformations i or iii are mixed in one chain, the alkyl side chains get randomly attached to the aromatic main chains. These chain conformation may hinder the crystallization of the alkyl side chain between the aromatic layers. Thus, in this phase we assume that the pyromellitic ester moieties were confined to one conformation.

Later we next focus on the ester bond between the phenyl rings of the hydroquinone and pyromellitic moieties. Two sharp peaks due to the aromatic carbon C2 were observed at 125.3 and 123.0 ppm and a C1 carbon peak is observed at 149.4 ppm. As discussed in the conformational study of B-Cn, a C2 carbon peak splits into two peaks with a decrease in dihedral angle ψ (as shown in Figure 6-6), between the phenyl rings of the hydroquinone and pyromellitic moieties. The observed difference between two peaks is 1.6 ppm. To precisely clarify the relationship between the dihedral angle ψ and the chemical shift value of C2 carbon, we measured the solid-state ^{13}C NMR spectrum of diacetoxy benzene in the crystal.

In this spectrum, the ^{13}C chemical shift values of C2 were observed at 125.3 and 123.7 ppm and that of C1 is 149.5 ppm, as shown in Table 6-1. These values are nearly the same as in Kc crystal. Coulter and Windle report that the dihedral angle ψ is idealized to 68.4° in the crystalline state based on X-ray diffraction studies, which suggests that this twisted conformation is very stable[44]. Thus, in Kc, the ester bond is believed to be twisted by about 70°.

This conclusion is also consistent with that deduced from the X-ray observation, according to which the interchain distance of 4.90 Å between neighboring main chains within a layer in Kc crystal is reasonable for the main chains in a suitable twisted conformation.

To confirm this suggestion on the conformation, the INDO calculations

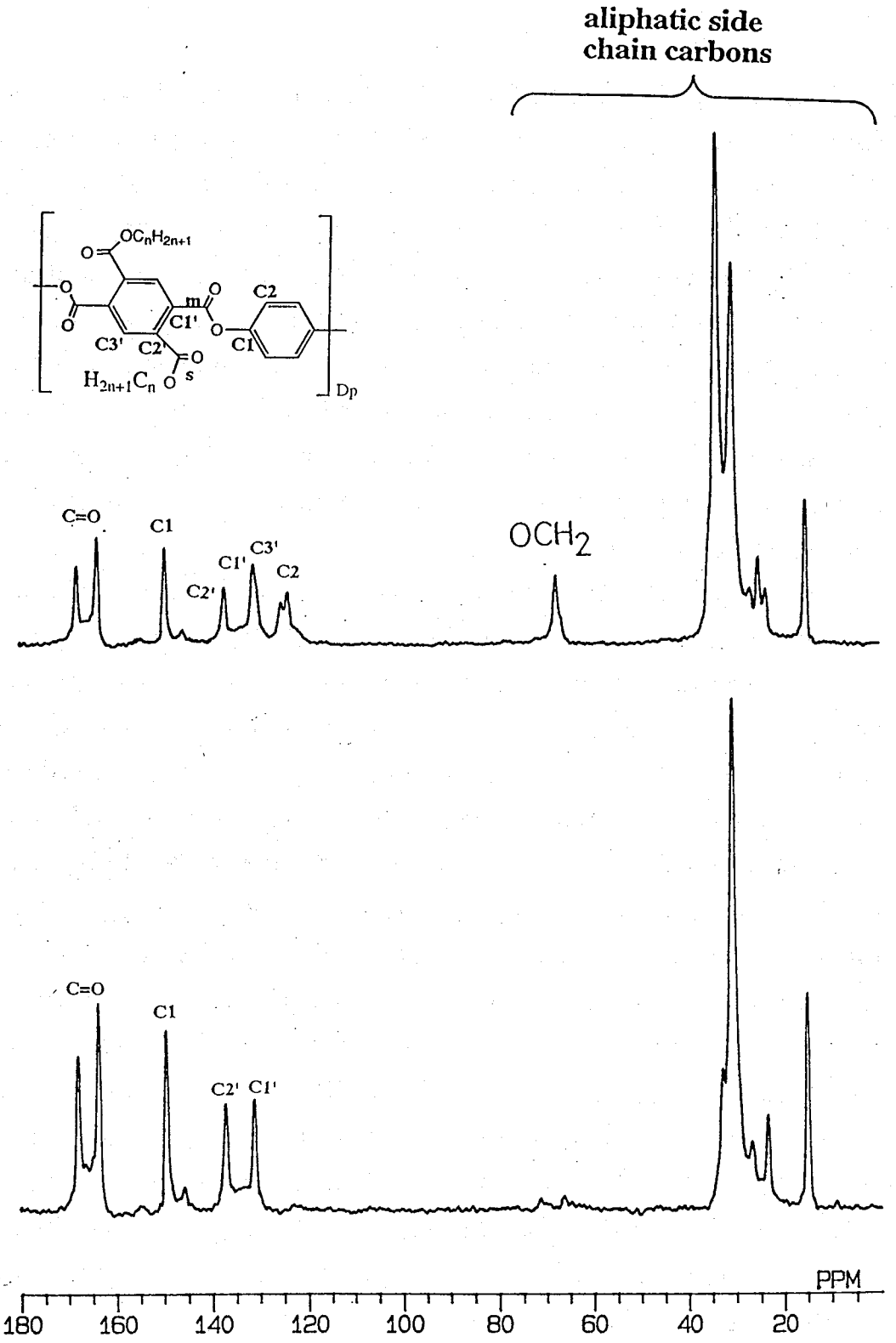

Figure 6-2. ^{13}C TOSS MAS NMR spectra for Kc crystal of B-C16 polyesters using (a) CP and (b) dipolar dephasing methods.

Table 6-1

Observed ^{13}C NMR Chemical shifts for the aromatic carbons of the H-Cn polyesters in the various crystalline state.

	Observed ^{13}C NMR Chemical shift (ppm)						
	C=O						
	m[a]	s[b]	C1	C1'	C2'	C3'	C2
H-C16soln[c].	165.3	164.8	149.5	134.5	134.5	130.0	122.6
Kc Crystal							
H-C14	167.6	163.5	149.5	137.1	131.1	130.2	125.3,123.8
H-C16	167.9	163.6	149.5	137.1	131.0	130.4	125.3 123.8
H-C18	167.8	163.5	149.4	137.1	131.0	130.1	125.2,123.8
Km1 Crystal							
H-C14	167.9	162.8	146.0	136.3,134.3	132.8	129.4	122.9
H-C16	167.8	165.4	145.5	136.0	132.9	128.9	122.0
H-C18	167.9	165.0	145.9	136.2	132.7	129.1	122.2
Km2 Crystal							
H-C6	167.3,165.0	168.8,163.0	149.0,147.0	139.0,133.0	131.6,136.0	128.9	122.0
H-C8	167.3,165.5	168.8,162.8	148.7,147.0	138.7,132.8	131.8,136.2	129.2	122.7
H-C10	167.2,165.4	168.4,162.8	149.1,146.3	139.1,133.8	131.8,137.0	129.1	122.3
H-C12	167.6,165.0	168.4,162.9	148.8,145.6	139.9,133.6	132.7,138.7	129.1	121.7
Kh Crystal							
H-C6	165.4	162.9	150.0	134.2	133.5	128.6	123.2

m[a]; main chain s[b]; side chain c; $CDCL_3$ solution

Table 6-2

Observed ^{13}C NMR Chemical shifts for the aliphatic carbons of the H-Cn polyesters in the various crystalline state.

			^{13}C NMR chemical shifts / ppm						
			Interior CH_2		δ	α		CH_3	
Temp/°C	OCH_2	β	Cryst.	Amor.		Cryst.	Amor.	Cryst.	Amor.
Soln.($CDCl_3$)	66.9	31.8		29.5	25.9	--	22.7	--	14.1
Kc Crystal									
H-C14	67.1	--	33.6	30.5	26.7	24.6	23.2	--	14.8
H-C16	67.6	--	33.7	30.4	26.8	24.9	23.3	--	14.8
H-C18	67.0	--	33.6	30.1	26.7	24.8	23.0	--	14.3
Km1 Crystal									
H-C14	67.8	--	34.0	30.5	26.6	24.7	23.5	--	14.7
H-C16	67.0	--	33.2	30.9	27.4	24.7	23.8	--	14.9
H-C18	67.9	--	34.0	30.8	--	24.8	23.8	--	14.8
Km2 Crystal									
H-C6	68.9,67.2	32.2	--	29.2	25.9	--	23.0	--	14.3
H-C8	68.9,66.7	32.3	--	29.6	26.4	--	23.2	--	14.4
H-C10	68.9,66.6	32.4	--	29.9	26.4	--	23.1	--	14.3

*Cryst. and Amor. indicate the crystalline and noncrystalline state, respectively.

of ^{13}C NMR shieldings based on FPT theory for the model compound of Figure 6-6 were performed as a function of the torsion angle ψ. The geometric parameters given in Figure 6-6 are based upon X-ray diffraction data of aromatic ester compounds.

Figure 6-7 shows the calculated ^{13}C NMR shieldings with the torsion angle ψ. This Figure indicates that the ^{13}C chemical shifts strongly depend on the torsion angle ψ so as to allow the determination of the conformation based upon these values. When ψ decreases from 90° to 0°, that is , when the conformation changes from the twisted to coplanar one, the C2 carbon signal undergoes a large splitting into two distinct components at lower field and the C1 carbon peak shifts slightly to a lower field. Compared to the observed data in Figure 6-2, this trend in the calculated ^{13}C NMR shieldings qualitatively corresponds to that observed experimentally. The observed splitting of the C2 carbon peaks means that the ester bonds are twisted. Thus, the FPT-INDO calculations support our suggestion that the main chain in the Kc crystal assumes a twisted conformation with the dihedral angle ψ being about 70°. This dihedral angle dependence of the ^{13}C chemical shifts in the aromatic molecules was reported previously[23]. Using all of the above data, the possible conformation is illustrated in Figure 6-8.

Figure 6-9 shows the expanded aliphatic region of the ^{13}C CP/MAS spectrum of Kc crystal. The peak assignment is summarized in Table 6-2. These observed chemical shift values of the interior chains do not correspond to as that observed in the triclinic, orthorhombic and rotator phase. Thus, in Kc, the aliphatic side chains between the aromatic layers are partially crystallized.

[3] Km1 Crystal

Km1 crystals formed from H-C12 to 18 were obtained on annealing the melt quenched sample. In Km1 crystals, the aromatic main chains are fully extended with a repeat length of 12 Å and are regularly packed in a monolayer. The lateral packing distance of the main chains within a layer is 3.85 Å and this short spacing indicates an unusual dense packing of the

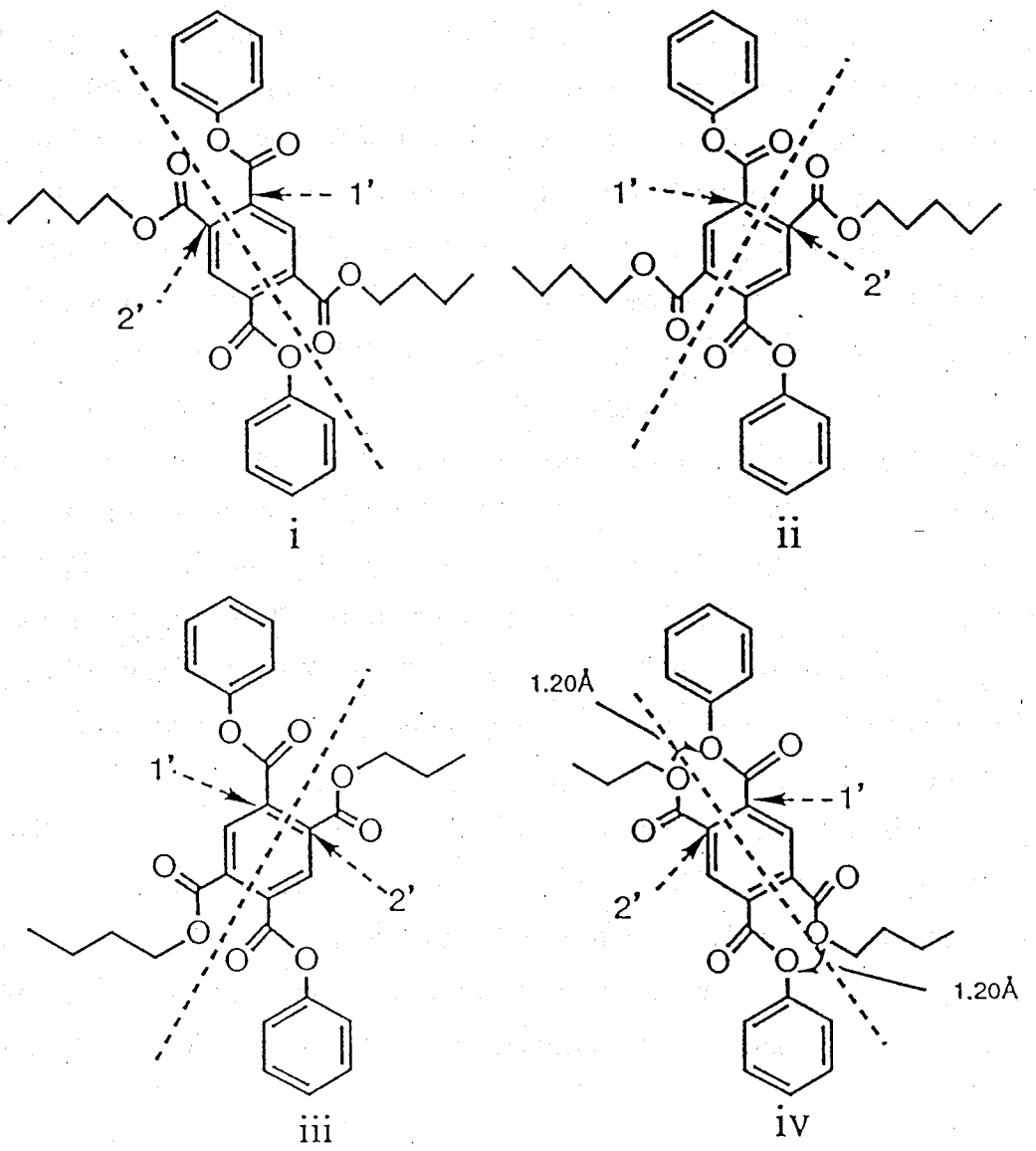

Figure 6-3. Four possible conformations for the pyromellitic ester moieties of the H-Cn polyesters.

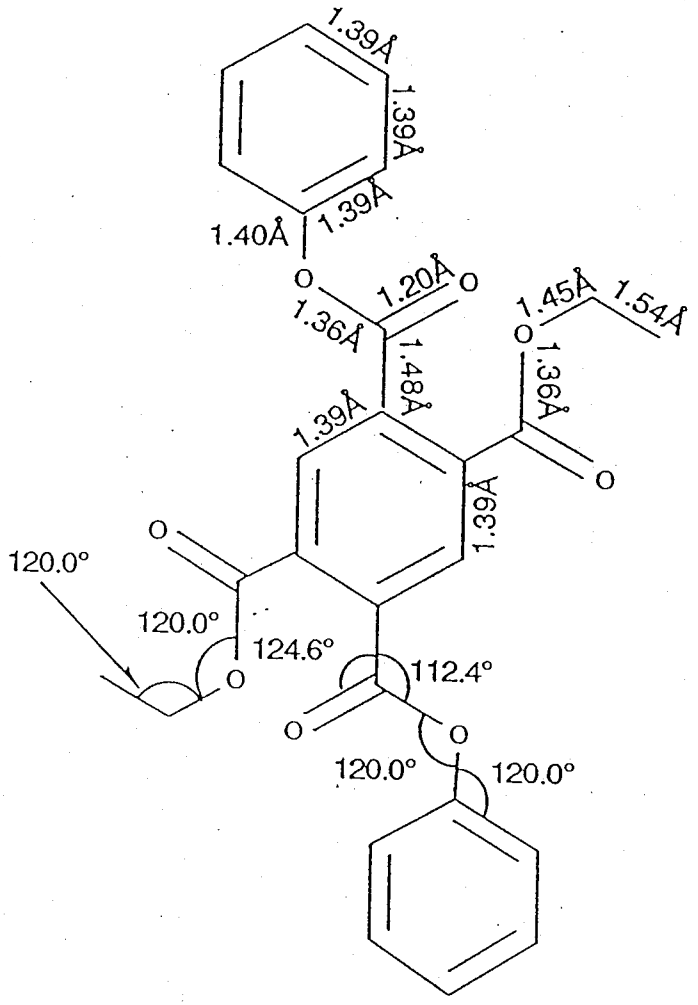

Figure 6-4. Model compound and the geometric parameters of pyromellitic ester moiety for the FPT-INDO calculation.

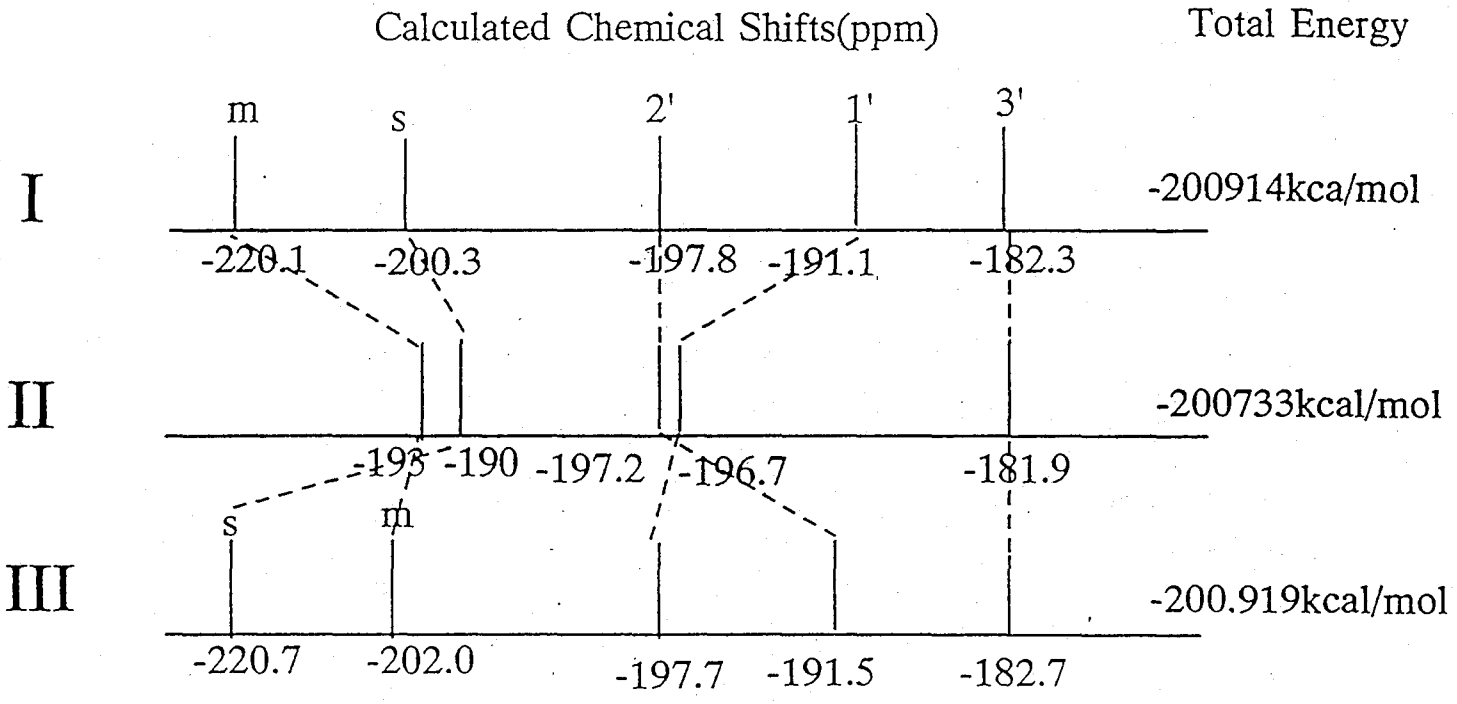

Figure 6-5. Diagram of the calculated NMRshieldings in the pyromellitic moiety in Kc crystal.

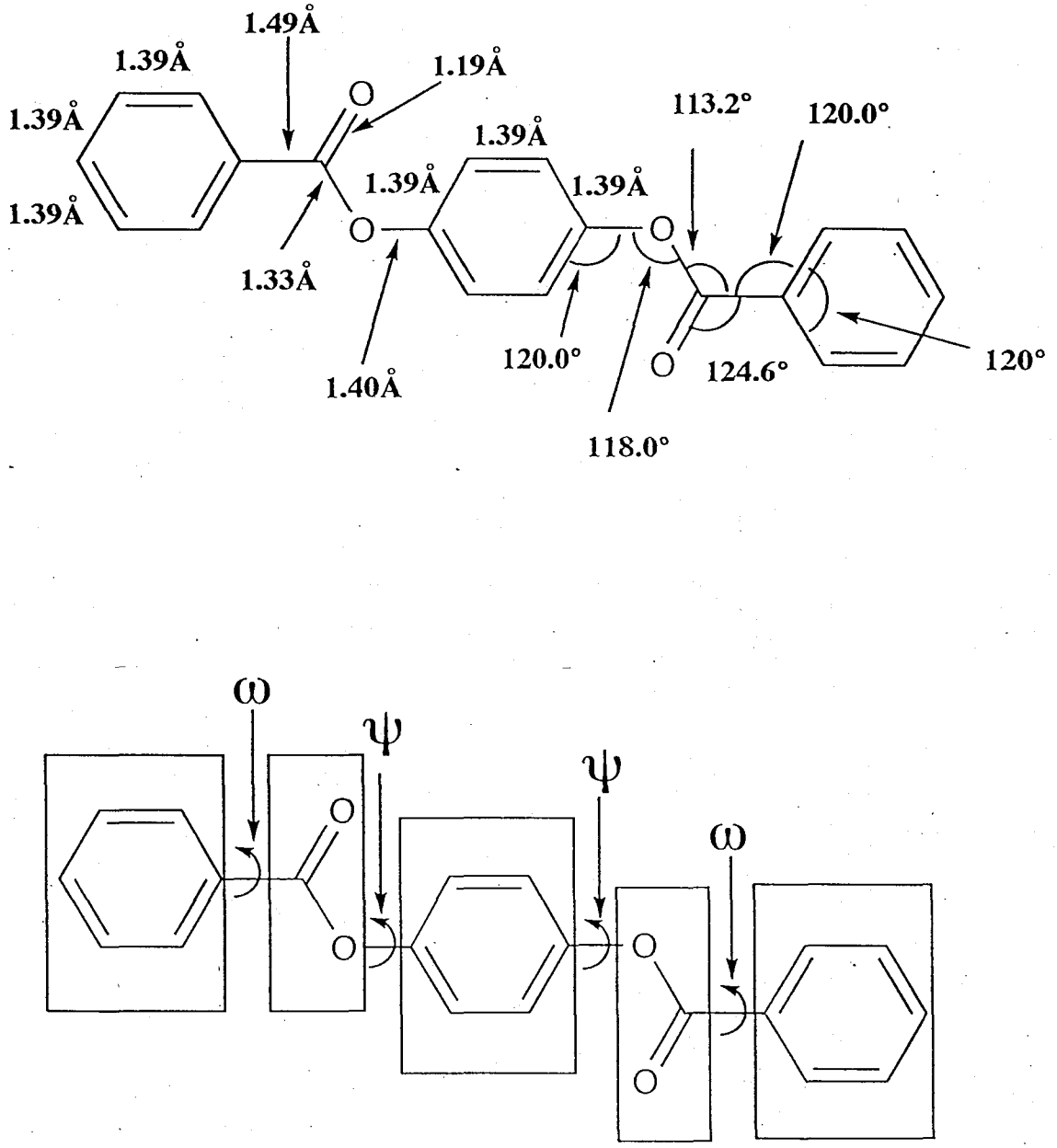

Figure 6-6. Model compound and the geometric parameters of the main chain of H-Cn polyester for the FPT-INDO calculation.

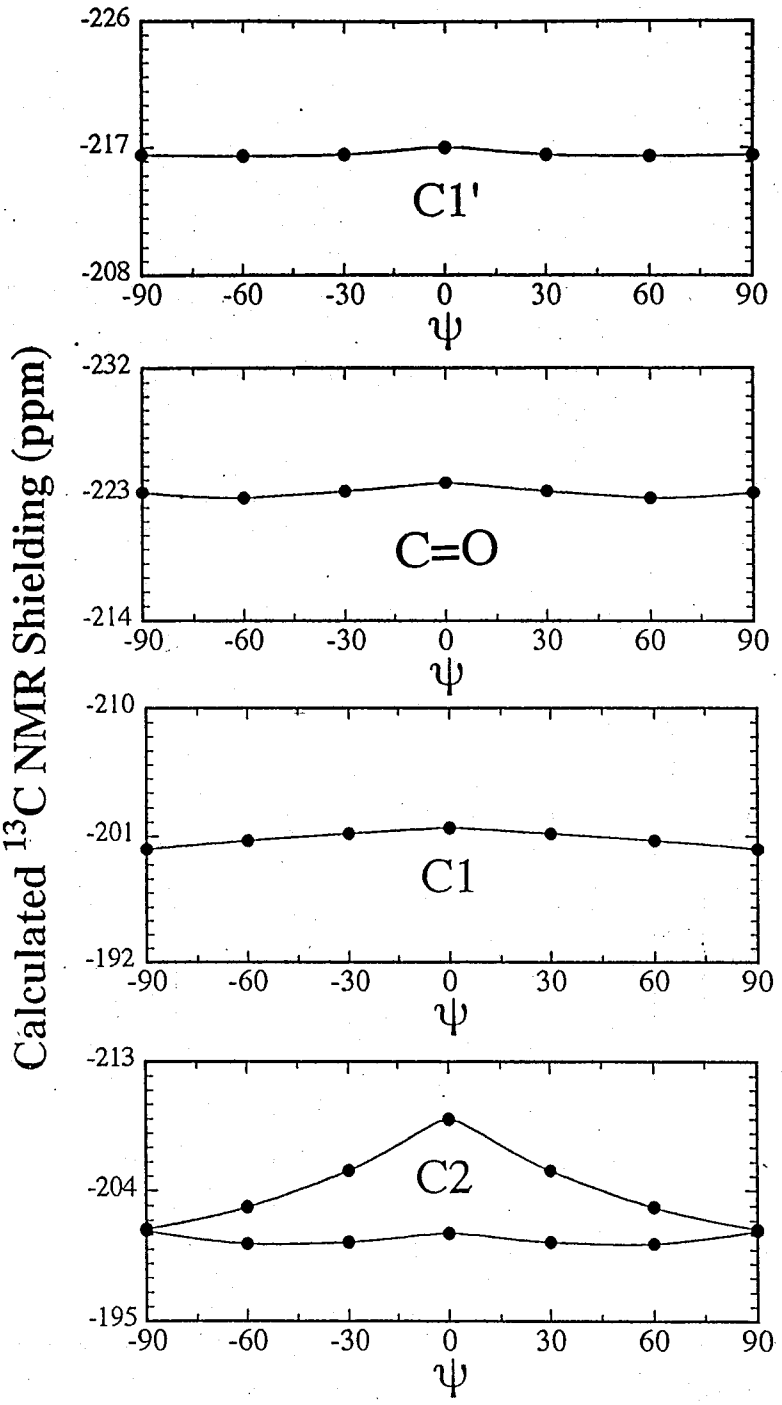

Figure 6-7. Calculated ^{13}C NMRshieldings of the carbons of the ester bond as a function of the relative torsion angle, ψ, under the condition ω = 0°. The negative sign indicates deshielding.

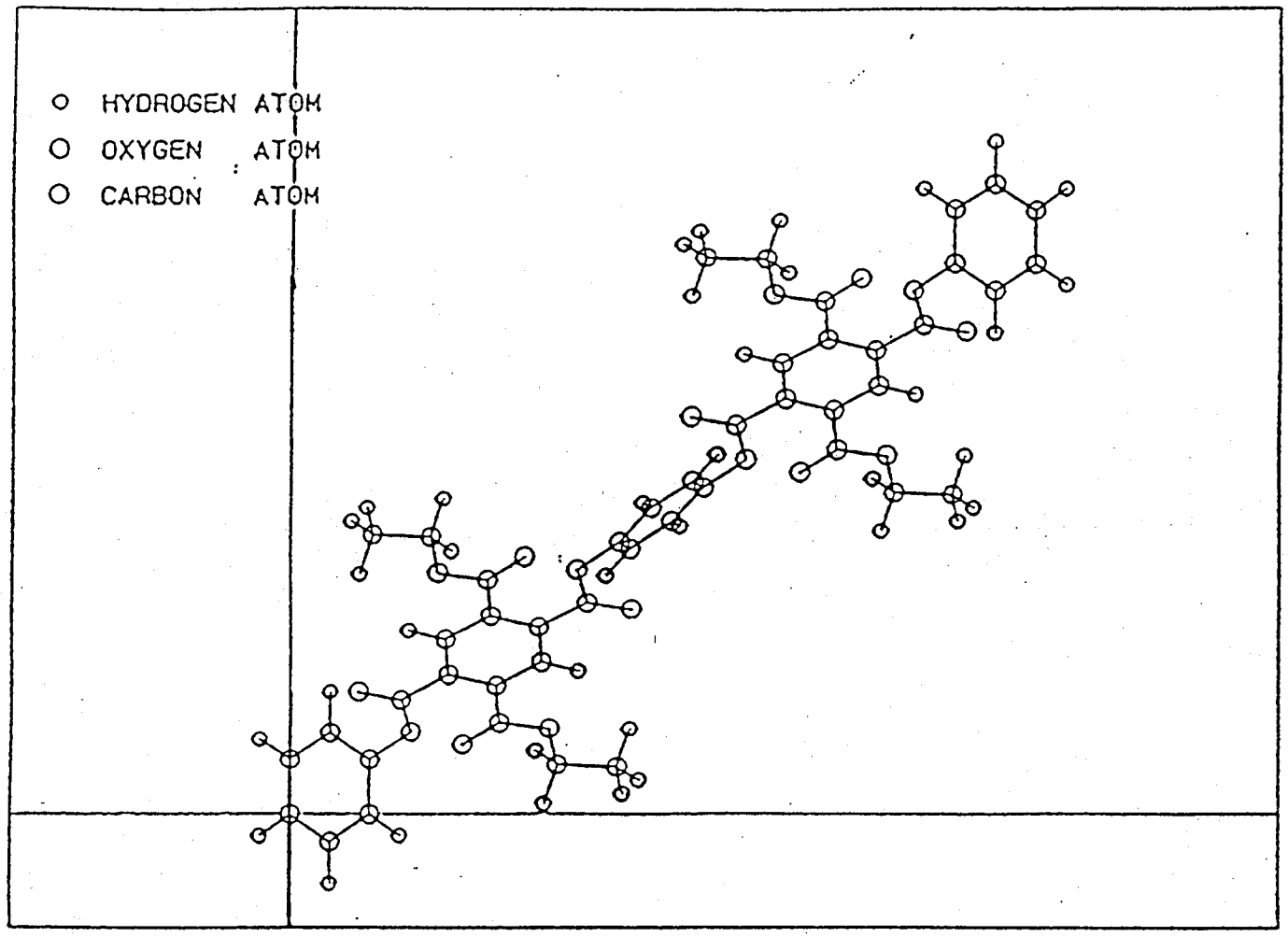

Figure 6-8. Chain conformation in Kc crystals according to the FPT-INDO calculation.

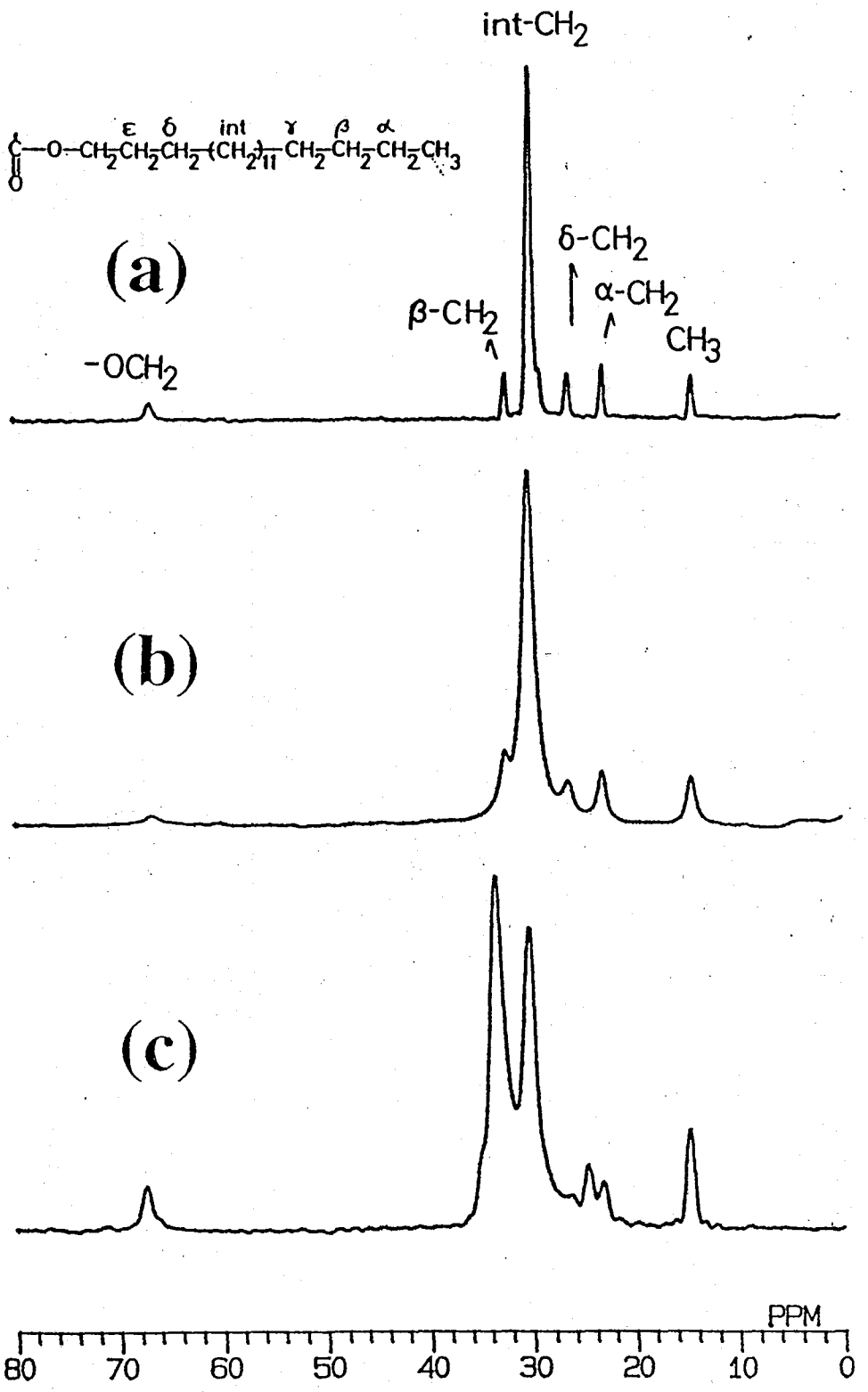

Figure 6-9. Expanded aliphatic region of the ^{13}C TOSS MAS spectra for (a)Isotropic liquid, (b) liquid crystal as observed by the gated decoupling method and (c) Kc crystal as observed by CP method.

aromatic chains that requires an anomal conformation.

Figure 6-10 shows a typical example of ^{13}C CP/MAS spectrum for H-Cn in the Km1 crystal (HC-16) as obtained on annealing the quenched sample at 60°C. The observed ^{13}C chemical shift values are summarized in Table 6-1.

Two sharp peaks due to the main- and side-chain carbonyl carbons in Km1 crystal were observed at 167.6 and 163.9 ppm, and the two aromatic carbon peaks C1' and C2' were observed at 136.0 and 132.9 ppm. The aromatic carbon peak C3' was observed at 128.9 ppm.

As discussed in conformational studies in two crystals of B-Cn and Kc crystal of H-Cn, the conformation for the pyromellitic ester groups is coplanar with the aromatic moiety. In fact the aromatic carbon peaks, C1' and C2', were observed at about 136.0 or 131.0 ppm as a single overlapped sharp peak or two split sharp peaks. However, in Km1, the higher field aromatic carbon peak C1' shifts about 2 ppm from 131.0 to 133.0 ppm comparing that in Kc. Hence, we arrive at a preliminary conclusion that the ester group in Km1 may not be in a coplanar conformation. Figure 6-11 show the diagram of the ^{13}C chemical shift behavior in Kc and Km1.

To verify the above suggestion, the calculation of the ^{13}C NMR shielding constants was performed for model compound as shown in Figure 6-6 as a function of the dihedral angle ω. Figure 6-12 shows the dihedral angle dependence of the chemical shifts of the carbon atoms Cm, C1', C1 and C2. These calculated results show that an increase in the torsional angle ω shifts the carbon peaks, Cm and C1', into the lower field. As compared with the observed data in Figure 6-11, this trend in the calculated ^{13}C NMR shieldings qualitatively corresponds to that observed experimentally. Thus, the dihedral angle ω in Km1 is considerably larger than that in Kc crystal.

We next focus on the ester bond between the phenyl rings of the hydroquinone and pyromellitic moieties. The peaks of the aromatic carbons C1 and C2 were observed at 145.5 and 121.9 ppm, respectively. The chemical shift value, 121.9 ppm, of the C2 carbon is almost same as that in solution or isotropic phase. The peak C1 shifts by about 4 ppm to higher field compared to that in Kc.

Figure 6-7 shows the variation of chemical shift with torsional angle ψ. An increase in the angle ψ results in a shift of the C1 carbon peak to higher field. These calculated results indicate that the ester bond is twisted with larger angle than that in Kc seen from the chemical shift changes of C1 and C2 carbons. Comparing the chemical shift value in Kc and isotropic phase, we could tentatively suggest that the ester bond is twisted and the ester moiety is perpendicular to the phenyl ring of the hydroquinone.

Thus, there are four different points on the the main chain conformation of Km1. [1] The main chain is fully extended as determined from the X-ray diffraction pattern. [2] The main chains are packed in a monolayer with an unusual interchain distance of 3.85 Å. [3] The dihedral angle ψ is about 90° on the basis of the chemical shift values for the C1 and C2 carbons. [4] The dihedral angle ω is effectively larger as determined from the chemical shift values of C1' carbon peak. These results dictate the prediction of main chain conformation such that the main chain takes a stairlike conformation with both the torsional angles ψ and ω being 90°.

Moreover, since the chemical shift change of C1' carbon peak was observed in the higher field, the conformation of pyromellitic moiety is considered to be of conformation i as discussed before for the conformation of Kc. From this result, we can find that the main chain conformation of Km1 is confined uniquely about the pyromellitic moiety and ester bonds. Hence the possible main chain conformation is shown in Figure 6-13, which is deduced from the complete data.

Figure 6-9(c) shows the extended aliphatic region of the ^{13}C CP/MAS spectra for Km1 crystal. The assignments are summarized in Table 6-2. This data shows same results as Kc that the side chains are crystallized partially between the aromatic layers.

[4] Layered mesophase

Figure 6-14 shows an expansion of the aromatic region of the ^{13}C CP/MAS spectra of H-C16 in Kc and Km1 crystals and LC phase. These spectra show that the main chain conformation in LC takes almost the same conformation as in Km1 crystal although a significant difference in the

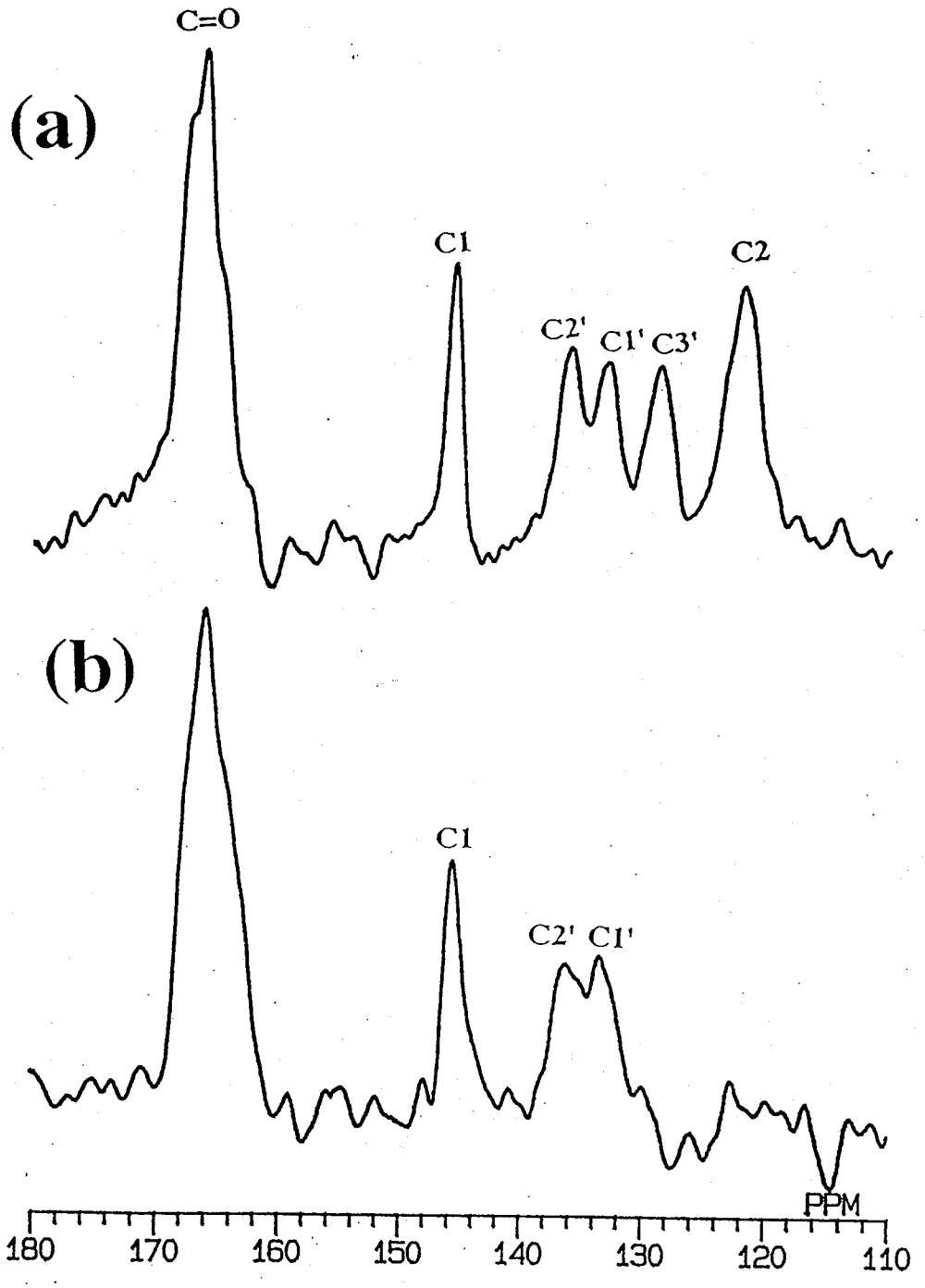

Figure 6-10. Expanded aromatic region of the ^{13}C TOSS MAS NMR spectra for Km1 crystal of B-C16 polyesters using (a) CP and (b) dipolar dephasing methods.

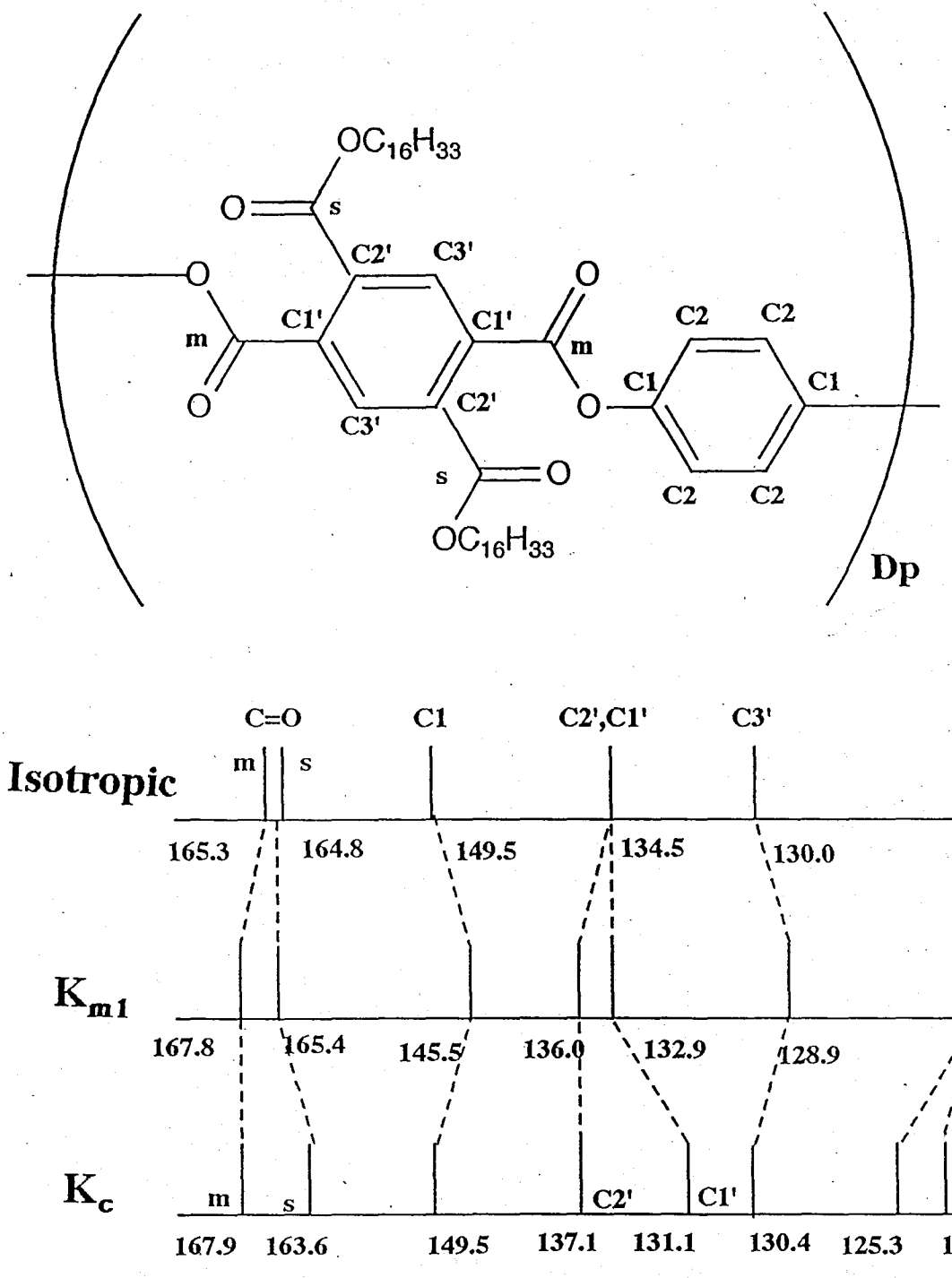

Figure 6-11. Diagram of the observed ^{13}C chemical shifts of the carbon in the main chains in Isotropic liquid, Kc crystal and Km1 crystal.

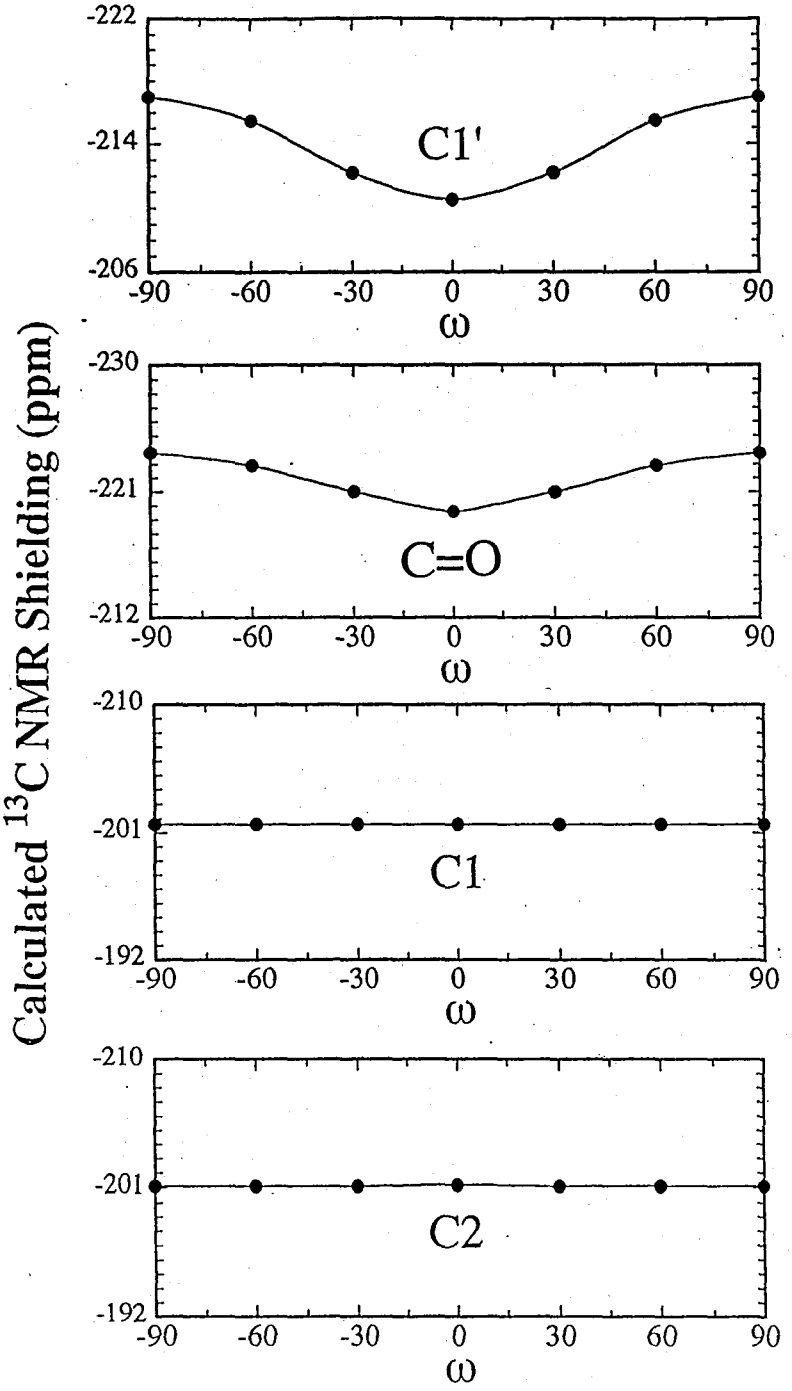

Figure 6-12. Calculated ^{13}C NMRshieldings of the carbons of the ester bond as a function of the relative torsion angle, ω1, under the condition ψ = 60°. The negative sign indicates deshielding.

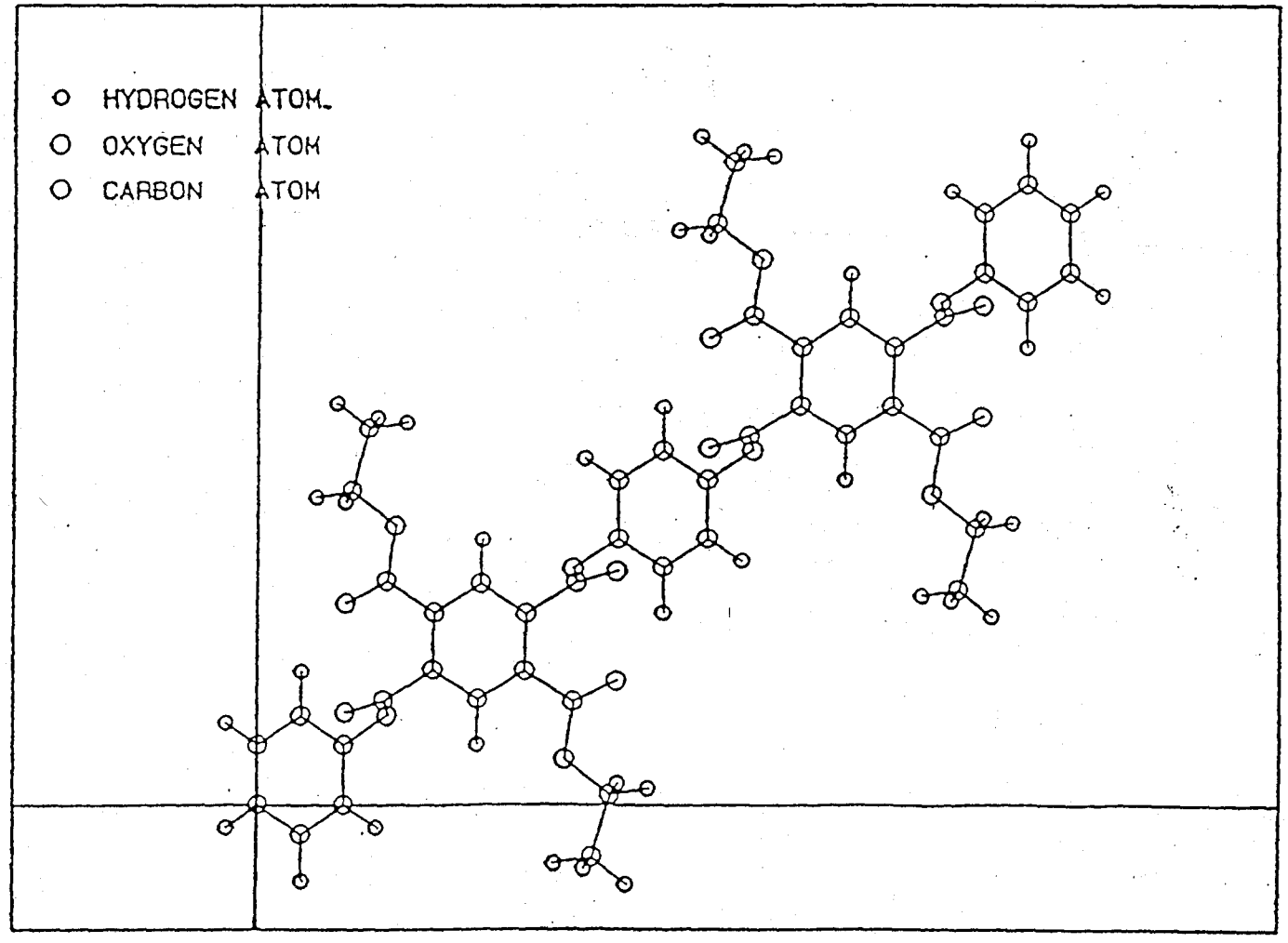

Figure 6-13. Chain conformation in Km1 crystals according to the FPT-INDO calculation.

chemical shifts of the aromatic carbons C1' and C2' is observed. This difference may result from a greater degree of molecular motion in the mesophase of the main and side chains.

Figure 6-15 shows an expanded aliphatic region of the spectra for Kc, LC and isotropic phase. The chemical shifts are listed in Table 6-3 and 6-4. The chemical shift values clearly show that the aliphatic side chains are in a molten state in liquid crystalline phase as well as in isotropic phase. Furthermore, it is apparent from Figure 6-9 that in liquid crystalline phase the half width of the O-CH_2 and δ-CH_2 carbon atoms, which are located near the main chain, are larger than those of other carbons although in isotropic phase the width of all the aliphatic carbons is nearly the same. These differences are believed to originate from inhomogeneities in the molecular motion of the alkyl side chains. Therefore, in layered liquid crystals, the aliphatic carbons near the main chain have less mobility than the other carbons. The formation of the layered structure is believed to restrict the molecular motion of the aliphatic carbon atoms close to the main chains.

[5] Km2 Crystal

In Chapter 4, It was found that H-Cn with n = 6 to 10 form a characteristic layered structure in which the aromatic main chains are packed like zigzag sheet within a layer. Thus, in this phase, the main chains are not packed laterally in a monolayer and thus might take a different conformation from that in Km1 and Kc.

Figure 6-15 show the ^{13}C CP/MAS spectra of H-C6, 8 and 10 in Km2 estimated from X-ray diffraction patterns. These spectra are the same for chemical shift values but are different from that of Km1 and Kc crystals. Especially, the number of peaks in the carbonyl and the aromatic region are larger than that in the Kc and Km1. Considering the conformation of Kc and Km1, it is found that different conformations are mixed in Km2. Moreover, it is very interesting that the side-chains assume a complete amorphous state although these X-ray patterns show that this crystal has three dimensional order. The observed chemical shift values are summarized

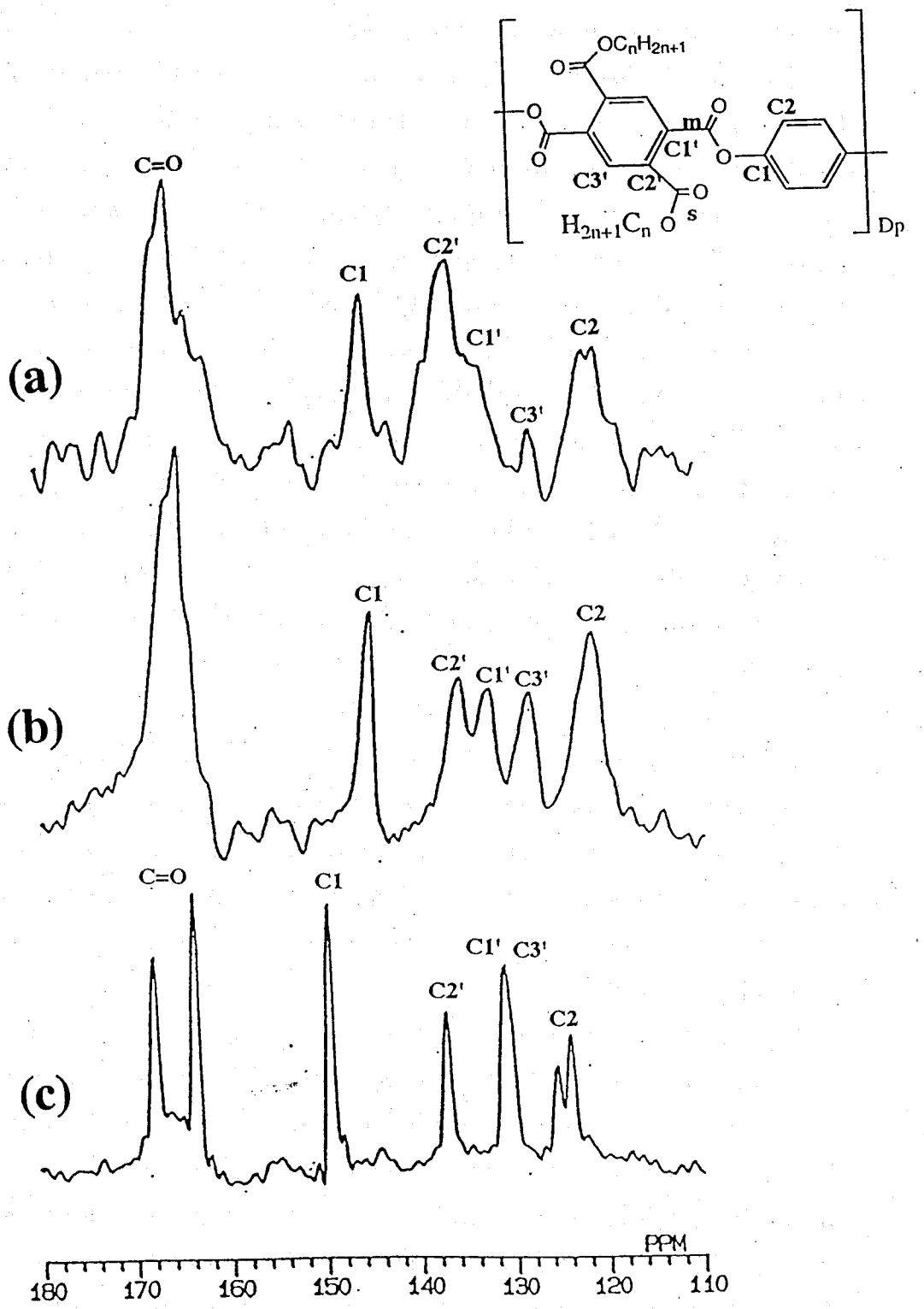

Figure 6-14. Expanded aromatic region of the ^{13}C TOSS CP/MAS spectra for (a) liquid crystal, (b) Kc crystal and (c) Km1 crystal.

Table 6-3

Observed ^{13}C NMR Chemical shifts for the aromatic carbons of the H-C16 polyesters in the various state.

	Observed ^{13}C NMR Chemical shift (ppm)						
	C=O						
	m[a]	s[b]	C1	C1'	C2'	C3'	C2
Soln[c].	165.3	164.8	149.5	134.5	134.5	130.0	122.6
Isotropic	165.7	165.7	135.3	135.3	135.3	130.3	122.6
Liquid Crystal	170.9	167.9	145.5	136.2	133.1	129.8	121.2
Kc Crystal	167.9	163.6	149.5	137.1	131.0	130.4	125.3 123.8
Km1 Crystal	167.8	165.4	145.5	136.0	132.9	128.9	122.0

m[a]; main chain s[b]; side chain c; $CDCL_3$ solution

in Tables 6-1 and 6-2.

Four sharp peaks due to the main and side chain carbonyl carbons in Km2 were observed at 168.7, 167.0, 165 and 163.0 ppm. The four split aromatic carbons, C1' and C2' were observed at 138.3, 135.3, 133.6 and 132.8 ppm. The aromatic carbon C3' was observed at 128.6 ppm. Comparing the pairs of peaks in Km2 with those in Km1, we can recognize the existence of the main chain conformation of Km1 with the chemical shift values of C1' and C2' (135.3 and 133.6 ppm) and those of carbonyl carbons (167.0 and 163.0 ppm). The two split peaks of C1 carbon were observed at 146.2 and 149 ppm and that in Km1 at 146.0 ppm. The change in the relative intensity of the peaks implies the mixing of the different main chain conformations. Hence we can easily separate two components in the Km2. Figure 6-16 shows a diagram of the observed chemical shift values of H-Cn in Km2 and Km1.

Except for the pair of peaks in main chain conformation observed in Km1, other pair of the carbon peaks was observed at 138.3 and 132.8 ppm for C1' and C2' carbons and at 168.7 and 165.0 ppm for carbonyl carbons and 148.9 ppm for C1 carbon, respectively. In a section on Km1 we proposed, on the basis of the chemical shift values, that the main chain in Km1 takes a stairlike conformation with the dihedral angle ω2 being 180° ; i-s conformation as shown in Figure 6-16, while we can find the existence of another stairlike conformation with ω2 being 0°; iii-s conformation. The ^{13}C shielding calculation of model compound indicate that an increase of the dihedral angle ω1 shifts the peak of C1' carbon into the lower field. Thus, we could arrive at a conclusion that the stairlike conformation with the dihedral angle ω2 being 180° shows the chemical shifts at 135.3 and 133.6 ppm (C2' and C1'), 167.0 and 163.0 ppm (carbonyl carbons) and 146.2 ppm (C1) while another one with ω2 being 0° shows the ^{13}C chemical shifts at 138.3 and 132.8 ppm (C1' and C2'), 168.7 and 165.0 ppm (carbonyl carbons) and 149.0 ppm (C1).

[6] Kh Crystal

In Kh crystal of H-C6, the aromatic main chains are packed in a

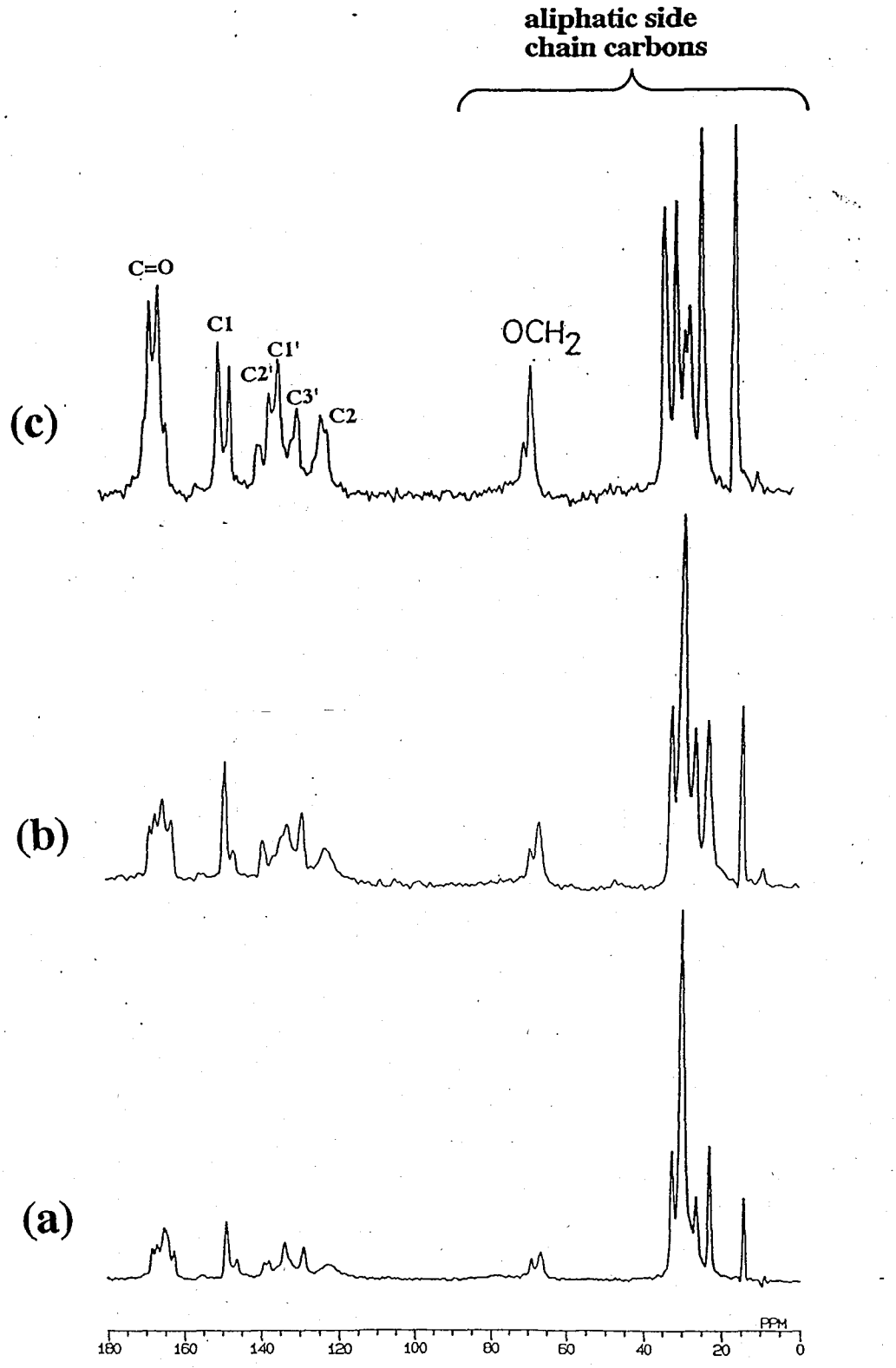

Figure 6-15. ^{13}C TOSS CP/MAS NMR spectra for Km2 crystal of B-Cn polyesters; (a) H-C10, (b) H-C8 and (C) H-C6 polyesters.

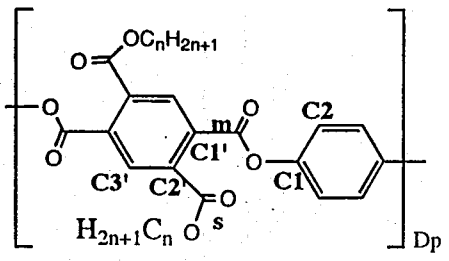

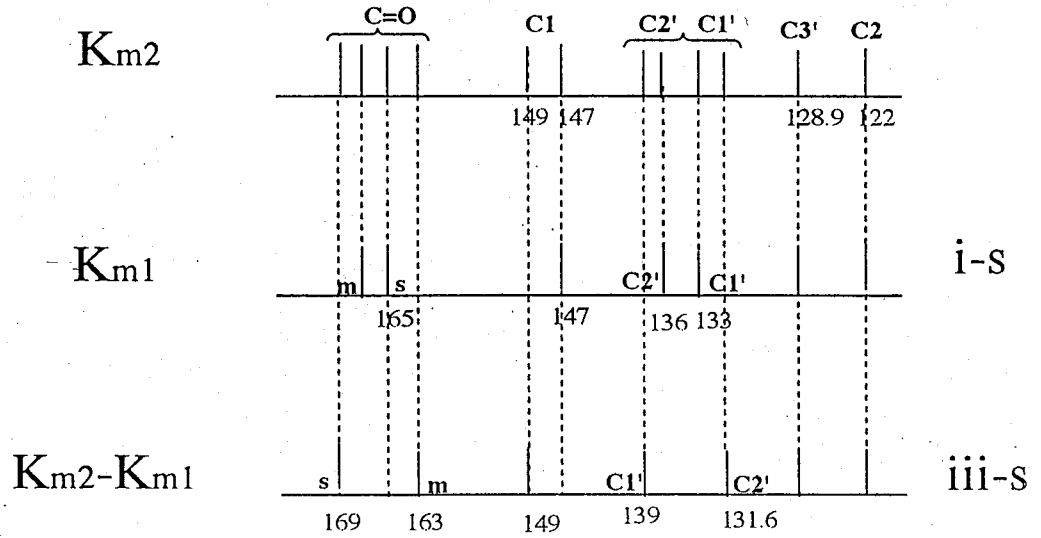

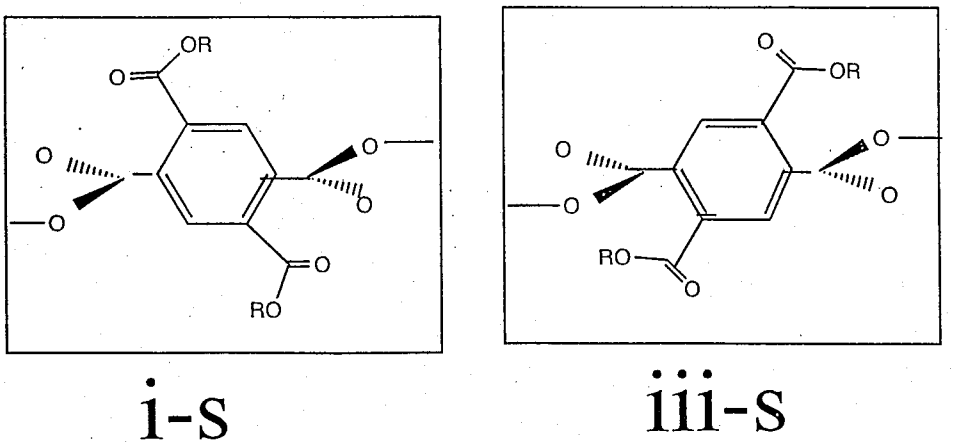

i-S iii-S

Figure 6-16. Diagram of the observed ^{13}C chemical shifts of the carbon in the main chains in Km2 and Km1 crystal.

Table 6-4

Observed ^{13}C NMR Chemical shifts for the aliphatic carbons of the H-C16 polyesters in the various state.

	^{13}C NMR chemical shifts / ppm								
			Interior CH_2		δ	α		CH_3	
Temp/°C	OCH_2	β	Cryst.	Amor.		Cryst.	Amor.	Cryst.	Amor.
Soln.($CDCl_3$)	66.9	31.8	--	29.5	25.9	--	22.7	--	14.1
Isotropic	66.6	32.5	--	30.2	26.6	--	23.2	--	14.4
Liq.Cryst.	66.3	32.6	--	30.4	26.8	--	23.4	--	14.8
Kc Crystal	67.6	--	33.7	30.4	26.8	24.9	23.3	--	14.8
Km1Crystal	67.0	--	33.2	30.9	27.4	24.7	23.8	--	14.9

*Cryst. and Amor. indicate the crystalline and noncrystalline state, respectively.

hexagonal lattice and this crystal has three dimensional positional orders.

Figure 6-17 shows the ^{13}C MAS spectra of H-C6 in Kh, Km2 and isotropic phase. All the spectra show the alkyl side chains in these three phases in a molten state. In Km2, the aromatic and carbonyl carbon peaks are sharp and split into many peaks while all of the peaks in Kh are broad which means that the main chain conformation is not confined and it has a large distribution of the conformations. The peaks of C1' and C2' carbons are broad at around 133.0 ppm and C1 and C2 peaks appear at 149.0 and 123 ppm as well as in isotropic phase.

This result means that the hexagonal packing of the main chain would never restrict the main chain conformation while the main chain conformation is confined in layered mesophase and crystals. It should be pointed that Kh crystal is highly ordered with the main and side chains assuming a molten state.

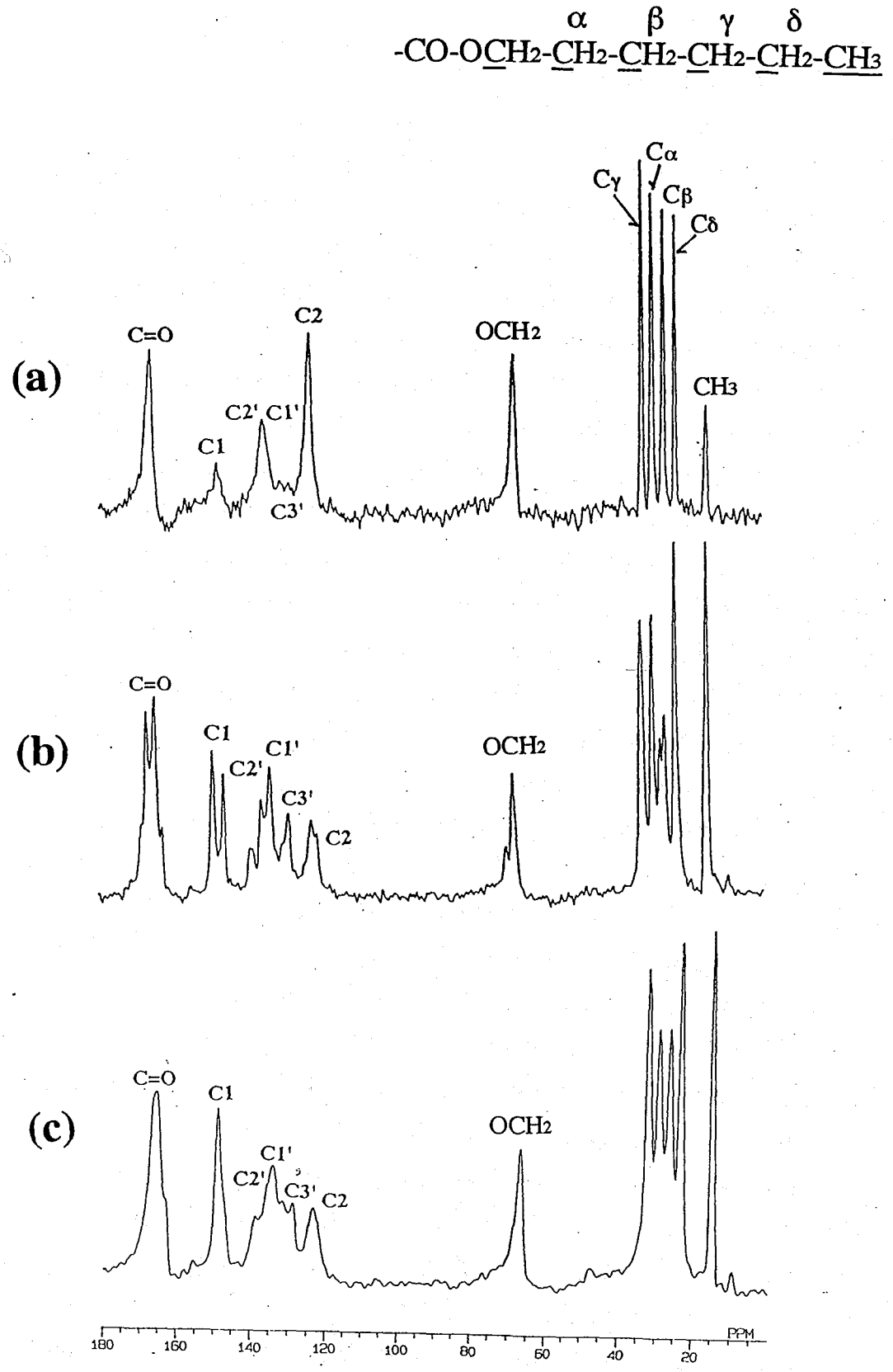

Figure 6-1ㄱ. ^{13}C TOSS MAS NMR spectra for Kh crystal of B-C6 polyesters. (a) Isotropic liquid as observed by the gated decoupling method, (b) Km2 crystal and (c) Kh crystal as observed by CP method.

6-4 Concluding Remarks

High resolution solid state ^{13}C NMR spectra have provided detailed informations about the main and side chain conformations in the crystalline and liquid crystalline phases of H-Cn polyesters. In Kc crystal, the ester bonds assume a twisted conformation with the pyromellitic ester functionalities situated asymmetrically about an axis drawn between the C1' and C2' carbons. In Km1 crystal, the main chain takes a stairlike conformation that all the phenyl rings lie parallel to each other with the pyromellitic ester functionalities situated like conformation i. In Kc and Km1 crystals, the alkyl side chains are crystallized between the main chain layers. In the liquid crystalline phase, the main chain conformation takes that in Km1. Thus, the main chain conformations are restricted in a monolayer of Kc, Km1 and layered mesophase.

In Km2 crystal, the main chain takes two types of stairlike conformations with the amorphous side chain. Thus, different conformations are mixed in Km2 crystal. In Kh crystal, the main and side chain are in an isotropic state in which there is a large distribution of the conformations and thus the conformation is not confined. It is of interest that alkyl side chain is amorphous in Kh and Km2 although H-Cn polyesters form highly ordered crystal with three dimensional positional orders. On the point of category for the polymeric material, the Km2 and Kh crystals could belong to ''condis crystal'' (conformational disordered crystal) proposed by Wunderlich[46].

Coulter and Windle[44] report that most stable is a conformation in which the dihedral angles ψ and ω are about 45° and 0°, respectively, in liquid crystalline polymers, on the basis of experimental and calculated results. Considering this results, the main chain conformation in Kc is most stable while that in Km1, LC and Km2 is energetically unstable. It is believed that the anomal stairlike conformation observed in Km1, Km2 and LC phases is mainly forced by the layered segregation of the aromatic main chains and the long aliphatic side chains.

This conformational analysis and same analysis of B-Cn show one

conclusion that an anomal chain conformation is confined by a monolayer packing in layered structure. Recently, we consider that two factors could confine the main chain conformation in the aromatic layer of the layered structure. One factor is a monolayer packing caused by segregation of aliphatic and aromatic domains. This phenomenon in layered structure is likely to be a microphase separation of triblock polymers. With short component of the alkyl side chains, H-Cn form cylindrical phase while with longer side chain H-Cn form layered phase. In layered phase, the aromatic main chains are confined to monolayer packing.

Another factor is a formation of a ground state charge transfer complex between neighboring chains in a monolayer[13]. This complex is measured by fluorescence and recognized the stability in high temperature. In a monolayer between the aliphatic domains, a charge transfer interaction make the aromatic main chains to assume most suitable conformation for a confined space between the layers. Especially, H-Cn with n = 12 to 18 form two types of main chain packing. The conformation in Km1 is more stable than that in Kc although that in Km1 is unstable than that in Kc for a single chain. Thus, a transition from Kc to LC (thus Km1) can be interpreted to be a exchange between the two ground state charge transfer complexes.

Unger proposed the classification of the polymeric materials on the basis of the dimension for long range positional order and orientational order and a conformational disorder[46,47]. On the classification, Kc and Km1 could belong to 'crystal' because this has three dimensional positional orders, orientational orders and confined conformation[46]. Layered mesophase could be in 'liquid crystal' with one dimensional long range positional order and orientational order. Moreover, Km2 and Kh might belong to 'condis crystal' because it has dynamic conformational disorder and long range positional and orientational order. The mechanism of a formation of Km2 and Kc is not solved and many factors might influence these formation for the deriving force. This matter has been studied and will be reported in further.

6-5 References and Notes

(1) Ballauff, M. Macromol. Chem., Rapid Commun. 1986, **7**, 407.

(2) Ballauff, M. Angew. Chem., Int. Ed. Engl. 1987, **28**, 253.

(3) Ballauff, M.; Schmidt, G.F. Mol. Cryst. Liq. Cryst. 1987, **147**, 163.

(4) Stern, R.; Ballauff, M.; Wegner, G. Macromol. Chem., Macromol. Symp. 1989, **423**, 373.

(5) Rodrigues-Parada, J. M.; Duran, R.; Wegner, G. Macromolecules 1989, **22**, 2507.

(6) Ebert, M.; Herrmann-Schenherr, O.; Wendorf, J.; Ringsdorf, H.; Tschirner, P. Liq. Cryst. 1990, **7**, 63.

(7) Adam, A.; Spiess, H. M. Macromol. Chem., Rapid Commun. 1990, **11**, 249.

(8) Frech, C. H.; Adam, A.; Falk, U.; Boeffel, C.; Spiess, H. W. New Polym. Mater. 1990, **2**, 267.

(9) Stern, R.; Ballauff, M.; Lieser, G.; Wegner, G. Polymer 1991, **32**, 2079.

(10) Harkness, B. R.; Watanabe, J. Macromolecules 1991, **24**, 6759.

(11) Watanabe, J.; Harkness, B.R.; Sone, M. Polym. J. 1992, **24**, 1119.

(12) Cervinka, L.; Ballauff, M. Colloid Polym. Sci. 1992, **270**, 859.

(13) Sone, M.; Harkness, B.R.; Watanabe, J.; Torii, T.; Yamashita, T.; Horie, K. Polym. J. 1993, **25**, 997.

(14) Galda, P.; Kistner, D.; Martin, A.; Ballauff, M. Macromolecules 1993, **26**, 1595.

(15) Marz, K.; Lindner, P.; Urban, J.; Ballauff, M.; Fischer, E. W. Acta Polym. 1993, **44**,139.

(16) Damman, S. B.; Mercx, F. R. P.; Kootwijk-Damman, C. M. Polymer 1993, **34**, 1891.

(17) Damman, S. B.; Mercx, F. P. M. J. Polym. Sci., Polym. Phys. 1993, **31**, 1759.

(18) Damman, S. B.; Mercx, F. P. M.; Lemstra, P. J. Polymer 1993, **34**, 2726.

(19) Damman, S. B.; Vroege, G. J. Polymer 1993, **34**, 2732.

(20) Kakimoto, M.; Orikabe, H.; Imai, Y. ACS Polym. Prep. 1993, **34**, 746.

(21) Steuer, M.; Hortz, M.; Ballauff, M. J. Polym. Sci., Polym. Chem. 1993, **31**, 1609.
(22) Watanabe, J.; Harkness, B.R.; Sone, M.; Ichimura, H. Macromolecules 1994, **27**, 507.
(23) Sone, M.; Harkness, B. R.; Kurosu, H.; Ando, I.; Watanabe, J. Macromolecules 1994, **27**, 2769.
(24) Damman, S. B.; Buijs, J. A. H. M.; Polymer 1994, **35**, 2559.
(25) Damman, S. B.; Buijs, J. A. H. M.; van Turnhout, J. Polymer 1994, **35**, 2364.
(26) Buijs, J. A. H. M.; Damman, S. B. J. Polym. Sci., Polym. Phys. 1994, **32**, 851.
(27) Sone, M.; Harkness, B. R.; Kawasaki, H.; Watanabe, J. to be published.
(28) Sekine, N.; Watanabe, J.; Sone, M. Macromolecules to be submitted.
(29) Watanabe, J.; Ono, H.; Uematsu, I.; Abe, A. Macromolecules 1985, **18**, 2141.
(30) Watanabe, J.; Takashina, Y. Macromolecules 1991, **24**, 3423.
(31) Watanabe, J.; Takashina, Y. Polym. J. 1992, **24**, 709.
(32) Yamagishi, T.; Fukuda, T.; Miyamoto, T.; Yakoh, Y.; Watanabe, J. Mol. Cryst. Liq. Cryst. 1990, **7**, 155.
(33) Yamagishi, T.; Fukuda, T.; Miyamoto, T.; Yakoh, Y.; Takashina, Y.; Watanabe, J. Liq. Cryst. 1991, **10**, 467.
(34) Ando, I.; Yamanobe, T.; Kurosu, H.; Webb, G. A. Annu. Rep. NMR Spectrosc. 1990, **22**, 205.
(35) Ando, I.; Yamanobe, T.; Asakura, T. Prog. NMR Spectrosc. 1990, **7**, 839.
(36) Kurosu, H.; Yamanobe, T.; Ando, I. J. Chem. Phys. 1988, **89**, 5216.
(37) Sone, M.; Yoshimizu, H.; Kurosu, H.; Ando, I. J. Mol. Struct. 1993, **301**, 227.; 1994, **317**, 111.
(38) Asakawa, N.; Kurosu, H.; Ando, I.; Shoji, A.; Ozaki, T. J. Mol. Struct. 1994, **317**, 119.
(39) Bruck, D.; Rabinovits, M. Tetrahedron Lett. 1977, **47**, 4121.
(40) VanderHart, D. L.; J. Magn. Reson. 1981, **44**, 117.
(41) Ishikawa, S.; Kurosu, H.; Ando, I. J. Mol. Struct. 1990, **248**, 361.

(42) Yamanobe, T.; Tsukahara, M.; Komoto, T.; Watanabe, J.; Ando, I.; Uematsu, I.; Deguchi, K.; Fujito, T.; Imanari, M. Macromolecules 1988, **21**, 48.
(43) Simmons, A.; Natansohn, A. Macromolecules 1992, **25**, 3881.
(44) Coulter, P.; Windle, A.H. Macromolecules 1989, **22**, 1129.
(45) Uryu, T.; Kato, T. Macromolecules 1988, **21**, 378.
(46) Wunderlich, B.; Moeller, M.; Grebowitz, J.; Baur, H. Adv. Polym. Sci. 1988, **87**, 1.
(47) Unger, G. Polymer 1993, **34**, 2050.

Chapter 7

Charge Transfer Complex Formation in Layered Phases of B-Cn Polyesters Analyzed with Variable Temperature Fluorescence Spectroscopy

7-1 Introduction

There has been a great deal of interest in rigid-rod polyesters with flexible side chains in the past decade or since the discovery of the ability to form thermotropic liquid crystalline phase[1-29]. The liquid crystal has been characterized by a layered segregated structure in which the rigid-rod main chains are laterally packed into monolayer with the flexible side chains occupying the space between the layers. It has been postulated that the driving force for the adoption of such a structure is a segregation of the aliphatic and aromatic domains. In these layered structures, the liquid crystallinity is the result of a partial or total lack of positional order with respect to the main chain packing within the layers and also by the fluidlike disordered alkyl side chains between the layers. Moreover, these layered liquid crystalline phases are classified on the basis of the positional order with respect to the main chain packing within the layers[22].

In this thesis new rigid-rod polyesters with long alkyl side chains denoted as B-Cn or H-Cn polyesters have been prepared where n refers to the number of carbon atoms in the alkyl side chain[10,11,22]. The H-Cn polyesters in which the alkyl side chain length were greater than 10 carbon atoms formed highly ordered thermotropic mesophases that have a layered structure like those observed for similar types of rigid-rod polyesters with long flexible side chains[11]. On the other hand, the B-Cn polyesters with n = 14, 16 and 18 were found two novel thermotropic mesophases with the nature of the layered structure depending on temperature[22]. These two structures were different from the layered structure with respect to the degree of ordering and the packing arrangement of the chains within the

layers. In this layered structure, it has been clarified from the X-ray diffraction pattern that the aromatic main chains are in an extended form (repeat length of 16.6 Å) and are packed into a layered structure with positional order perpendicular to their long axes. Averaged lateral packing distance of main chain within a layer is 3.45 Å, indicating that the aromatic main chains are closely associated with each other. These imply the specific interaction or association of the pyromellitic ester group and biphenyl group which are included in the repeat unit of main chain.

Several recent studies[30-35] have shown that fluorescence measurements can be a valuable tool in elucidating the state of intra- and intermolecular aggregation of aromatic polymers in solid and liquid crystalline phases. The value of this technique lies in the fact that fluorescence measurements are sensitive to interactions between neighboring chromophore which in turn can be translated to give some information concerning the spatial geometry of these groups. The aim of this study is to clarify the intermolecular aggregation in the layered crystal and mesophase of B-Cn by examining the fluorescence behavior. Moreover, we demonstrate the change in the intermolecular aggregation between different layered structures during the phase transitions by using variable- temperature fluorescence spectroscopy.

7-2 Experimental

The synthesis of B-Cn polyesters (n; the carbon number of the alkyl side chain).

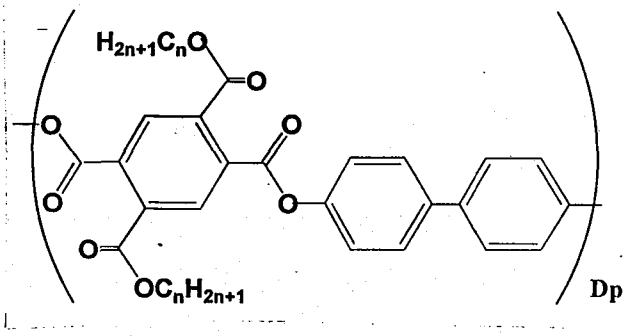

has been described in chapter 2[10,11]. Here the B-C14 polyesters were employed.

DSC measurements were performed with a Perkin-Elmer DSC II differential scanning calorimeter. Samples of about 10 mg were examined at a scanning rate of 10 °C/min under a flow of dry nitrogen.

WAXD measurements were carried out with a Rigaku Denki RU-200 X-ray generator system equipped with a flat plate camera using nickel filtered Cu Kα radiation. The distance from the sample to film was determined by using silicon powder. The sample temperature was controlled by a Mettler FP-80 hot stage with FP-82 central processor.

Steady-state fluorescence spectra were measured with a Hitachi 850 fluorescence spectrophotometer equipped with a 30 kV xenon lamp. The bandpasses were 5 nm for both excitation and emission monochrometors. The fluorescence and its excitation spectra for $10^{-1} \sim 10^{-4}$ M solution of model compound and polymers were measured by using a 1 mm quartz cell in side-face detection. For the crystal of model compound, the fluorescence spectra and its excitation spectra were measured at the surface of a 1 cm quartz cell. Those for the liquid crystalline polymers were measured in a front-face arrangement to minimize the self-absorption. The temperature of the liquid crystalline polymers was controlled by mean of an ALPHA engineering thermostat coupled with a temperature-controlling unit.

7-3 Results and Discussion

[1] Thermotropic Phase Behavior and Phase Structure of the B-Cn Polyesters

In Chapter 3[10,13,22], we reported that the B-Cn polyesters form two layered crystals (K1 and K2) and two liquid crystalline phases (LC-1 and LC-2). The phase behavior depends on the side chain length as depicted in Figure 7-1.

In the layered K1 and K2 crystalline phases, the aromatic main chains are in a fully extended conformation with a repeat length of 16.6 Å and these are regularly packed within a layer. In addition, the side chains are also in a crystalline state between the layers. The X-ray pattern is indicative of a crystal structure with three-dimensional order, which demands that the positional correlation between adjacent layers is maintained through the side chains crystals. Thus, the crystal structure is likely built up by a close coupling of the main chains crystals and the side chain crystals. It is interesting to note that the main chains in the K1 and K2 crystals are packed in a different manner. For the K1 crystal, which is formed from the B-Cn polyesters with side chains shorter than n = 12, the lateral packing distance of the main chains within a layer is 4.6 Å, but this reduces to 3.45 Å for the K2 crystal in the B-Cn polyesters with side chains longer than n = 16. The polyester B-C14 has been found to have characteristics of both types of crystalline phases depending on the crystallization temperature. The packing distance of 4.6 Å in the K1 crystal is reasonable for the main chains in a stable twisted conformation. In contrast, the short spacing of 3.45 Å in the K2 crystal indicates an unusually dense packing of the main chains that requires a conformation in which all the phenyl rings adopt a coplanar arrangement.

The LC-2 phase, the lower temperature mesophase, also has a layered segregated structure similar to that of the crystalline phase although its

fundamental structure is remarkably altered in several aspects from the crystal structure. The main chains are still in an elongated conformation (a repeat length of 16.6 Å) as in the crystalline phase, but they are packed into a layer having positional order only along the chain axis but not in the lateral direction. The side chains placed between the layers are in a molten state, which gives rise to the liquid crystalline fluidity of the phase. This type of liquid crystalline phase appears only for the B-Cn polyesters in which the alkyl side chains are longer than n = 14 (see Figure 7-2).

The LC-1 phase, the longer temperature mesophase observed for all specimens, displays a nematiclike optical texture, but a classic nematic phase cannot be postulated because it still exhibits a lateral packing spacing as large as that in the LC-2 phase. A biaxial nematic phase has been tentatively proposed such that the layers are retained, but there are frequently irregularities in their packing.

This study begins with an analysis of the main chain and side chain conformations in the layered K1 and K2 crystals, and in subsequent sections this is extended to measurements of the layered LC-1 and LC-2 mesophases.

[2] Fluorescence study of B-Cn polyesters

Origin of Fluorescence Initially, the excitation and emission spectra of the fluorescence were measured for the THF solution of B-C14 polyesters as a function of concentration. The data are shown in Figure 7-3. The fluorescence spectrum for the dilute solution of the B-C14 polyester at the concentration of 10^{-4} M (mol repeat unit/ L) shows a structured band with a maximum at 355 nm (excitation wavelength at 287 nm). This band can be attributed to an overlap of monomer fluorescence bands of both the biphenyl and pyromellitic ester moieties individually, since the fluorescence band for the biphenyl moiety may appear about 327 nm (excitation at 260 nm) as has been deduced from the fluorescence spectrum for diacetoxybiphenyl and that for the pyromellitic ester moiety may appear at 354 nm (excitation at 267 nm) as measured for the 1,4-ditetradecylester of pyromellitic acid (see later curves a and b in Figure 7-4).

Increasing the concentration of the polymer results in a profound change

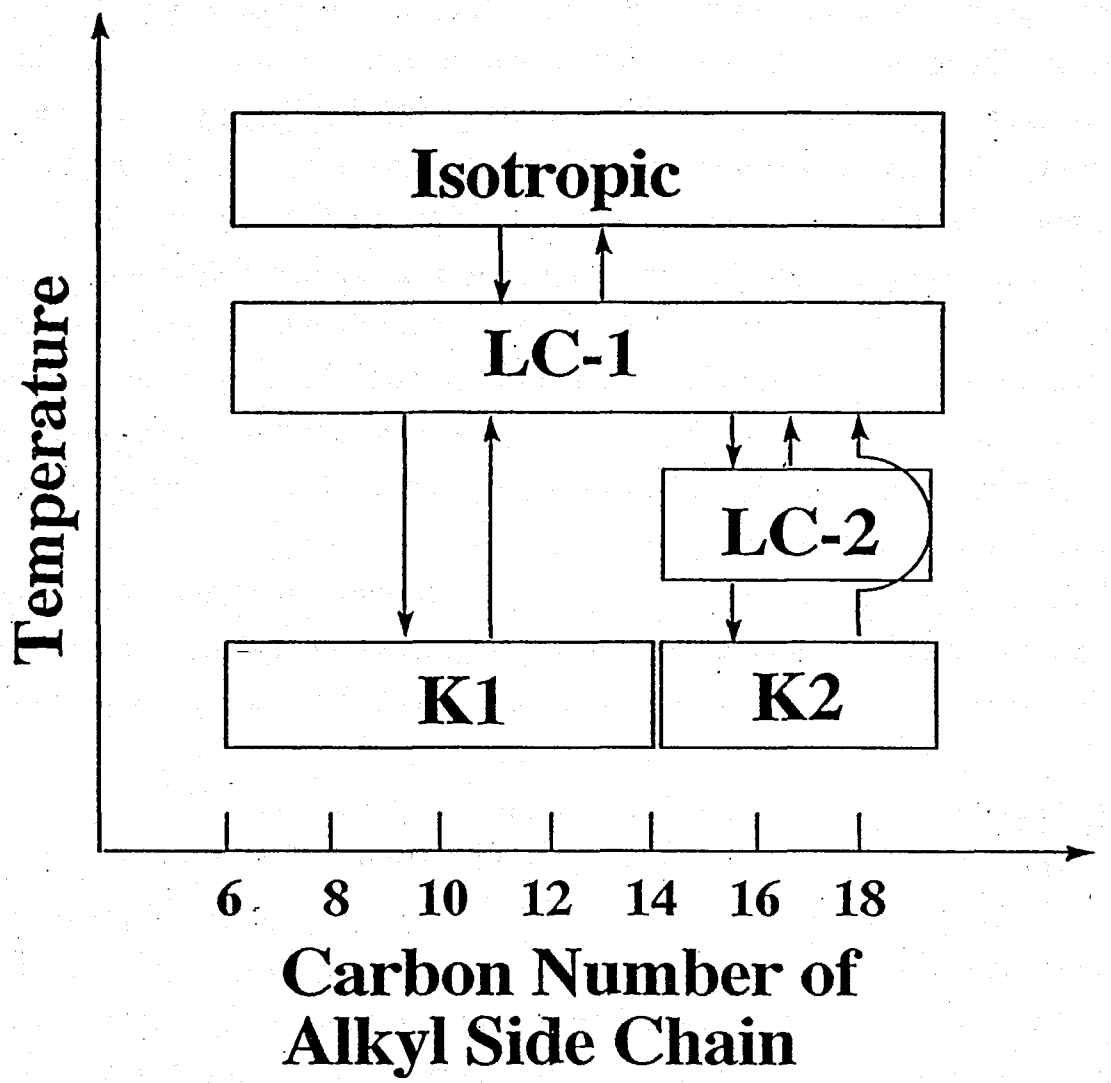

Figure 7-1. Schematic illustration of thermotropic phase behavior in B-Cn polyesters.

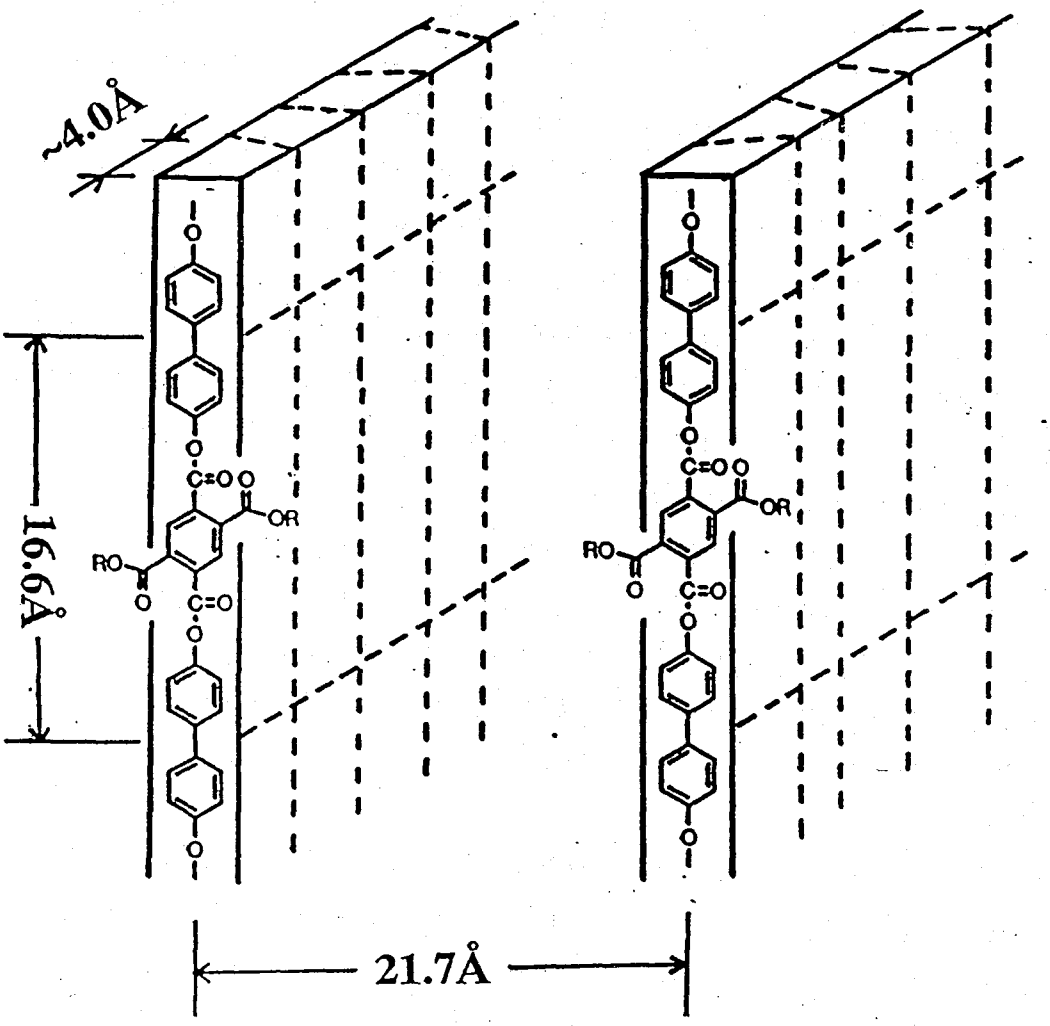

Figure 7-2. A proposed layered structure for the liquid crystalline phase of B-Cn polyester. In this layered structure, the aromatic main chains in the extended form pack into layers with positional order only in the lateral direction, and the aliphatic side chains in the disordered form occupy the space between the layers.

in both the excitation and emission spectra. The new broad excitation and emission bands (given by dashed curves) appear at longer wavelengths with the increase of the concentration from 10^{-4} to 10^{-1} M. Finally, they becomes predominant at the concentrations above 10^{-1} M; a excitation at 410 nm gives rise to a fluorescence band at 490 nm. Further, these are structureless. This result simply indicates that an increase in the concentration of the concentration of B-C14 cause a change in the electronic state of the biphenyl and pyromellitic ester chromophores. This would be due to an aggregation process which results in a ground state complex of charge transfer nature between the donor and acceptor groups. The excited state of the charge transfer complex becomes more stable than the change in ground state, emitting fluorescence at a longer wavelength. With respect to the B-Cn polyesters, there exists a donor group (biphenyl moiety) and an acceptor group (pyromellitic ester moiety) within an aromatic main chain, thus it can be predicted that a charge transfer complex is formed between these two units when they are in a suitable geometry and at a suitable distance.

To test this hypothesis, the fluorescence spectra for a mixture of two model compounds, 4,4'-diacetoxybiphenyl and 1,4-ditetradecylester of pyromellitic acid were examined at a concentration of 10^{-1} M. Figure 7-5 shows the fluorescence spectra for the individual compounds (curve a and b) and their equimolar mixture (curve c). Visually, the mixture of two compounds gave a slightly yellow collar as a result of molecular complex formation[36]. In addition, the mixture showed a structureless fluorescence band with a maximum at 470 nm which is similar to that observed in concentrated solution of B-C14 and is completely absent in the spectra of the individual compounds. This observation supports the proposal that the ground state molecular complex between biphenyl and pyromellitic ester groups exists in the concentrated solutions of B-C14. For forming such a complex it is necessary that the pyromellitic ester and biphenyl groups achieve a spatial orientation in which these groups are adjacent to one another in an alternating fashion although at this time we can gave no detailed aggregation structure in concentrated solutions.

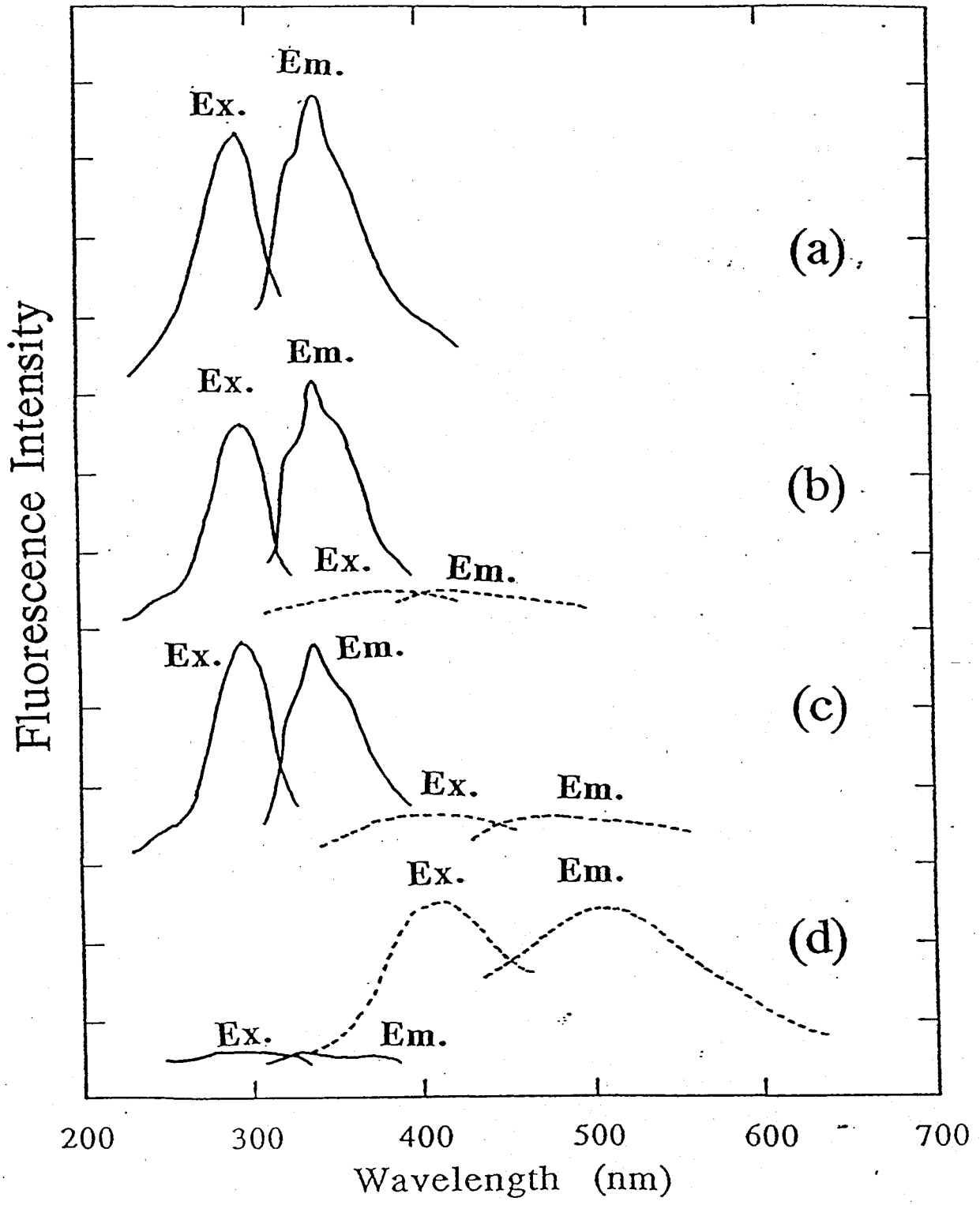

Figure 7-3. The fluorescence and its excitation spectra of B-C14 in Chloroform solutions at the concentrations of 10^{-4}M, 10^{-3}M, 10^{-2}M and 10^{-1}M. A pair of the fluorescence and excitation spectra are given by the solid curve or dash line.

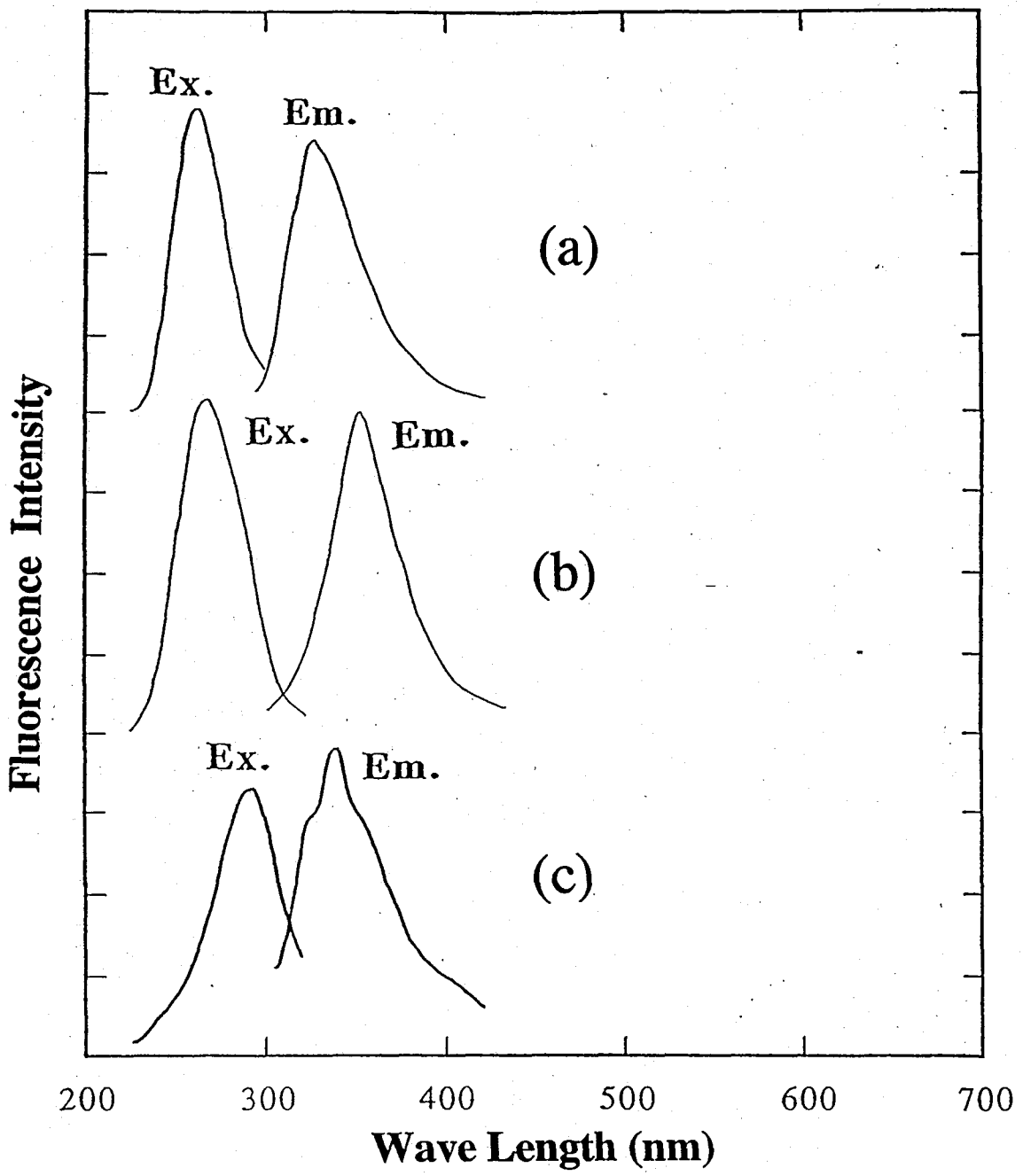

Figure 7-4. The fluorescence and its excitation spectra for (a) diacetoxy biphenyl, (b) 1,4-hexadecyl pyromellitic acid, and (c) B-C16 polyesters in chloroform solution of 10^{-1}M.

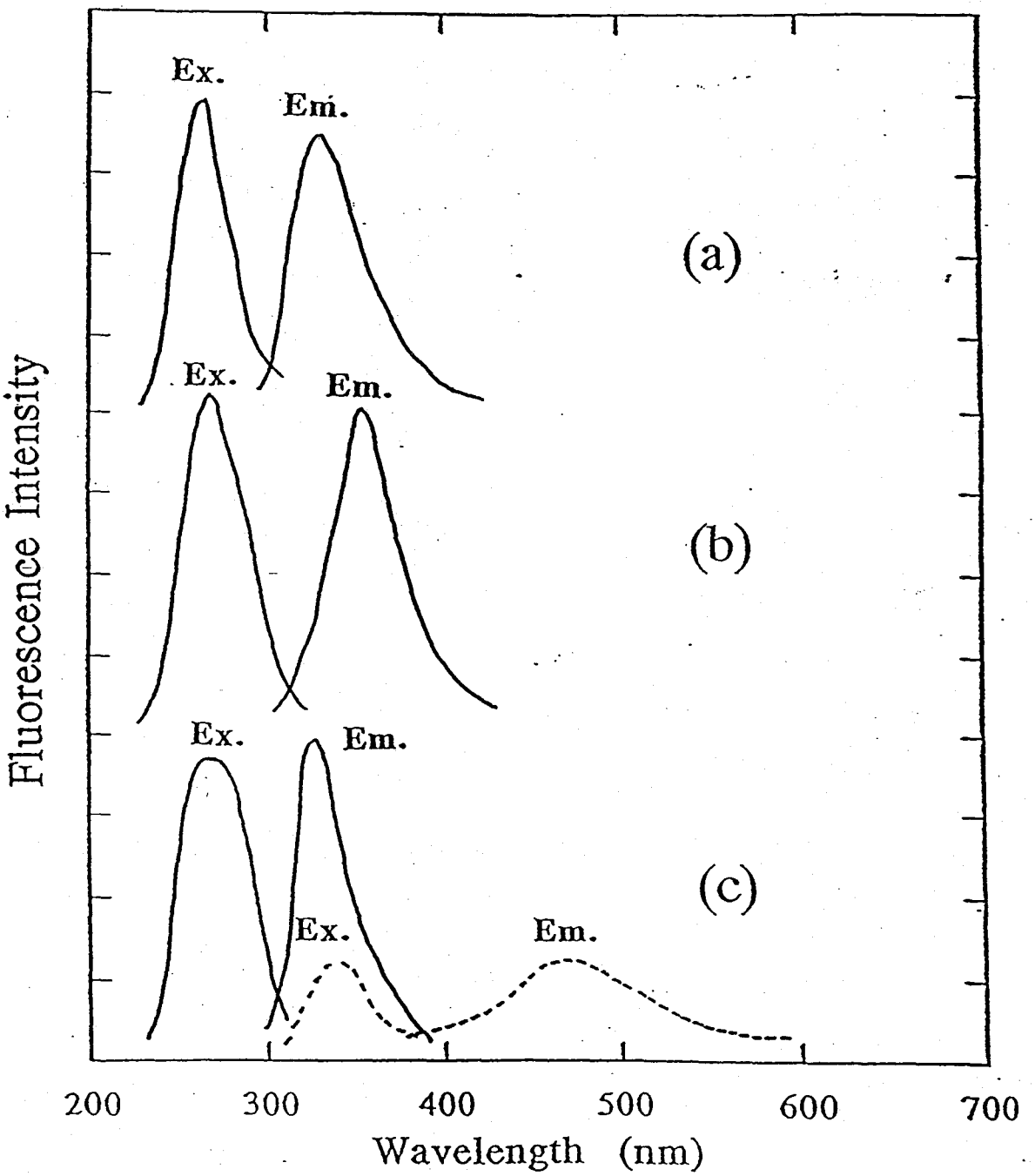

Figure 7-5. The fluorescence and its excitation spectra for (a) diacetoxy biphenyl, (b) 1,4-hexadecyl pyromellitic acid, and (c) their equimolar mixture in chloroform solution of 10^{-1}M.

Figure 7-1.
Wavelengths of the observed fluorescence and its excitation spectra for the layered crystals of B-Cn polyesters and the $CHCl_3$ solution of model compound.

sample	Wave length (nm) Excitation	Emission
$CHCl_3$ Solution		
B-C16	287	355
diacetoxybiphenyl	260	323
16PI[1]	267	354
Charge transfer band		
K1 crystal		
B-C6	396	475
B-C12	400	473
B-C14	400	470
K2 crystal		
B-C16	425	505
B-C18	420	500
diphenyl		
ground-state dimer (crystal)	330	360
monomer[2]	255	321

[1] dihexadecylester of pyromellitic acid. [2] acetonitrile solution.

Moreover, the concentration dependence of the fluorescence wavelength indicates that the charge transfer band comes from the intermolecular aggregation. An increasing in concentration of solution corresponds to a shortening of the intermolecular distance between the neighboring electron donor and accepting units which means the change in the intermolecular aggregation.

Aggregated structure proposed by fluorescence study Formerly, the crystalline structure based on X-ray diffraction study were proposed[22]. In this layered structure, it has been clarified from the X-ray diffraction pattern that the aromatic main chains are in an extended form (repeat length of 16.6 Å) and are packed into a layered structure with positional order perpendicular to their long axes. We further found that the averaged lateral packing distance of main chain within a layer for B-C14 is 3.45 Å, indicating that the aromatic main chains are closely associated with each other. These values imply the specific interaction or association of the pyromellitic ester group and the biphenyl group which are included in the repeat unit of main chain.

Keeping these results in mind, the fluorescence spectra were measured for the layered liquid crystalline phase of B-C14. Here, a small amount of the sample was heated to the mesophase temperature at 100 °C using a standard hot plate, spread between quartz slides and then quickly cooled to room temperature. The sample thickness is about 20 μm. The fluorescence spectrum is shown in Figure 7-6. It is obvious that the fluorescence behavior is completely similar to that observed in the concentrated solution of 10^{-1} M (refer to curve d of Figure 7-3), again indicating that a charge transfer complex is formed between two components; biphenyl and pyromellitic ester moieties. Moreover, the absorption spectrum of the B-C14 cast film is shown in Figure 7-7. By comparing to the absorption spectrum for B-C14 in dilute solution (Fig 6b), marked tailing of absorption for longer wavelength region is observed for that of B-C14 film. This difference in the longer wavelength is considered to be a ground state aggregation[36]. This observation dictated that the main chains within a

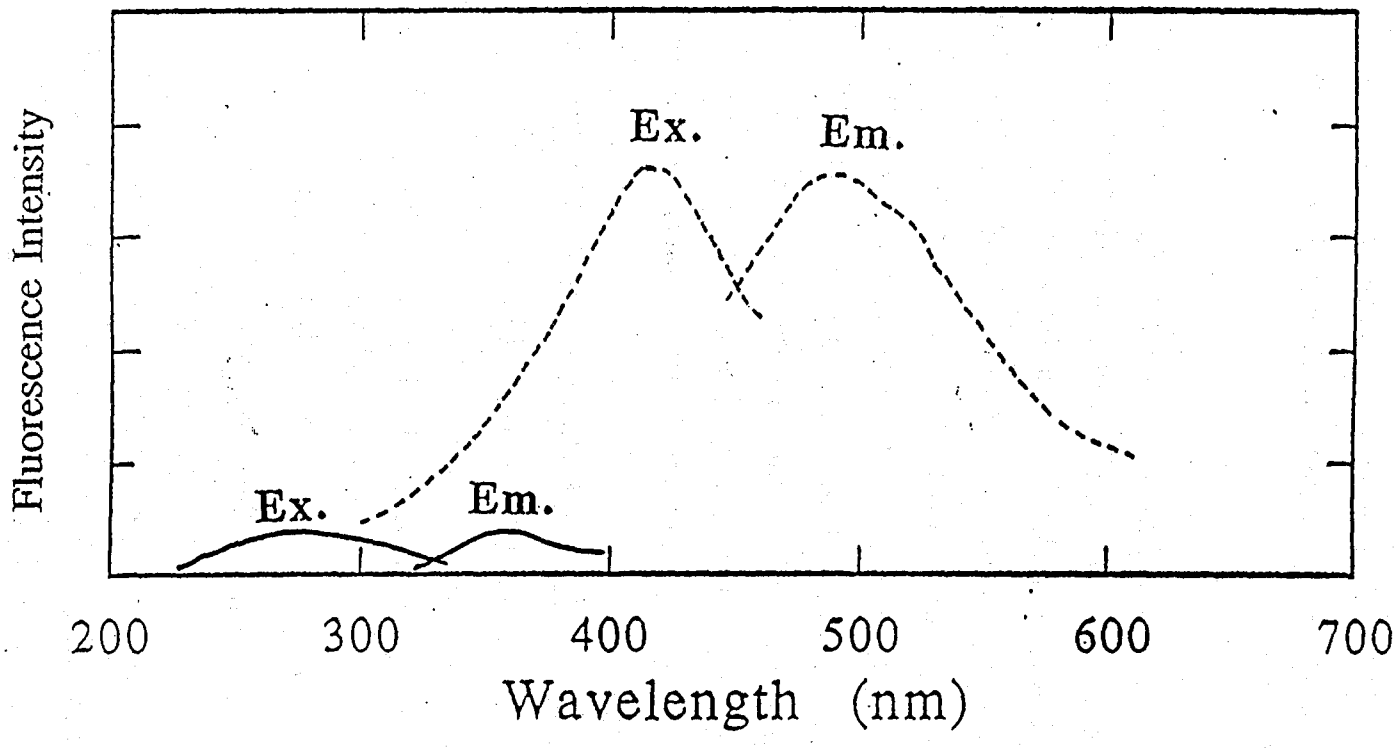

Figure 7-6. The fluorescnce and its excitatioin spectra for the layered crystals of B-C16 polyesters, which was prepared between quartz slides. The sample thickness is about 0.5 mm.

layer are laterally packed in such a way that the biphenyl moieties of one polymer chain are adjacent to the pyromellitic ester moieties of the neighboring chain as illustrated in Figure 7-8. This can produce no positional order of main chain packing along their chain axes which has been proposed in the X-ray measurement since the pyromellitic ester group is approximately the twice length as the biphenyl group. In addition, the formation of a ground state complex may help to explain the unusually short distances between the main chains in the individual layers (d = 3.45 Å).

Moreover, it is interesting that the fluorescence wavelengths of K1 and K2 crystals are different from each other as shown in Figure 7-9. Observed data are summarized in Table 7-1. The fluorescence peak for K1 crystals of B-C6, 12 polyesters are observed at 475 nm (excited at 396 nm), 473 nm (excited at 400 nm) and 470 nm (excited at 400 nm), respectively. The fluorescence peak for K2 crystals of B-C16 and 18 are observed at 505 nm (excited at 425 nm) and 500 nm excited at 420 nm. X-ray diffraction patterns show that the interchain length between the adjacent aromatic main chains is 3.45 Å in K2 and 4.6 Å in K1 crystal. Mulliken clarified the relationship between the frequency (υ) of absorption band and the intermolecular length (r) between the electron donor and the acceptor[36].

$h\nu = Ip - Ea - e^2/r$

where Ip is an ionization potential of an electron-donating molecules, Ea is an electron affinity of electron-accepting molecules and r is a distance between electron donating and accepting molecules. This equation shows that the change in frequency of absorption band corresponds to that in distance between the electron donating and accepting units. The wavelengths (frequency) of the excitation spectra are different between the two crystals because of the difference in the interchain distance in the aromatic layers. The difference in the distance at the ground state could also influence that at the excited states. It has been found that the fluorescence is sensitive to the intermolecular distance between the donor and acceptor groups.

Change in the fluorescence wavelength of he ground state complex during phase transition as a function of temperature Figure 7-10

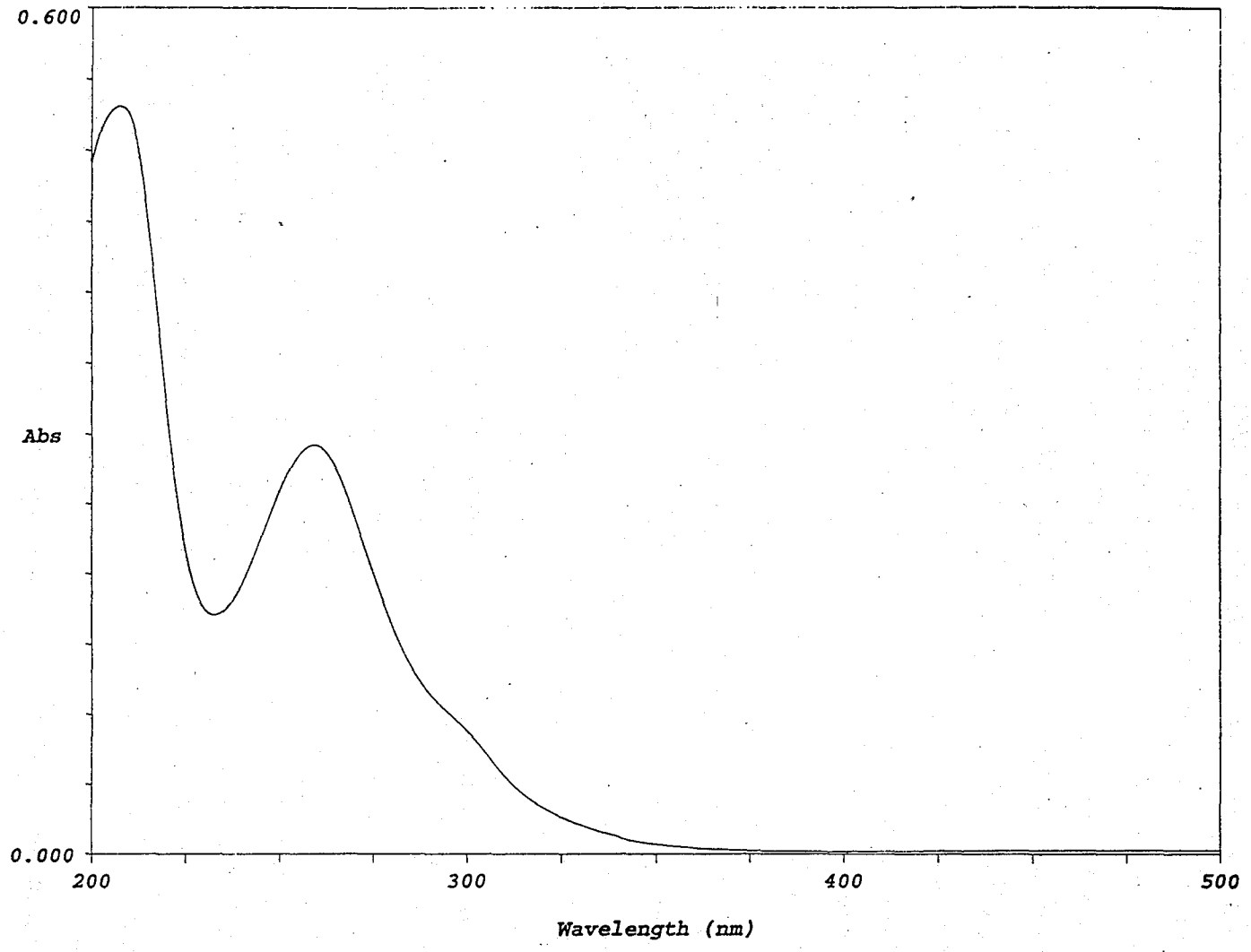

Figure 7-7. The absorption spectrum of B-C16 cast film (K2).

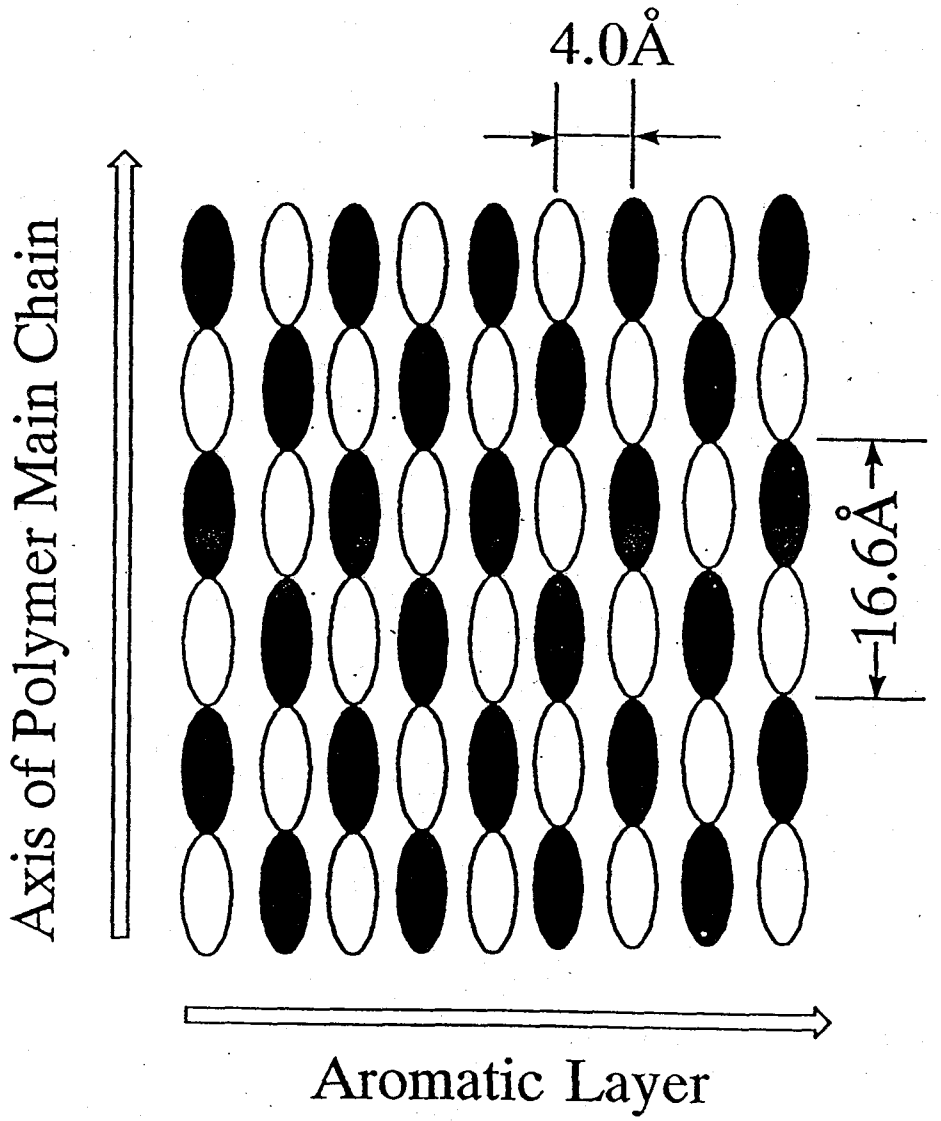

Figure 7-8. The illustration for ideal packing structure of aromatic main chains within a layer, as proposed according to the fluorescence studies, in which the biphenyl moieties (open ellipses) lie adjacent to the pyromellitic ester groups (closed ellipses). (a) an ordered packing structure, (b) a disordered packing structure to the chain axis.

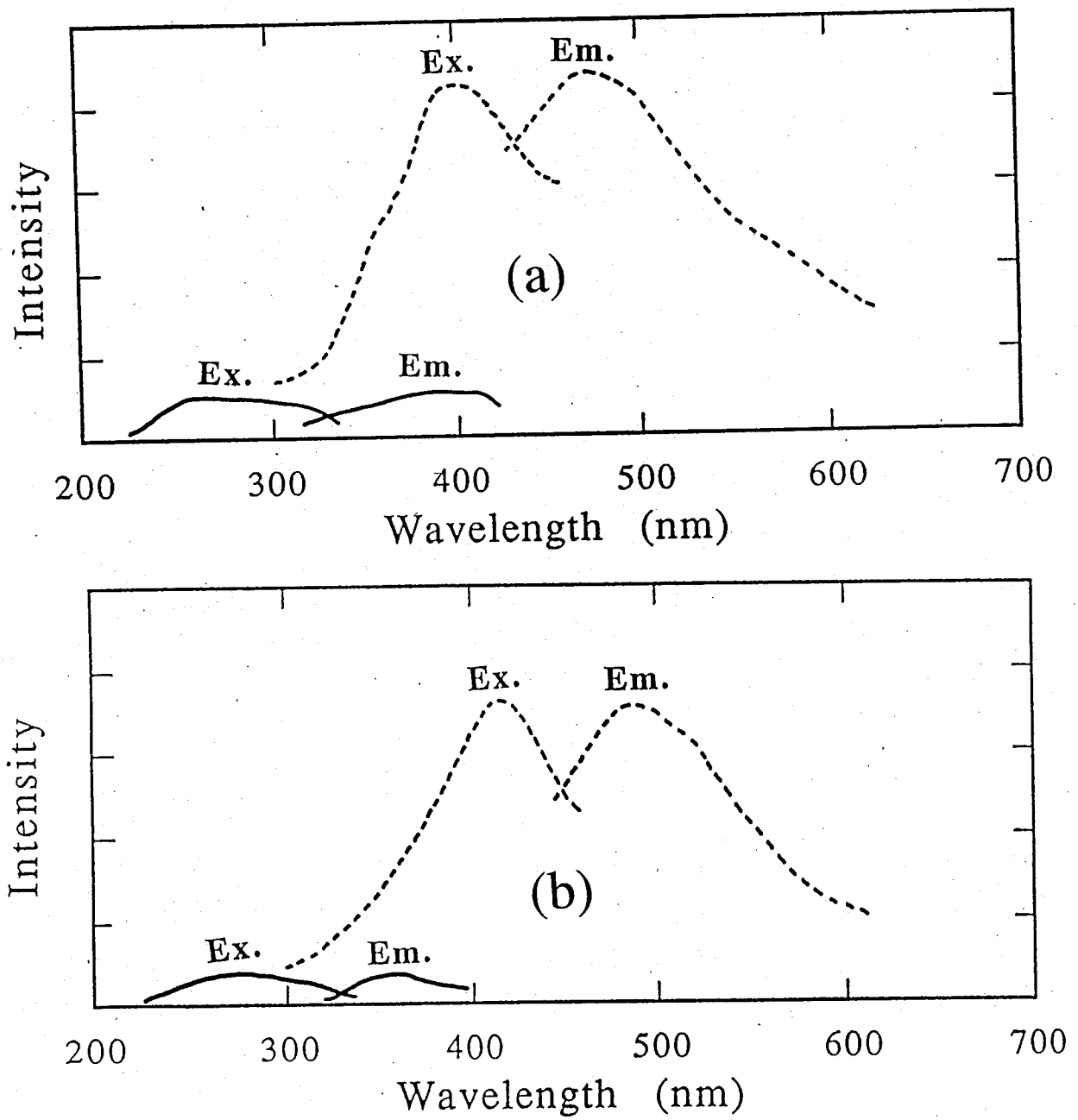

Figure 7-9. The fluorescnce and its excitatioin spectra for the layered crystals (a) K1 crystal of B-C12 polyester and (b) K2 crystal of B-C16 polyesters, which was prepared between quartz slides. The sample thickness is about 0.5 mm.

shows the fluorescence and its excitation spectra of B-C14 polyesters from 25 °C to 224 °C. The fluorescence of the inter-chain charge transfer complex between the biphenyl and the pyromellitic ester moieties was observed in the K2 crystal, the layered liquid crystalline phase and the isotropic phase. This mean that the segregated structure between the aromatic and aliphatic domains is maintained in all the phases. It is interesting that the charge transfer bond was observed also in the isotropic phase. This result dictated that the layered segregated structure is maintained in the isotropic phase and the anisotropy of the molecular order is lost. The wavelength of the excitation and emission spectra does not change in all the phases. This means that the polarization of the electronic states in the excited and ground state do not change in all the phases.

Molecular motion in various phases proposed by the fluorescence intensity as a function of temperature. In order to investigate the deactivation process of various intermolecular ground state complexes during the heating process, we illustrated their Arrhenius-plots for the change in fluorescence intensity in the heating process as shown in Figure 7-11. From this figure we notice that the fluorescence intensity decreases gradually from 25 to 224 °C. This change is considered to be due to the increase in radiationless transition. This is also due to the differences in the states and in the molecular arrangement of main intermolecular interaction for various temperature range. In addition, since the degree of the molecular motion increases with the increase of temperature, the frequency of quenching the excited state increases.

The temperature dependence of fluorescence intensity is generally affected by both the activation energy for radiationless transition and the change in the number of species emitting fluorescence. In this case, since the layered structure is maintained in various phases, there would be no change in the number of various ground state complexes. Hence, the main reason for the decrease of fluorescence intensity of the ground state charge transfer complexes is considered to be the radiationless transition. The quenching of the excited states between the biphenyl and the pyromellitic moieties

become more frequent with an increase in molecular motion. The observed activation energy is considered to reflect an activation energy for the non-radiative deactivation process of charge transfer complex.

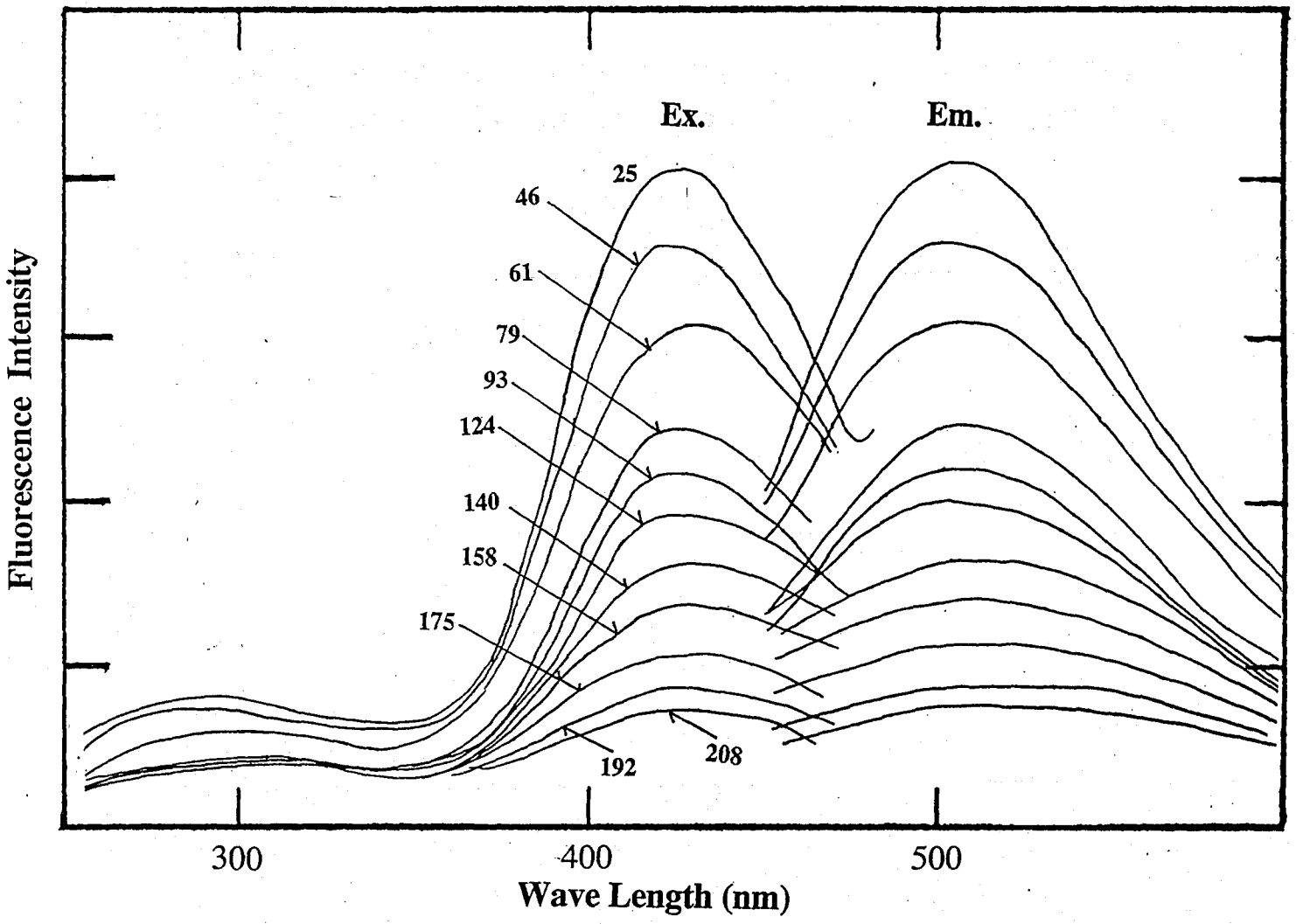

Figure 7-10. The fluorescence and its excitation spectra of B-C16 polyesters in the heating process.

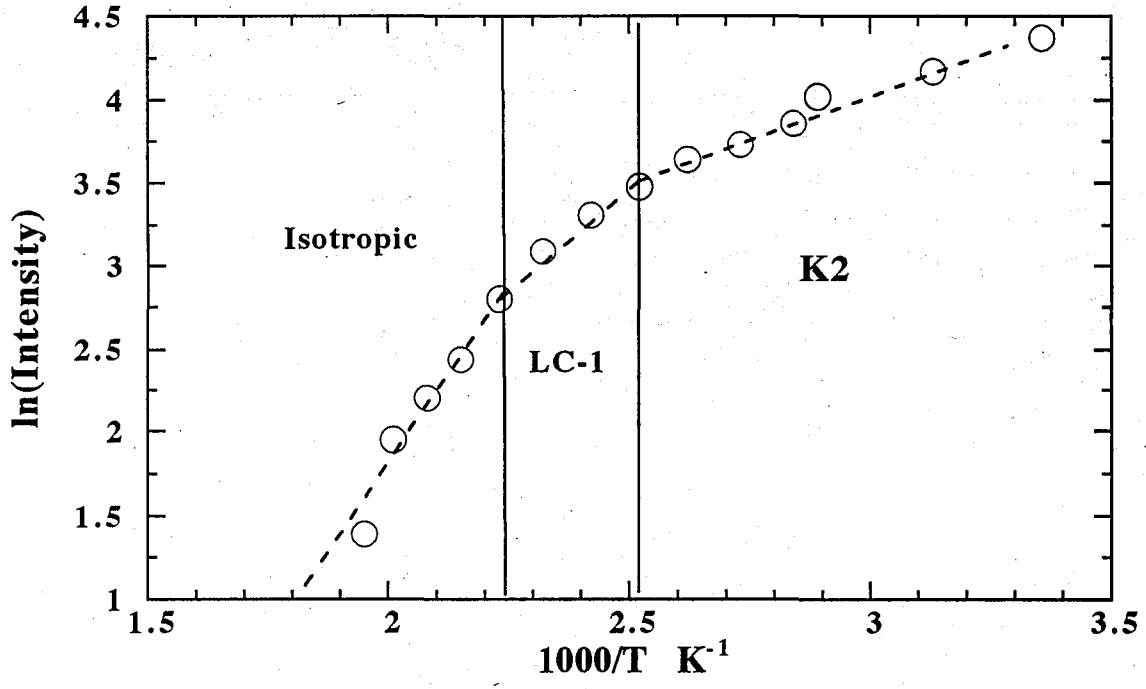

Figure 7-11. Arrhenius-type plots for the change in fluorescence intensity of intermolecular ground-state complexes of B-C14 polyesters during heating process.

7-4 Concluding Remarks

Fluorescence measurements at various temperatures have provided detailed informations about the aggregation state and structure of B-Cn polyesters in the crystalline, liquid crystalline and isotropic phases. In K2 crystal, the ground-state charge transfer fluorescence was observed at 500 nm (excited at 420 nm) and that in K1 was about 475 nm (excited at 400 nm). Layered mesophase shows the charge transfer fluorescence at 500 nm and its excitation spectra at 420 nm. This charge transfer complex is found between the biphenyl and the pyromellitic ester moieties in the neighboring chains within a layer. Moreover, the wavelength for the fluorescence and its excitation spectra is found to be sensitive to the intermolecular length between the electron donating and accepting units. These results dictate that the fluorescence measurements is a powerful tool to elucidate the intermolecular interaction in the liquid crystalline phases.

The wavelength of the excitation and emission spectra does not change through the phases. This means that the polarization of the electronic state in the ground and excited state don not change in all the phases. In isotropic phase we also observed the charge transfer complex band at 500 nm, which means that in isotropic phase the segregated structures are maintained between the aliphatic and aromatic domains while the molecular ordering becomes isotropic. This conclusion is based on the results that in this phase we can not observe an increase in fluorescence intensity from an isolated chains.

Hence, we can discuss about driving forces responsible for the organization of these molecules into layered liquid crystalline structures. As has been widely accepted, most reliable force is segregation between the aromatic and aliphatic domains. However this study suggests that the formation of interchain complex in the aromatic main chains also plays a significant role in the formation of the characteristic layered structure.

7-5 Reference and notes

(1) Ballauff, M. Macromol. Chem., Rapid Comun. 1986, **7**, 407.

(2) Ballauff, M. Angew. Chem., Int. Ed. Engl. 1987, **28**, 253.

(3) Ballauff, M.; Schmidt, G. F. Mol.Cryst.Liq.Cryst. 1987, **147**, 163.

(4) Stern, R.; Ballauff, M.; Wegner, G. Macromol. Chem., Macromol. Symp. 1989, **423**, 373.

(5) Rodrigues-Parada, J. M.; Duran, R.; Wegner, G. Macromolecules 1989, **22**, 2507.

(6) Ebert, M.; Herrmann-Schenherr, O.; Wendorf, J.; Ringsdorf, H.; Tschirner, P. Liq. Cryst. 1990, **7**, 63.

(7) Adam, A.; Spiess, H. W. Macromol. Chem., Rapid Comun. 1990, **11**, 249.

(8) Frech, C. H.; Adam, A.; Falk, U.; Boeffel, C.; Spiess, H. W. New Polym. Mater. 1990, **2**, 267.

(9) Stern, R.; Ballauff, M.; Lieser, G.; Wegner, G. Polymer 1991, **32**, 2079.

(10) Harkness, B. R.; Watanabe, J. Macromolecules 1991, **24**, 6759.

(11) Watanabe, J.; Harkness, B. R.; Sone, M. Polym. J. 1992, **24**, 1119.

(12) Cervinka, L.; Ballauff, M. Colloid Polym. Sci. 1992, **270**, 859.

(13) Sone, M.; Harkness, B. R.; Watanabe, J.; Torii, T.; Yamashita, T.; Horie, K. Polym. J. 1993, **25**, 997.

(14) Galda, P.; Kistner, D.; Martin, A.; Ballauff, M. Macromolecules 1993, **26**, 1595.

(15) Marz, K.; Lindner, P.; Urban, J.; Ballauff, M.; Fisher, E. W. Acta Polym. 1993, **44**, 139.

(16) Damman, S. B.; Mercx, F. R. P.; Kootwijk-Damman, C. M. Polymer 1993, **34**, 1891.

(17) Damman, S. B.; Mercx, F. P. M. J. Polym. Sci., Polym. Phys. 1993, **31**, 1759.

(18) Damman, S. B.; Mercx, F. P. M. J.; Lemstra, P. J. Polymer 1993, **34**, 2726.

(19) Damman, S. B.; Vroege, G. J. Polymer 1993, **34**, 2732.

(20) Kakimoto, M.; Orikabe, H.; Imai, Y. ACS Polym. Prep. 1993, **34**, 746.

(21) Steuner, M.; Hortz, M.; Ballauff, M. J. Polym. Sci., Polym. Chem. 1993, **31**, 1609.
(22) Watanabe, J.; Harkness, B. R.; Sone, M.; Ichimura, H. Macromolecules 1994, **27**, 507.
(23) Sone, M.; Harkness, B. R.; Kurosu, H.; Ando, I.; Watanabe, J. Macromolecules 1994, **27**, 2769.
(24) Damman, S. B.; Buijs, J. A. H. M. Polymer 1994, **35**, 2559.
(25) Damman, S. B.; Buijs, J. A. H. M.; van Turnhout, J. Polymer 1994, **35**, 2364.
(26) Buijs, J. A. H. M.; Damman, S. B. J. Polym. Sci.; Polym. Phys. 1994, **32**, 851.
(27) Tiesler,U.; Pulina,T.; Rehahn,M.; Ballauff,M.; Mol.Cryst.Liq.Cryst. 1994, **41**,525.
(28) Voigt-Martin, I. G.; Simon, P.; Bauer, S.; Ringsdorf, H. Macromolecules 1995, **28**, 236.
(29) Voigt-Martin, I. G.; Simon, P.; Yan, D.; Yakimansky, A.; Bauer, S.; Ringsdorf, H. Macromolecules 1995, **28**, 243.
(30) Itagaki, H.; Horie, K.; Mita, I. Prog. Polym. Sci. 19990, **15**, 36.
(31) Hasegawa, H.; Mita, I.; Kochi, M.; Yokota, R. J. Polym. Sci. Part C: Polym. Lett. 1989, **27**, 263.
(31) Hasegawa, H.; Kochi, M.; Yokota, R. Polymer 1991, **32**, 3225.
(32) Hasegawa, H.; Arai, H.; Mita, I.; Yokota, R. Polym. J. 1990, **22**, 875.
(33) Hashimoto, H.; Hasegawa, M.; Horie, K.; Yamashita, T.; Mita, I, Ushiki, H. J. Polym. Sci. Polym. Phys. Ed. 1993, **31**, 1187.
(34) Huang, H. W.; Horie, K.; Yamashita, T. J. Polym. Sci. Polym. Phys. Ed. 1995, **33**, 1673.
(35) Huang, H. W.; Horie, K.; Yamashita, T.; Machida, S.; Sone, M.; Mabuchi, T.; Watanabe, J.; Maeda, Y. Macromolecules 1996 in press.
(36) Mataga, N.; Kubota, T. "Molecular Interaction and Electronic Spectra" Marcel Dekker, Inc., New York (1970).

Chapter 8

Charge Transfer Complex Formation in Layered Phases of H-Cn Polyesters Analyzed with Variable Temperature Fluorescence Spectroscopy

8-1 Introduction

Rigid-rod polyesters with long flexible side chains, over a past decade, have been investigated in a rapidly growing number of papers because of the ability to form thermotropic liquid crystalline phases[1-29]. The most interesting property of these materials is the ability to form layered segregated structures in crystals and liquid crystals when the alkyl side chains reach a critical length. The layered phases are characterized by a segregated structure in which the rigid-rod main chains are laterally packed into monolayer with the flexible side chains occupying the space between the layers. It has been postulated that the driving force for the adoption of such a structure is a segregation of the aliphatic and aromatic domains. In these layered structures, the liquid crystallinity is the result of a partial or total lack of positional order with respect to the main chain packing within the layers and also by the fluidlike disordered alkyl side chains between the layers.

In chapters 4, the thermotropic phase behavior of H-Cn polyesters is studied as a function of side chain length. It is interesting that H-Cn polyesters, with n = 12, 14, 16 and 18, form a two layered crystals, Kc and Km1. The layered crystal Kc is translated to the high ordered layered mesophase $\Sigma ou_{\perp}$. It has been recognized that the morphology observed in a bulk film may depend on the solvent. Such nonequiliblium morphologies are metastable, so annealing the film at elevated temperatures hold in principle return the sample to the equilibrium morphology. Layered Km1 crystal annealing a melt spun fiber of H-C16 is considered to be the equilibrium state although the chain conformation is energetically unstable than ordinary

aromatic polyesters as discussed in Chapter 6. These results might indicate an existence of a specific interaction in layered modifications.

Recently, several studies have shown that fluorescence measurements can be a valuable tool in elucidating the state of intra- and intermolecular aggregation of aromatic polymers in solid and liquid crystalline phases[30-35]. The values of this technique lies in the fact that fluorescence measurements are sensitive to interactions between neighboring chromophore which in tern can be translated to give some information concerning the spatial geometry of these groups. In this chapter, we aim to clarify the intermolecular aggregation in the two layered crystals and mesophase of H-Cn by examining the fluorescence behavior. Moreover, we examine the change of the intermolecular aggregation between different layered structures on the phase transition through the use of variable temperature fluorescence spectroscopy.

8-2 Experimental

The synthesis of H-Cn polyesters (n; the carbon number of the alkyl side chain).

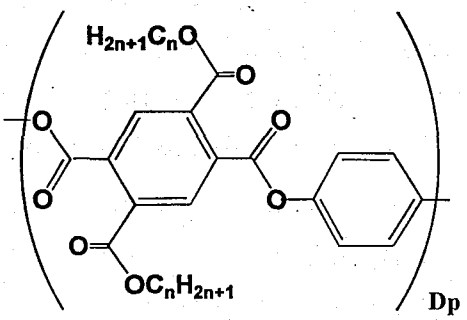

has been described in a previous paper. Here, the H-C14 polyesters were employed.

DSC measurements were performed with a Perkin-Elmer DSC II differential scanning calorimeter. Samples of about 10 mg were examined at a scanning rate of 10 °C/min under a flow of dry nitrogen.

WAXD measurements were carried out with a Rigaku Denki RU-200 X-ray generator system equipped with a flat plate camera using nickel filtered Cu Ka radiation. The distance from the sample to film was determined by using silicon powder. The sample temperature was controlled by a Mettler FP-80 hot stage with FP-82 central processor.

Steady-state fluorescence spectra were measured with a Hitachi 850 fluorescence spectrophotometer equipped with a 30 kV xenon lamp. The bandpasses were 5 nm for both excitation and emission monochrometors. The fluorescence and its excitation spectra for $10^{-1} \sim 10^{-4}$ M solution of model compound and polymers were measured by using a 1 mm quartz cell in side-face detection. For the crystal of model compound, the fluorescence spectra and its excitation spectra were measured at the surface of a 1 cm quartz cell. Those for the LCPs were measured in a front-face arrangement to minimize the self-absorption. The temperature of the LCPs was controlled by mean of an ALPHA engineering thermostat coupled with a temperature-controlling unit.

8-3 Results and Discussion

[1] Thermotropic Phase Behavior and Structure

In Chapter 4, we reported that H-Cn polyesters form four types of crystals and a layered mesophase as a function of side chain length as shown in Figure 8-1.

With n=12, 14, 16 and 18, H-Cn forms a highly ordered thermotropic mesophase (LC) and two crystalline phases (Kc and Km1) with the nature of layered structure. The Kc were obtained by casting from $CHCl_3$ and THF solution. The Km1 was obtained by annealing the quenched sample from liquid crystalline state at 60 °C for a month. In layered Kc and Km1 crystalline phases, the aromatic main chains are in a fully extended conformation with a repeat length of 12 Å and they are regularly packed within a monolayer. In addition, the side chains are also in a crystalline state between the layers. It is of interest that the main chains in Kc and Km1 are packed in a different manner. For Kc, the lateral packing distance of the main chains within a layer is 4.89 Å. But this reduces to 3.85 Å for Km1. A liquid crystalline phase is observed following the melting of the crystallites as indicated by the high birefringence and their ability of flow.

[2] Fluorescence study of H-Cn polyesters

Origin of Fluorescence Initially, the excitation and emission spectra of the fluorescence were measured for the $CHCl_3$ solution of H-C16 polyesters as a function of concentration. The data are shown in Figure 8-2. The fluorescence spectrum for the dilute solution of the H-C16 polyester at the concentration of 10^{-4} M (mol repeat unit/ L) shows a structured band with a maximum at 350 nm (excitation wavelength at 270 nm). This band can be attributed to an overlap of the fluorescence bands of both the biphenyl and pyromellitic ester moieties individually, the fluorescence band for the hydroquinone moiety may appear about 300 nm (excitation at 250 nm) as has been deduced from the fluorescence spectrum for 4,4'-diacetoxybiphenyl and that for the pyromellitic ester moiety may appear at 354 nm (excitation

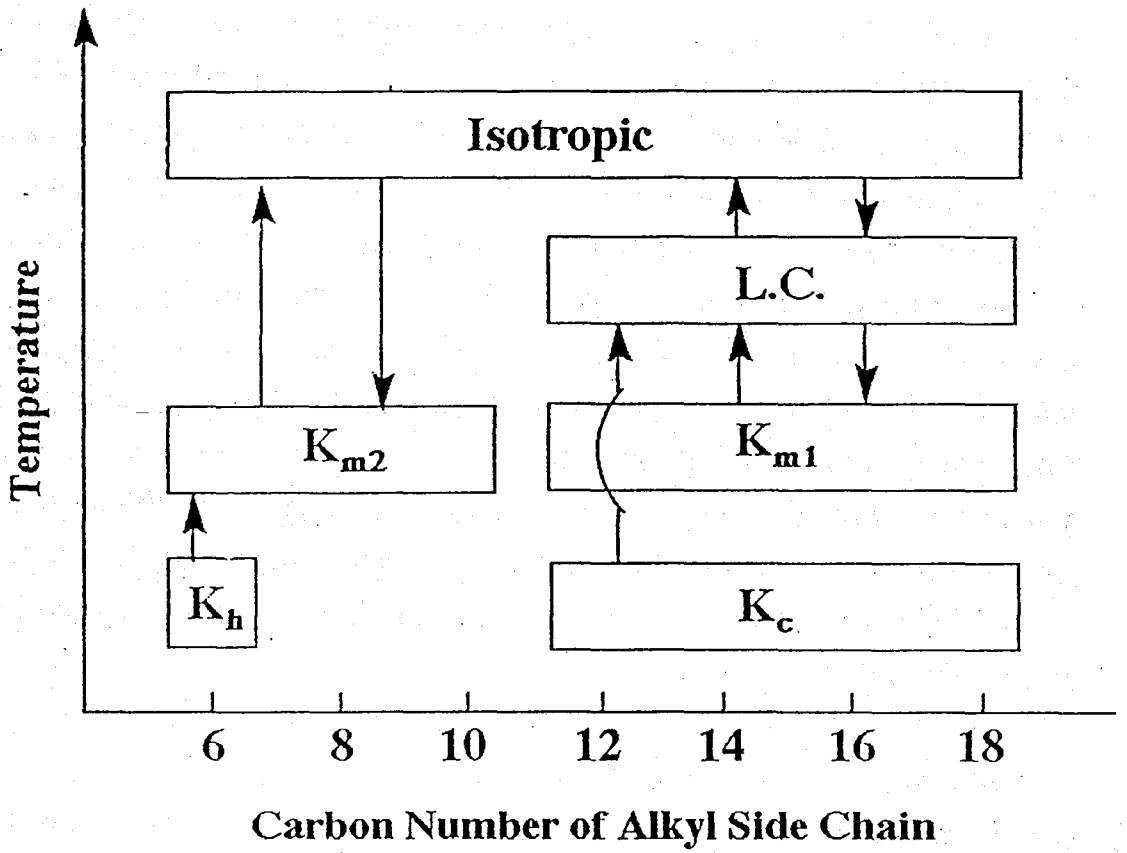

Figure 8-1. Schematic illustration of thermotropic phase behavior in H-Cn polyesters.

at 267 nm) as measured for the 1,4-ditetradecylester of pyromellitic acid (see later curves a and b in Figure 8-3).

Increasing the concentration of the polymer results in a profound change in both the excitation and emission spectra. The new broad excitation and emission bands (given by dashed curves) appear at larger wavelengths with the increase of the concentration from 10^{-4} to 10^{-1} M. Finally, they become predominant in the concentrations above 10-1 M; a excitation at 350 nm gives rise to a fluorescence band at 468 nm. Further, we found that these bands are structureless. This results simply indicate that an increase of the concentration of H-C14 cause a change in the electronic state of the hydroquinone and pyromellitic ester chromophores. This provides the ground state in the concentrated solution to be at a lower energy level (a more stable excited state formed by the charge transfer between the donor and acceptor group) than in dilute solution and thus emitting at a higher wavelength. This could be due to an aggregation process which results in a ground state dimerization to give a charge transfer complex. With respect to the H-Cn polyesters, their exists a donor group (hydroquinone moiety) and an acceptor group (pyromellitic ester moiety) within an aromatic main chain, thus it can be predicted that a charge transfer complex is formed between these two units when they are in a suitable geometry and at a suitable distance.

To test this hypothesis, the fluorescence spectrum for a mixture of two model compounds, 4,4'-diacetoxy biphenyl and the 1,4-ditetradecylester of pyromellitic acid was examined at a concentration of 10^{-1} M. Figure 8-4 shows the fluorescence spectra for the individual compounds (curve a and b) and their equimolar mixture (curve c). Visually, the mixture of two compounds gave a slightly yellow collar as a result of a molecular complex formation. In addition the fluorescence spectrum for the mixture appeared similar to that observed in concentrated solution of H-C16, exhibiting a structureless fluorescence band with a maximum at 460 nm that is completely absent in the spectra of the individual compounds. Moreover, in this concentrated solution, all the molecules form complex because the fluorescence of the two model compounds disappears completely. This

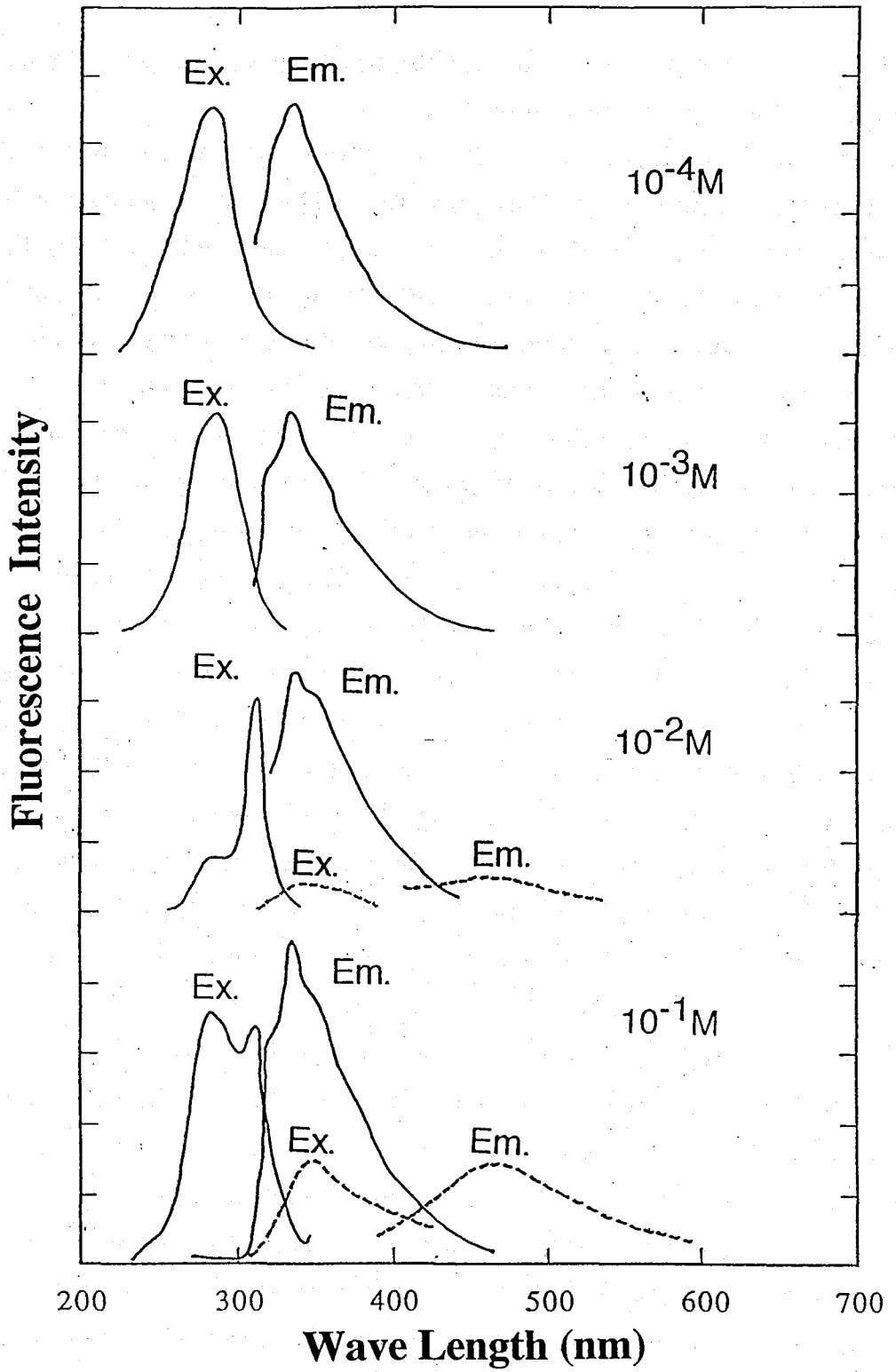

Figure 8-2. The fluorescence and its excitation spectra of H-C14 in Chloroform solutions at the concentrations of 10^{-4}M, 10^{-3}M, 10^{-2}M and 10^{-1}M. A pair of the fluorescence and excitation spectra are given by the solid curve or dash line.

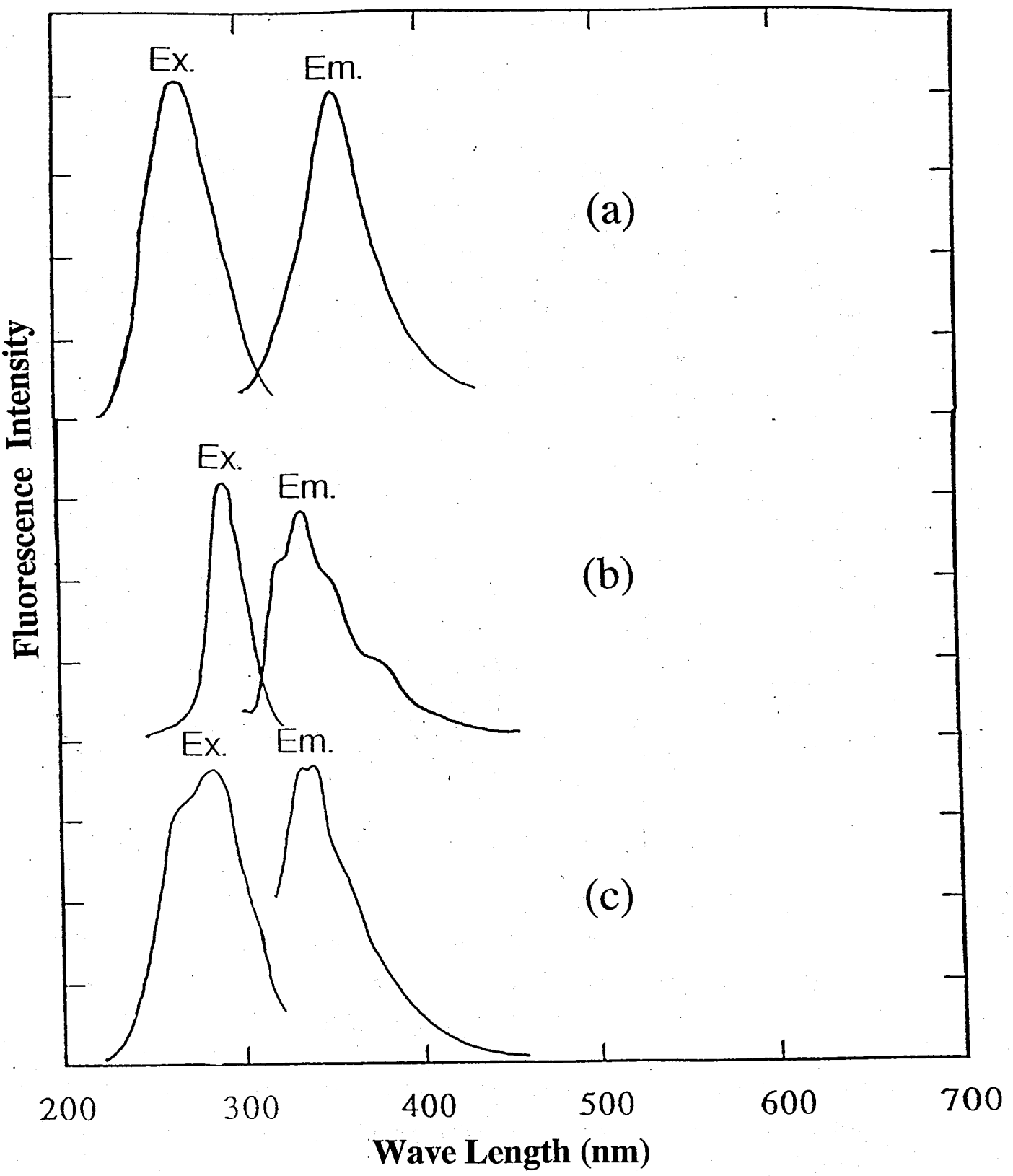

Figure 8-3. The fluorescence and its excitation spectra for (a) diacetoxy benzene, (b) 1,4-tetradecyl pyromellitic acid, and (c) H-C14 polyesters in chloroform solution of 10^{-1}M.

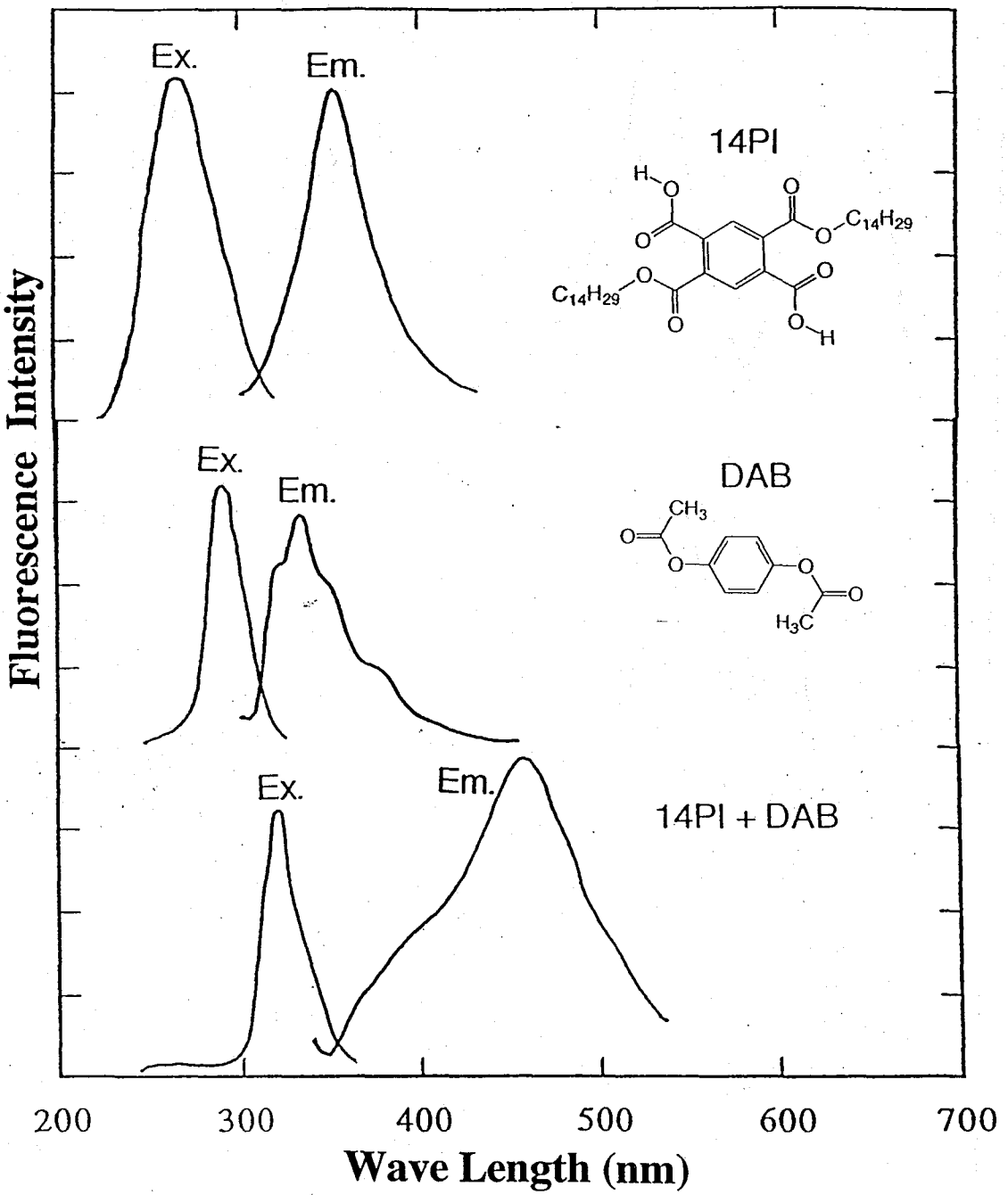

Figure 8-4. The fluorescence and its excitation spectra for (a) diacetoxy benzene, (b) 1,4-tetradecyl pyromellitic acid, and (c) their equimolar mixture in chloroform solution of 10^{-1}M.

mean that the complex between the diacetoxybenzene and the pyromellitic acid ester is very stable. This observation supports the proposal that the ground state molecular complex between hydroquinone and pyromellitic ester groups exists in the concentrated solutions of H-C16. For forming such a complex it is necessary that the pyromellitic ester and biphenyl groups achieve a spatial orientation in which these groups are adjacent to one another in an alternating fashion although at this time we can gave no detailed aggregation structure in concentrated solutions.

Moreover, the concentration dependence of the fluorescence wavelength indicates that the charge transfer band come from the intermolecular aggregation. Moreover, an increase of concentration of solution corresponds a shortening the intermolecular distance between the neighboring electron donor and accepting units and means the change of the intermolecular aggregation.

Aggregated structure proposed by fluorescence study Former, we describe the liquid crystalline structure based on X-ray diffraction study. In this layered structure, it has been clarified from the X-ray diffraction pattern that the aromatic main chains are in an extended form (repeat length of 12 Å) and are packed into a layered structure with a positional order perpendicular their long axes, as shown in Figure 8-5. We further found that the averaged lateral packing distance of main chains within a layer is 3.85 Å, indicating that the aromatic main chains are closely associated with each other. These imply the specific interaction or association of the pyromellitic ester group and the biphenyl group which are included in the repeat unit of main chain.

Keeping these results in mind, the fluorescence spectra were measured for the layered liquid crystalline phase of H-C14. Here, a small amount of the sample was heated to the mesophase temperature at 100 °C using a standard hot plate, spread between quartz slides and then quickly cooled to room temperature. The sample thickness is about 0.5 mm. The absorption spectrum is shown in Figure 8-6. In this absorption spectrum, the large shoulder at around 350 nm is observed in the higher wavelength region

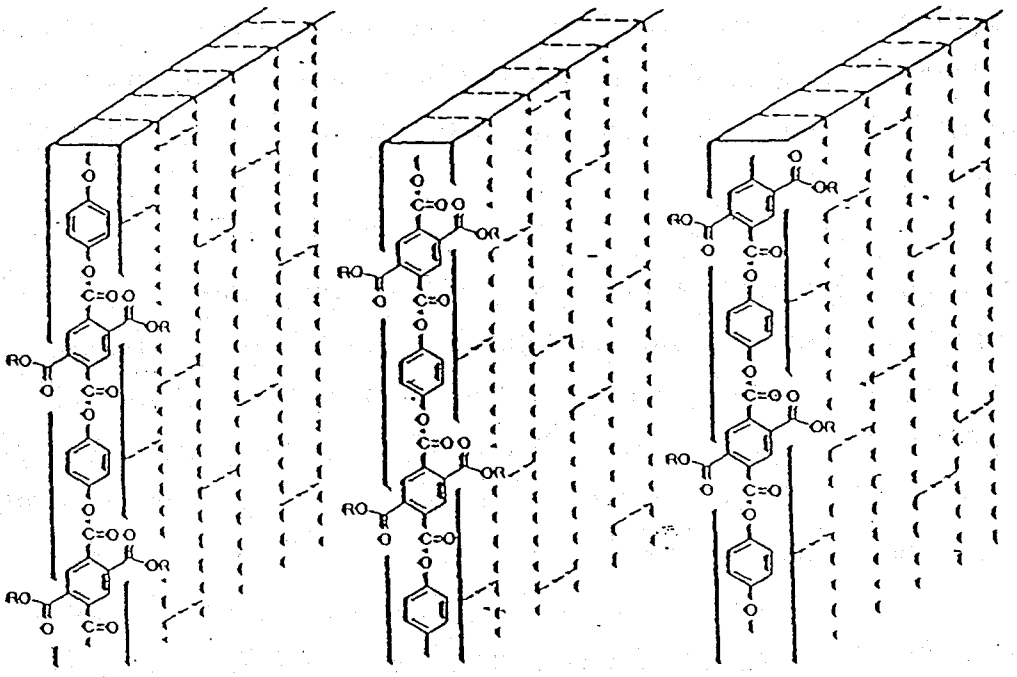

Figure 8-5. A proposed layered structure for the liquid crystalline phase of H-Cn polyester. In this layered structure, the aromatic main chains in the extended form pack into layers with positional order only in the lateral direction, and the aliphatic side chains in the disordered form occupy the space between the layers.

than the absorption peak of the isolated chain of H-C14 polyesters at 265 nm. This result means that the ground state aggregation is formed in the layered structure of H-C14 polyesters. Figure 8-7 shows the fluorescence and its excitation spectra of Kc crystal and Km1 crystals. It is obvious that the fluorescence behavior is similar to that observed in the concentrated solution of 10^{-1} M (refer to curve c of Figure 8-3), again indicating that a charge transfer complex is formed between two components; biphenyl and pyromellitic ester moieties. This observation dictated that the main chains within a layer are laterally packed in such a way that the biphenyl moieties of one polymer chain are adjacent to the pyromellitic ester moieties of the neighboring chain as illustrated in Figure 8-8. In this packing structure, two plausible model could be proposed. Figure 8-8(a) shows the high ordered packing to the polymer chain axis in the aromatic layers. Figure 8-8(b) shows the disordered packing structure. The latter model can produce no positional order of main chain packing along their chain axes which has been proposed in the X-ray measurement since the pyromellitic ester group is approximately the same length as the hydroquinone group. This result is in contrast to that result about layered mesophase of B-Cn, in which the positional order of the main chain packing along their chain axes exists in the aromatic layer because the pyromellitic ester group is approximately in the same length as the hydroquinone group. In addition, the formation of a ground state complex may help explain the unusually short distances between the main chains in the individual layers (d = 3.85 Å).

Moreover, it is interesting that the fluorescence wavelengths of Kc and Km1 crystals is different from each other. The wavelengths of the fluorescence and its excitation spectra of Kc crystal are 485 and 400 nm respectively. Those of Km1 crystal are 500 and 408 nm.. X-ray diffraction patterns show that the interchain length between the adjacent aromatic main chains is 3.85 Å in Km1 and 4.6 Å in Kc. Mulliken clarified the relationship between the wavelength (υ) of absorption band and the intermolecular length (r) between the electron donor and the acceptor.

$h\upsilon = Ip - Ea - e^2/r$

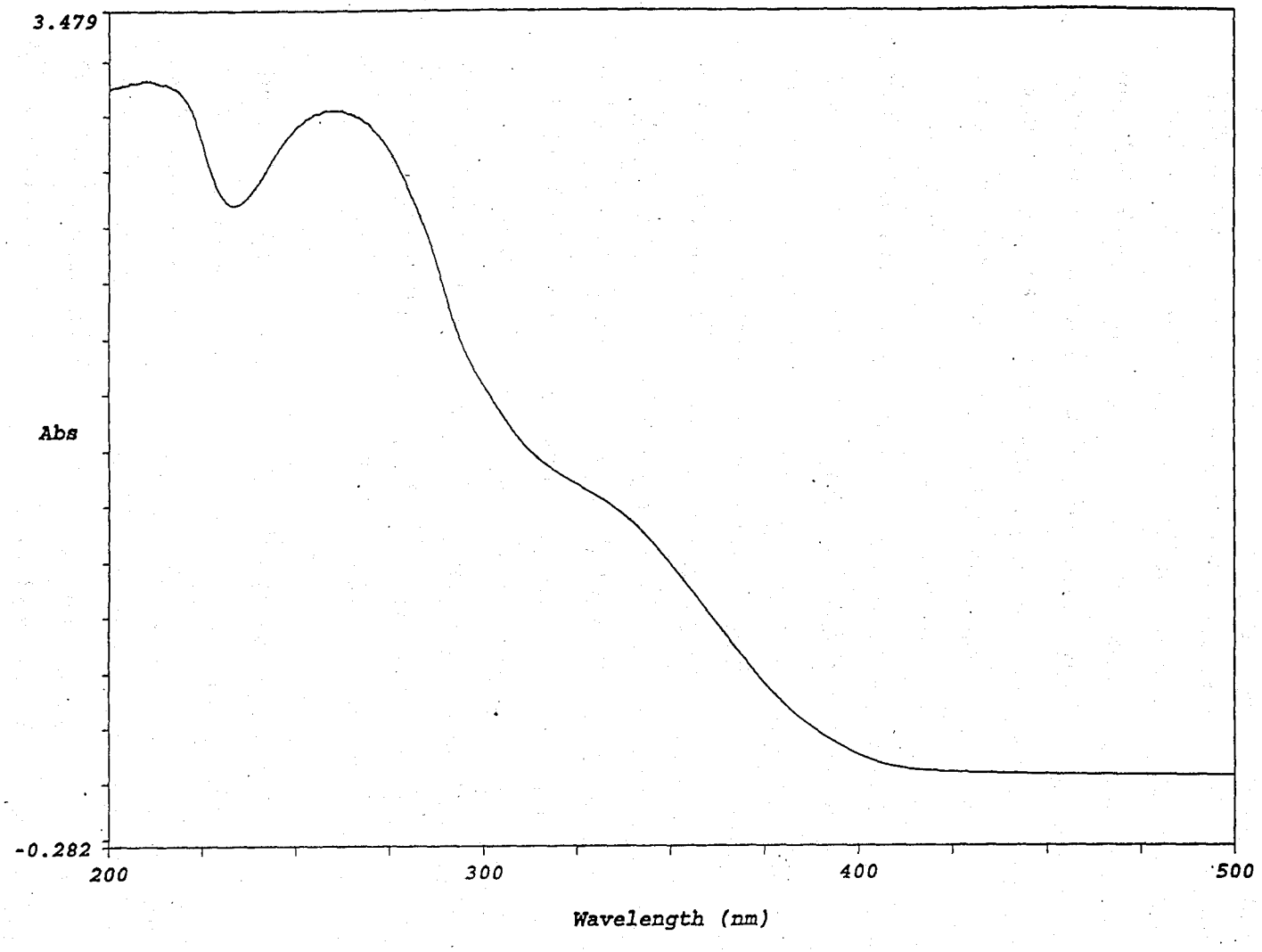

Figure 8-6. The absorption spectrum of H-C14 cast film (Kc).

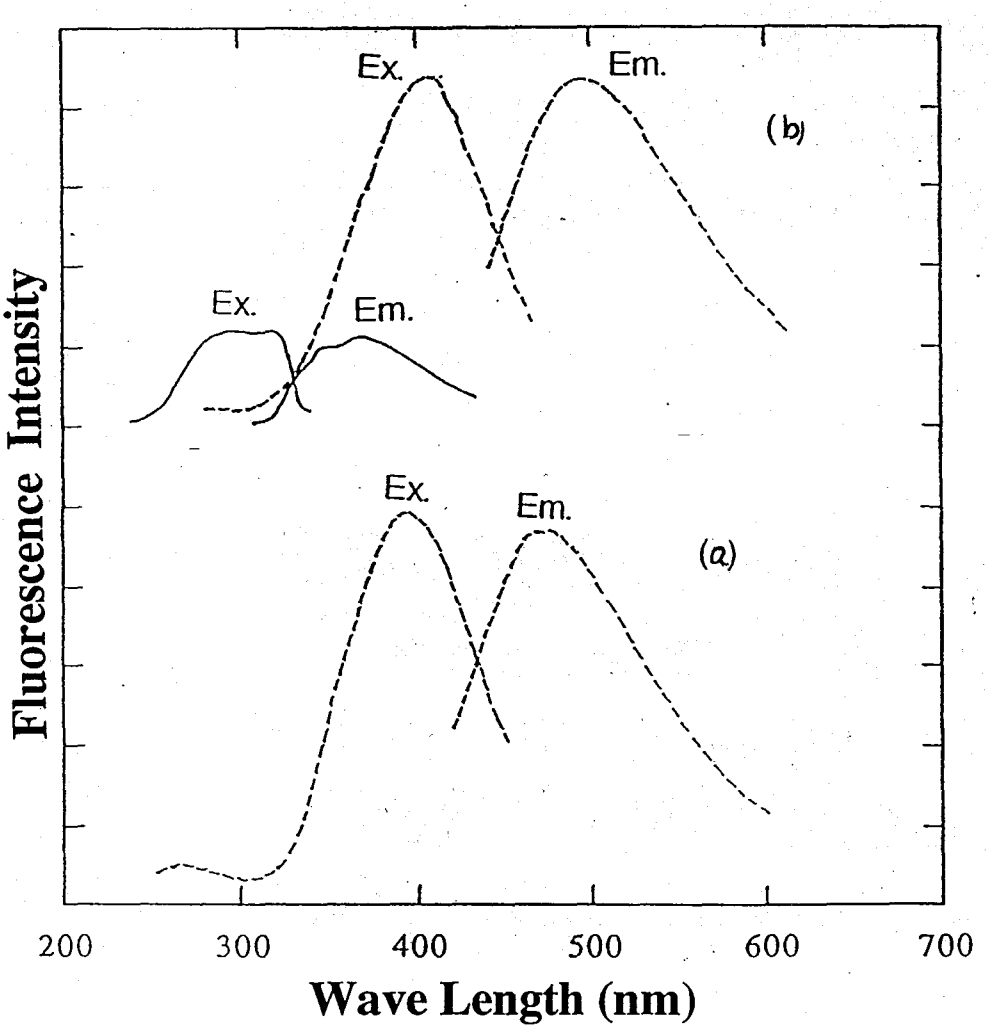

Figure 8-7. The fluorescnce and its excitatioin spectra for the layered crystals (a) Kc and (b) Km. of H-C14 polyesters, which was prepared between quartz slides. The sample thickness is about 0.5 mm.

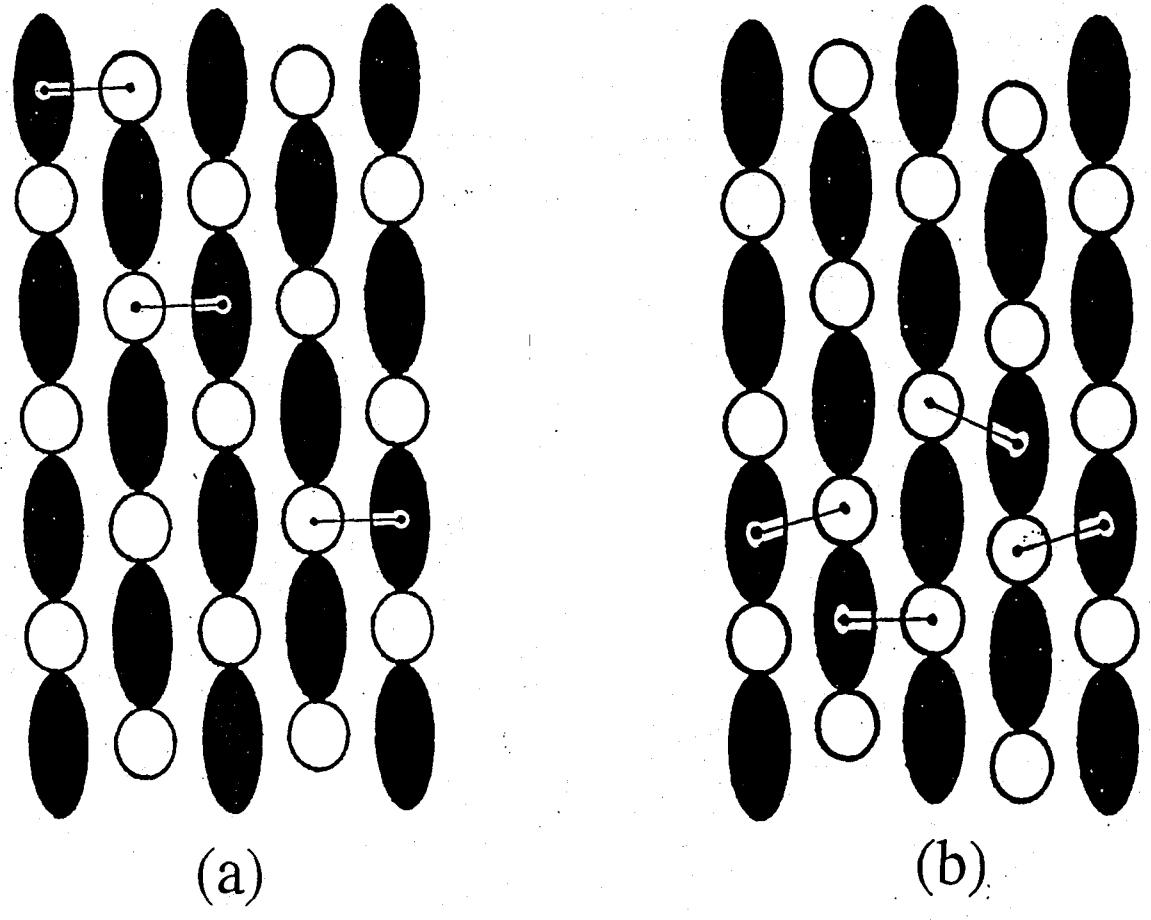

Figure 8-8. The illustration for ideal packing structure of aromatic main chains within a layer, as proposed according to the fluorescence studies, in which the biphenyl moieties (open ellipses) lie adjacent to the pyromellitic ester groups (closed ellipses). (a) an ordered packing structure, (b) a disordered packing structure to the chain axis.

where Ip is an ionization potential of an electronic donating molecules and Ea is an electron affinity of electronic accepting molecules and r is a distance between electron donating and accepting molecules. This equation shows that the change of wavelength of absorption band corresponds to that of distance between the electron donating and accepting units. Thus, the wavelength of the excitation spectra is different between the two crystals because of the difference of the interchain distance in the aromatic layers. The difference of the ground state could also influence the excited states. It is found that the fluorescence is sensitive to the intermolecular distance between the donor and acceptor groups.

Figure 8-9 shows fluorescence spectra of Kc crystal of H-C14 excited by different wavelengths. This figure indicates that the wavelength of fluorescence band is shifted by that of the excitation band and the stokes shifts (between excitation and emission bands) independent of the excitation wavelength. This results indicate the large distribution of the spatual arrangement between the hydroquinone moiety and the pyromellitic moiety in the ground state complex. When such an intermolecular lengths constantly situated, we might not observe such a dependency upon the excited wavelength. In fact we do not observe such a dependency in the charge transfer complex in layered structure of B-Cn. Thus a random displacement along to the polymer chain in an aromatic layer could cause the dependence of the fluorescence wavelength upon the excited wavelength and the large distribution of fluorescence band.

On a discussion about the packing structure of B-Cn layered mesophase, the length of electron donating unit (4,4'-biphenol) is same as that of electron accepting unit, thus a charge transfer complex causes a positional order along a polymer axis in the aromatic layers[13]. In contrast to B-Cn polyesters, the electron donating unit has half length of the electron accepting unit (pyromellitic ester moiety). These chemical structural feature might make the difference of positional order in a layered structure.

Ikeda et al.[37,38] studied the relationship between the excimer formation and phase structure of main chain and side chain liquid crystalline polymers. We reported the relationship between the intermolecular ground state

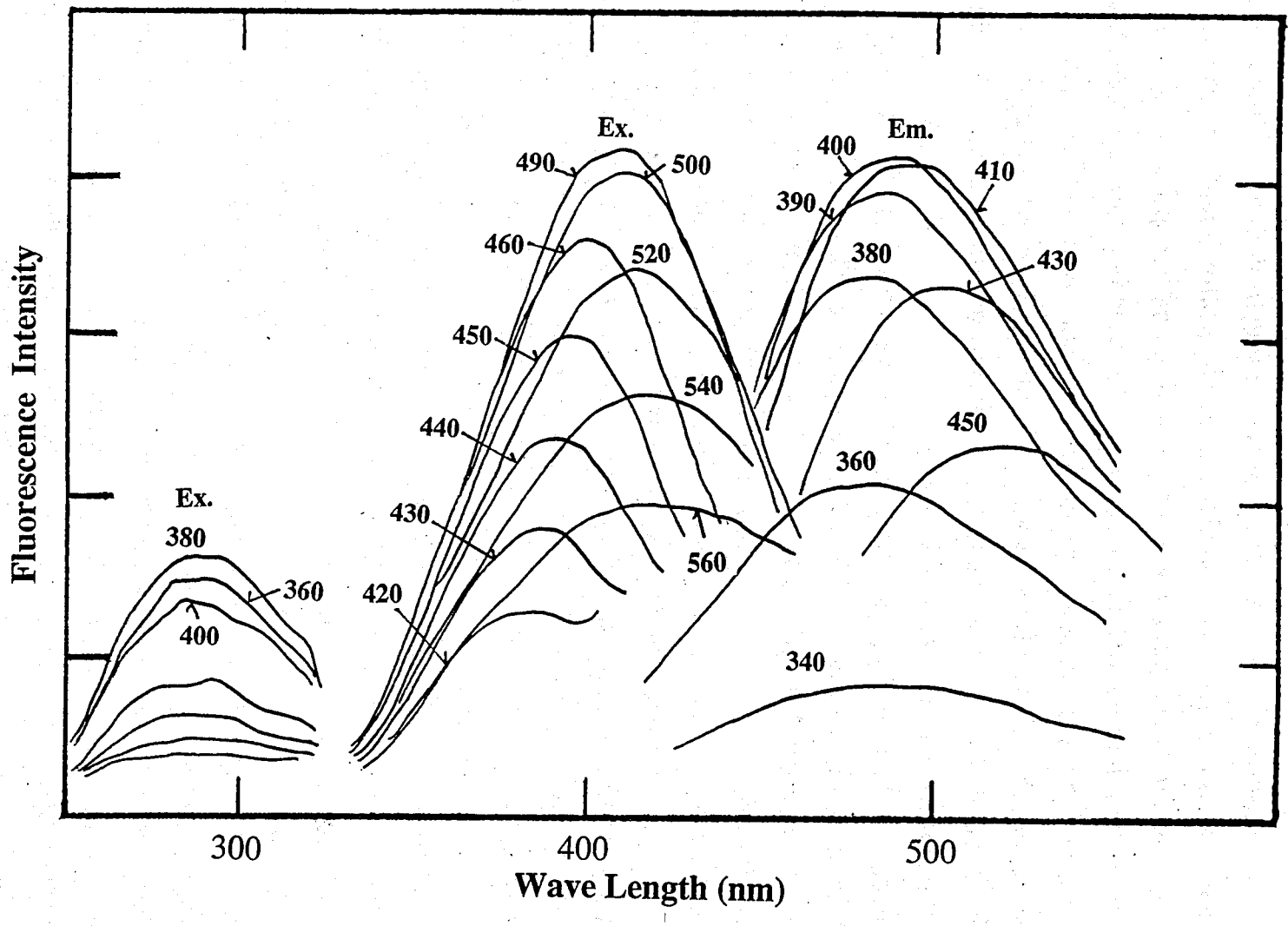

Figure 8-9. The fluorescnce excited by various wavelengths and its excitation spectra emitted by various wavelengths for the layered crystals Kc of H-C14 polyesters, which was prepared between quartz slides. The sample thickness is about 0.5 mm.

complex formation and microstructure change of a thermotropic liquid crystalline polyesters, and showed that the change in fluorescence peak wavelength strongly depends on the change in intermolecular interaction between the biphenyl and the pyromellitic moieties.

Change of ground state complex on phase transition through the wavelength of fluorescence as a function of temperature Figure 8-10 shows the fluorescence and its excitation spectra from 25 °C to 218 °C. With increase of temperature, the wavelength of fluorescence shifts to the higher. This means that the polarization of the electronic state in the excited state become larger in high temperature than that in room temperature. At the transition from Kc to Km1, the fluorescence peak of the intermolecular ground state complex shifts from 485 nm to 500 nm and its excitation peak shifts from 400 to 408 nm. The fluorescence intensity of the intermolecular ground state complex appearing at 485 to 500 nm decreases gradually up to the temperature.

The temperature dependence of the wavelengths of the fluorescence and its excitation peak on the heating Kc crystal is depicted in Figure 8-11. This figure show the change of the intermolecular aggregation of the polymer between the phase transitions, precisely to describe the change of the intermolecular length between the electronic donating units and the accepting units in the neighboring chains. As discussed in former, the distance between electron donating and accepting units decreases from Kc crystals to liquid crystalline phases. This structural result is supported with X-ray diffraction study, in which the interchain distance in the aromatic layer is 4.9 Å in Kc crystal and 3.85 Å in layered mesophase.

Thus a transition from Kc to layered mesophase means the change of ground state aggregation between the electron accepting and donating units and moreover the formation of very stable charge transfer complex between the layers of fluid-like alkyl side chain.

Interestingly, this intermolecular charge transfer bands are observed in isotropic phase. In this phase the fluorescence originated from the isolated chains is not observed. This results might imply that the segregation

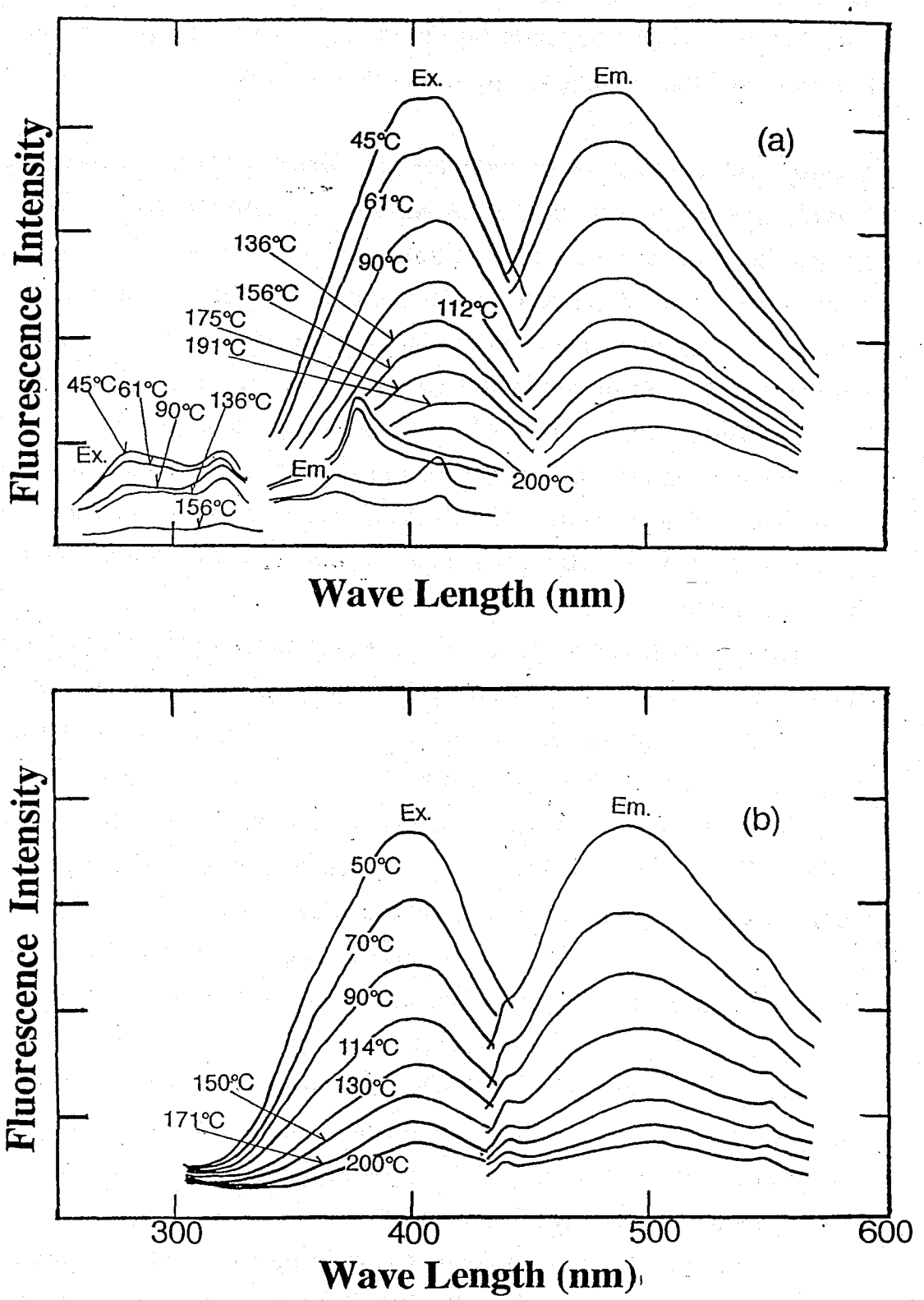

Figure 8-10. The fluorescence and its excitation spectra of H-C14 polyesters in the heating process.(a) the cast film, (b) melt annealed film.

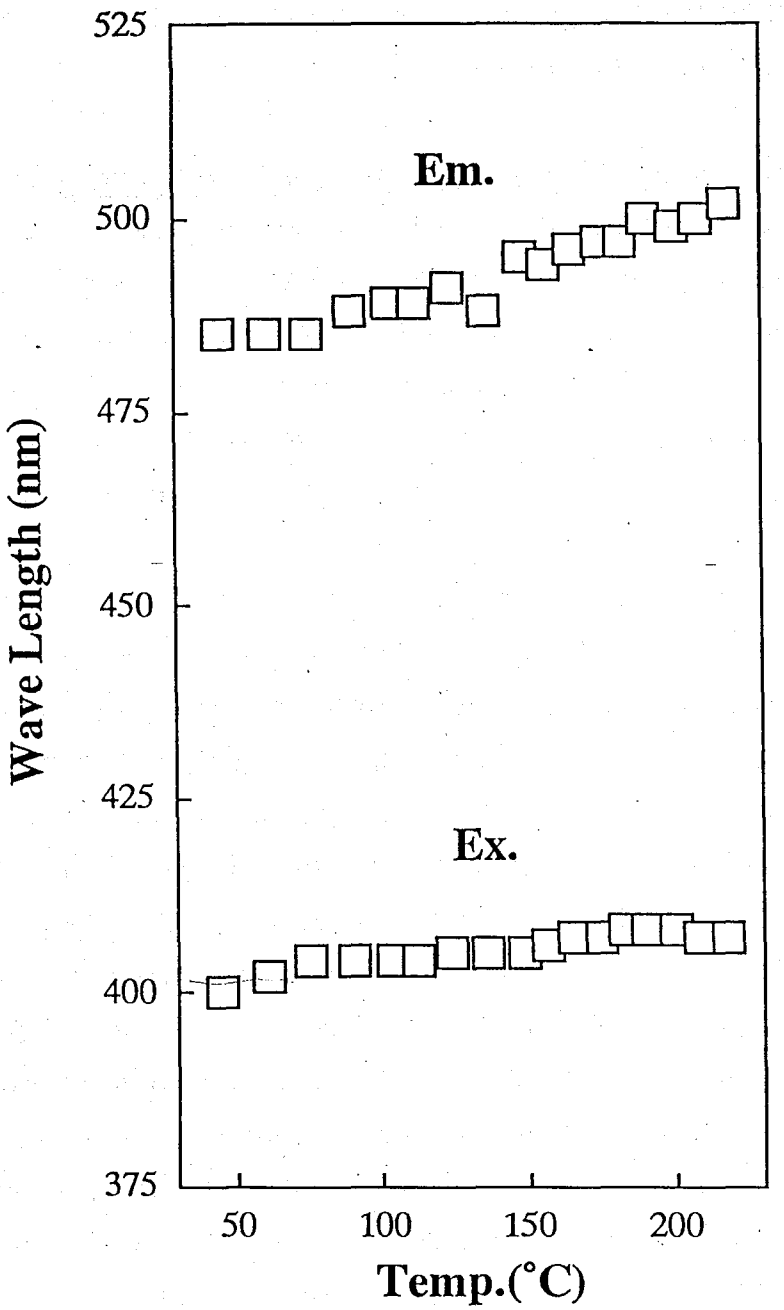

Figure 8-11. The changes of the peak wavelengths of the fluorescence and its excitation spectra of H-C14 polyesters in the heating process from the cast film (Kc crystal).

between the aliphatic and aromatic domains is maintained in isotropic phase. Thus, we can consider that the isotropic sate in rigid-rod polyesters with flexible side chains is a segregated state between the aliphatic and aromatic domains without anisotropy of molecular ordering. Moreover, the interlayer correlation between the aromatic layers disappears at the transition from the liquid crystal to the isotropic liquid.

Molecular motion in various phases through the intensity of fluorescence as a function of temperature. The logarithmic fluorescence intensity as a function of the reciprocal of absolute temperature is shown in Figure 8-12. From this figure we notice that the fluorescence intensity decreases gradually from 25 to 218 °C. This change is considered to be due to the increase in radiationless transition. With increase of temperature, the degree of the molecular motion increase, thus, the frequency of quenching the excited state increase.

In order to investigate the deactivation process of various intermolecular ground state complexes during the heating process, we illustrated their Arrhenius-plots for the change in fluorescence intensity in the heating process as shown in Figure 8-12. Fluorescence intensity decreases faster with increase of temperature, i.e., their temperature dependence of Arrhenius plots shows two breaks of straight lines with the slope, increasing with temperature. This is due to the differences in the states and in the molecular arrangement of main intermolecular interaction for various temperature range. In addition, the change in temperature dependence of fluorescence intensity at indicates that the local molecular mobility changes initially, then extends to the whole molecular mobility change.

The temperature dependence of fluorescence intensity is affected by both the activation energy for radiationless transition and the change in the number of various intermolecular ground state complexes. In this case, since the layered structure is maintained in various phase, there has to be no change in the number of various ground state complexes. Hence, the main reason for the decrease of fluorescence intensity of the ground state charge transfer complexes is considered to be the radiationless transition.

The quenching of the excited states between the biphenyl and the pyromellitic moieties become more frequent with an increase of the molecular motion. The observed activation energy is considered to be an activation energy for the occurrence of the fluorescence species. To discuss the difference of deactivation process among various intermolecular ground state complexes more precisely, the temperature dependence of fluorescence intensity, E, for various temperature ranges are calculated. Calculated activation energy in Km1 is 11.1 kJ/mol, in LC is 17.0 kJ/mol and in isotropic melt is 22.3 kJ/mol.

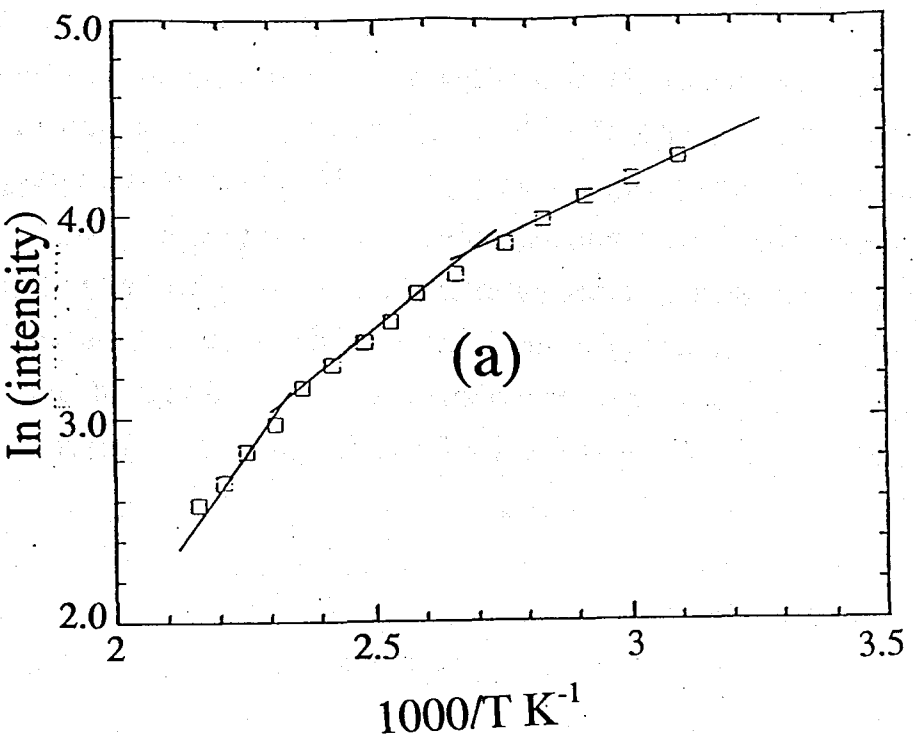

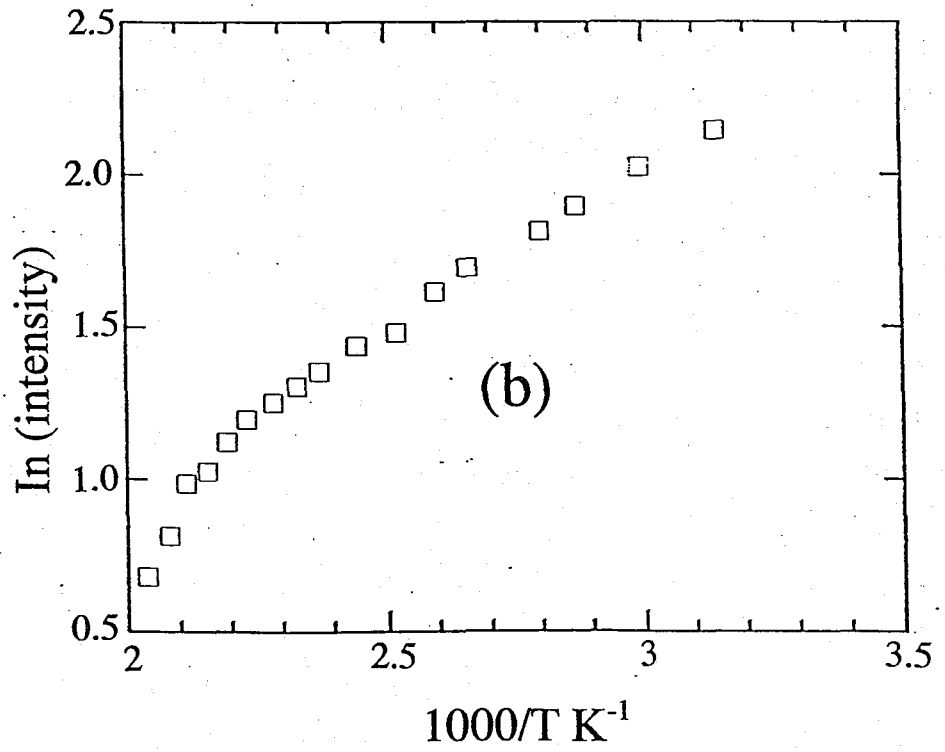

Figure 8-12. Arrhenius-type plots for the change in fluorescence intensity of intermolecular groun-state complexes of H-C14 polyesters during heating process from (a) the cast film (Kc crystal) and (b) the melt annealed film (Km1 crystal).

8-4 Concluding Remarks

Fluorescence measurement on various temperatures have provided detailed informations about the aggregation state and structure of polymers in the crystalline, liquid crystalline and isotropic phases of H-Cn polyesters. In Kc crystal, we observed the ground-state charge transfer fluorecsence at 480 nm (excited at 400 nm). This charge transfer complex is found between the hydroquinone and the pyromellitic ester moieties in the neighboring chains within a layer.

On heating the sample and when H-C16 polyesters translates from Kc to liquid crystalline layered phase, the wavelengths of the excitation and emission band of fluorescence are shifted to higher wavelength region. This means the change of ground-state molecular complex and moreover the intermolecular distance between the electron donating and accepting units in the neighboring chains become shorter than that in Kc crystal. Thus, in layered mesophase, the ground state charge transfer complexes are formed in an aromatic layer and the complex is different from that in Kc crystal. In isotropic phase we also observed the charge transfer complex band at 500 nm. This result means that in isotropic phase, the segregated structures are maintained between the aliphatic and aromatic domains and the molecular ordering become in an isotropic state. This conclusion is based on this results that in this phase we can not observe an increase of fluorescence intensity from an isolated chains. After melting, H-Cn do not form Kc crystal but Km1 crystal in which the intermolecular length is unusually short about 3.85 Å as much as layered mesophase. Fluorescence spectra in Km1 crystal is similar to that observed in layered mesophase.

These changes observed through fluorescence band correspond to that observed X-ray diffraction pattern. Hence a transition from Kc to LC (thus Km1) can be interpreted to be a change between the two ground state charge transfer complexes. Also, the isotropic state are interpreted to a segregated structure between the aliphatic and aromatic domains without the ordering of polymers.

We can discuss about driving forces responsible for the organization of these molecules into layered liquid crystalline structures. As has been widely accepted, most reliable force is segregation between the aromatic and aliphatic domain. However this study suggests that the formation of interchain complex in the aromatic main chains also plays a significant role in the formation of characteristic layered structure.

8-5 Reference and notes

(1) Ballauff, M. Macromol. Chem., Rapid Comun. 1986, **7**, 407.

(2) Ballauff, M. Angew. Chem., Int. Ed. Engl. 1987, **28**, 253.

(3) Ballauff, M.; Schmidt, G. F. Mol.Cryst.Liq.Cryst. 1987, **147**, 163.

(4) Stern, R.; Ballauff, M.; Wegner, G. Macromol. Chem., Macromol. Symp. 1989, **423**, 373.

(5) Rodrigues-Parada, J. M.; Duran, R.; Wegner, G. Macromolecules 1989, **22**, 2507.

(6) Ebert, M.; Herrmann-Schenherr, O.; Wendorf, J.; Ringsdorf, H.; Tschirner, P. Liq. Cryst. 1990, **7**, 63.

(7) Adam, A.; Spiess, H. W. Macromol. Chem., Rapid Comun. 1990, **11**, 249.

(8) Frech, C. H.; Adam, A.; Falk, U.; Boeffel, C.; Spiess, H. W. New Polym. Mater. 1990, **2**, 267.

(9) Stern, R.; Ballauff, M.; Lieser, G.; Wegner, G. Polymer 1991, **32**, 2079.

(10) Harkmess, B. R.; Watanabe, J. Macromolecules 1991, **24**, 6759.

(11) Watanabe, J.; Harkness, B. R.; Sone, M. Polym. J. 1992, **24**, 1119.

(12) Cervinka, L.; Ballauff, M. Colloid Polym. Sci. 1992, **270**, 859.

(13) Sone, M.; Harkness, B. R.; Watanabe, J.; Torii, T.; Yamashita, T.; Horie, K. Polym. J. 1993, **25**, 997.

(14) Galda, P.; Kistner, D.; Martin, A.; Ballauff, M. Macromolecules 1993, **26**, 1595.

(15) Marz, K.; Lindner, P.; Urban, J.; Ballauff, M.; Fisher, E. W. Acta Polym. 1993, **44**, 139.

(16) Damman, S. B.; Mercx, F. R. P.; Kootwijk-Damman, C. M. Polymer 1993, **34**, 1891.

(17) Damman, S. B.; Mercx, F. P. M. J. Polym. Sci., Polym. Phys. 1993, **31**, 1759.

(18) Damman, S. B.; Mercx, F. P. M. J.; Lemstra, P. J. Polymer 1993, **34**, 2726.

(19) Damman, S. B.; Vroege, G. J. Polymer 1993, **34**, 2732.

(20) Kakimoto, M.; Orikabe, H.; Imai, Y. ACS Polym. Prep. 1993, **34**, 746.
(21) Steuner, M.; Hortz, M.; Ballauff, M. J. Polym. Sci., Polym. Chem. 1993, **31**, 1609.
(22) Watanabe, J.; Harkness, B. R.; Sone, M.; Ichimura, H. Macromolecules 1994, **27**, 507.
(23) Sone, M.; Harkness, B. R.; Kurosu, H.; Ando, I.; Watanabe, J. Macromolecules 1994, **27**, 2769.
(24) Damman, S. B.; Buijs, J. A. H. M. Polymer 1994, **35**, 2559.
(25) Damman, S. B.; Buijs, J. A. H. M.; van Turnhout, J. Polymer 1994, **35**, 2364.
(26) Buijs, J. A. H. M.; Damman, S. B. J. Polym. Sci.; Polym. Phys. 1994, **32**, 851.
(27) Tiesler,U.; Pulina,T.; Rehahn,M.; Ballauff,M.; Mol.Cryst.Liq.Cryst. 1994, **41**, 525.
(28) Voigt-Martin, I. G.; Simon, P.; Bauer, S.; Ringsdorf, H. Macromolecules 1995, **28**, 236.
(29) Voigt-Martin, I. G.; Simon, P.; Yan, D.; Yakimansky, A.; Bauer, S.; Ringsdorf, H. Macromolecules 1995, **28**, 243.
(30) Itagaki, H.; Horie, K.; Mita, I. Prog. Polym. Sci. 19990, **15**, 36.
(31) Hasegawa, H.; Mita, I.; Kochi, M.; Yokota, R. J. Polym. Sci. Part C: Polym. Lett. 1989, **27**, 263.
(31) Hasegawa, H.; Kochi, M.; Yokota, R. Polymer 1991, **32**, 3225.
(32) Hasegawa, H.; Arai, H.; Mita, I.; Yokota, R. Polym. J. 1990, **22**, 875.
(33) Hashimoto, H.; Hasegawa, M.; Horie, K.; Yamashita, T.; Mita, I, Ushiki, H. J. Polym. Sci. Polym. Phys. Ed. 1993, **31**, 1187.
(34) Huang, H. W.; Horie, K.; Yamashita, T. J. Polym. Sci. Polym. Phys. Ed. 1995, **33**, 1673.
(35) Huang, H. W.; Horie, K.; Yamashita, T.; Machida, S.; Sone, M.; Mabuchi, T.; Watanabe, J.; Maeda, Y. Macromolecules 1996 in press.
(36) Mataga, N.; Kubota, T. "Molecular Interaction and Electronic Spectra" Marcel Dekker, Inc., New York (1970).
(37) Ikeda, T.; Lee, C.H.; Sasaki, T,; Lee, B,; Tazuke, S. Macromolecules

1990, **23**, 1691.
(38) Kurihara, S.; Ikeda, T.; Tazuke,S. Macromolecules 1991, 24, 627; 1993, **26**, 1993.

Chapter 9

Summary

In this discussion, the thermotropic behaviors and phase structures of the rigid-rod polyesters with flexible side chains are systematically studied and understood as a function of temperature. These results effectively showed that a thermotropic phase structure could be controlled by a molecular design of thermotropic liquid crystalline polymers with considerations about three different factors; a segregation, an intermolecular interaction and a molecular shape. Morphology for the liquid crystal of the rigid-rod polyesters with flexible side chains is dominated by the segregation of the aliphatic and aromatic domains. The degree of the segregation is controlled by the length of the alkyl side chains. The structural order of the layered structure is influenced by the intermolecular interaction such as the charge transfer interaction. The charge transfer interaction could be controlled by the considering the charge transfer between an electron donating and accepting units in the main chains. In this layered structure, various specific chain conformations for the aromatic main chains are found through high resolution solid-state ^{13}C NMR spectroscopy. This finding would help a fine controlling the mesophase structure.

These studies are also important for the methodologies for examining a structure and properties of liquid crystalline phases. X-ray diffraction pattern shows an ordered structure of liquid crystalline phases. Solid-state ^{13}C NMR spectroscopy provides an information of chain conformation in liquid crystal. Moreover fluorescence methods provides an information about intermolecular charge transfer interaction in thermotropic liquid crystalline phases. The detailed concluding remarks are shown in following.

Chapter 2 A series of rigid-rod polyesters with long alkyl side chains, denoted as B-Cn and H-Cn, have been prepared by condensing esters of

pyromellitic acid with 4,4'-biphenyl and hydroquinone, respectively. The alkyl side chain lengths were varied from excel (n = 6) to octadecyl groups (n = 18).

Chapter 3 The thermotropic transition behavior and mesophase structure of B-Cn polyesters were examined by optical microscopy, DSC and X-ray measurements. An increase in the length of side chain decreases remarkably the melting point of the crystalline phase, giving rise to a liquid crystalline phase. Two types of liquid crystalline phases with layer-like modifications, LC-1 and LC-2 have been observed. The transition behavior of these liquid crystalline phases is described as a function of the side chain length. In addition, the structural characteristics of the liquid crystalline phases as well as the crystalline phase are described as based upon X-ray data collected for oriented specimens.

Chapter 4 The thermotropic transition behavior and phase structure of H-Cn polyesters were examined by optical microscopy, DSC and X-ray measurements. H-Cn forms one type of liquid crystalline phase and four types of crystalline phases depending on side chain length. The crystalline phases , Kc and Km1 formed by H-C12 to 18 are characterized by a layered structure, in which the aromatic main chains are packed into monolayer with the side chains crystallized in the space between the layers. Km2 formed by H-C6 to 10 is also characterized by a layered structure, in which the aromatic main chains are packed like a zigzag sheet with amorphous side chains. In Kh formed by H-C6, the main chains are packed in a hexagonal lattice in which unit cell six numbers of the repeating units are contained. The liquid crystalline phase is also a layered structure which belongs to Σo_{1} according to classification of layered mesophase. The driving force for the adoption of such various structure as a function of side chain lengths is considered to be a segregation of the aliphatic and aromatic domains.

Chapter 5 Rigid-rod aromatic B-Cn polyesters with long alkyl side chains, composed of 1,4-dialkyl esters of pyromellitic acid and 4,4'-biphenol, form two distinct types of crystalline phases, K1 and K2, depending on the length of alkyl side chain. These crystalline phases are characterized by a layered structure, in which the aromatic main chains are packed into a layer with the side chains crystallized in the space between the layers. The detailed structures for these two crystalline phases were studied by ^{13}C solid-state NMR spectroscopy from which it was found that there are remarkable differences in the main chain conformation and in the packing structure of the side chains. In the K1 crystal formed by the B-Cn polymers with shorter side chains, the aromatic main chain assumes a twisted conformation with the side chains packed into an orthorhombic lattice. In contrast, in the K2 crystal of the longer side chain B-Cn polymers, the main chains assume a coplanar conformation with the side chains packed into triclinic lattice. The NMR studies have also been extended to the two types of layered mesophases, LC-1 and LC-2, formed by these polymers. In these phases, the side chains are molten, with the main chains in the LC-1 and LC-2 phases assuming conformations similar to those in the K1 and K2 crystals, respectively. FPT-INDO calculations for the conformational energy have shown that the coplanar conformation in the K2 and LC-2 phases is strongly disfavored whereas the twisted conformation is stable. It is believed that the disfavored coplanar conformation observed in the K2 and LC-2 phases is forced by the layered segregation of the aromatic main chains and the aliphatic side chains.

Chapter 6 Rigid-rod aromatic H-Cn polyesters with long alkyl side-chain, composed of 1,4-dialkylesters of pyromellitic acid and hydroquinone, form four distinct types of crystalline phases, Kc, Km1, Km2 and Kh, depending on the length of alkyl side-chain. The crystalline phases, Kc and Km1, formed by H-C12 to 18 are characterized by a layered structure, in which the aromatic main chains are packed into monolayer with the side-chains crystallized in the space between the layers. Km2

formed by H-C6 to 10 is also characterized by a layered structure, in which the aromatic main-chains are packed like a zigzag sheet between the aliphatic layers. In Kh formed by H-C6, the main chains are packed in a hexagonal lattice. The detailed structures for these four crystalline phases were studied by solid-state ^{13}C NMR spectroscopy from which it was found that there are remarkable differences in the main-chain conformation and in the packing structure of the side-chains. With the observed ^{13}C chemical shift values and calculated NMR shielding by FPT-INDO calculation, we can successfully estimate the polymer conformation in these phases. In the Kc crystal, the aromatic main chain assumes a twisted conformation with the side chain crystallized. In contrast, the main chain in Km1 assumes a stairlike conformation with crystallized side chains. In the Km2 and Kh, the main chain conformations are not uniquely confined but mixed. Interestingly, Km2 and Kh crystals has three dimensional long range positional orders with disordered chain conformation and these structural properties indicate that these crystals are classified into 'condis crystal'. The NMR studies have also been extended to the layered mesophase. In this phase, the side-chains are molten, with the main-chains assuming conformation similar to those in Km1 crystals. The driving force for the adoption of such various structure is considered to be both a segregation of aliphatic and aromatic domains and an interchain charge transfer complex formation between the hydroquinone and pyromellitic ester moieties.

Chapter 7 Rigid-rod B-Cn polyesters form two types of the layered crystals and two types of the layered mesophase. These layered phases are characterized by a layered structure, in which the aromatic main chains are packed into a layer with the side chains occupying the space between the layers. The detailed aggregated structures for these two crystalline phases were studied by fluorescence spectroscopy from which it was found that the ground-state charge transfer complexes are formed between the biphenyl and pyromellitic moieties in the adjacent main chains. Two layered crystals, K1 and K2, shows the charge transfer fluorescence and its excitation spectra in the different wavelengths. This difference of the

wavelengths come from that of the interchain lengths between the electron donating and accepting units in the adjacent chains. Thus the charge transfer complexes in the two layered crystals is different from each other. In the isotropic phase, the charge transfer bands were also observed. This result means that the isotropic state in this polymeric system could be defined by the state that a layered segregation is maintained but the molecular ordering and the interlayer correlation are lost. It is well known that the driving force of the adoption for layered structure is a segregation of aliphatic and aromatic domains and moreover we demonstrated that a charge transfer interaction between the electron donating and accepting units in the neighboring main chains attributes the organization of phase structure and spatual arrangements. This study also proved that the fluorescence spectroscopy is a powerful tool for examining the intermolecular interaction in the liquid crystalline phase.

Chapter 8 Rigid-rod aromatic H-C14 polyesters with long alkyl side chains, composed of 1,4-dialkylesters of pyromellitic acid and hydroquinone, form three types of layered modification; Kc, Km1 crystals and a layered mesophase, as a function of temperature. The crystalline phases Kc and Km1 are characterized by a layered structure, in which the aromatic main chains are packed into monolayer with the side chains crystallized in the space between the layers. The packing modification of aromatic main chains in two crystals differ from each other about the interchain distance which is 4.89 Å in Kc and that is 3.85 Å in Km1.

The aggregation structure for these phases were studied by variable temperature fluorescence spectroscopy from which it was found that ground state charge transfer complexes are formed between pyromellitic and hydroquinone moieties in neighboring aromatic chains. Remarkable differences in these complexes between Kc and Km1 is found through the measurement of wavelengths for excitation and emission bands of fluorescence spectra. The intensity of charge transfer fluorescence as a function of temperature shows differences of molecular motion among these three phases; isotropic, layered mesophase and layered crystals. From

this result we found that a layered segregated structure is kept in isotropic phase in which the orientational order of layers is lost.

It is well known that the driving force of the adoption for layered structure is a segregation of aliphatic and aromatic domains and moreover we demonstrated that a charge transfer interaction between the electron donating and accepting units in the neighboring main chains attributes the organization of phase structure and spatual arrangements.

Acknowledgments

The author wishes to express his sincere gratitude to Professor J. Watanabe for his inspired supervision, friendship and valuable discussions. He also wishes to thank Dr B.R. Harkness for his kind advice and useful discussions. He is also grateful to Mr N. Sekine, Mr H. Ichimura, Mr N. Kawasaki, Mr T.Wada, Mr T. Hironaka, Ms H. Bhavna and Mr M. Tokita for their collaborations, and other members of the Watanabe Lab. in Tokyo Institute of Technology for their kind consideration.

The author deeply thanks Professor I. Ando and Assistant Professor H. Kurosu, in Department of Polymer Chemistry at Tokyo Institute of Technology, for their valuable discussion in the High resolution solid state NMR method. He also wishes to thank Dr H. Yoshimizu (Assistant Professor in Nagoya Institute of Technology), Dr Y. Yasunaga (Assistant Professor in Kyoto Institute of Technology), Dr S. Kuroki, Dr N. Asakawa (Assistant Professor in Tokyo Institute of Technology) and other members in Ando Lab. for their kind advice and discussion.

The author deeply thanks Professor K. Horie, Associated Professor T. Yamashita and Assistant Professor S. Machida in Department of Chemistry and Biotechnology at Tokyo University, in valuable discussions in the Fluorescence method and their kindness for their giving opportunities to use their fluorescence spectrometers. He also wishes to thank Dr T. Torii, Dr S. Morino, Mr H. Takahashi and Mr H. W. Huang and other members in Horie Lab. for their great advice and discussion.

The author deeply thanks Professor Y. Imai, Associated Professor M. Kakimoto and Assistant Professor M. Jikei in Department of Organic and Polymeric Material at Tokyo Institute of Technology for their valuable discussion in synthesis of the Rigid-rod polyamide with flexible side chains.

The author deeply thanks Professor K. Okuyama and Assistant Professor K. Noguchi in Department of Biotechnology in Tokyo University of Agriculture and Technology for the discussion in the X-ray diffraction study to be reported in future. He also wish to thank Mr N. Yoshimatsu, Ms H. Muramatsu, and other members in Okuyama Lab. for their good advice and discussions. He wants to apologize to them for being unablt to finish "X-ray diffraction study of the Layered Crystals" for this thesis.

The author deeply thanks Professor S. Miyata and Assistant Professor T. Watanabe in Department of Biotechnology in Tokyo University of Agriculture and Technology for their adivice and discussion in SHG study of Rigid-rod polyesters.

The auther deeply thanks Professor Y. Takezoe, and Mr T. Furukawa in Department of Organic and Polymeric Material in Tokyo Institute of Technology for their excellent measurement and useful discussion of SHG activity of the Rigid-rod polyesters.

The author thanks Associated Professor K.Ishikawa and Dr K. H. Kim for providing the Raman spectra for B-Cn polymers.

The author thanks Associated Professor T. Kato of Tokyo University for his advice and encouragements in this study.

Lastly, He expresses thanks to his parents for their deep encouragements and support throughout the study.